Lactose permease LacY as a model for membrane transport proteins

S. Frillingos, 2014

Meta-genomic era of structure-function studies: The active transport proteins taxa

Μεμβρανικές πρωτεΐνες

~1/3 του συνόλου των πρωτεϊνών

Ενσωματωμένες (integral)

Περιφερειακές (peripheral)

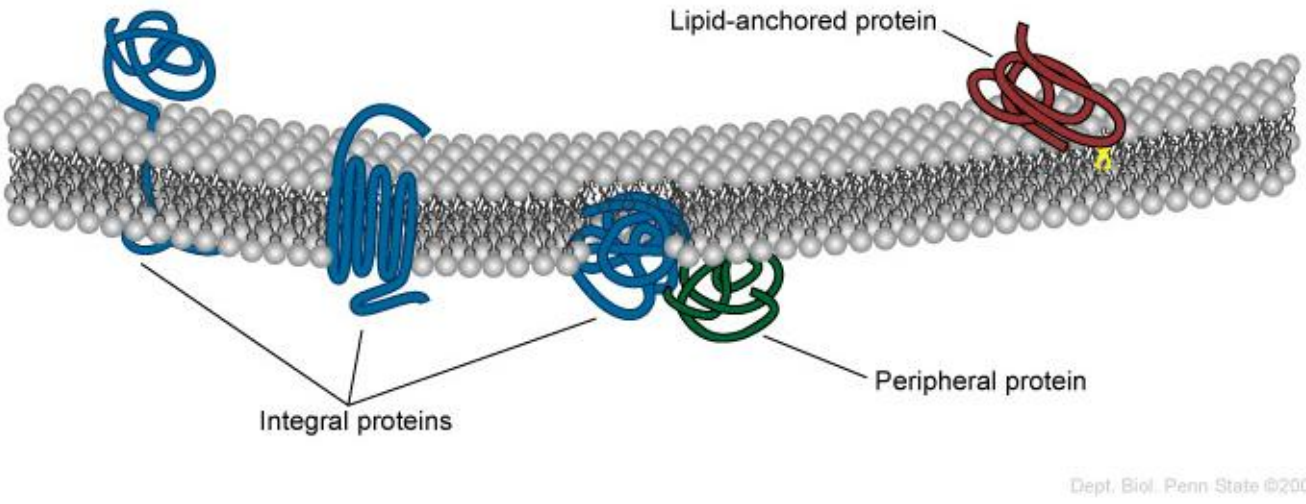

- ✓Επικοινωνία κυττάρου – κυττάρου
- ✓Συντονισμός των κυτταρικών λειτουργιών
- ✓Προσαρμογή στις μεταβαλλόμενες συνθήκες του περιβάλλοντος

Μεμβρανικές πρωτεΐνες

~1/3 του συνόλου των πρωτεϊνών

Μεταγωγή ενέργειας (energy transduction)

Μεταβολικές δραστηριότητες (π.χ. αναπνευστική αλυσίδα)

Πρόσληψη – διαμεμβρανική μεταφορά μεταβολιτών, ιόντων

Μεταγωγή σημάτων (signal transduction)

Αντιδράσεις μοριακής αναγνώρισης

Αναγνώριση εξωκυττάριων μορίων-σημάτων (π.χ. ορμονών) και έναρξη ενδοκυτταρικής σηματοδότησης

Ενδοκυττάρωση – εξωκυττάρωση
Ανακύκλωση υποδοχέων μεταξύ κυτταρικής μεμβράνης και ενδο-μεμβρανικών διαμερισμάτων

Μεμβρανικές πρωτεΐνες

~1/3 του συνόλου των πρωτεϊνών

Μεταγωγή ενέργειας (energy transduction)

Μεταβολικές δραστηριότητες (π.χ. αναπνευστική αλυσίδα)

Πρόσληψη – διαμεμβρανική μεταφορά μεταβολιτών, ιόντων

Μεταγωγή σημάτων (signal transduction)

Αντιδράσεις μοριακής αναγνώρισης

Αναγνώριση εξωκυττάριων μορίων-σημάτων (π.χ. ορμονών) και έναρξη ενδοκυτταρικής σηματοδότησης

Ενδοκυττάρωση – εξωκυττάρωση
Ανακύκλωση υποδοχέων μεταξύ κυτταρικής μεμβράνης και ενδο-μεμβρανικών διαμερισμάτων

Δυσλειτουργίες των πρωτεϊνών μεταφοράς συνδέονται συχνά με σοβαρές ασθένειες:

- **Κυστική ίνωση** (CFTR, chloride carrier), 1989
- **Νόσος Darier (θυλακική δυσκεράτωση)** (muscle Ca^{2+} ATPase), 1999
- **Συμφορητική καρδιακή ανεπάρκεια** (Na^+/Ca^{2+} antiporter; Na^+/K^+ ATPase)
- **Ρύθμιση της ανθεκτικότητας έναντι φαρμάκων** (MDR1,2)

- **Δυσαπορρόφηση σακχάρων** (SGLT1, sodium-glucose carrier)
- **Συγγενής υποθυρεοειδισμός** (NIS, Na^+-iodide symporter)
- **Κυστινουρία** (SLC3A1, SLC7A9, cystine & dibasic amino acid carriers)

- **Σύνδρομο αργής ανταπόκρισης διαύλου** (AchR, acetylcholine-gated ion channel)
- **Αμυοτροφική πλευρική σκλήρυνση** (EAAT2, excitatory glutamate transporter)
- **Ιδεοψυχαναγκαστική διαταραχή** (SERT, serotonin transporter / *Prozac*)

Οι περισσότερες πρωτεΐνες μεταφοράς που έχουν μελετηθεί διεξοδικά προέρχονται από βακτήρια

- **Κατανόηση της βιοχημείας, μοριακής φυσιολογίας και οικολογίας**
  παθογόνων και μη βακτηρίων, και ειδικών μεταβολικών προσαρμογών

- **Ανάλυση κυτταρικών μηχανισμών αναγνώρισης και πρόσληψης**
  των μεταφερόμενων (θρεπτικών ή τοξικών) υποστρωμάτων

- **Δυνατότητες εφαρμογής για σχεδιασμό αντιμικροβιακών φαρμάκων**
  μέσω κατανόησης των αλληλεπιδράσεων μεταφορέων και προσδετών τους

- **Κατανόηση της μοριακής βάσης ομολόγων μεταφορέων από θηλαστικά**
  βάσει αναλύσεων σε υψηλή ευκρίνεια των βακτηριακών ομολόγων

Transporter types

Συστήματα μεταφοράς (transporters)

(5-15% των γονιδίων σε όλα τα γονιδιώματα)

Φορείς (carriers)	Δίαυλοι (channels)
Κέντρα δέσμευσης	Δίοδοι μέσω της μεμβράνης
«Ομοιότητες με ένζυμα»	Χωρίς ομοιότητες με ένζυμα
Αλλαγές διαμόρφωσης	Ελεγχόμενη δίοδος του υποστρώματος

Για έναν φορέα (carrier) υπάρχουν:
α) **συγκεκριμένες θέσεις** δέσμευσης ανά αριθμό μορίων υποστρώματος
β) κινητικά χαρακτηριστικά ***κορεσμού*** των θέσεων δέσμευσης σε υψηλή συγκέντρωση υποστρώματος,

γ) μπορούν να υπολογισθούν V_{max} και K_m (όπως στα ένζυμα).

Συστήματα μεταφοράς (transporters)

(5-15% των γονιδίων σε όλα τα γονιδιώματα)

Φορείς (carriers)

Ενεργός μεταφορά

ή

Διευκολυνόμενη διάχυση

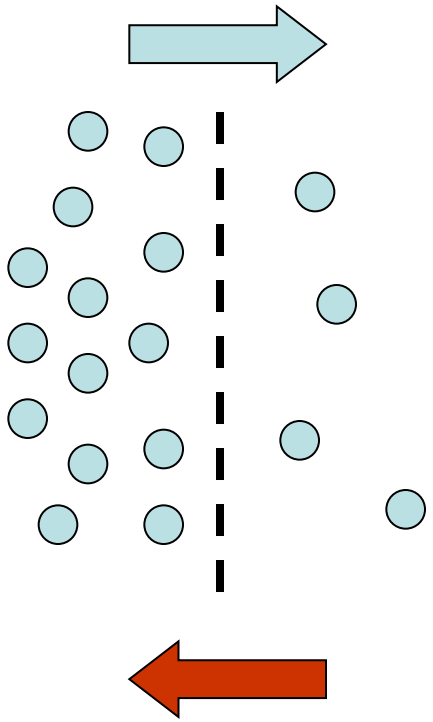

Δίαυλοι (channels)

Διευκολυνόμενη διάχυση

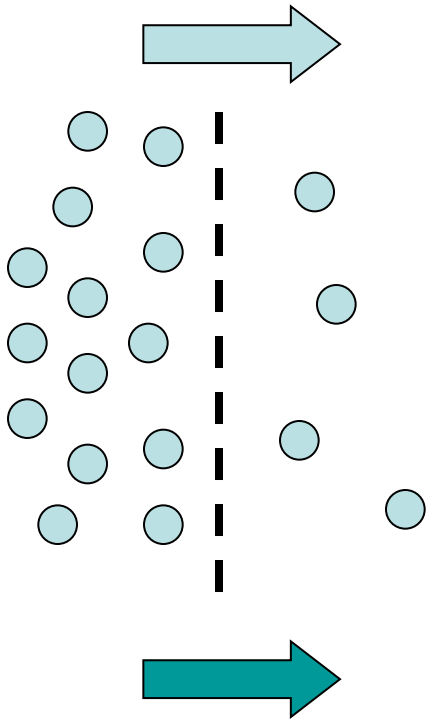

Συστήματα μεταφοράς (transporters)

(5-15% των γονιδίων σε όλα τα γονιδιώματα)

Φορείς (carriers)

Ενεργός μεταφορά

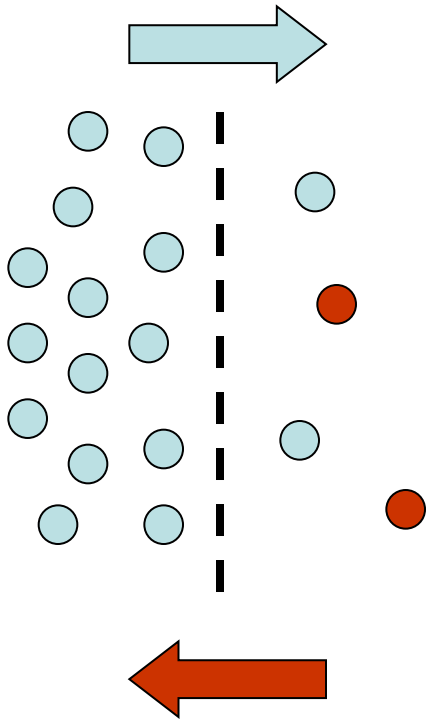

Δίαυλοι (channels)

Διευκολυνόμενη διάχυση

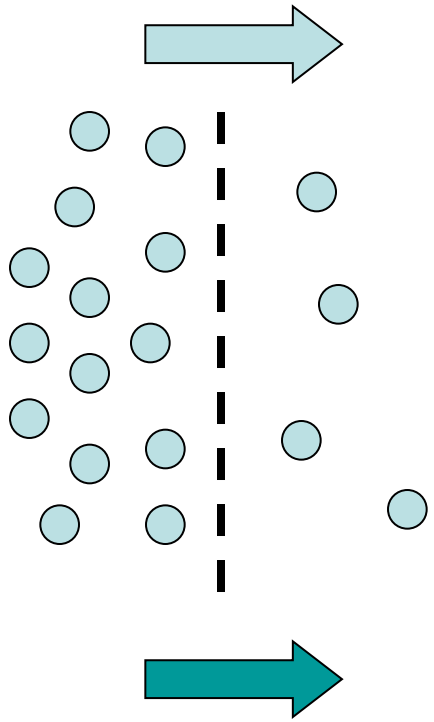

Συστήματα μεταφοράς (transporters)

(5-15% των γονιδίων σε όλα τα γονιδιώματα)

Φορείς (carriers)

Ενεργός μεταφορά

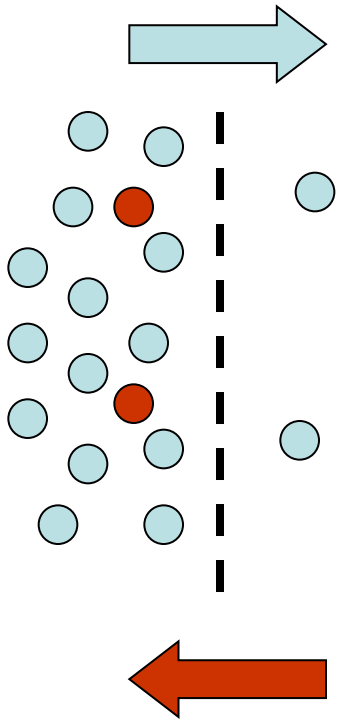

Δίαυλοι (channels)

Διευκολυνόμενη διάχυση

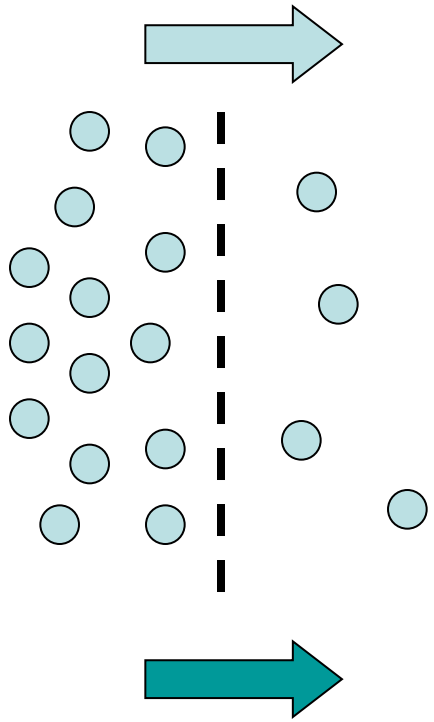

Συστήματα μεταφοράς (transporters)

(5-15% των γονιδίων σε όλα τα γονιδιώματα)

Φορείς (carriers)

Ενεργός μεταφορά

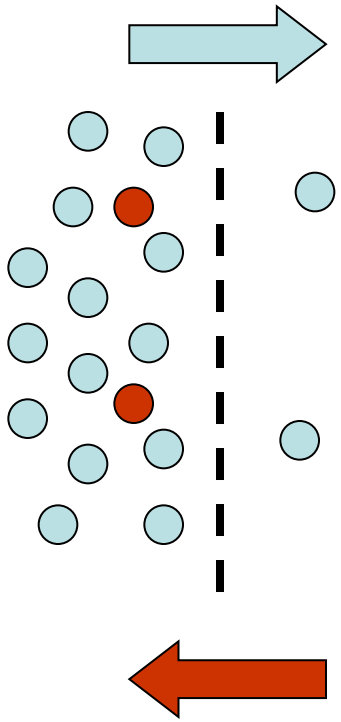

Δίαυλοι (channels)

Διευκολυνόμενη διάχυση

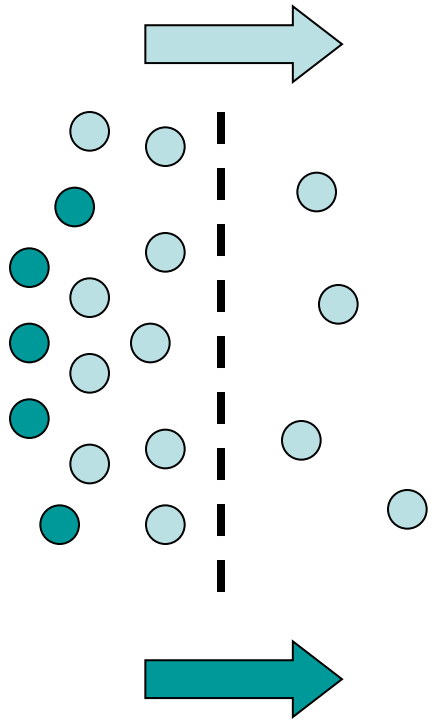

Συστήματα μεταφοράς (transporters)

(5-15% των γονιδίων σε όλα τα γονιδιώματα)

Φορείς (carriers)

Ενεργός μεταφορά

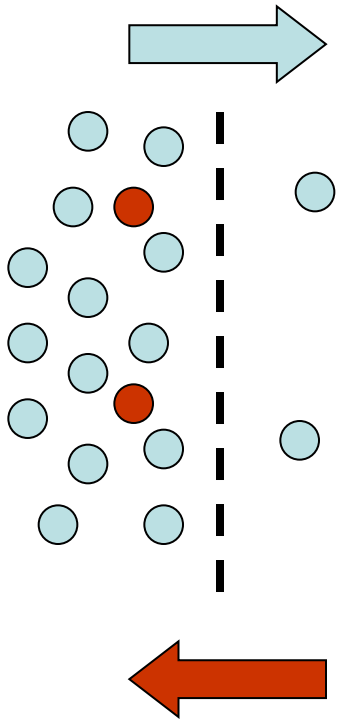

Δίαυλοι (channels)

Διευκολυνόμενη διάχυση

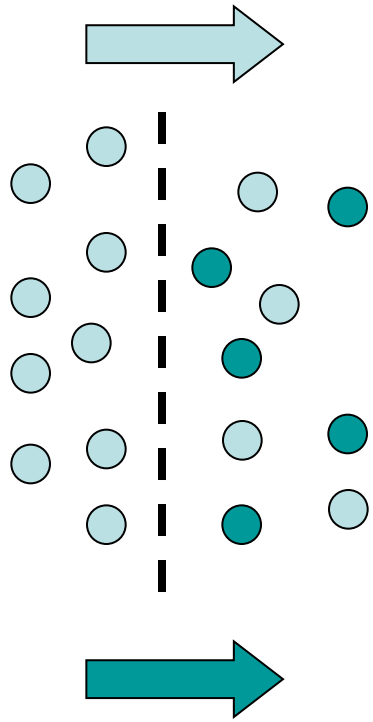

Συστήματα μεταφοράς (transporters)

(5-15% των γονιδίων σε όλα τα γονιδιώματα)

Φορείς (carriers)	Δίαυλοι (channels)
Ενεργός μεταφορά	Διευκολυνόμενη διάχυση

ΣΥΣΣΩΡΕΥΣΗ

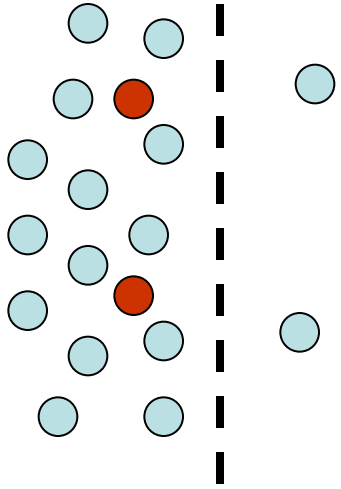

ΕΞΙΣΟΡΡΟΠΗΣΗ

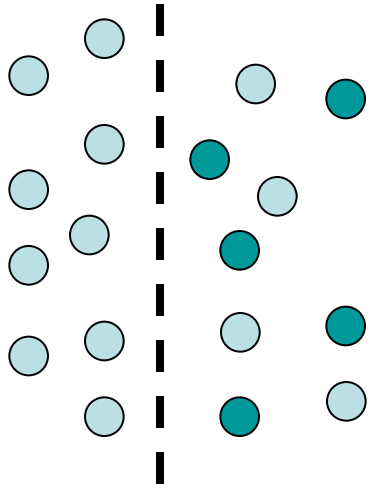

Από πού προέρχεται η ενέργεια που χρειάζεται για την ενεργό μεταφορά;

---

1. Από την υδρόλυση ATP (κυρίως) ή άλλες χημικές αντιδράσεις: <u>Πρωτογενούς τύπου</u>

2. Από ηλεκτροχημικές διαβαθμίσεις ιόντων (H^+ ή Na^+): <u>Δευτερογενούς τύπου</u>

Ηλεκτροχημική ενέργεια = Διαβάθμιση ιόντων

Συστήματα μεταφοράς (transporters)

(5-15% των γονιδίων σε όλα τα γονιδιώματα)

Φορείς (carriers) | **Δίαυλοι (channels)**

Ενεργός μεταφορά

δευτερογενούς τύπου (secondary active)

Ηλεκτροχημική διαβάθμιση ιόντων

πρωτογενούς τύπου (primary active)

Υδρόλυση του ATP

μεταφορείς ομάδας (group translocators)

Συστήματα μεταφοράς (transporters)

(5-15% των γονιδίων σε όλα τα γονιδιώματα)

Φορείς (carriers) | **Δίαυλοι (channels)**

Ενεργός μεταφορά

δευτερογενούς τύπου (secondary active)

Ηλεκτροχημική διαβάθμιση ιόντων

πρωτογενούς τύπου (primary active)

Υδρόλυση του ATP

μεταφορείς ομάδας (group translocators)

Αντιμεταφορείς (antiporters)

Συμμεταφορείς (symporters)

Μονομεταφορείς (uniporters)

Οικογένειες μεταφορέων – TCDB:

Δίαυλοι (channels)
TC 1

Φορείς (carriers)

Δευτερογενούς τύπου
TC 2

Πρωτογενούς τύπου
TC 3

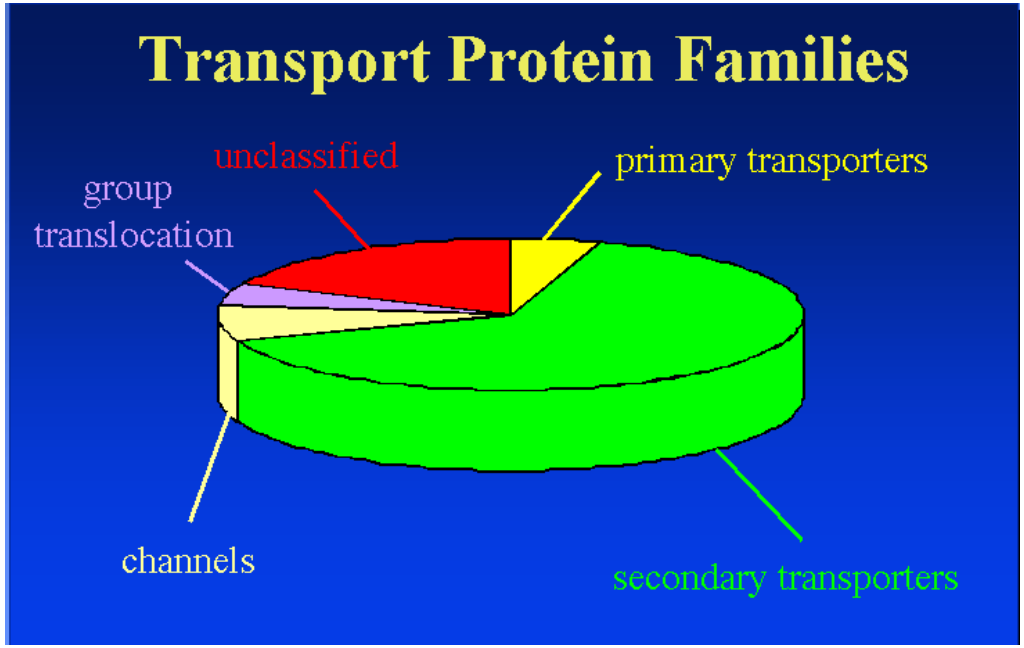

εντεροβακτήριο E. coli

Φορείς (carriers)

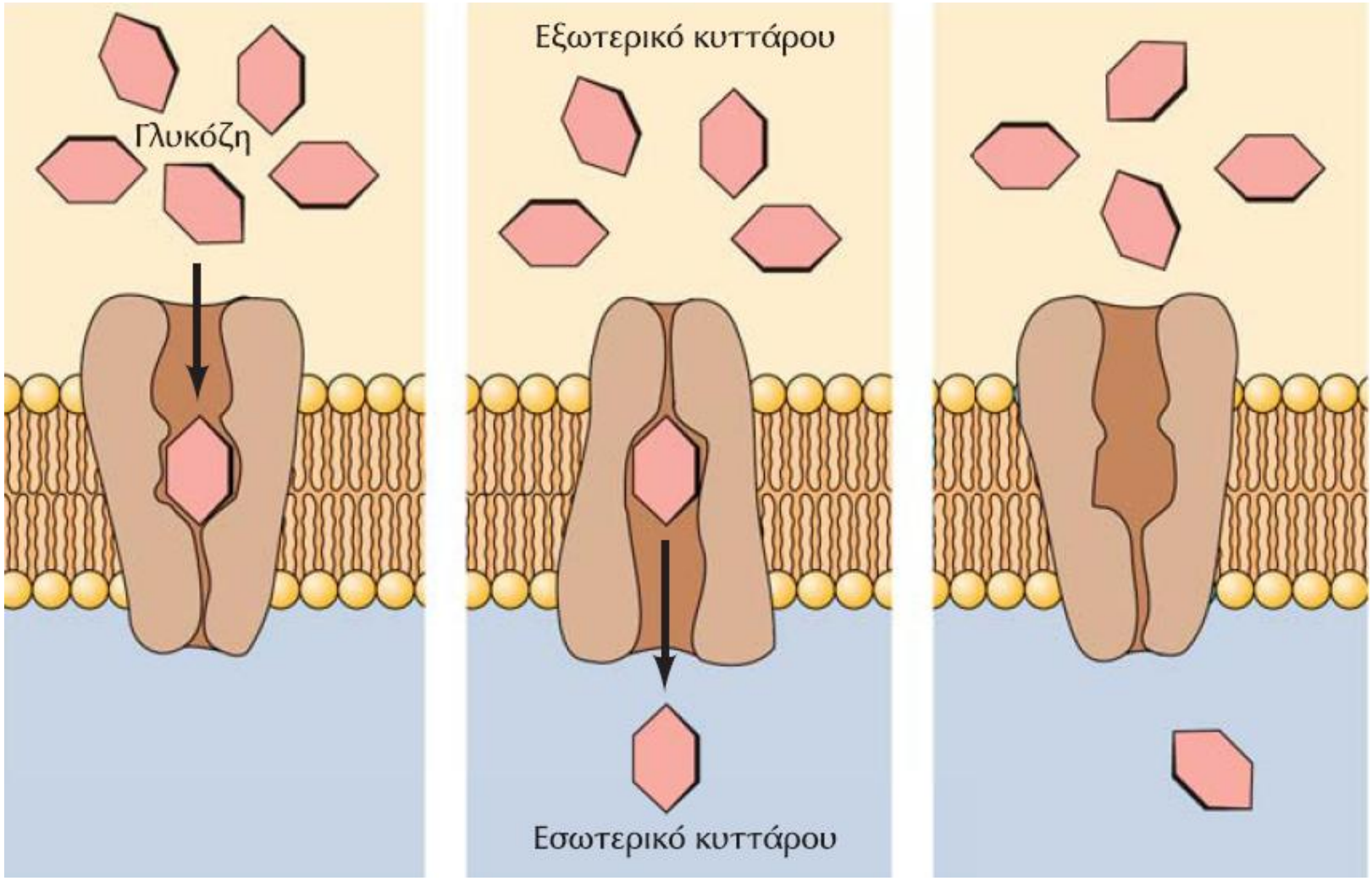

Πώς σχηματίζονται / λειτουργούν τα δυναμικά κέντρα δέσμευσης?

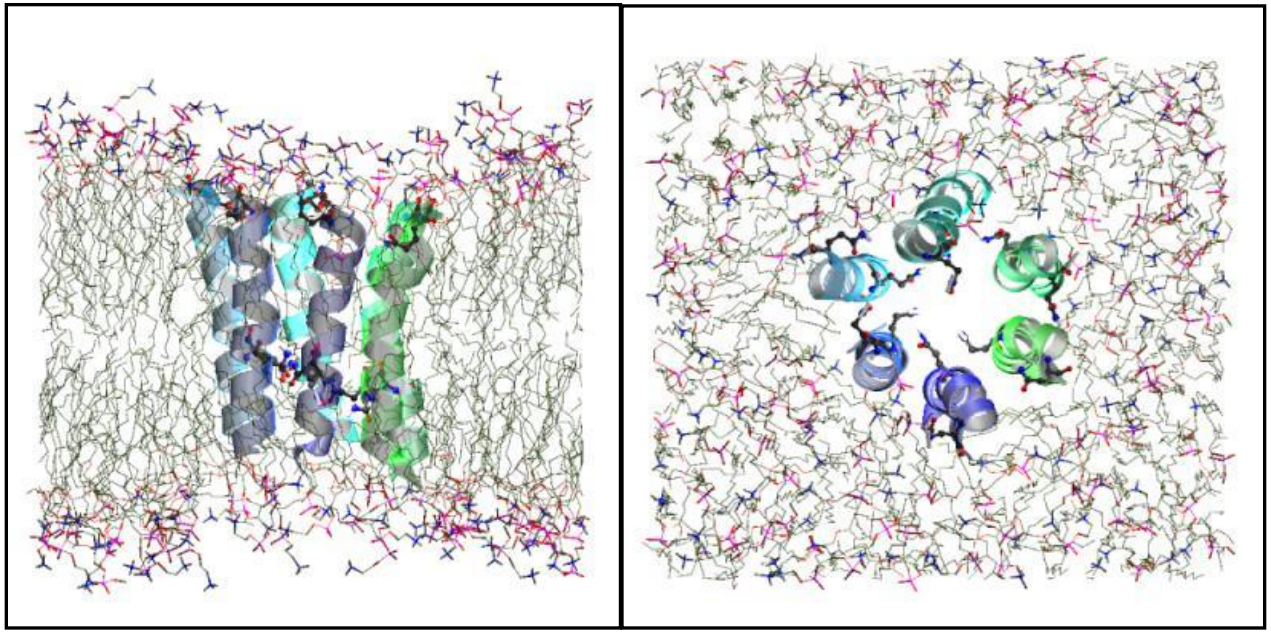

Το μοντέλο της εναλλασσόμενης πρόσβασης ενός δυναμικού κέντρου δέσμευσης (ΦΟΡΕΙΣ)

Alternating access

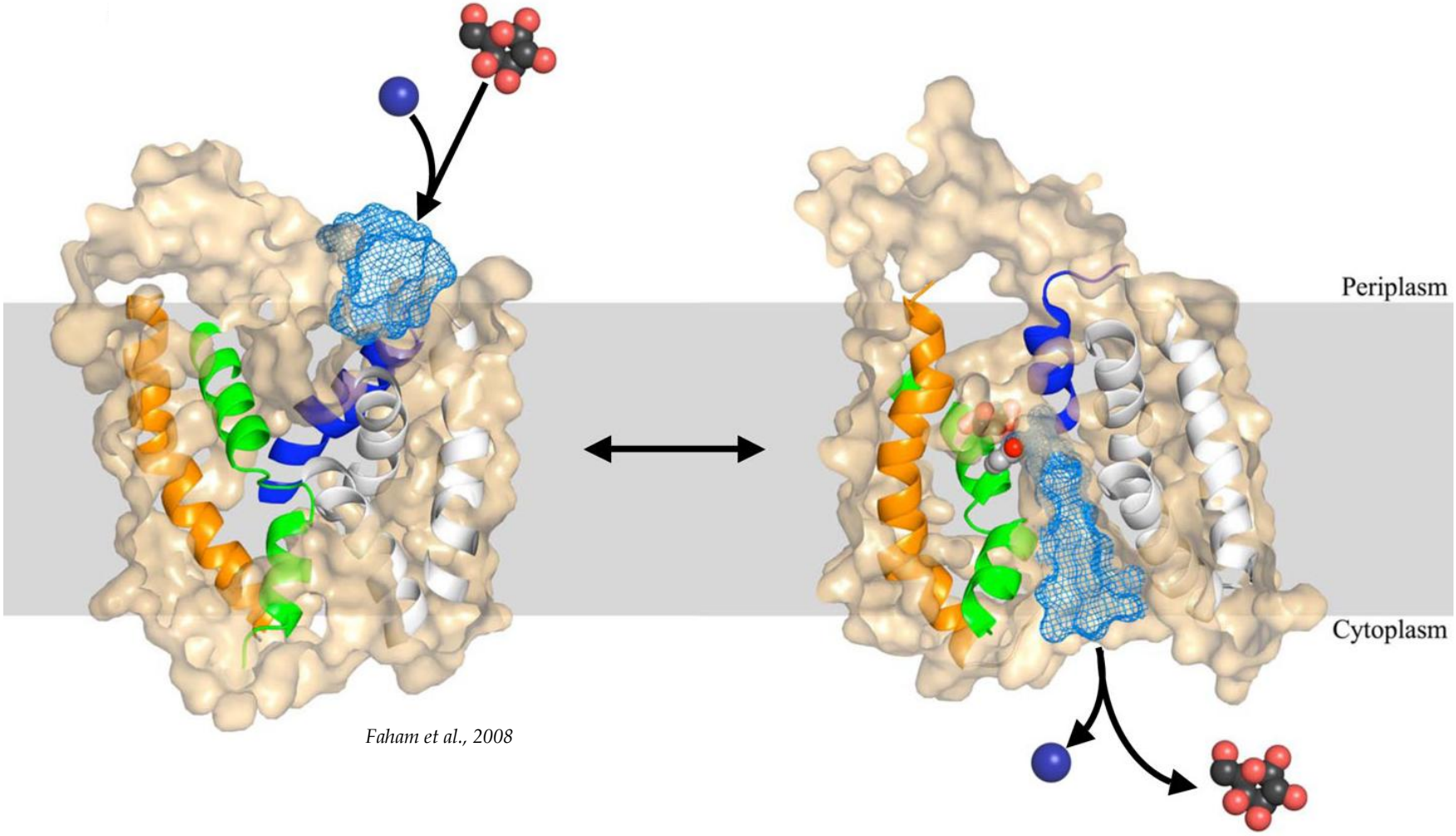

Faham et al., 2008

Widdas, 1952

Forrest et al., 2010

Το μοντέλο της εναλλασσόμενης πρόσβασης ενός δυναμικού κέντρου δέσμευσης (ΦΟΡΕΙΣ)

Alternating access

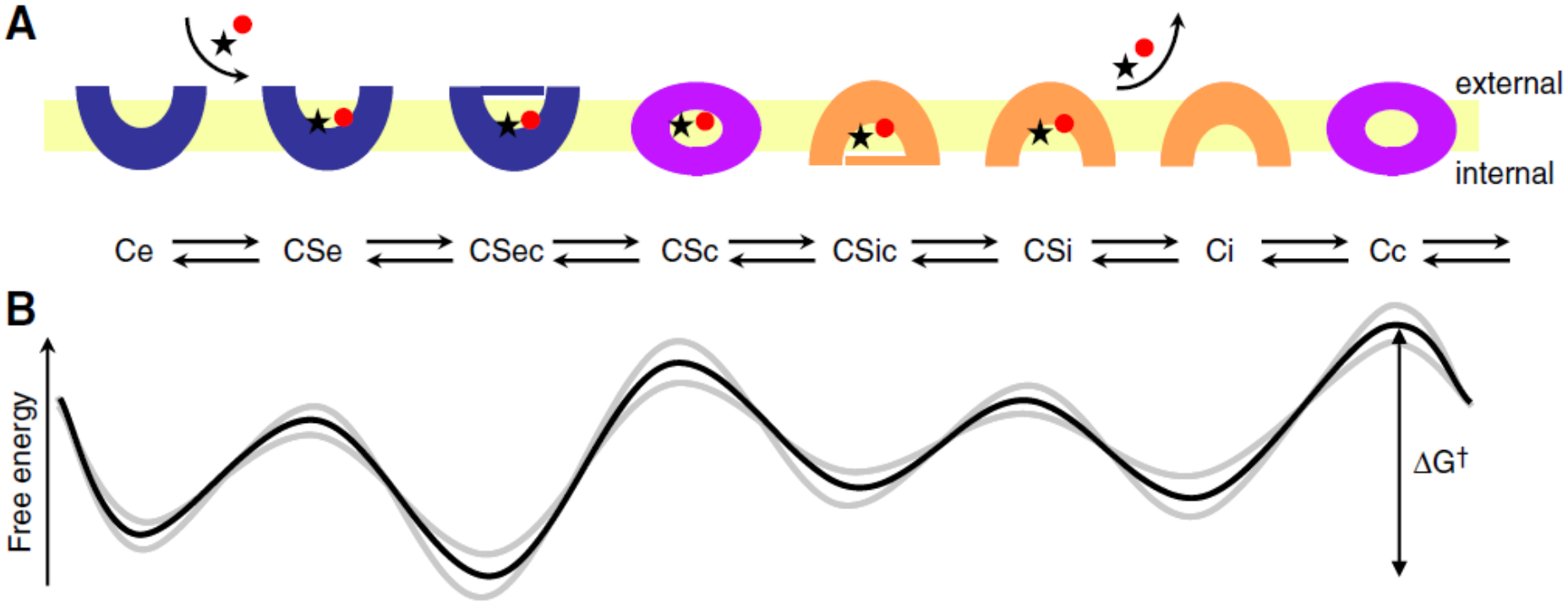

Πώς εξασφαλίζεται η εξειδίκευση?

C, φορέας (carrier)
S, υπόστρωμα (substrate)
e, προς τα έξω (external facing)
i, προς τα μέσα (internal facing)
c, κλειστό (closed)

Κέντρο δέσμευσης (binding site)
Συμμετοχή μοριακών φίλτρων (selectivity filters) που περιορίζουν την πρόσβαση στο κέντρο δέσμευσης ή την έξοδο από αυτό

Forrest et al., 2010

Οι δυσκολίες μελέτης των διαμεμβρανικών πρωτεϊνών ενεργού μεταφοράς

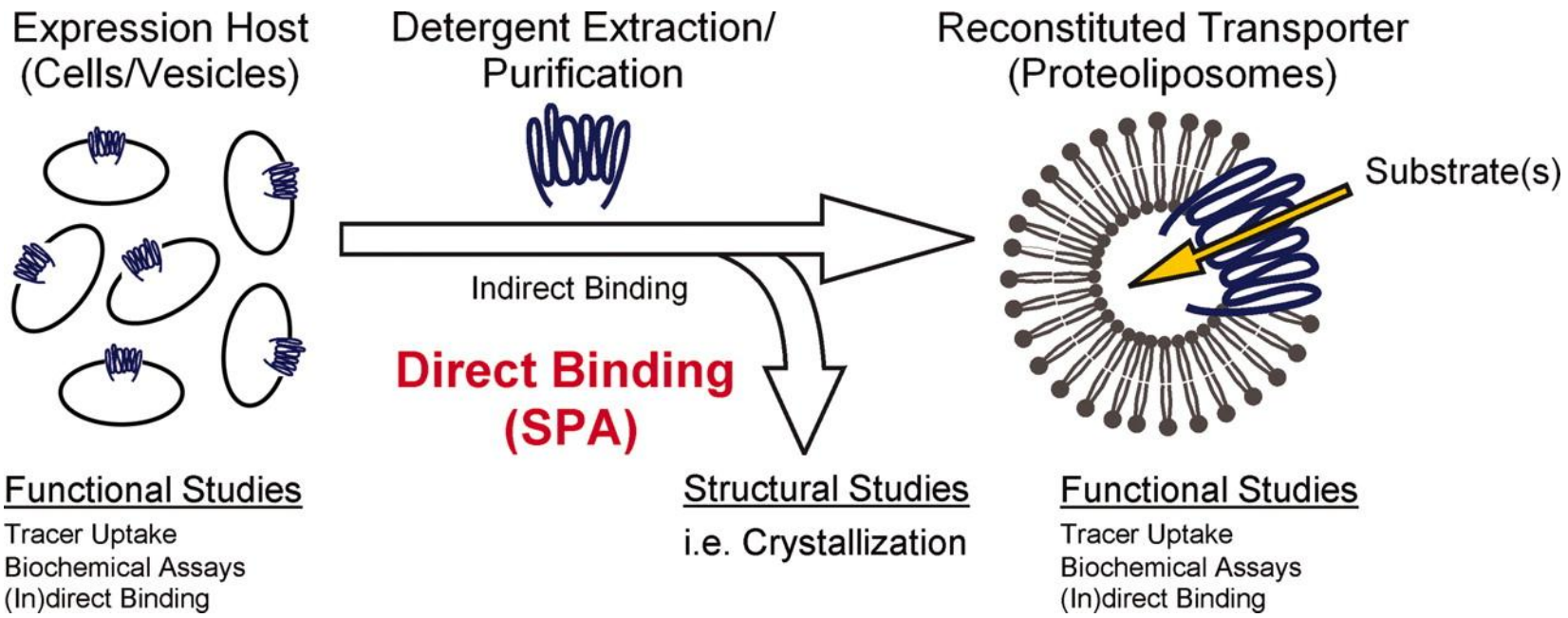

Quick M , Javitch JA, *PNAS* 2007;104:3603-8

Meta-crystallographic era of transporters

FIGURE 1. Progress in determining membrane protein structures.

From the following article:

Biophysical dissection of membrane proteins

Stephen H. White

Nature 459, 344-346(21 May 2009)

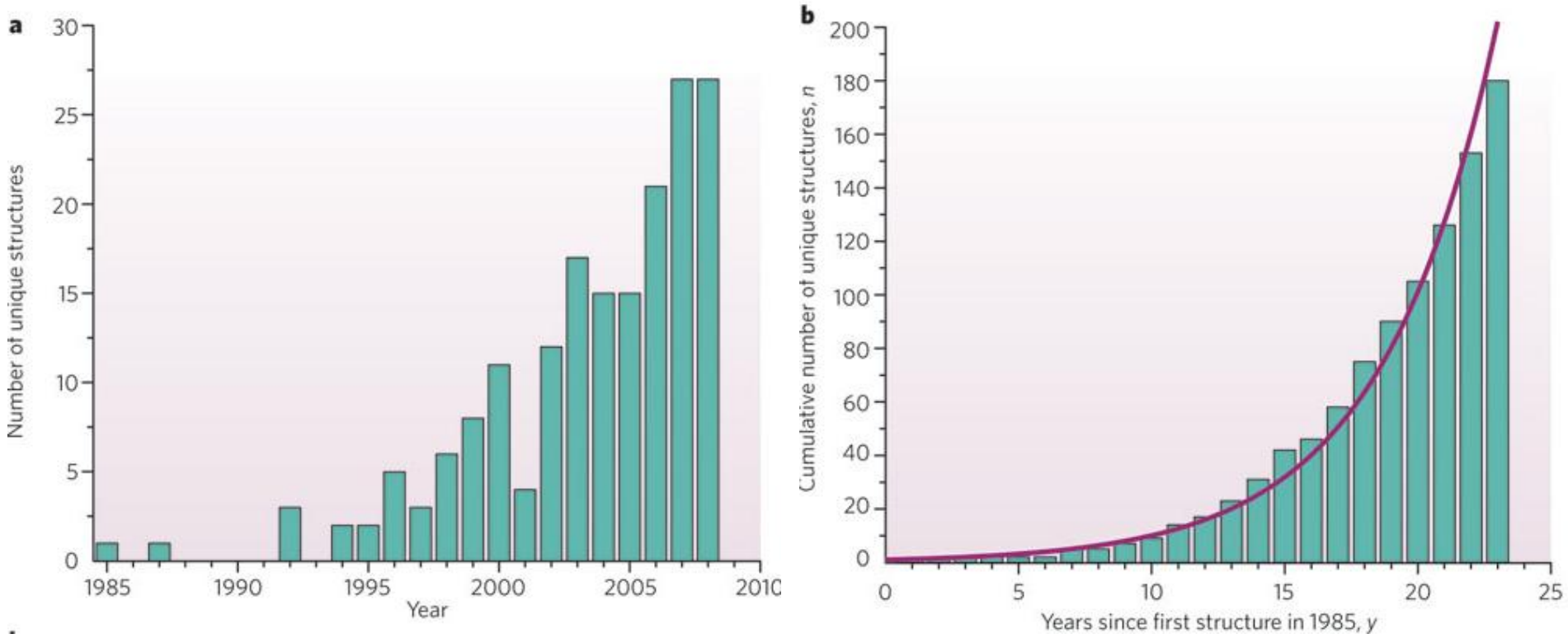

Only unique structures are included in the statistics. Proteins of the same type from different species are included, but structures of mutagenized versions of proteins are excluded, as are proteins that differ only in terms of substrate bound or physiological state. **a,** The number of structures reported each year since 1985. **b,** The bars represent the cumulative number (n) of structures plotted against the number of years (y) since the first structure was reported. The solid curve is the best fit to the equation $n = \exp(ay)$, where $a = 0.23$; the reduced x^2 of the fit is 0.6. Data are from a curated database of membrane proteins of known structure at http://blanco.biomol.uci.edu/Membrane_Proteins_xtal.html.

The structure images are not enough ; they need complementation with functional data

Lac permease
is the best studied paradigm
of an active transporter

for many reasons…

Περμεάση λακτόζης

LacY

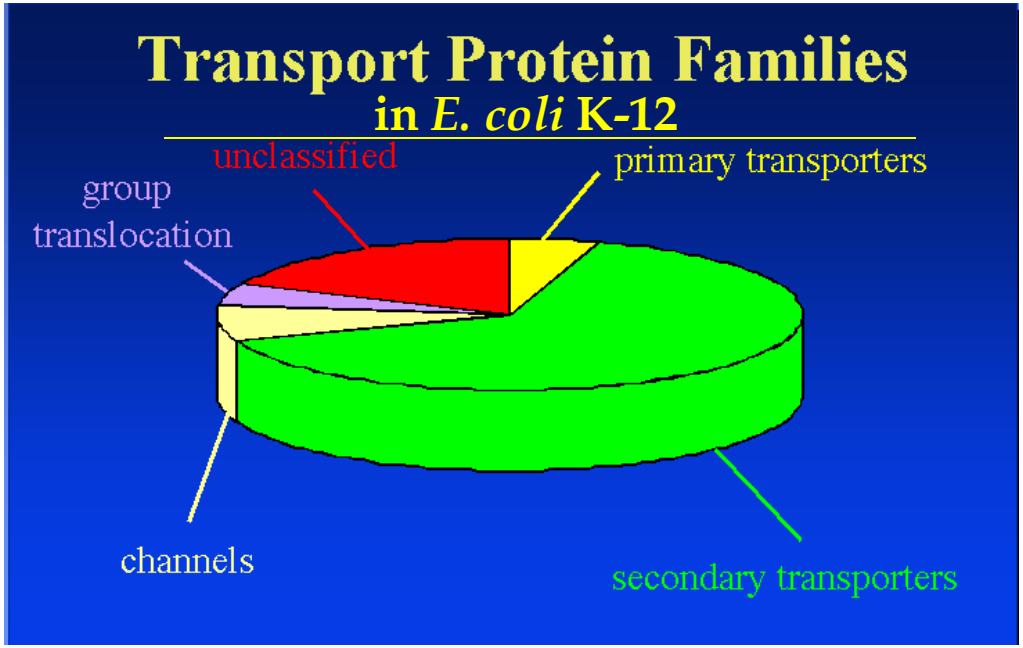

Περμεάση λακτόζης

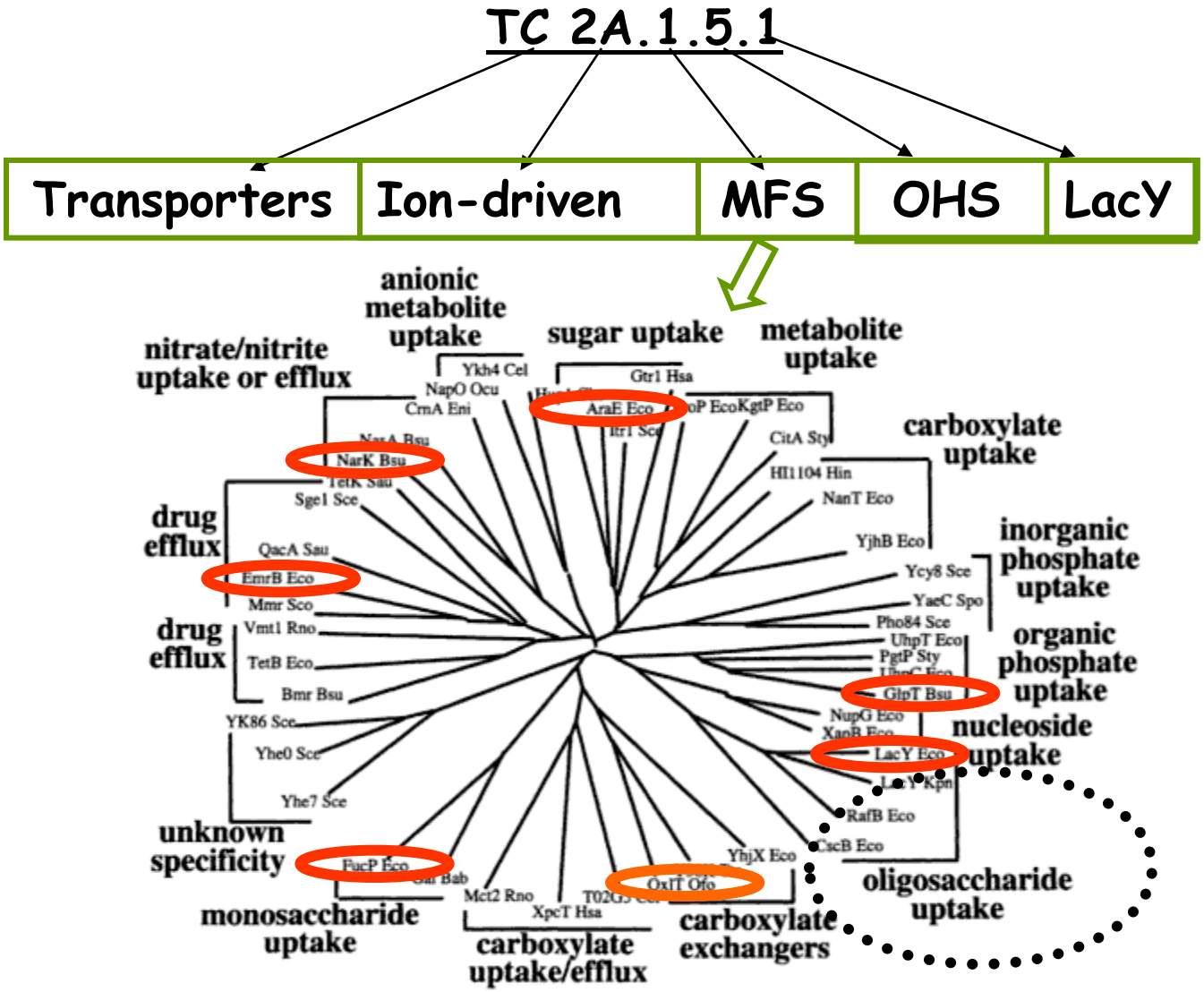

Saier, 1998-9
TCDB site

«Δεύτερο δομικό γονίδιο» στο οπερόνιο της λακτόζης

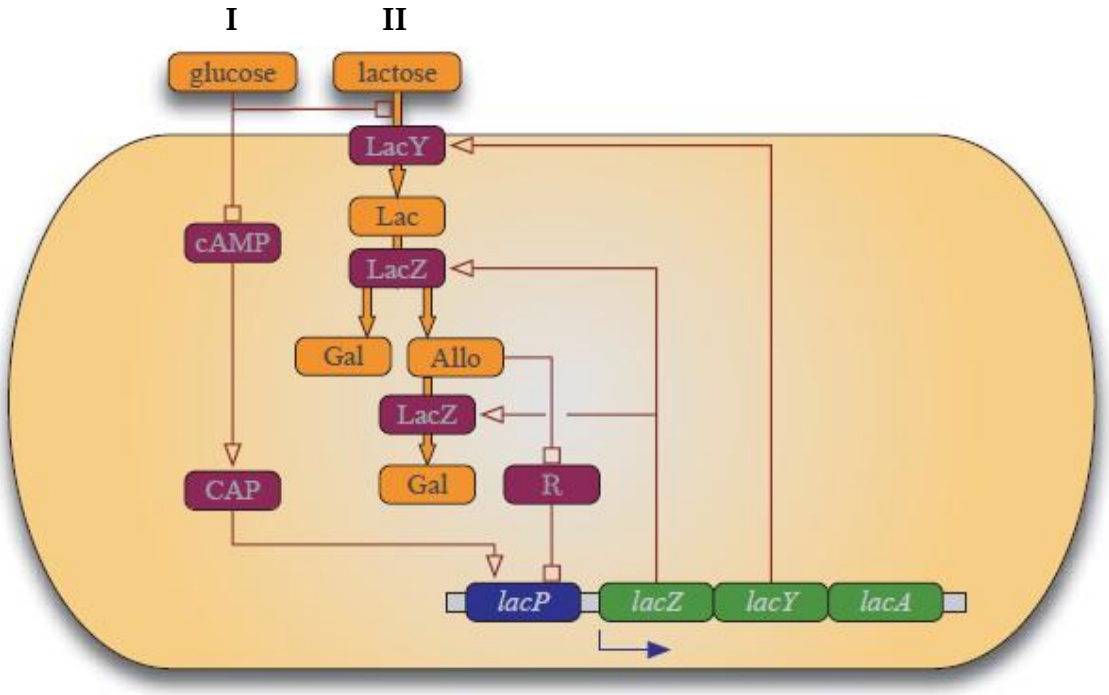

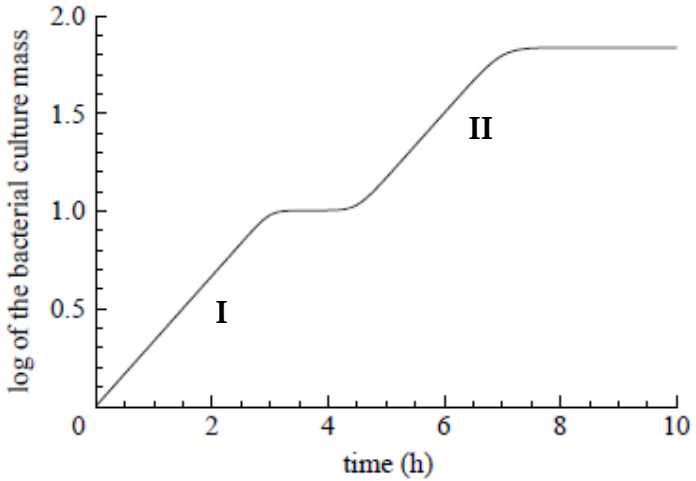

Monod, 1941
Jacob & Monod, 1961

Osbudak, 2004
Santillán, 2008

Μηχανισμός της καταβολικής καταστολής (catabolite repression)

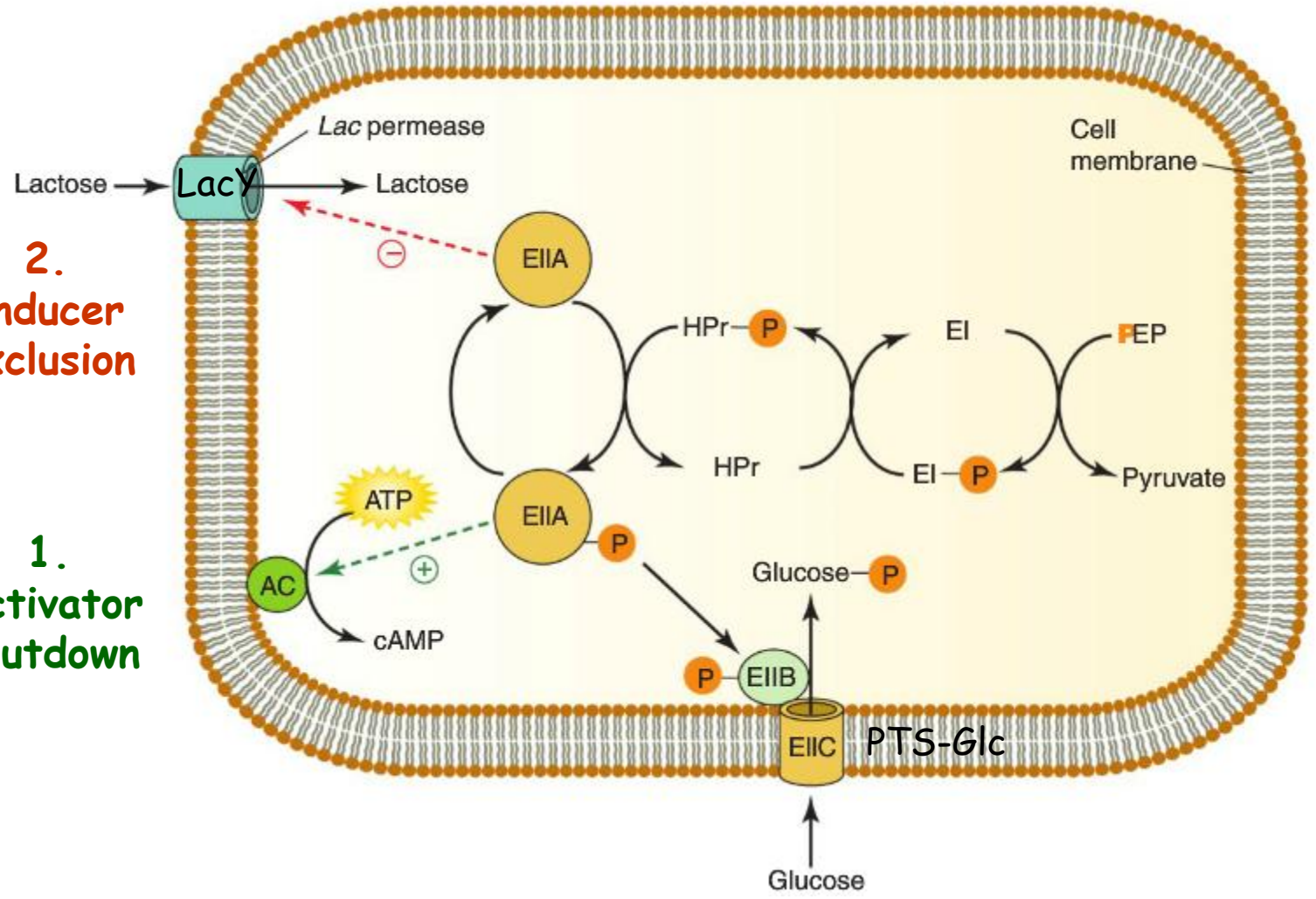

Tropp B.E., Principles of Molecular Biology-2014 Chapter 12:bacterial transcription

«Πρώτος διαμεμβρανικός μεταφορέας» που αποδείχθηκε ότι λειτουργεί χρησιμοποιώντας τη διαβάθμιση πρωτονίων

H. Ronald Kaback

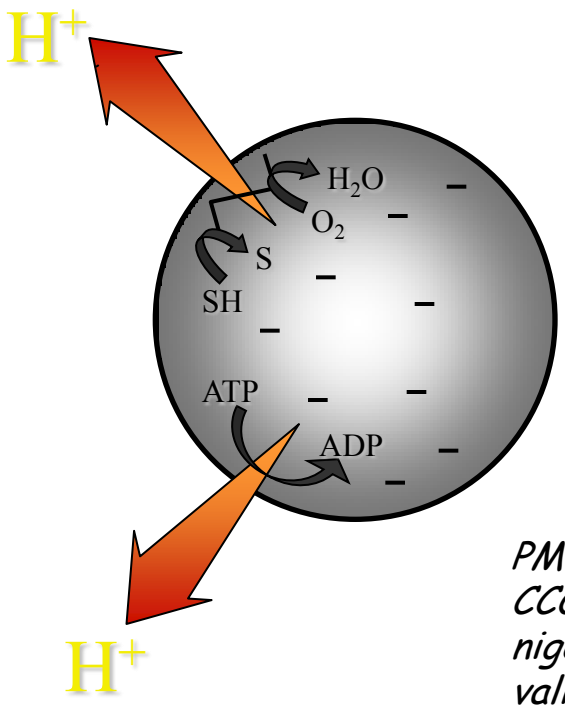

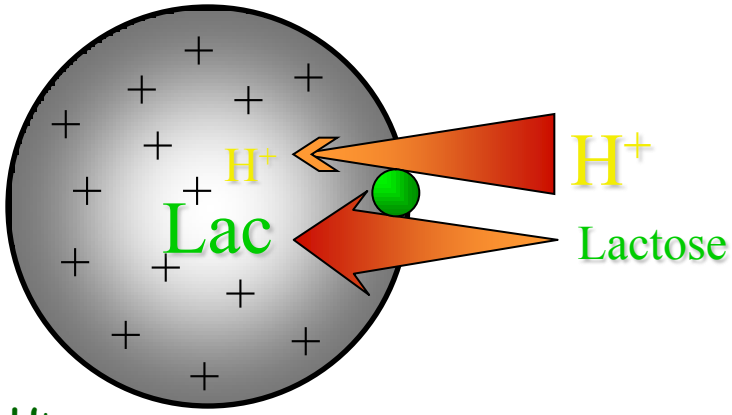

PMS/Ascorbate $\Delta\mu H^+$
CCCP, FCCP $\Delta\mu H^+$
nigericin (H^+/K^+) ΔpH
valinomycin (K^+) $\Delta\Psi$

Mitcell, 1963
Kaback, 1971

right-side-out (RSO) membrane vesicles

Περμεάση λακτόζης

Ηλεκτροχημική διαβάθμιση πρωτονίων

Ηλεκτροχημική διαβάθμιση λακτόζης

Μπορεί να λειτουργήσει και αντίστροφα

right-side-out (RSO) membrane vesicles

1980s

«Πρώτος διαμεμβρανικός μεταφορέας» που υπερεκφράσθηκε, απομονώθηκε σε καθαρή μορφή και μελετήθηκε σε πρωτεολιποσωμάτια (PLs)

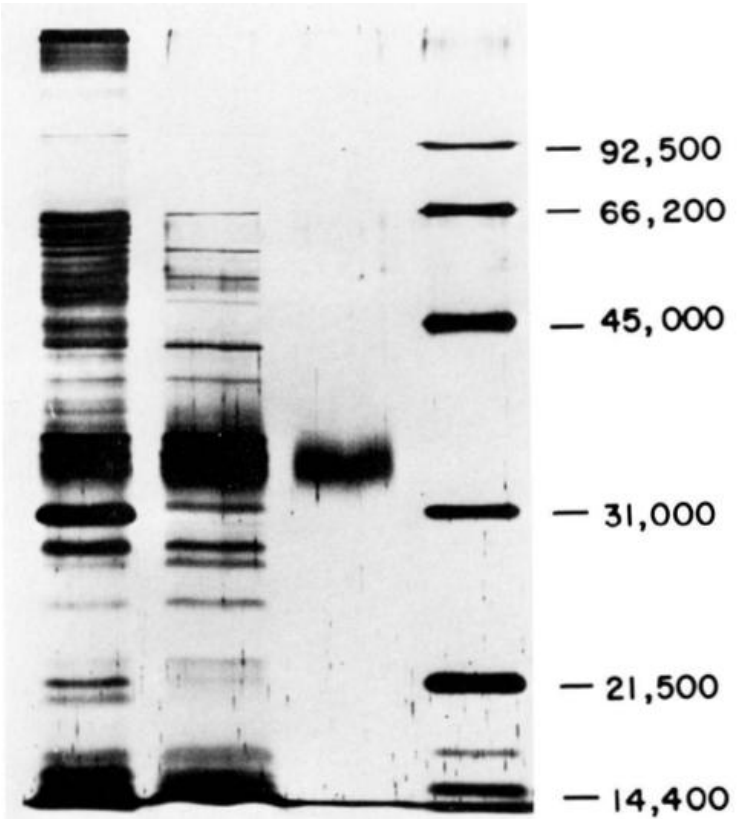

Newman et al., 1981

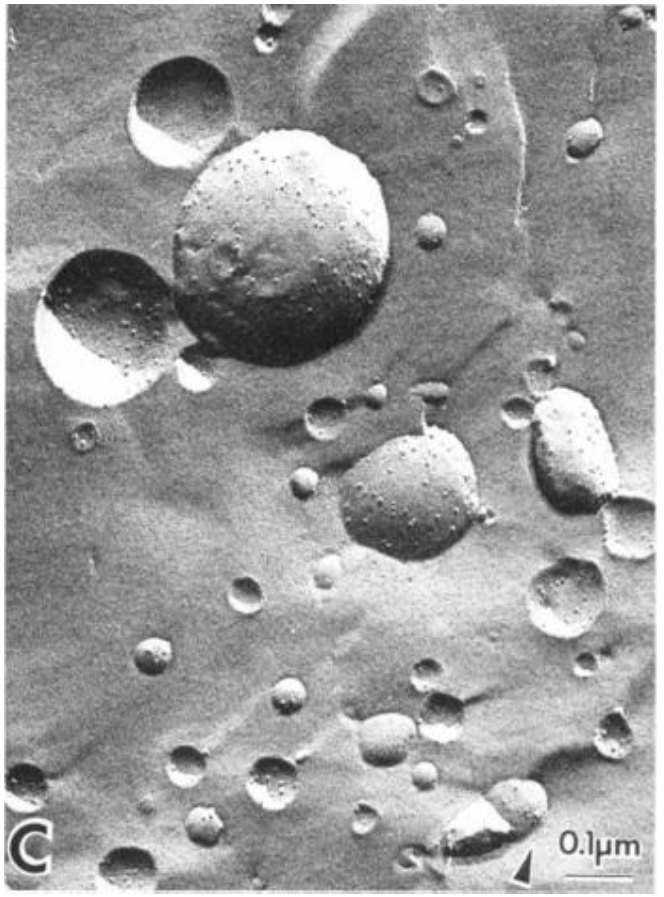

Costello et al., 1984

Περμεάση λακτόζης

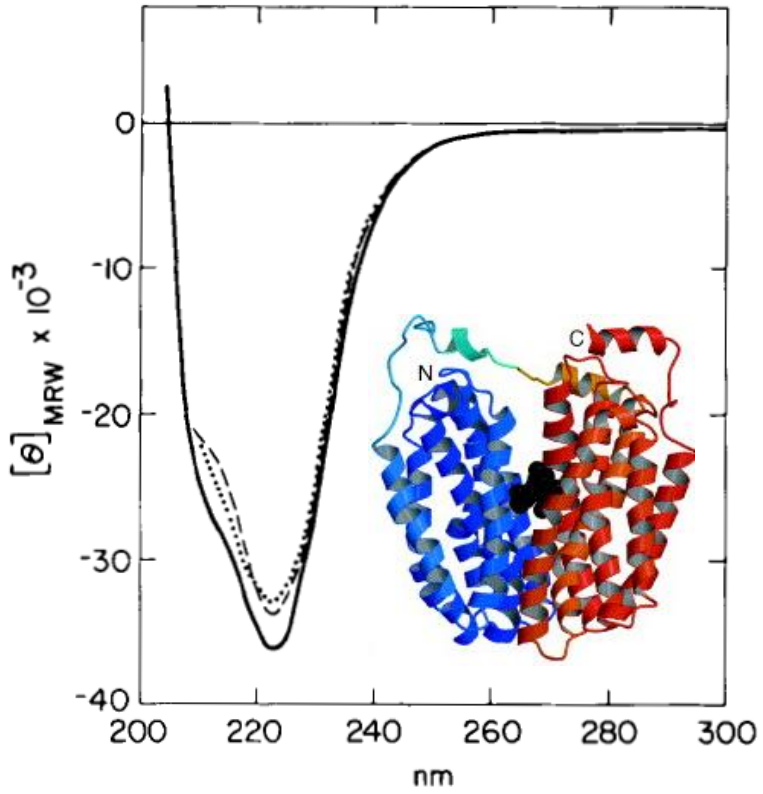

80% σε διαμόρφωση α-έλικας (12 TMs) (CD, διάλυμα DDM)

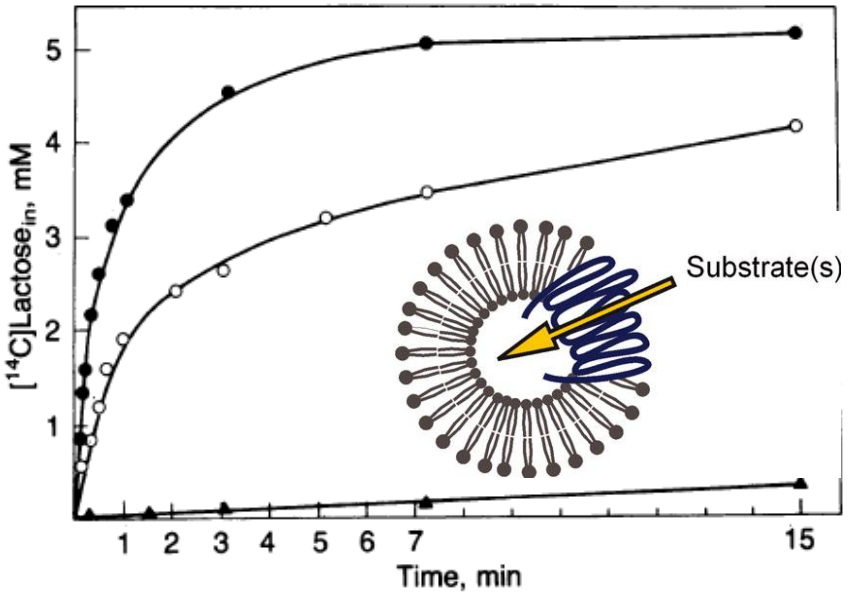

Πλήρως λειτουργική μετά από ανασύσταση σε PLs (διευκολυνόμενη διάχυση λακτόζης)

Foster et al., 1983

Viitanen et al., 1984

«Πρώτος διαμεμβρανικός μεταφορέας» που μελετήθηκε αναλυτικά ως προς τις σχέσεις δομής-λειτουργίας του με μεταλλαξιγένεση

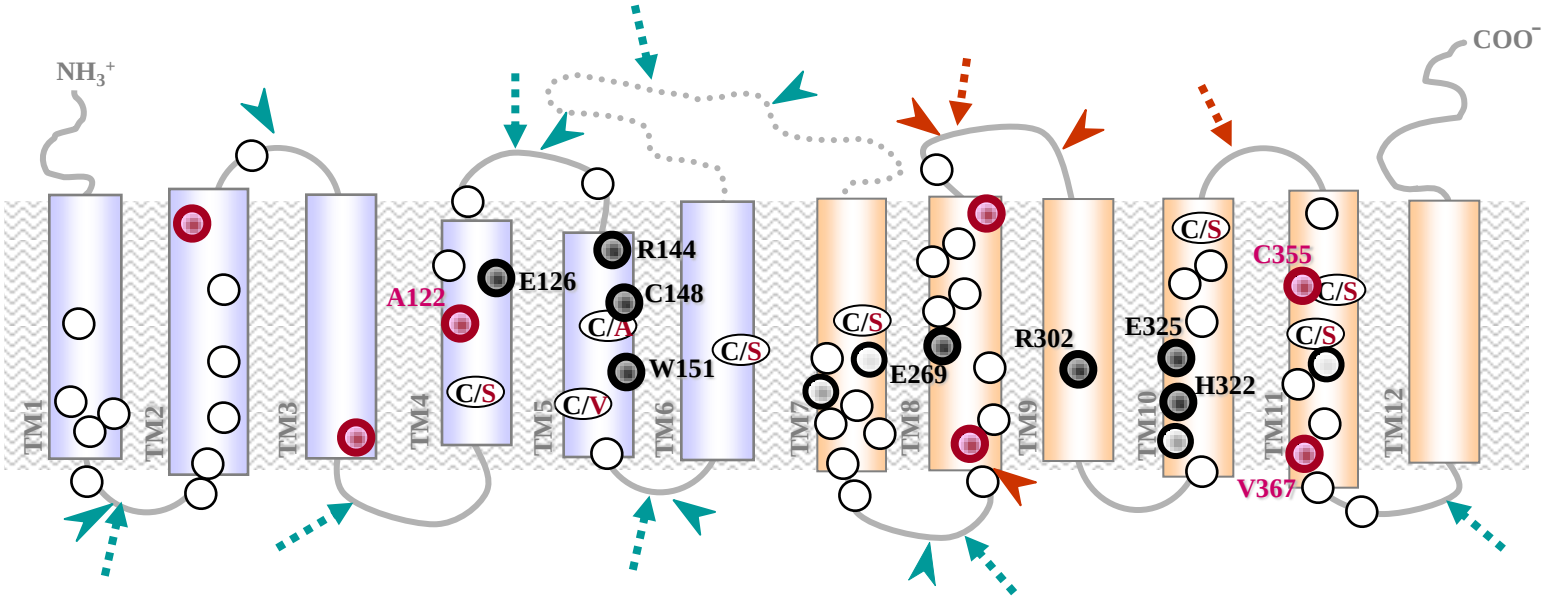

LacY

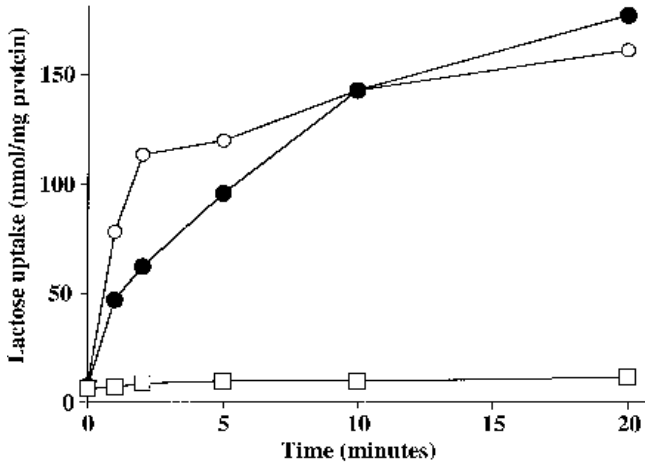

wild-type
split N6-C6

N6 alone
C6 alone

Bibi & Kaback, 1990

Kaback et al., 2001

Frillingos, 2013

«Πρώτος διαμεμβρανικός μεταφορέας» που μελετήθηκε αναλυτικά ως προς τις σχέσεις δομής-λειτουργίας του με μεταλλαξιγένεση

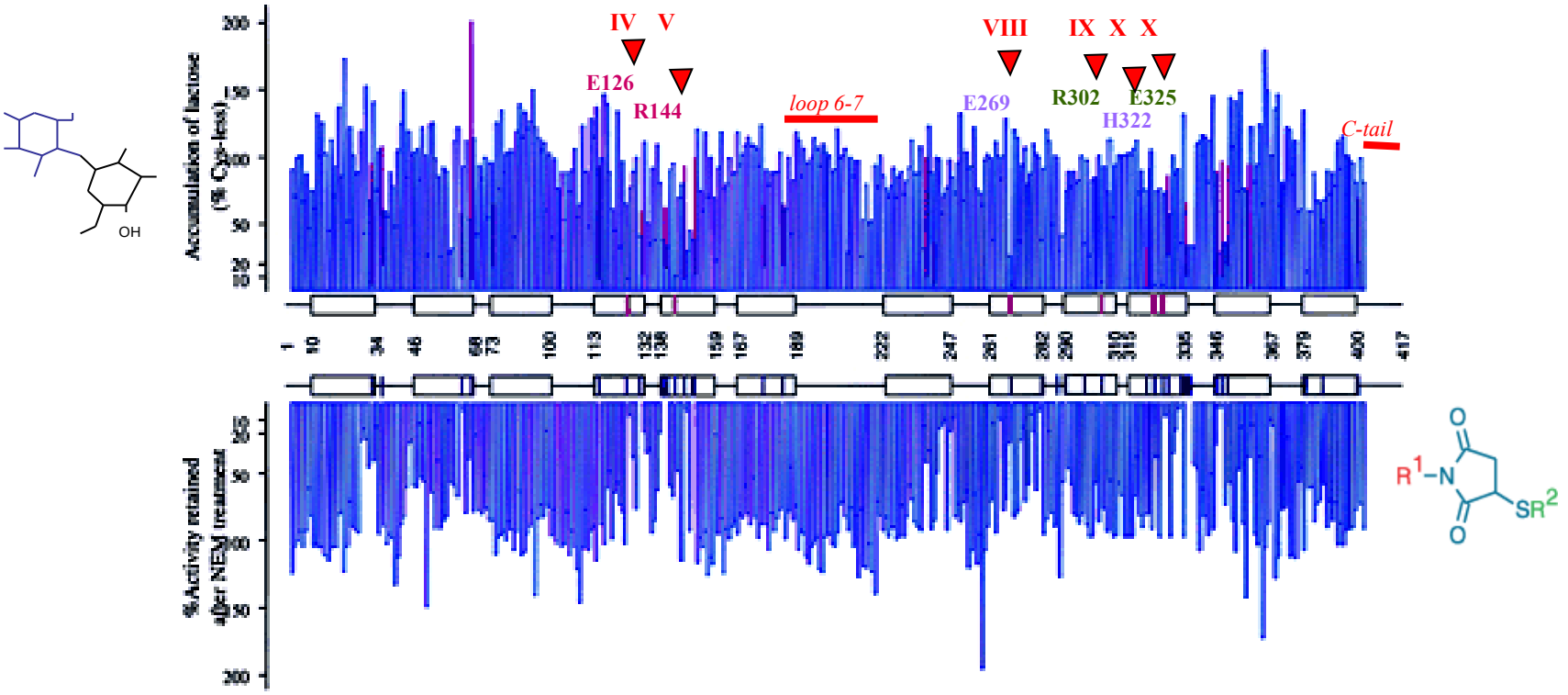

Μεταλλαξιγένεση κυστεϊνικής σάρωσης: δύο επίπεδα ανάλυσης (γενετική τροποποίηση DNA – ειδική χημική τροποποίηση πρωτεΐνης)

Frillingos et al., 1998

Μεταλλαξιγένεση κυστεϊνικής σάρωσης
Ανάλυση «προσβασιμότητας» κυστεϊνών (SCAM)

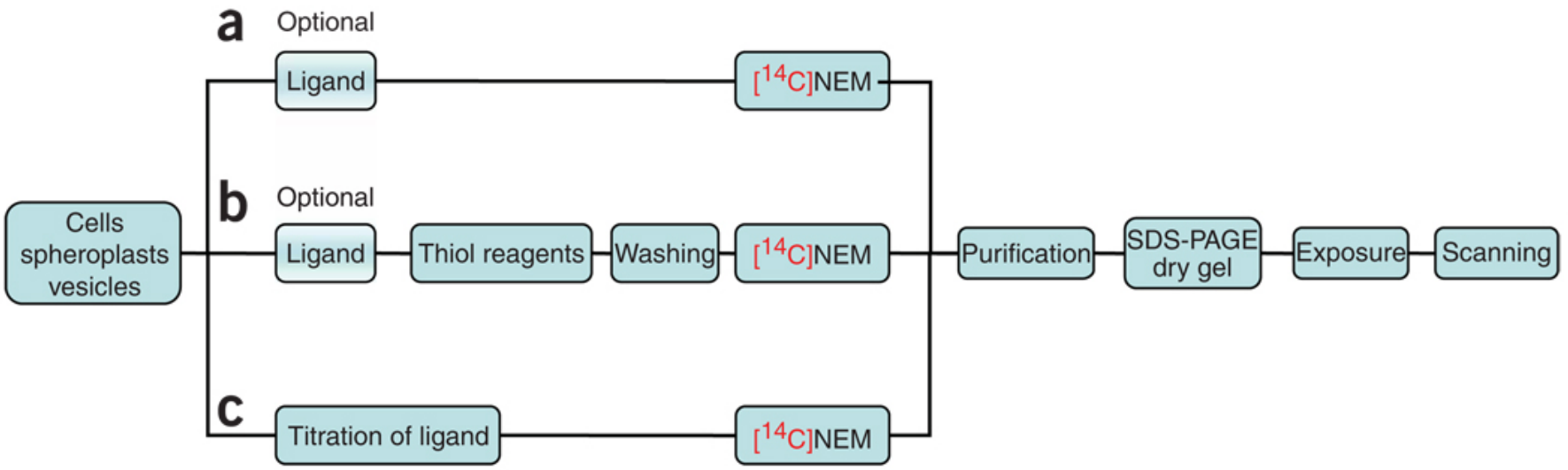

N-αιθυλμηλεϊμίδιο (NEM)
([^{14}C], αυτοραδιογραφία)

Frillingos & Kaback, 1996

Guan & Kaback, 2007

Μεταλλαξιγένεση κυστεϊνικής σάρωσης
Ανάλυση «προσβασιμότητας» κυστεϊνών (SCAM)

καθαρισμός σε μικρή κλίμακα
(αβιδίνη ή σφαιρίδια νικελίου)

Frillingos & Kaback, 1996

Guan & Kaback, 2007

Μεταλλαξιγένεση κυστεϊνικής σάρωσης
Ανάλυση «προσβασιμότητας» κυστεϊνών (SCAM)

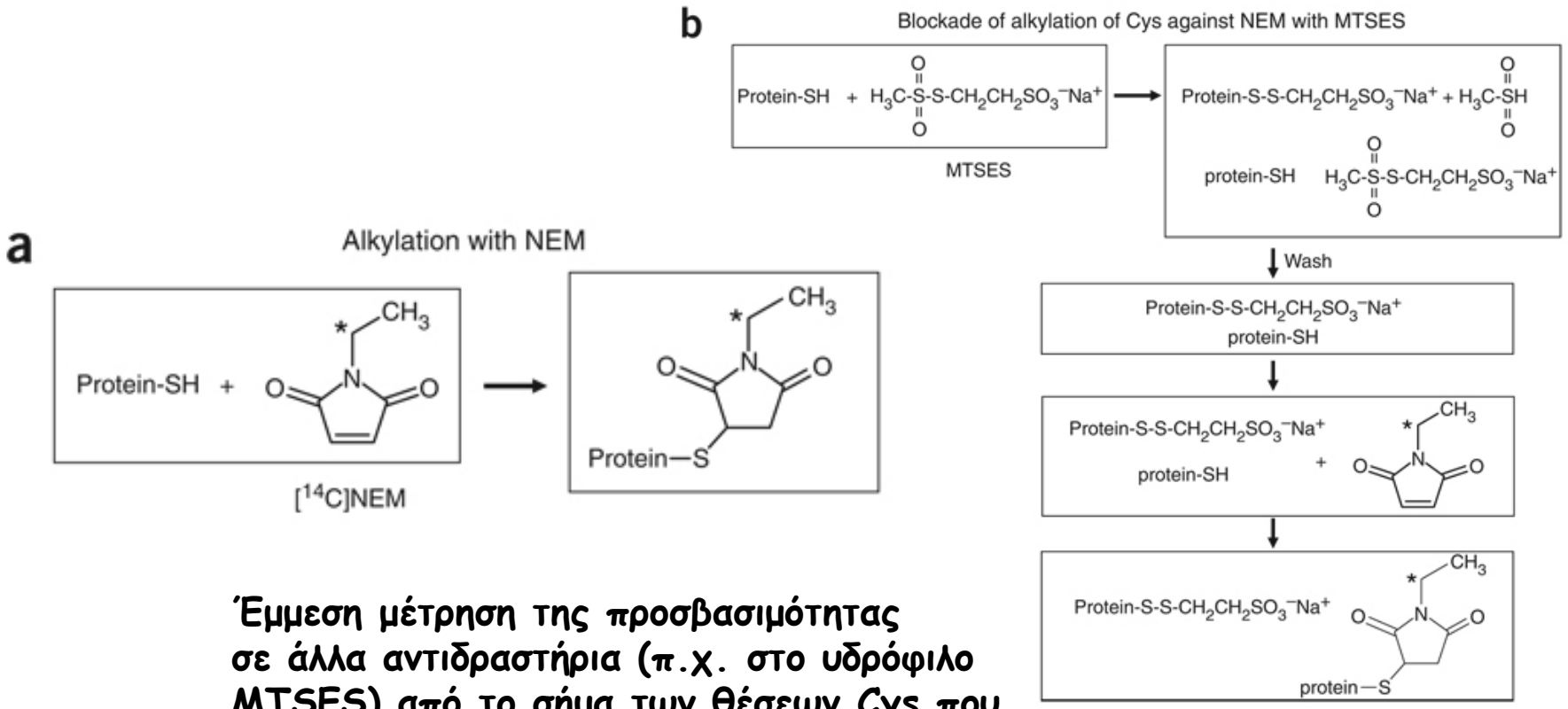

Έμμεση μέτρηση της προσβασιμότητας σε άλλα αντιδραστήρια (π.χ. στο υδρόφιλο MTSES) από το σήμα των θέσεων Cys που παραμένουν ελεύθερες και στη συνέχεια αντιδρούν με [^{14}C]NEM

Frillingos & Kaback, 1996

Guan & Kaback, 2007

Μεταλλαξιγένεση κυστεϊνικής σάρωσης
Ανάλυση «προσβασιμότητας» κυστεϊνών (SCAM)

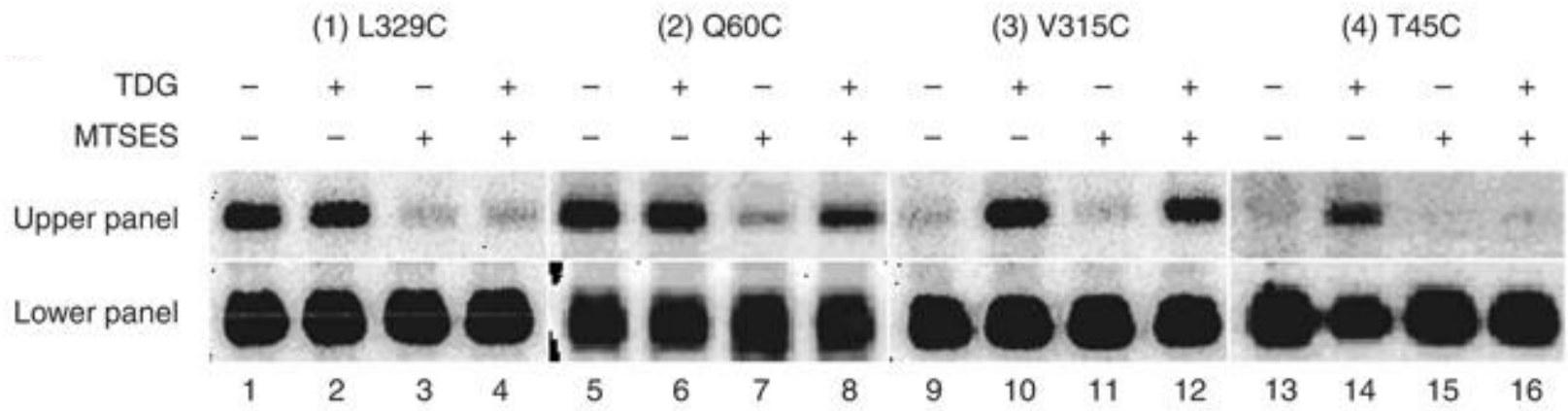

Αντίδραση με MTSES : Μειωμένο σήμα [^{14}C]NEM όταν έχει προηγηθεί επώαση με το MTSES
Ομαλοποίηση έναντι του συνολικού ποσού της περμεάσης στο δείγμα (loading)

Frillingos & Kaback, 1996

Guan & Kaback, 2007

Ανάλυση «προσβασιμότητας» (SCAM) με το φθορίζον TMRM

A

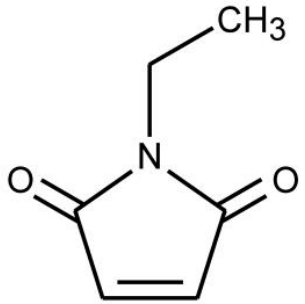

B

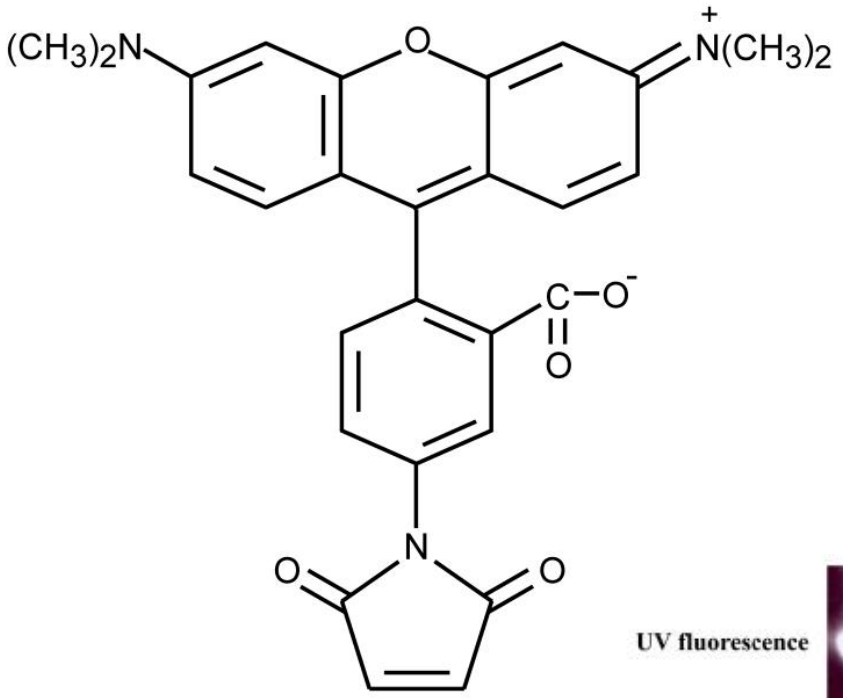

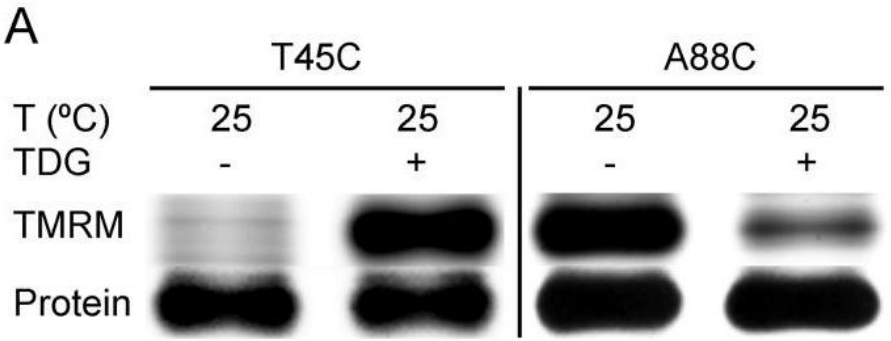

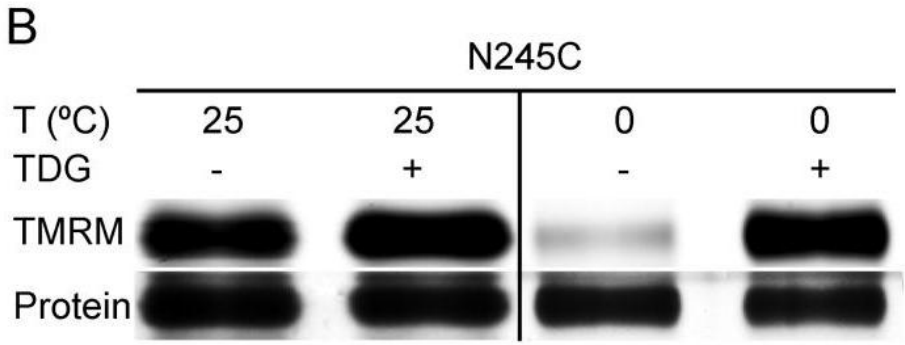

Μηλεϊμίδιο τετραμεθυλοροδαμίνης (TMRM) (φθορισμός, απευθείας σήμα)

Nie et al., 2007

A second, chemical "mutagenesis" on the background of the first, site-directed genetic mutagenesis

Interpretations of alkylation-sensitive single-Cys mutants

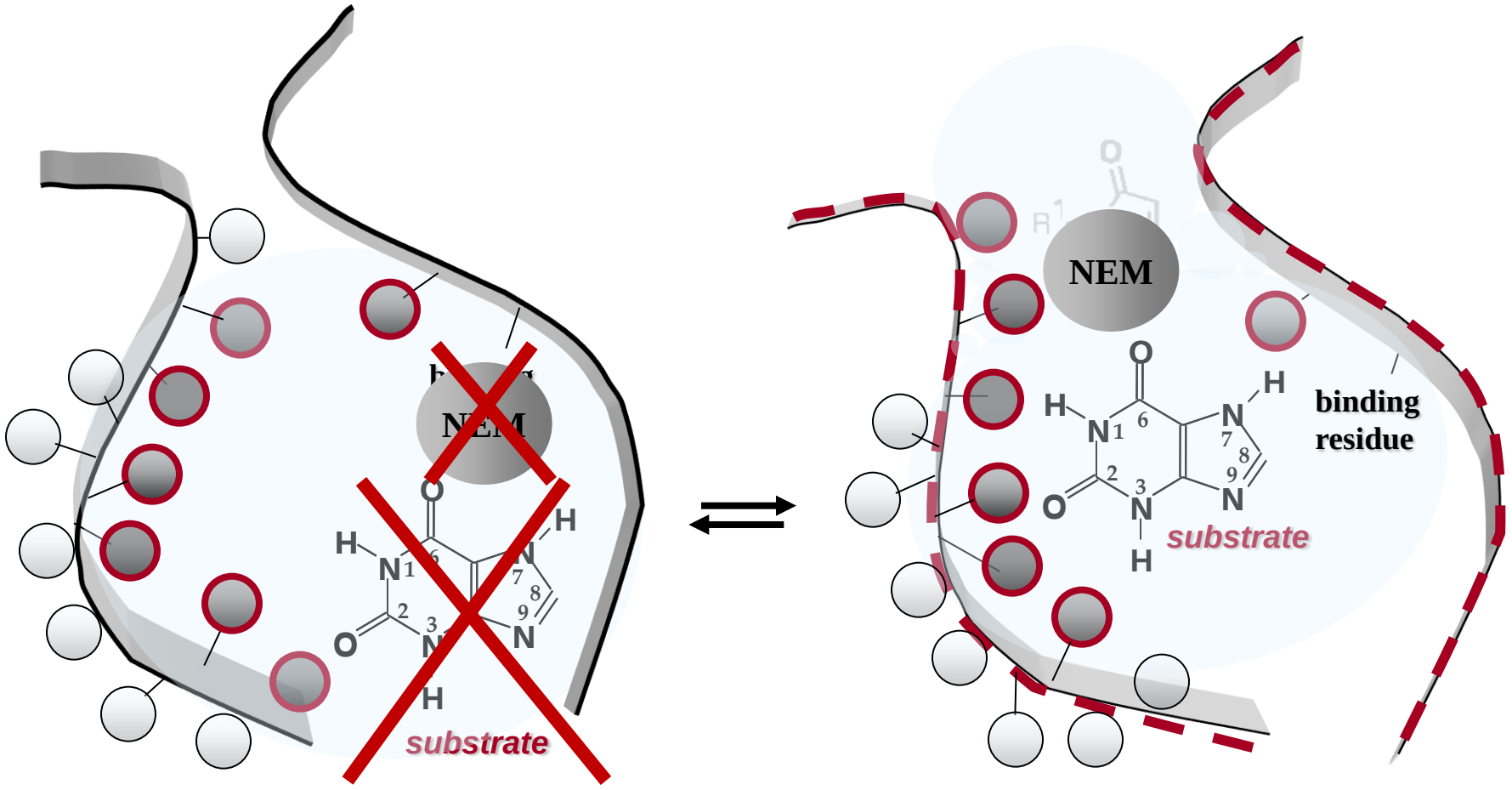

Steric hindrance (incompatible with substrate binding)

Conformation bottleneck (substrate-induced change)

Frillingos (2012) *Int. J. Bioch. Mol. Biol.* 3, 250-272

Coupling codon changes (genetic) with further amino-acid modifications (chemical) for structure-function analysis

1. Ala-scanning *vs.* Cys-scanning approaches
2. Cysteine; SH-modification reagents (*Molecular Probes*)
3. Probing the site microenvironment; conformation *dynamics*
4. Fluorescence; cross linking; hydrophobic/hydrophilic probes
5. Other side chains; carboxylic (carbodiimide), tryptophan (NBS)

Frillingos *et al.* (1998) *FASEB J.* 12, 1281-1299

Modification of a binding-site Glu to probe substrate binding after CNBr-cleavage and mass spectrometry (ESI-MS)

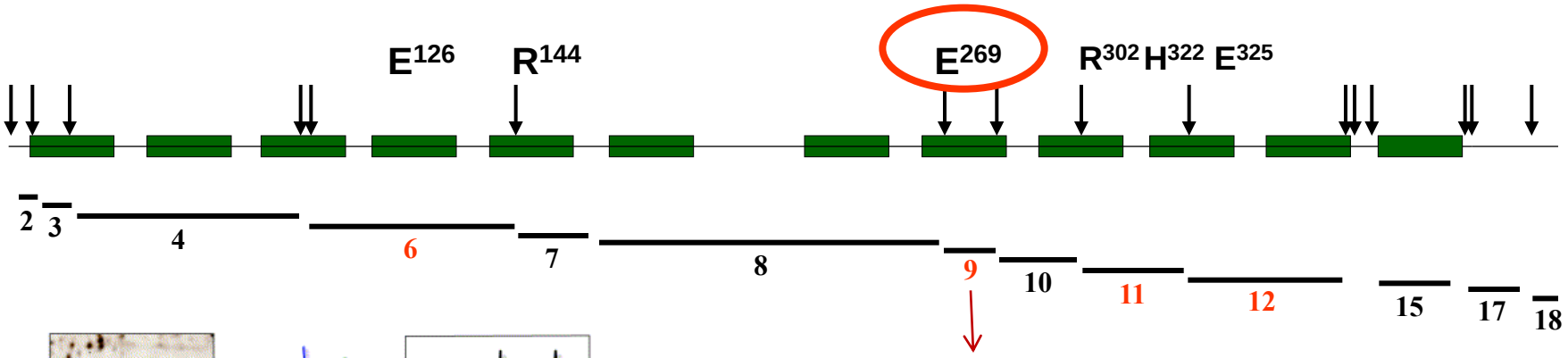

Peptide-9 : 899.7 Da (±126 Da)

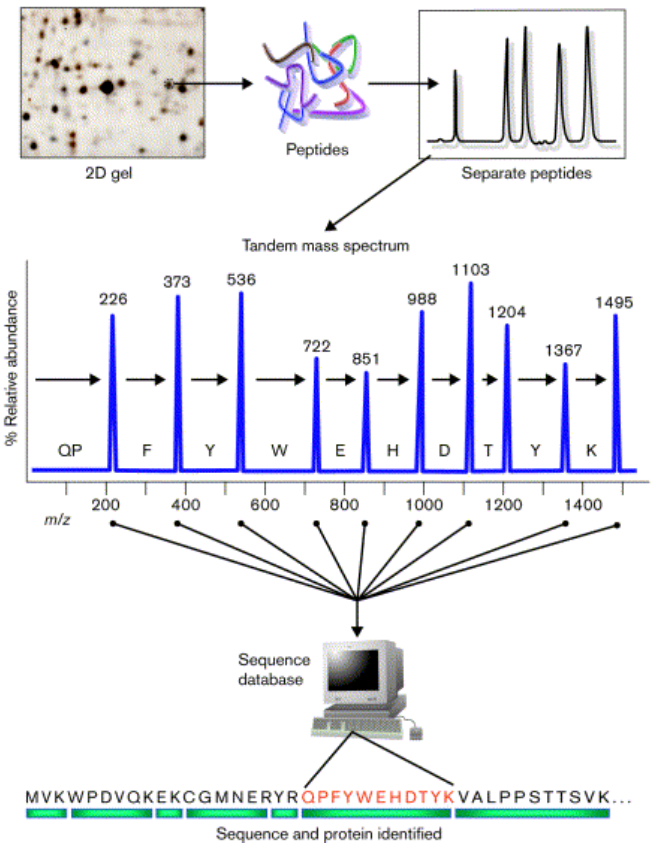

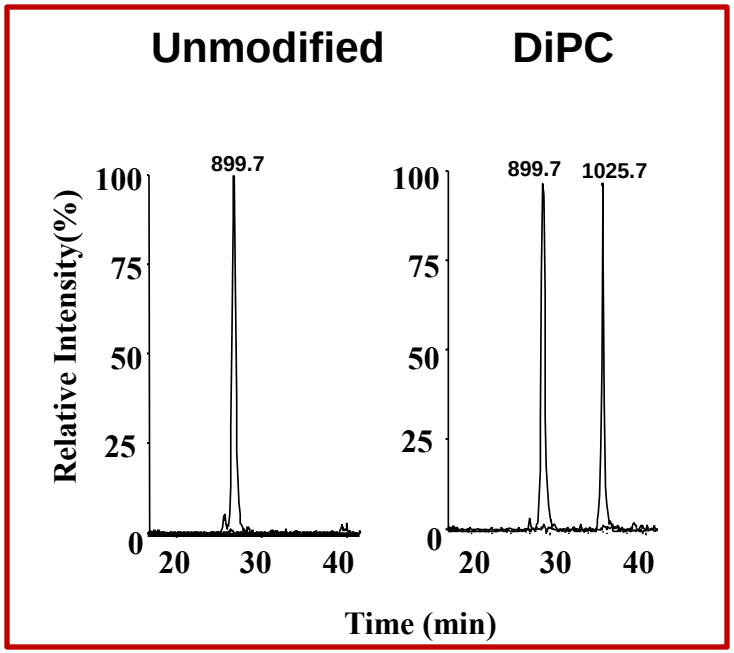

Weinglass *et al.* (2003) *EMBO J.* 22, 1467-77

Using fluorescence spectroscopy and FRET to detect/probe substrate binding and conformational alterations in a protein

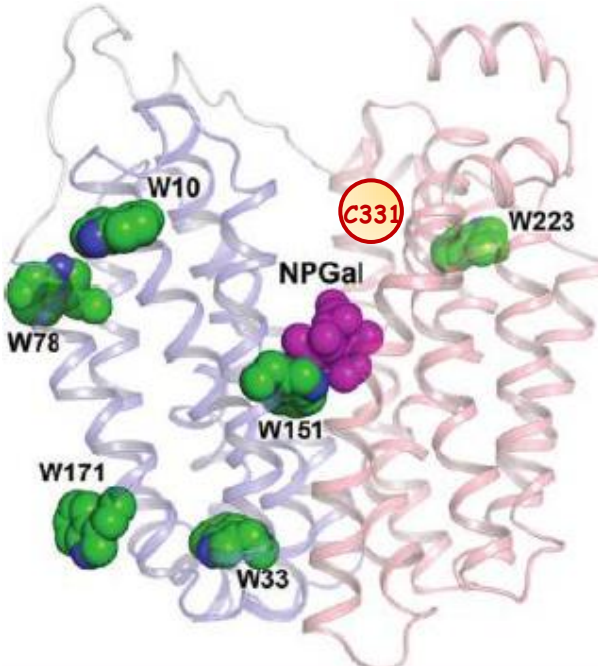

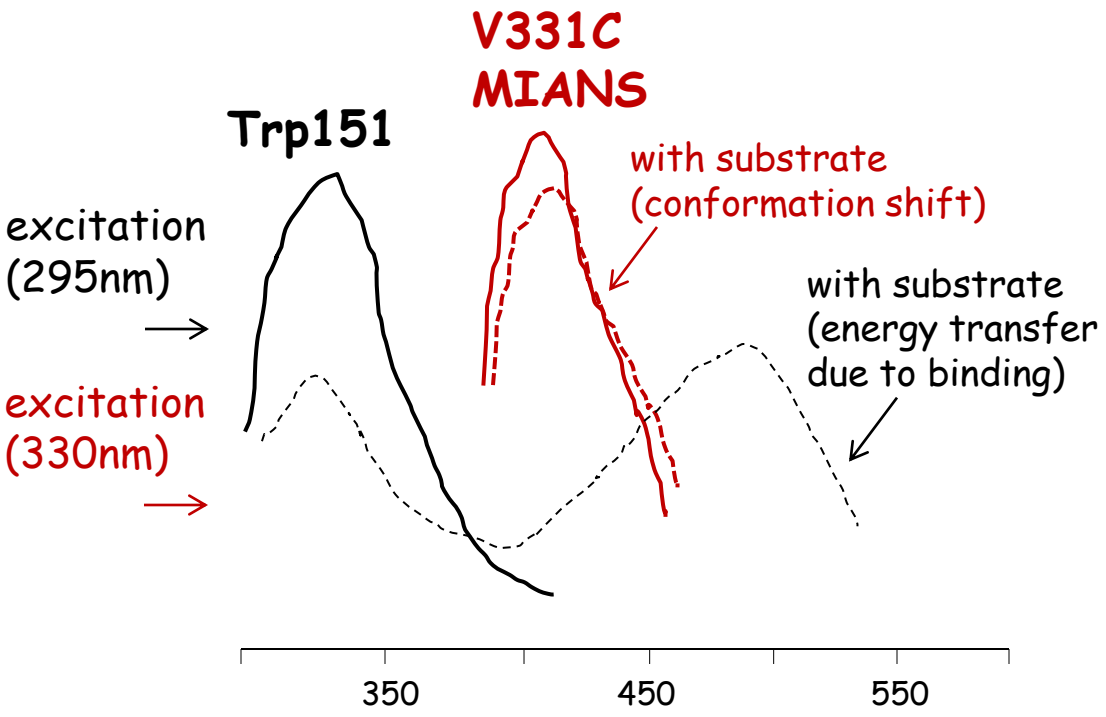

NPGal : substrate analog acting as a FRET acceptor from the binding-site Trp (W151) (exc. 295nm, em. 334nm, with FRET shift to 500nm)

Smirnova *et al.* (2006) *Biochemistry* 45, 15279-87

Titration of substrate binding in LacY; mechanistic insights

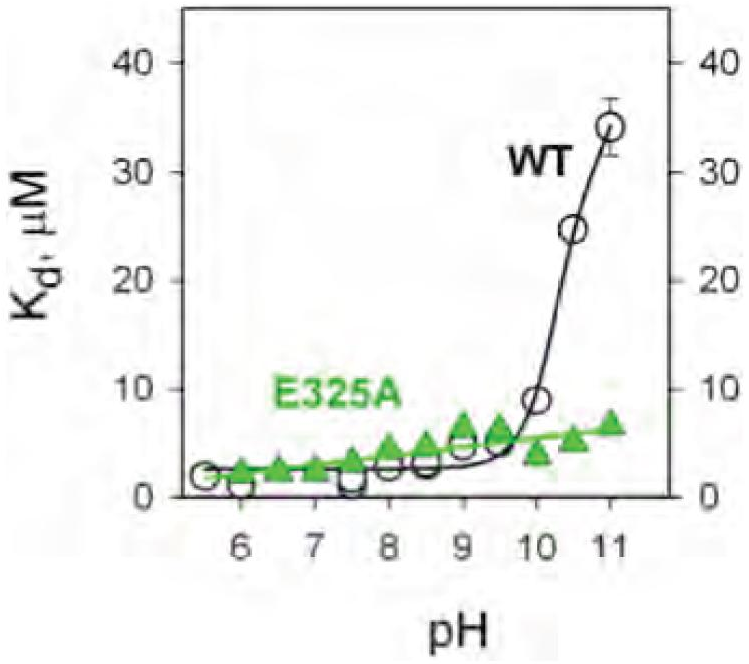

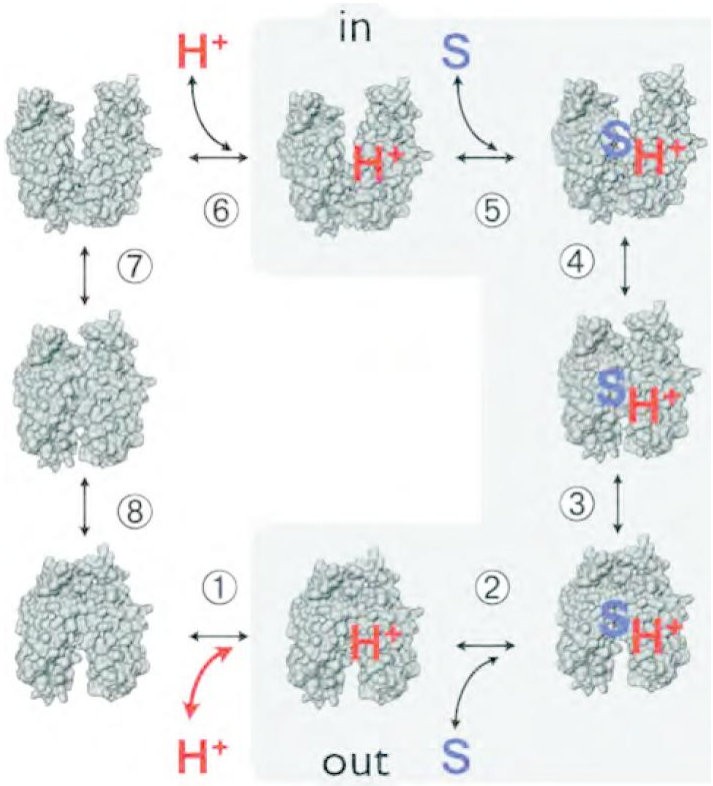

Kaback , 2015

Περμεάση λακτόζης

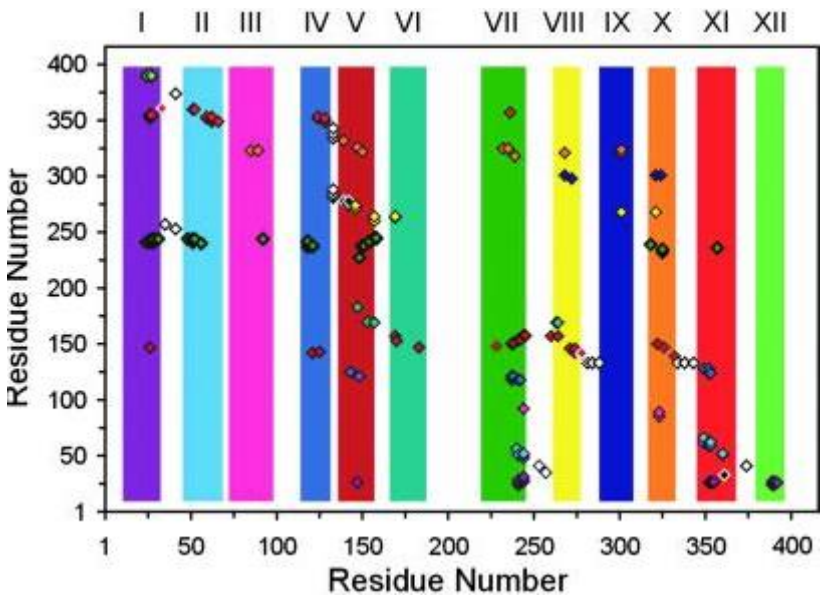

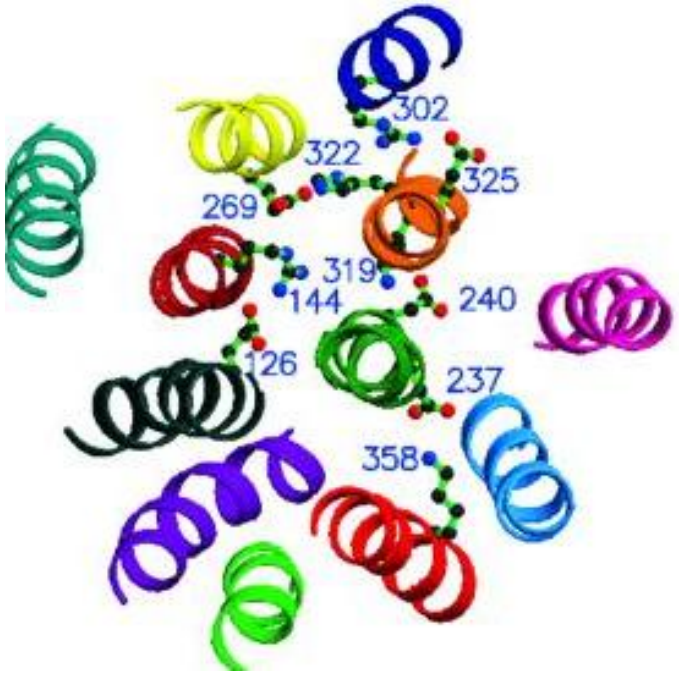

Ένα πρώτο μοντέλο οργάνωσης των διαμεμβρανικών α-ελίκων με βάση πειράματα διασύνδεσης Cys-Cys (cross-linking)

Sorgen et al., 2002

«Πρώτος διαμεμβρανικός μεταφορέας» δευτερογενούς τύπου (ιοντο-εξαρτώμενος) που αναλύθηκε με κρυσταλλογραφία

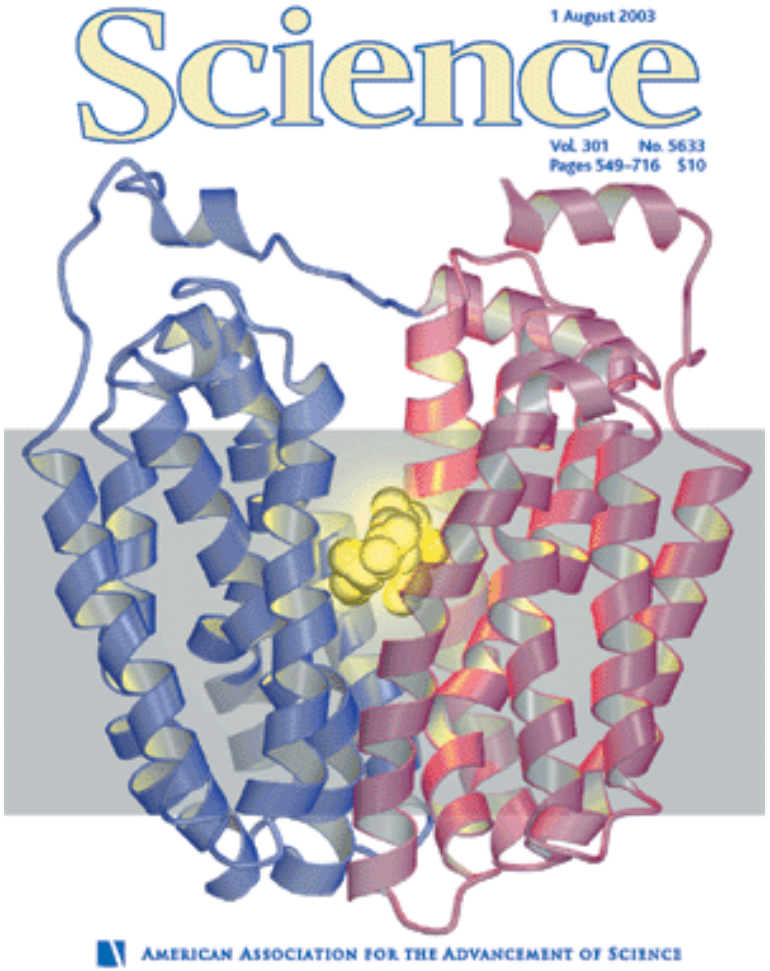

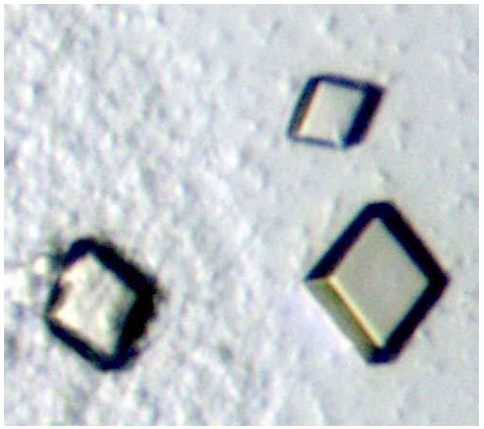

Abramson et al., 2003

Περμεάση λακτόζης

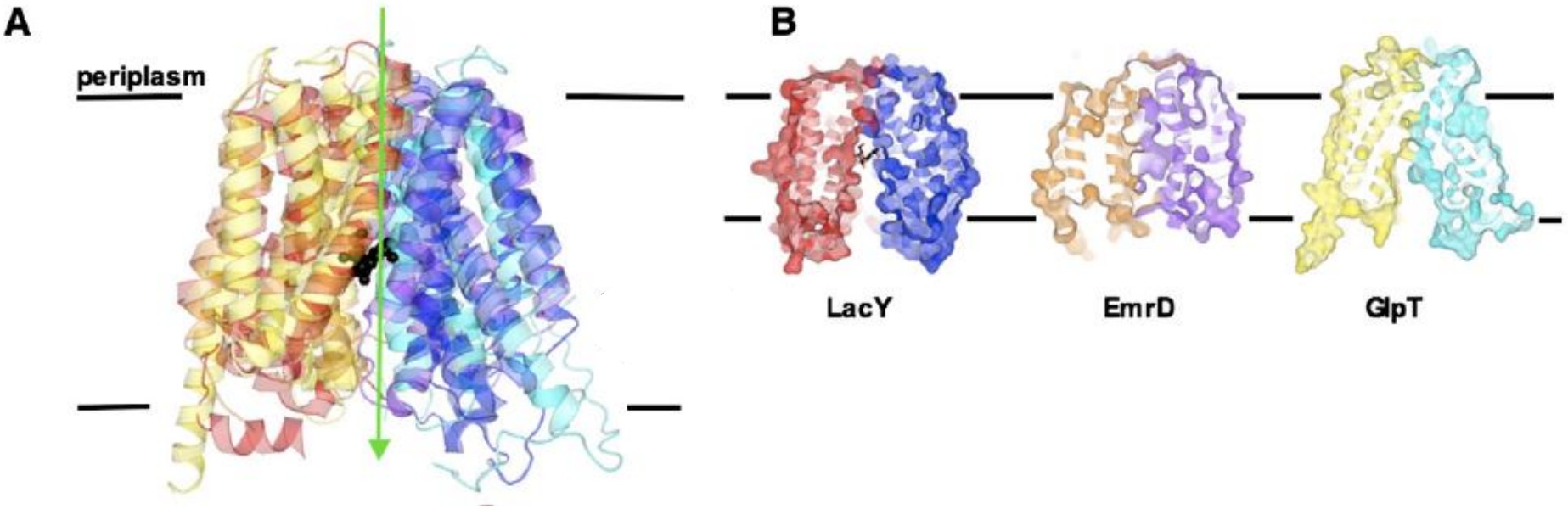

Δομικό-μηχανιστικό μοντέλο για >30% των μεταφορέων δευτερογενούς τύπου (υπεροικογένεια MFS)

Two domains

LacY

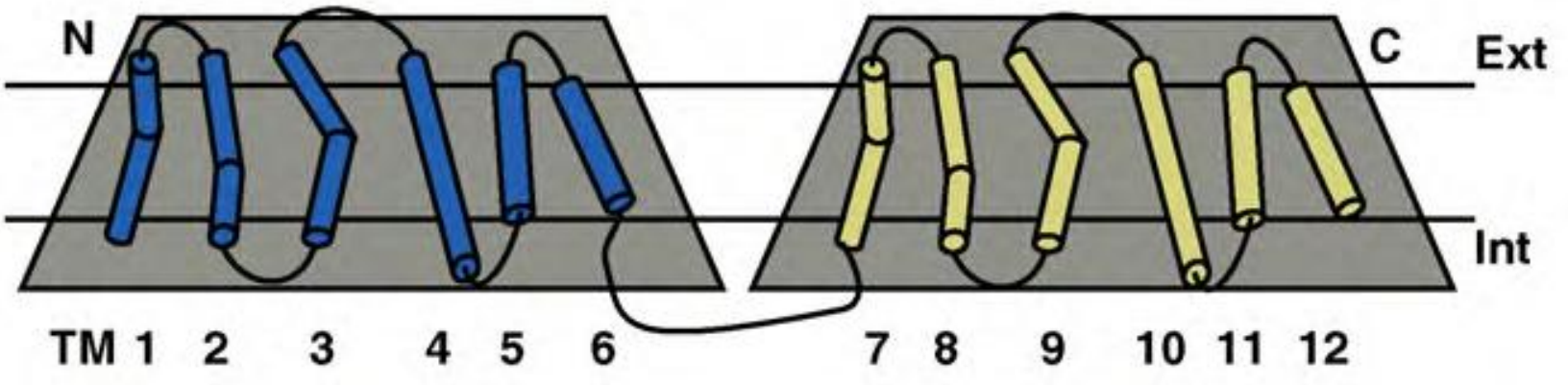

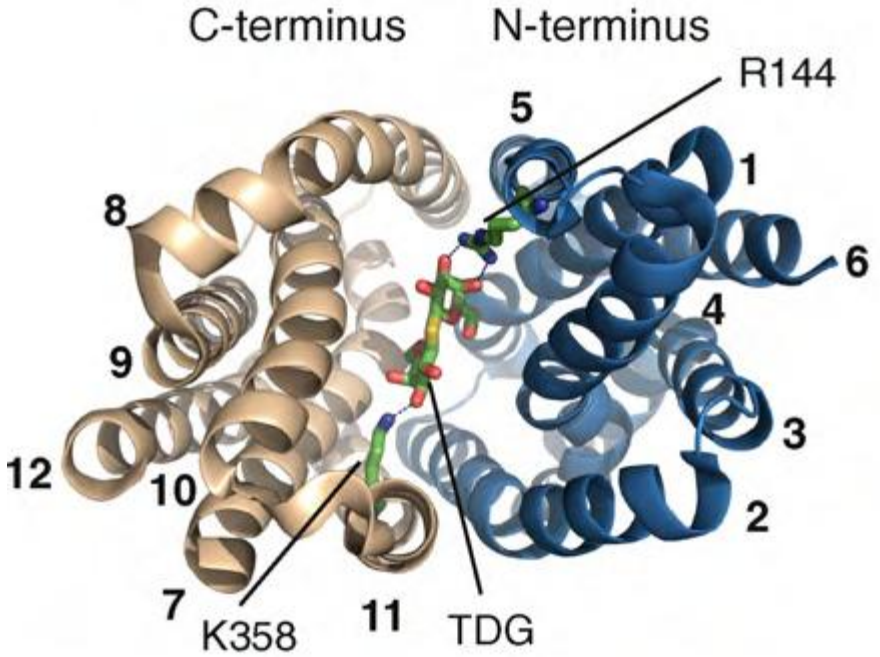

Boudker & Vernon, 2010

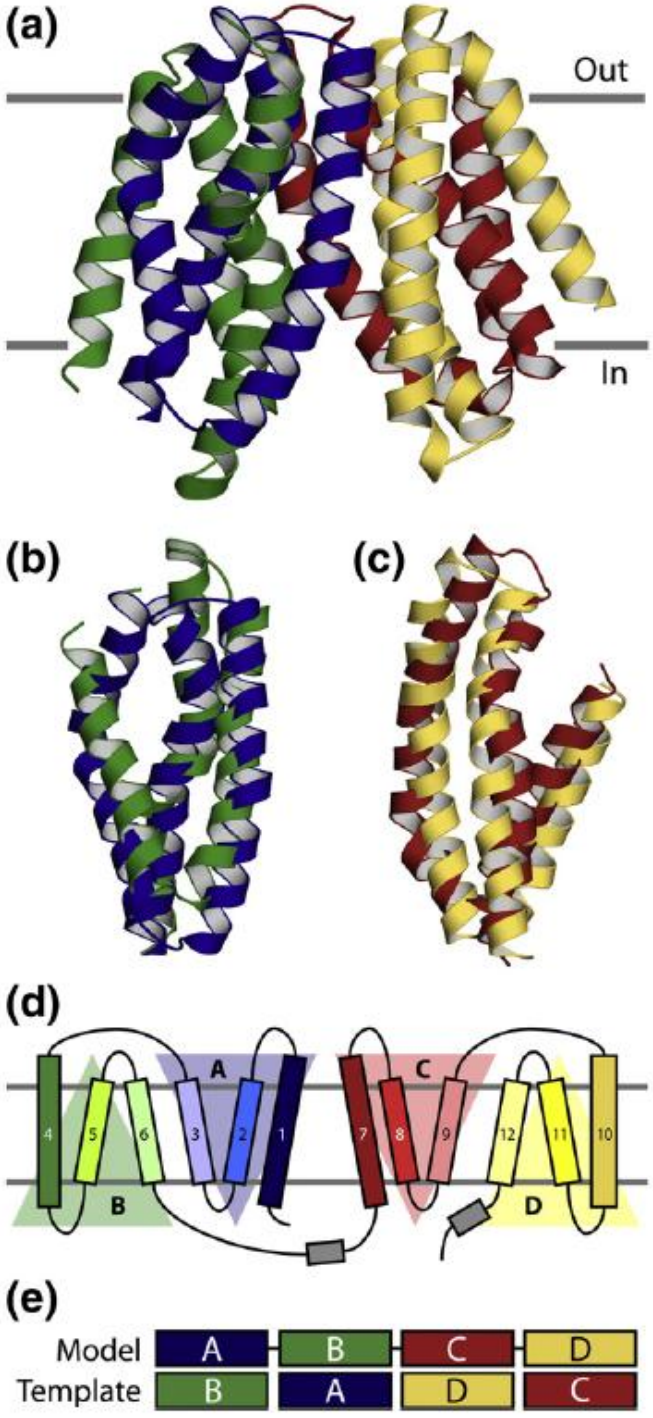

Radestock & Forrest, 2011

Two internally inverted repeats

Evolutionary mix and match with MFS transporters

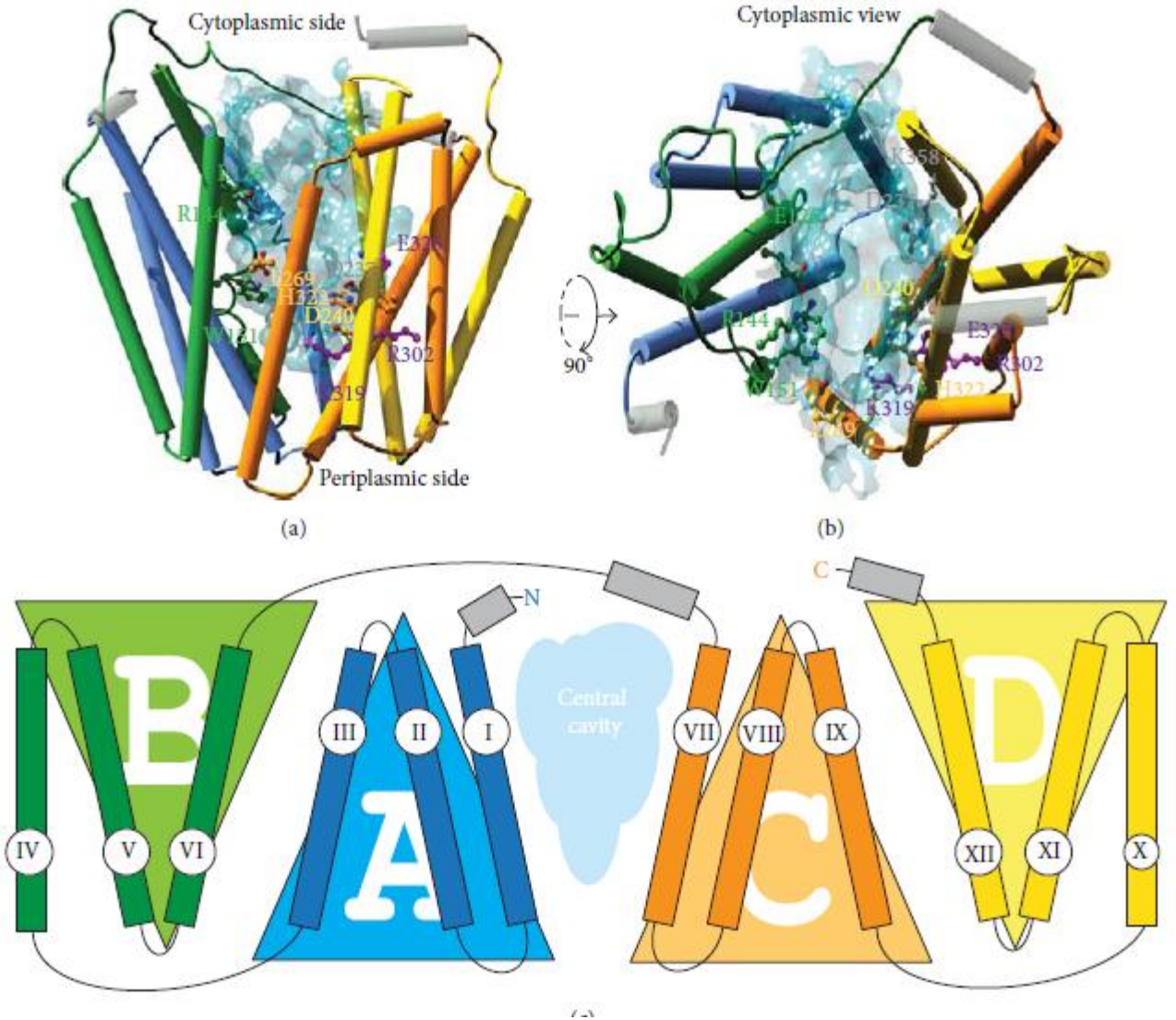

Madej, Adv. Biol. 2014

Evolutionary mix and match with MFS transporters

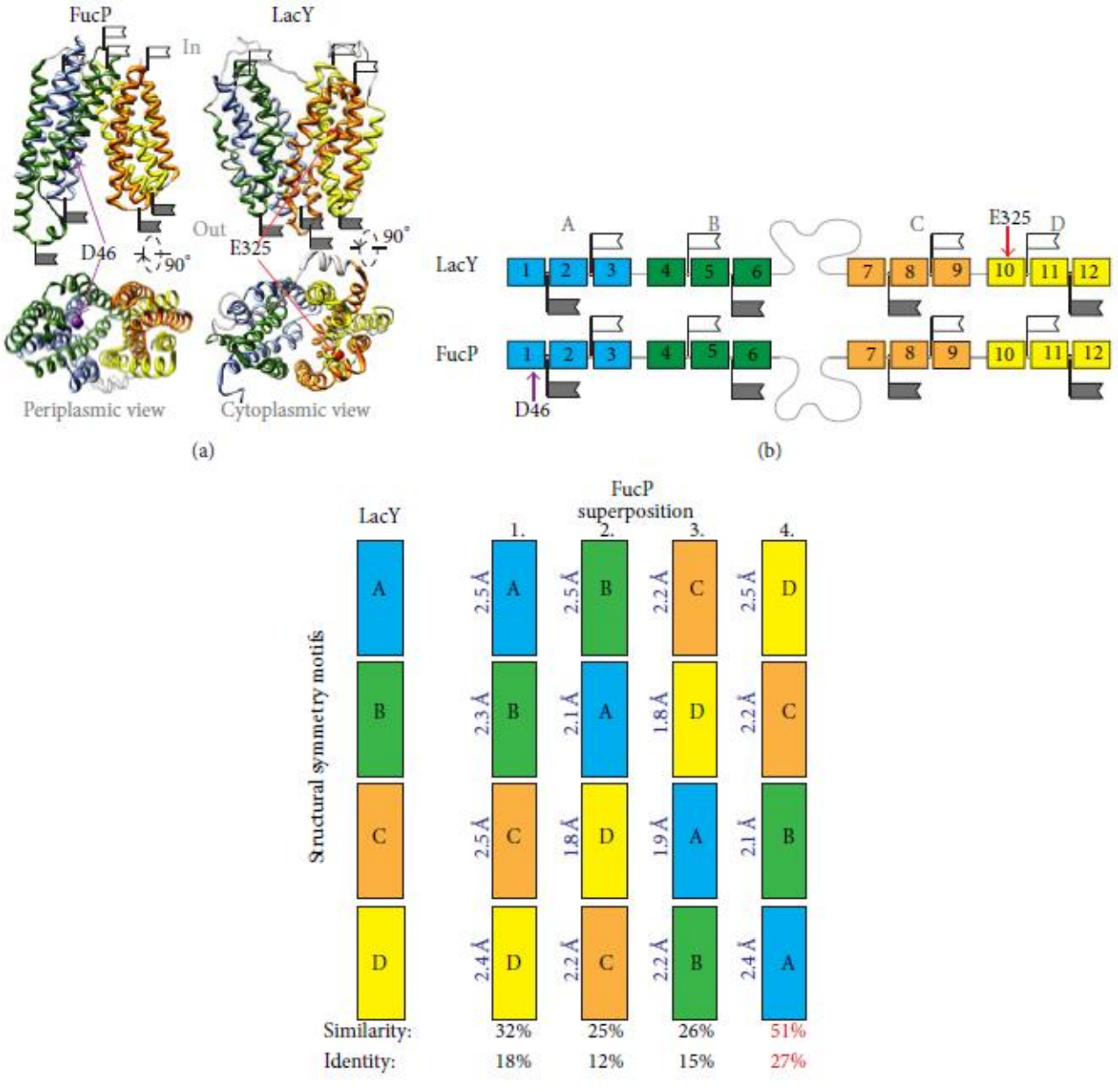

Madej, Adv. Biol. 2014

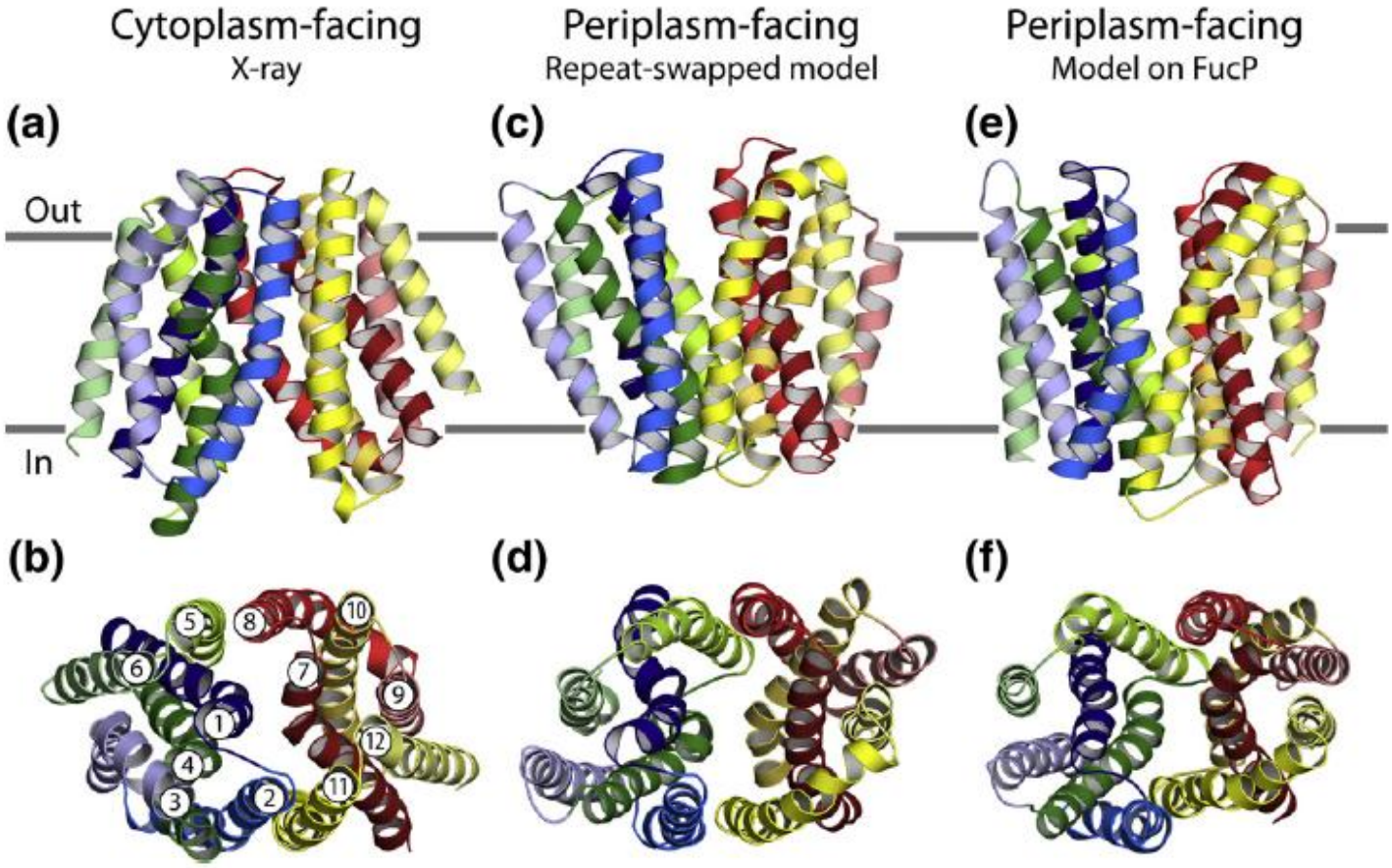

Radestock & Forrest, 2011

LeuT

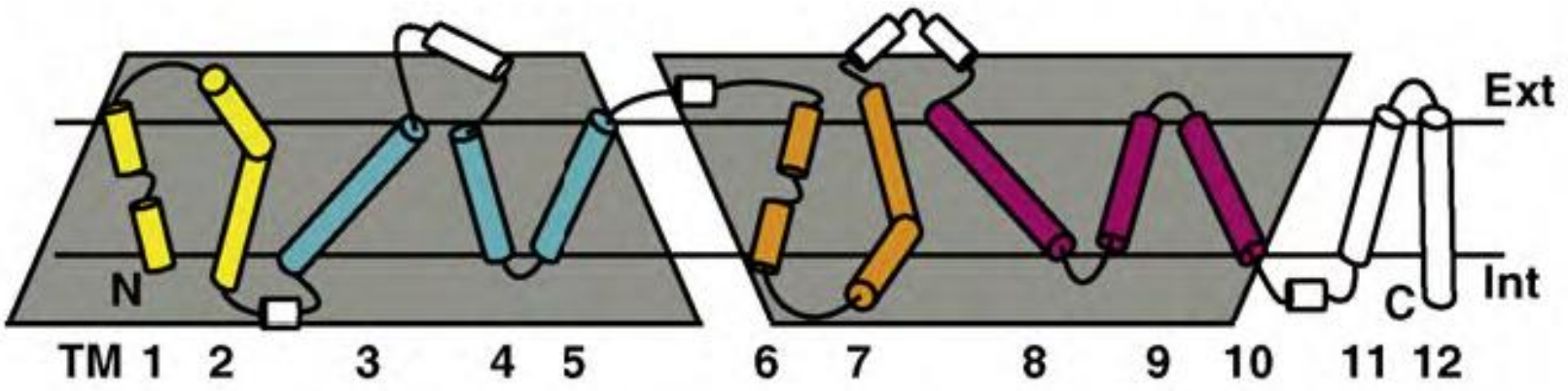

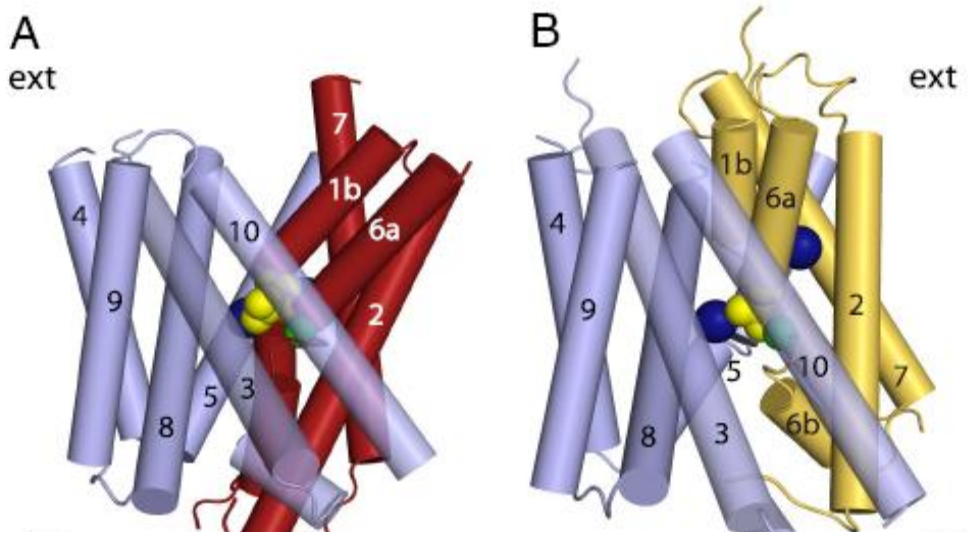

Δομικό-μηχανιστικό μοντέλο για >30% των μεταφορέων δευτερογενούς τύπου (οικογένειες NSS, SSS, APC, BCCT, NCS1)

Forrest et al., 2008

Boudker & Vernon, 2010

Evolutionary scenario

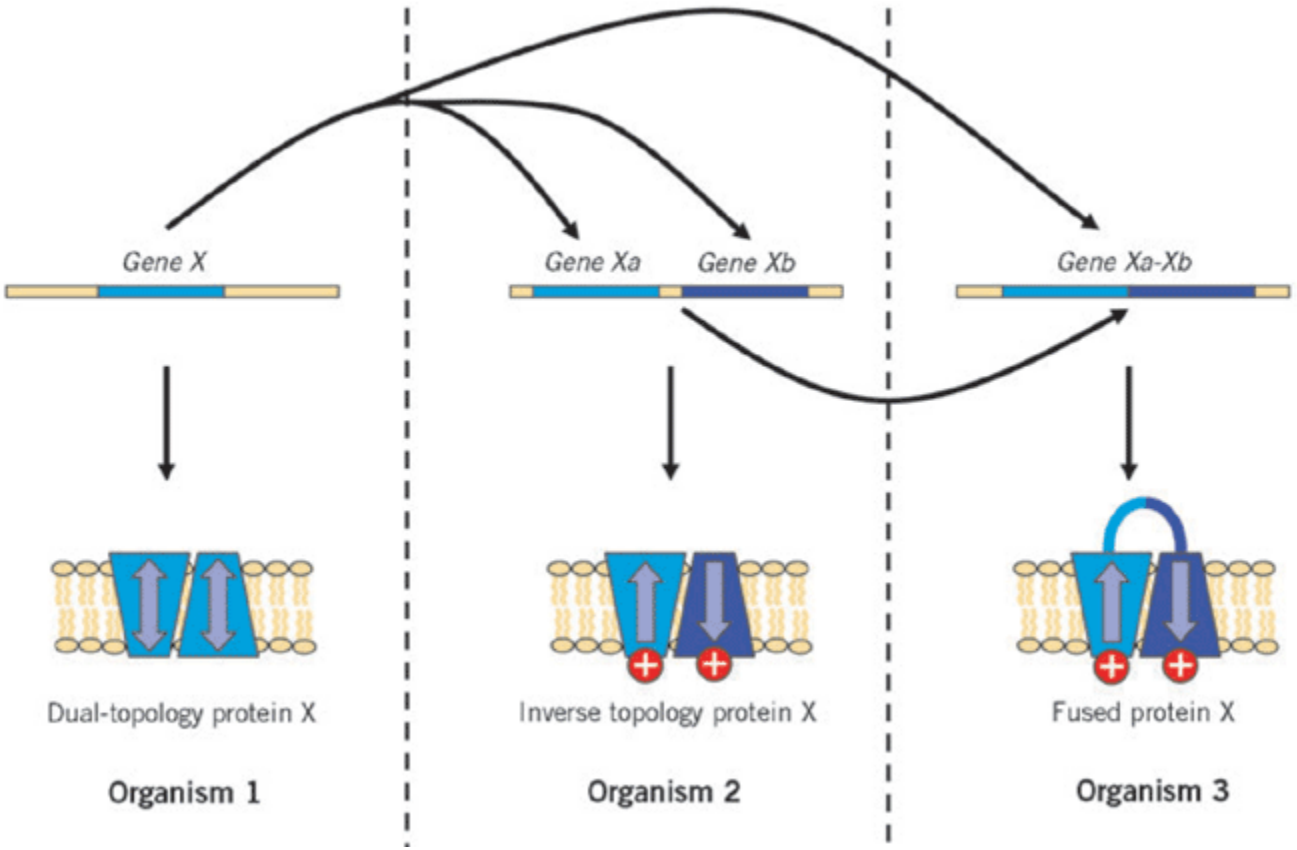

Rapp et al., *Science* 2007

Science. 2007 Mar 2;315(5816):1282-4. Epub 2007 Jan 25.

Comment in: Science. 2007 Mar 2;315(5816):1229-31.

Emulating membrane protein evolution by rational design.

Rapp M, Seppälä S, Granseth E, von Heijne G.
Center for Biomembrane Research, Department of Biochemistry and Biophysics, Stockholm University, SE-106 91 Stockholm, Sweden.

How do integral membrane proteins evolve in size and complexity? Using the small multidrug-resistance protein EmrE from Escherichia coli as a model, we experimentally demonstrated that the evolution of membrane proteins composed of two homologous but oppositely oriented domains can occur in a small number of steps: An original dual-topology protein evolves, through a gene-duplication event, to a heterodimer formed by two oppositely oriented monomers. This simple evolutionary pathway can explain the frequent occurrence of membrane proteins with an internal pseudo-two-fold symmetry axis in the plane of the membrane.
PMID: 17255477 [PubMed - indexed for MEDLINE]

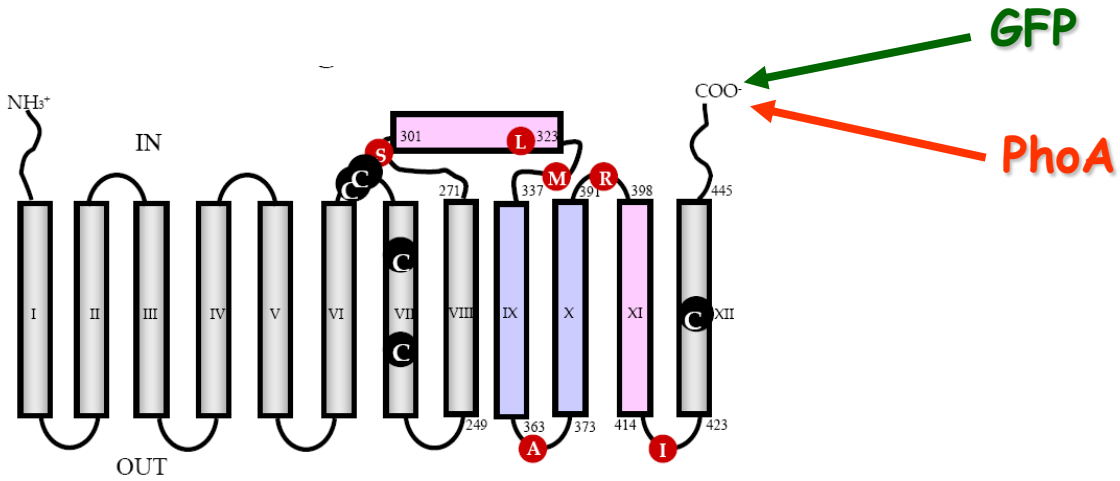

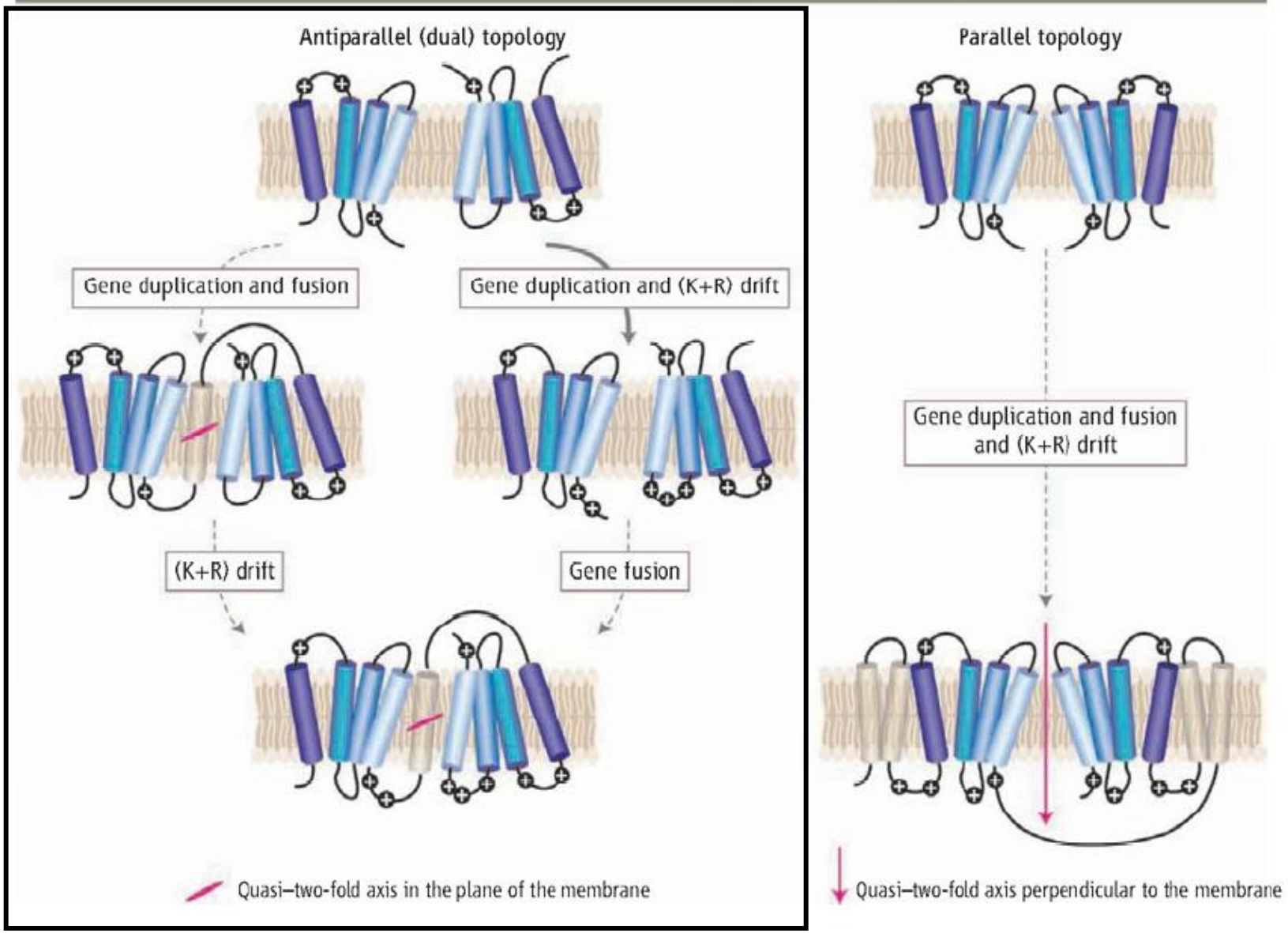

Plausible evolutionary paths. Membrane proteins with multiple homologous domains may have evolved through gene duplication, gene fusion, and drift events [bias to lysine (K) and arginine (R) residues in cytoplasmic regions of the protein]. The resulting proteins have similar domains with either antiparallel topologies (**bottom left**), or parallel topology (**bottom right**). Shaded cylinders depict additionally inserted transmembrane segments. Bold arrow indicates the evolutionary path simulated by Rapp *et al.* (*1*); dashed arrows indicate hypothetical events.

". . . the involvement of repeated structural elements is clearly an elegant and appealing solution to the problem of bringing the substrate into the binding site from one side of the membrane and allowing it to exit on the opposite side . . ."

Forrest et al., *BBA-Bioenergetics* 2010

Alternating access

Η ιδέα της «εναλλασσόμενης πρόσβασης» του κέντρου δέσμευσης των διαμεμβρανικών πρωτεϊνών ενεργού μεταφοράς (alternating access)

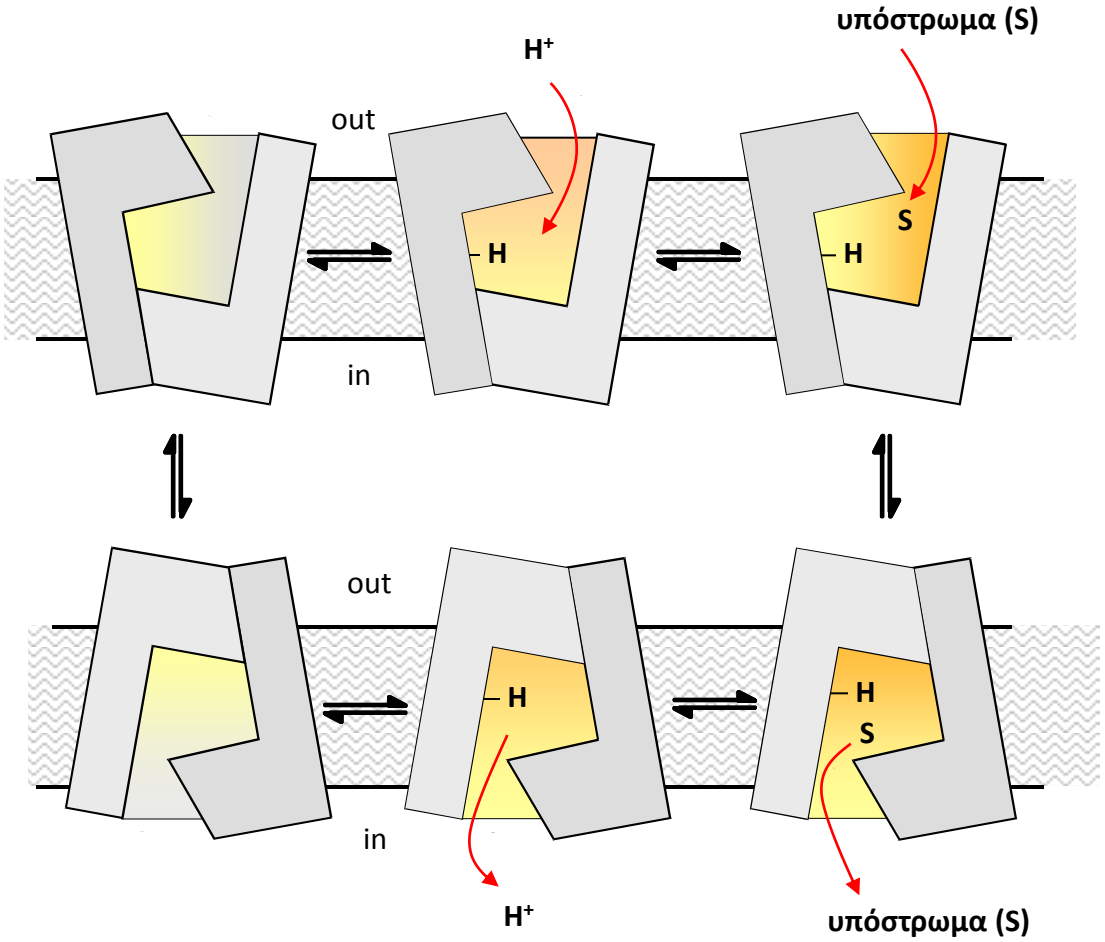

Widdas, 1952

Ο μηχανισμός της ενεργού μεταφοράς: Το μοντέλο «εναλλασσόμενης πρόσβασης»

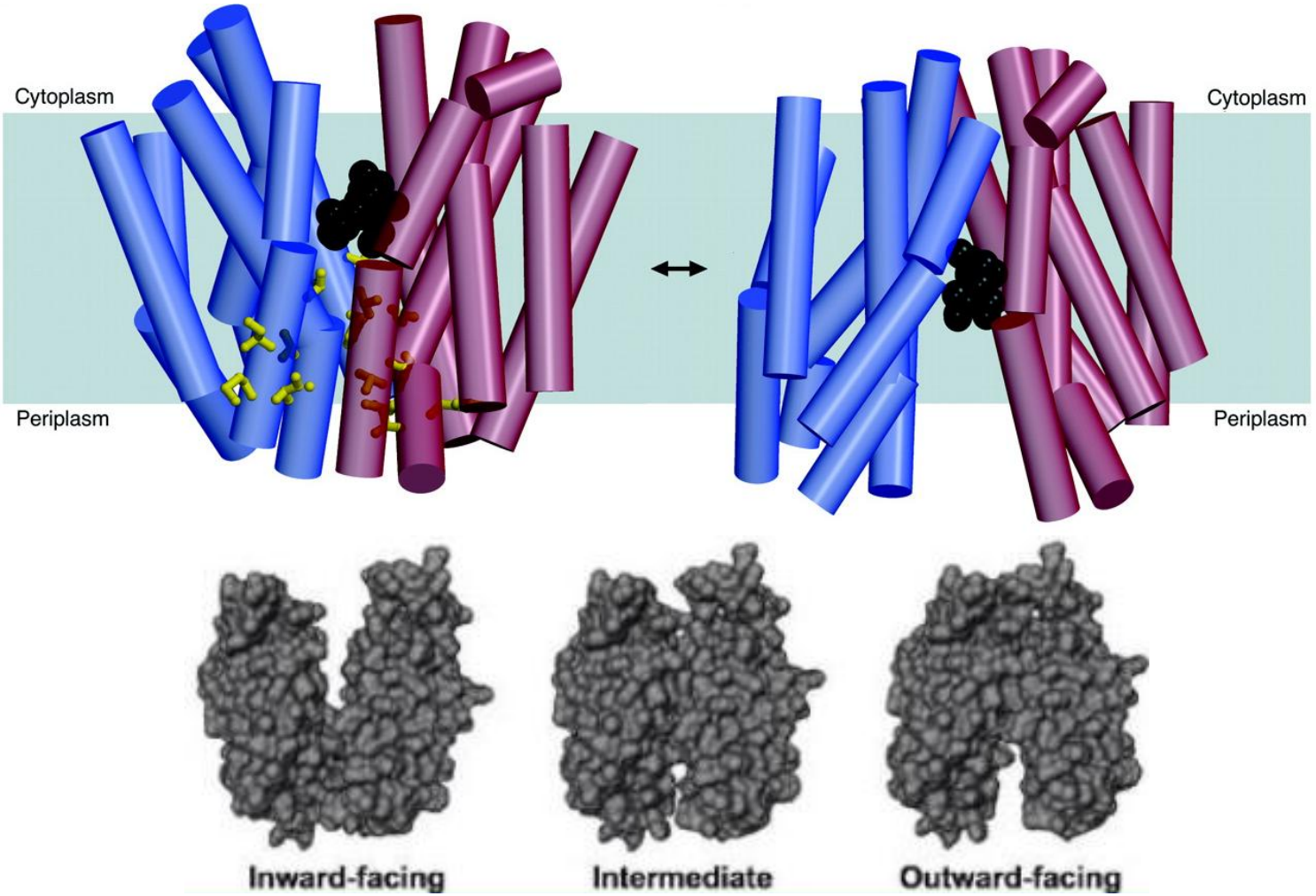

Widdas, 1952

«Ο διαμεμβρανικός μεταφορέας» που έχει μελετηθεί διεξοδικά με ένα σύνολο διαφορετικών μεθοδολογιών από πολλά πεδία

Site-directed alkylation (SCAM)

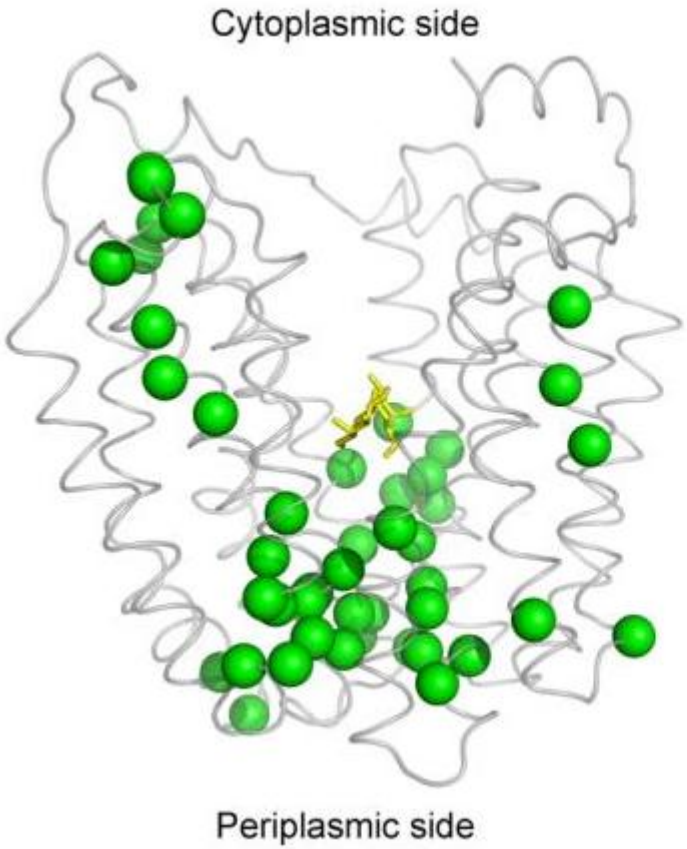

Θέσεις των οποίων η προσβασιμότητα *αυξάνεται* με τη δέσμευση υποστρώματος

Kaback et al., 2007

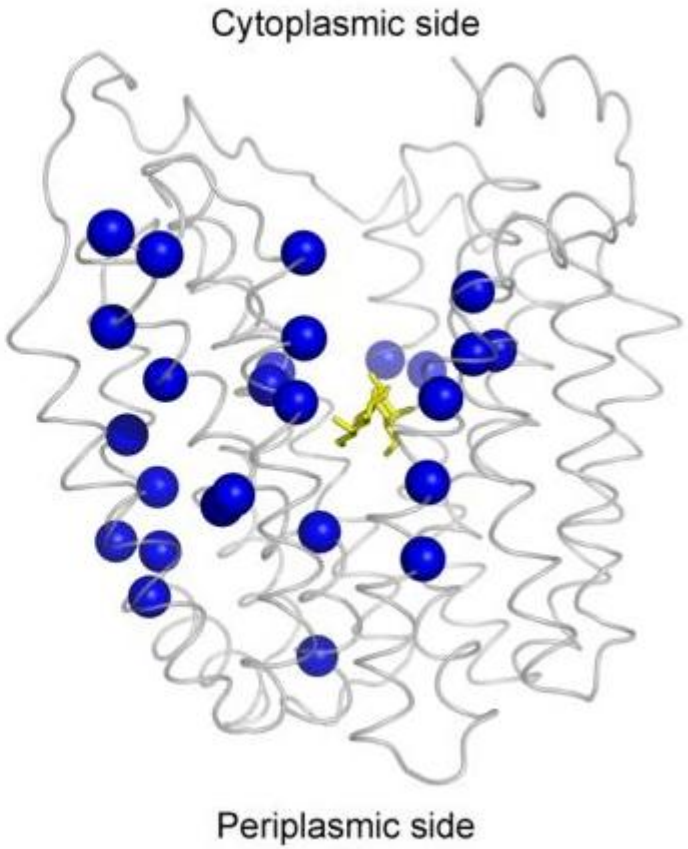

Θέσεις των οποίων η προσβασιμότητα *μειώνεται* με τη δέσμευση υποστρώματος

Nie et al., 2007

«Ο διαμεμβρανικός μεταφορέας» που έχει μελετηθεί διεξοδικά με ένα σύνολο διαφορετικών μεθοδολογιών από πολλά πεδία

Site-directed alkylation (SCAM)

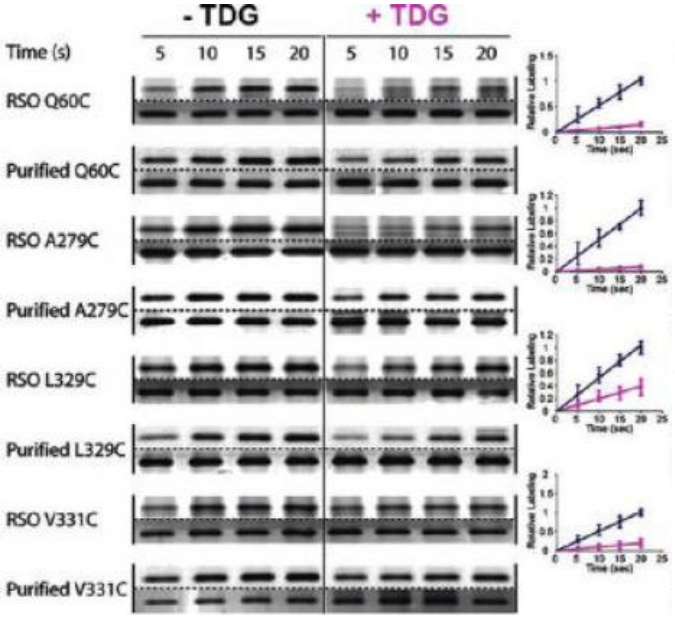

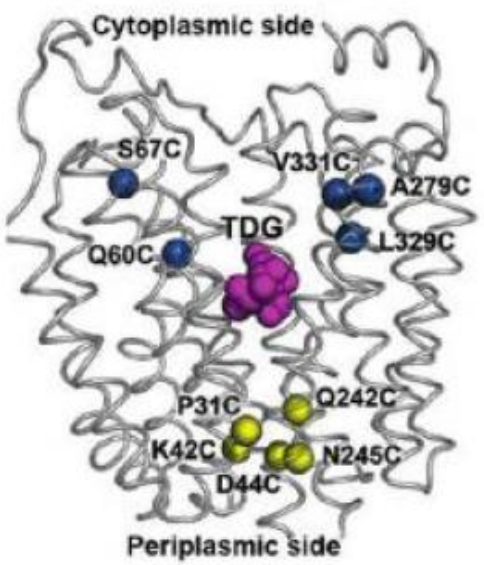

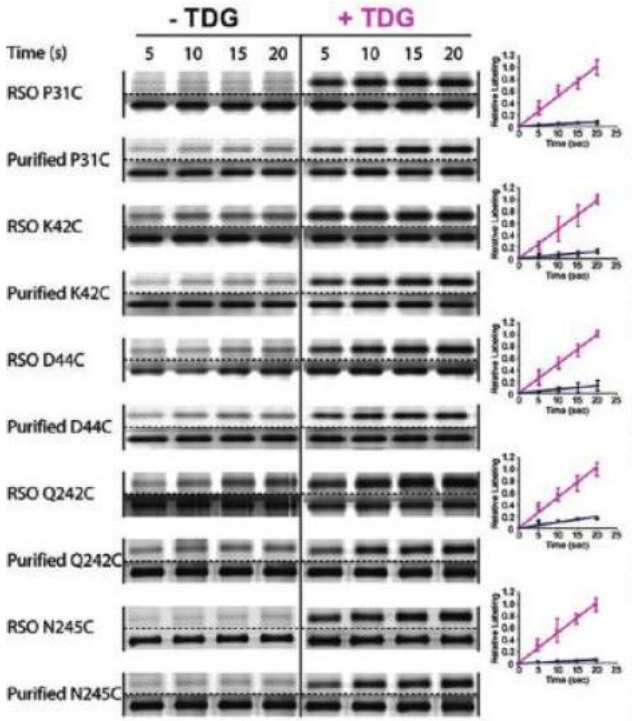

Μείωση της προσβασιμότητας στην πλευρά που βλέπει προς το κυτταρόπλασμα

Αύξηση της προσβασιμότητας στην πλευρά που βλέπει προς το περίπλασμα

Nie et al., 2007

«Ο διαμεμβρανικός μεταφορέας» που έχει μελετηθεί διεξοδικά με ένα σύνολο διαφορετικών μεθοδολογιών από πολλά πεδία

Trp fluorescence quenching
(Trp/His pairs)

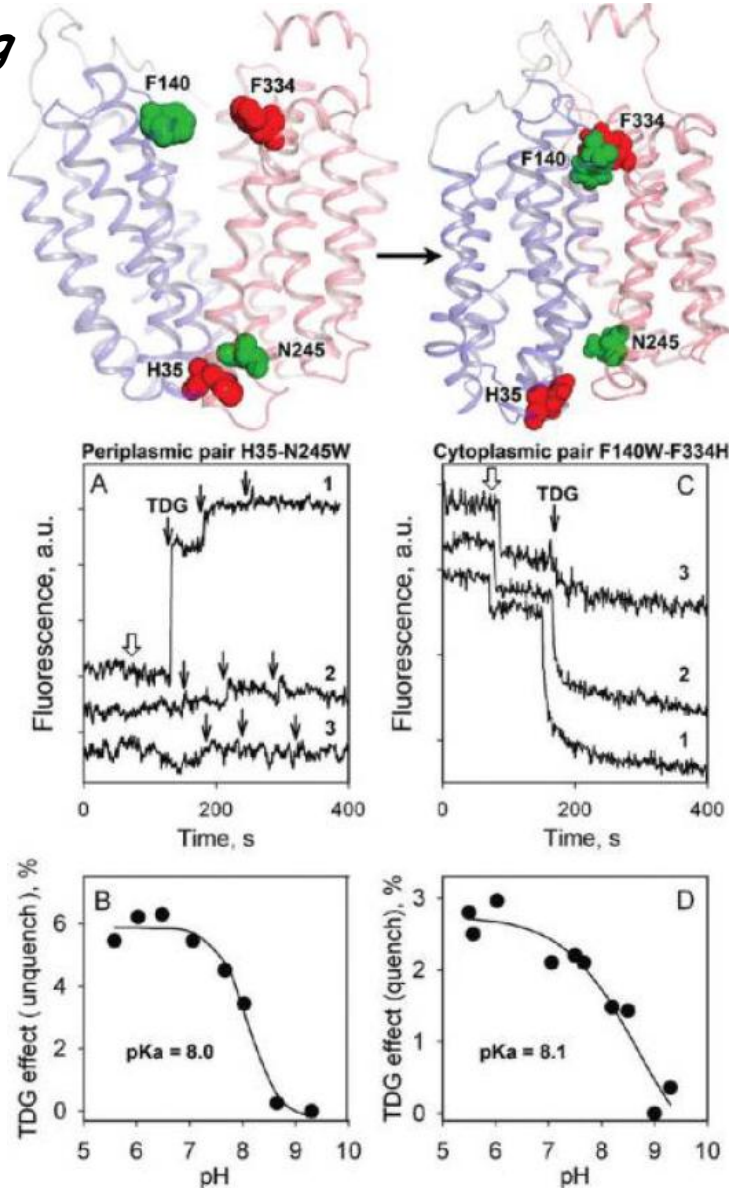

Άνοιγμα της «διάβασης» στο περιπλασμικό άκρο

Κλείσιμο της «διάβασης» στο κυτταροπλασμικό άκρο

Smirnova et al., 2011

«Ο διαμεμβρανικός μεταφορέας» που έχει μελετηθεί διεξοδικά με ένα σύνολο διαφορετικών μεθοδολογιών από πολλά πεδία

Site-directed spin labeling (SDSL)
Double electron-electron resonance (DEER)

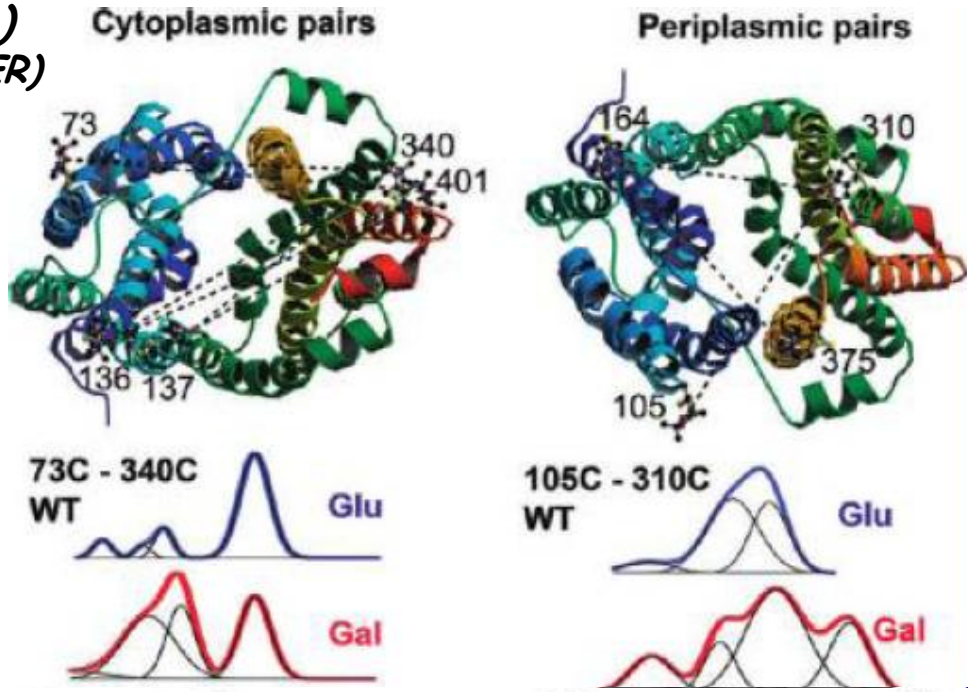

Μείωση των αποστάσεων στο κυτταροπλασμικό άκρο

Αύξηση των αποστάσεων στο περιπλασμικό άκρο

Ενδιάμεσες διαμορφώσεις (occluded states)

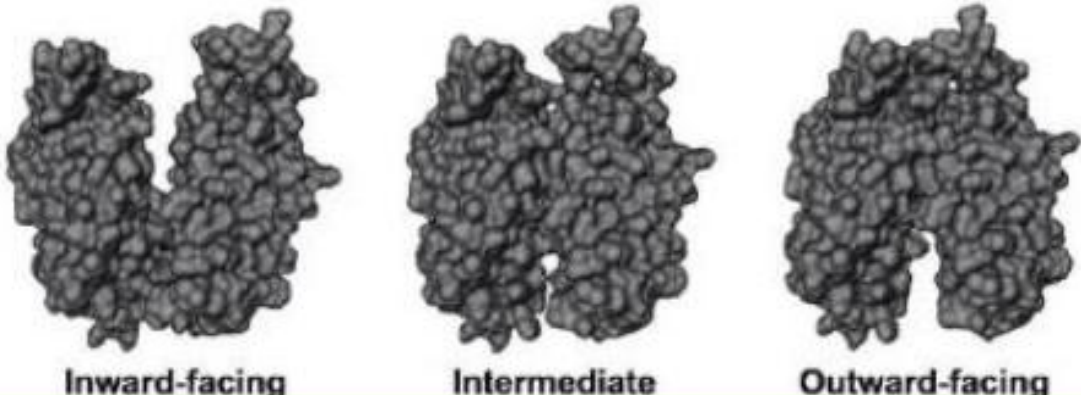

Madej et al., 2012

Smirnova et al., 2011

2003-2014: A compilation of MFS structures (περμεάση λακτόζης και ομόλογοι μεταφορείς)

x-ray crystallography (≥3.0 Å resolution)
Homology modeling/Molecular Dynamics

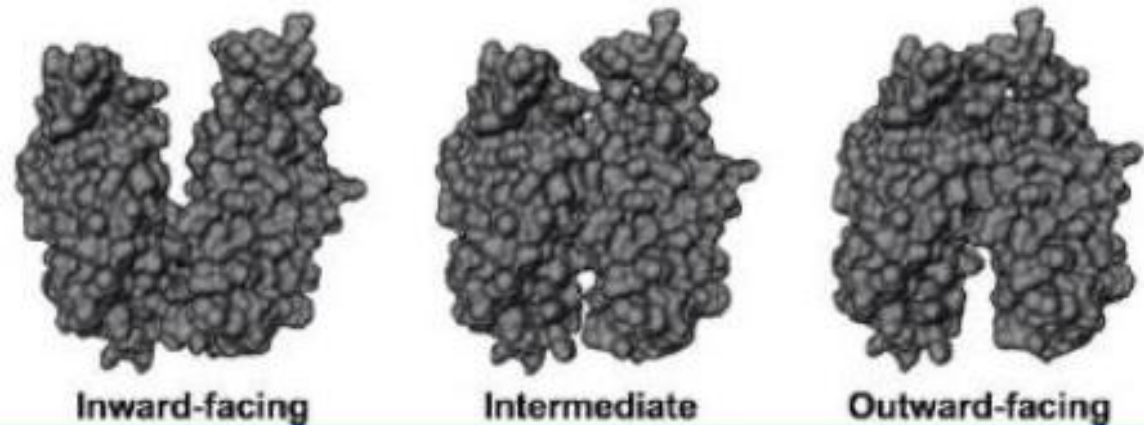

LacY (2003)
LacY (2006)
LacY (2006)
LacY (2007)
LacY (2011)
GlpT (2003)
GLUT1 (2014)

LacY (2014)
EmrD (2006)
PepT (2011)
NarK (2013)
NarU (2013)

FucP (2011)

Υπάρχει κρυσταλλογραφική μαρτυρία για ενδιάμεσες διαμορφώσεις

Deng et al., 2014

Kumar et al., 2014

Chaptal et al., 2011

«Ο διαμεμβρανικός μεταφορέας» που έχει μελετηθεί διεξοδικά με ένα σύνολο διαφορετικών μεθοδολογιών από πολλά πεδία

Site-directed cross-linking

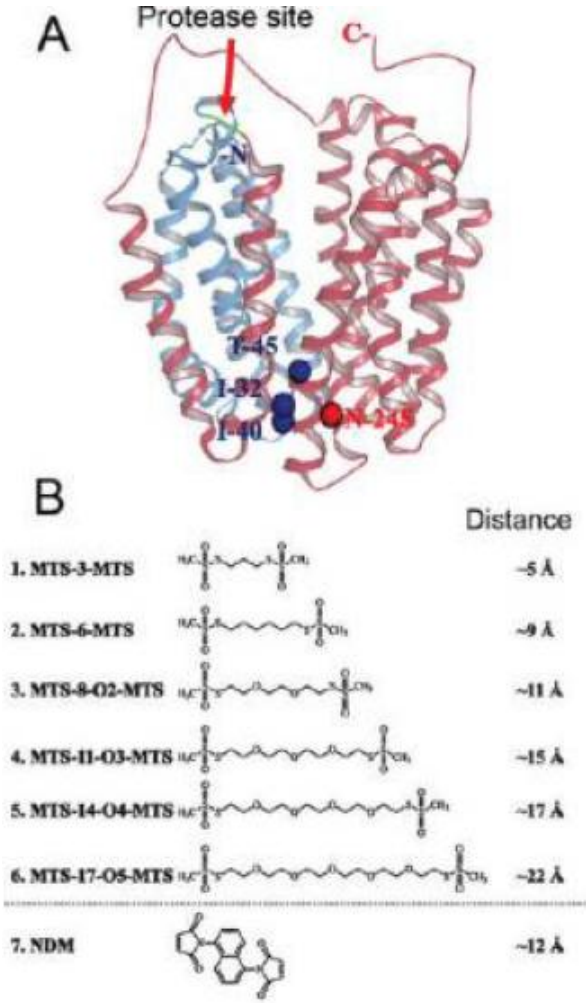

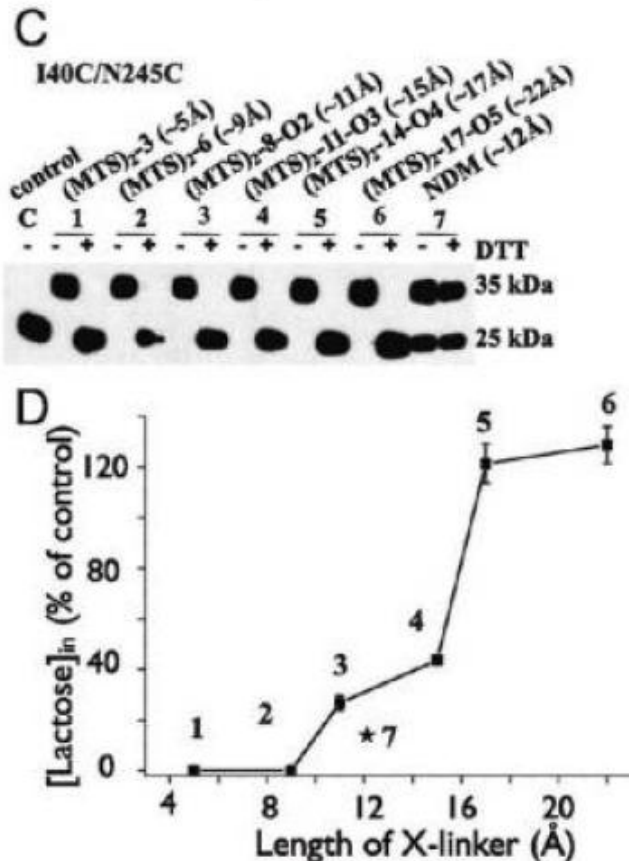

Χρειάζεται διαδοχικά άνοιγμα και κλείσιμο του περιπλασμικού άκρου. Απαιτείται >10Å απόσταση μεταξύ των ζευγών Cys (και >17Å για πλήρη ενεργότητα)

Zhou et al., 2008

«Ο διαμεμβρανικός μεταφορέας» που έχει μελετηθεί διεξοδικά με ένα σύνολο διαφορετικών μεθοδολογιών από πολλά πεδία

Trp151→NPG fluorescence resonance energy transfer (FRET)
Binding measurements

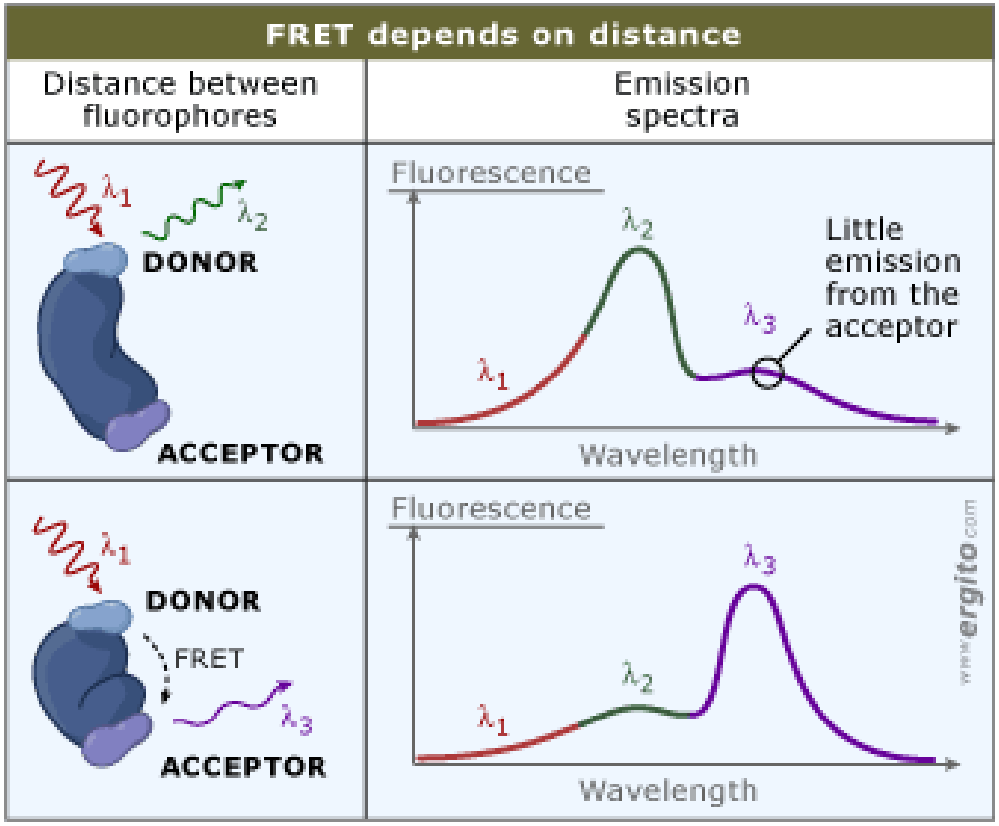

Smirnova et al., 2006

Smirnova et al., 2011

2010s

«Ο διαμεμβρανικός μεταφορέας» που έχει μελετηθεί διεξοδικά με ένα σύνολο διαφορετικών μεθοδολογιών από πολλά πεδία

Trp151→NPG fluorescence resonance energy transfer (FRET)

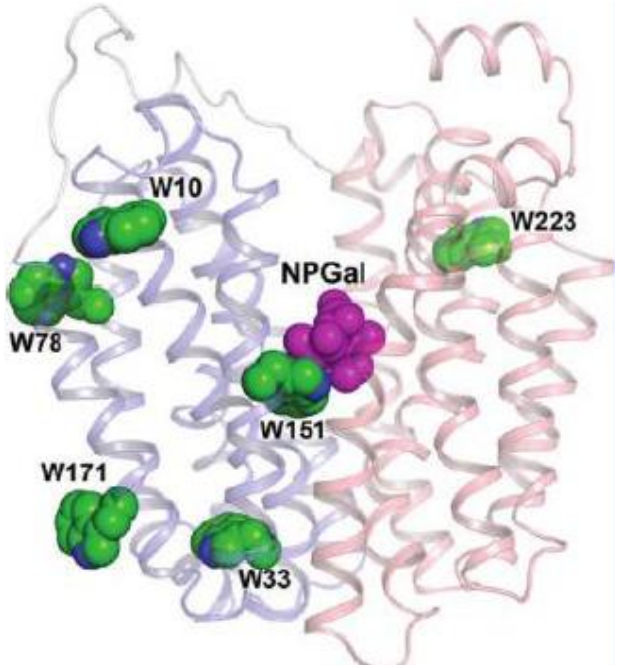

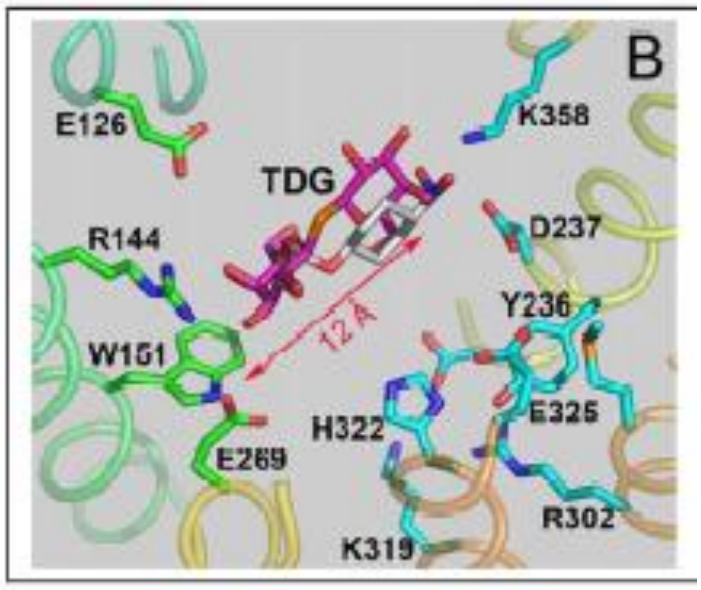

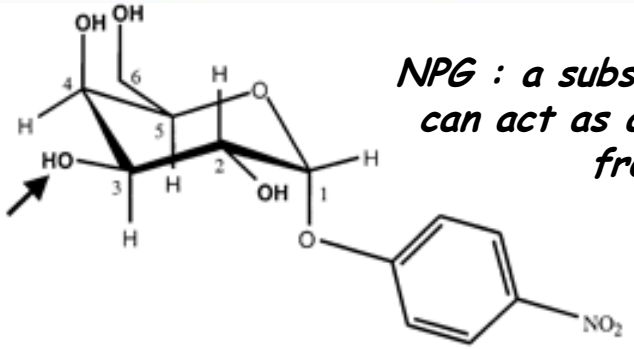

NPG : a substrate analog that can act as a FRET acceptor from Trp

Smirnova et al., 2006

Smirnova et al., 2011

«Ο διαμεμβρανικός μεταφορέας» που έχει μελετηθεί διεξοδικά με ένα σύνολο διαφορετικών μεθοδολογιών από πολλά πεδία

Trp151→NPG fluorescence resonance energy transfer (FRET)

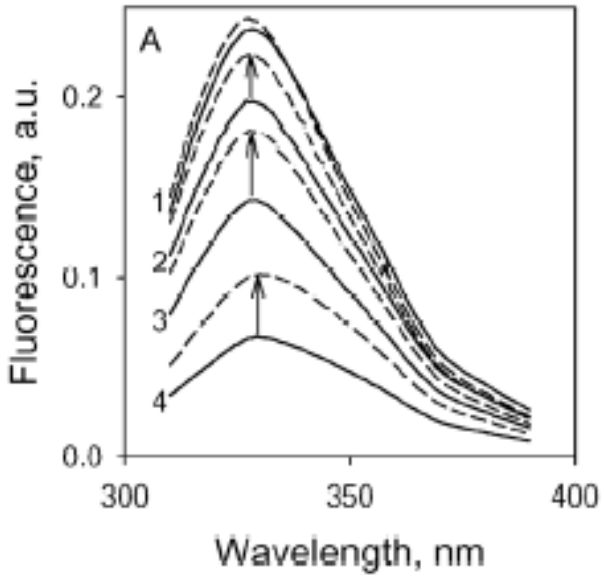

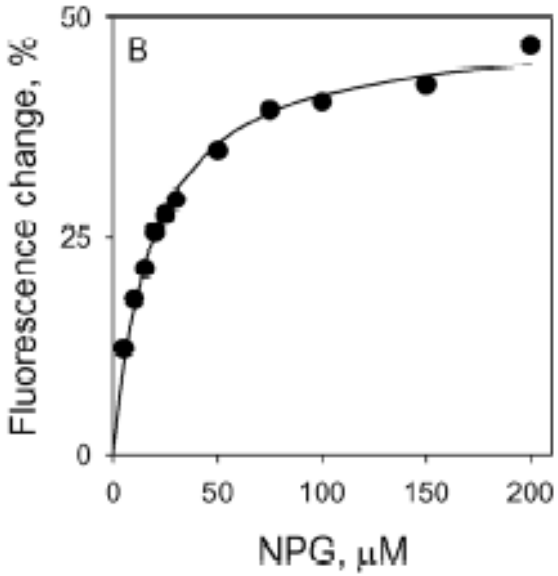

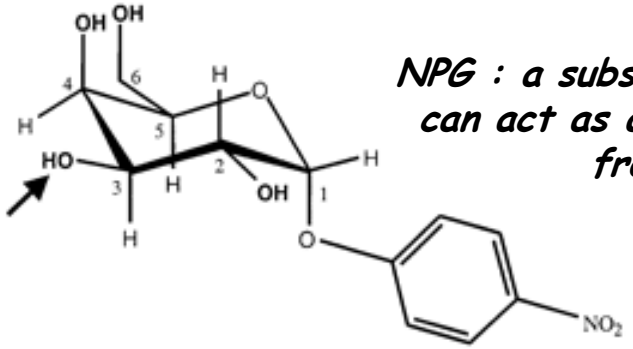

NPG : a substrate analog that can act as a FRET acceptor from Trp

Smirnova et al., 2006

Smirnova et al., 2011

«Ο διαμεμβρανικός μεταφορέας» που έχει μελετηθεί διεξοδικά με ένα σύνολο διαφορετικών μεθοδολογιών από πολλά πεδία

Trp151→NPG fluorescence resonance energy transfer (FRET)

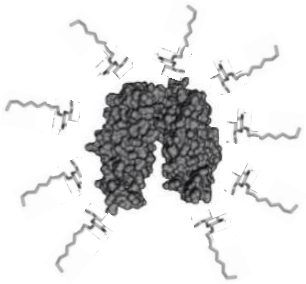

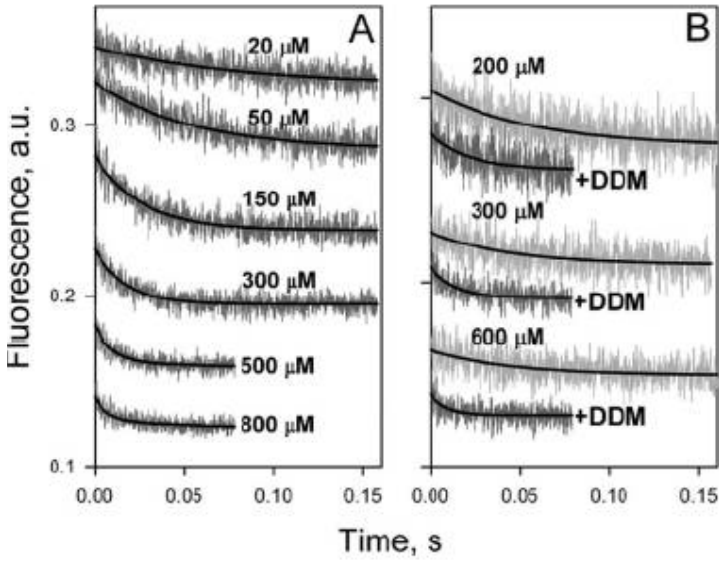

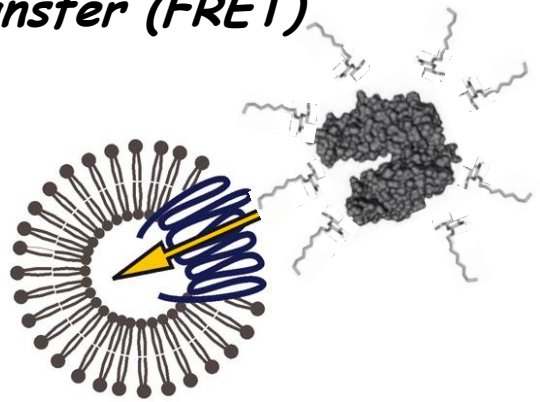

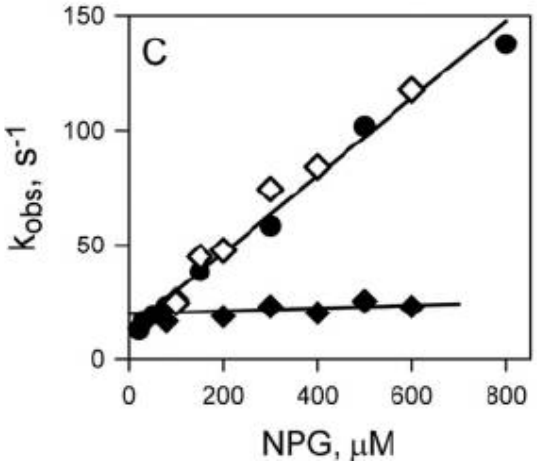

*Στα πρωτεολιποσωμάτια (καθώς και στην κυτταρική μεμβράνη), η LacY βρίσκεται σε διαμόρφωση **κλειστή προς το περίπλασμα**. Για τη δέσμευση υποστρώματος θα πρέπει να προηγηθεί το άνοιγμα του περιπλασμικού της άκρου που θα επιτρέψει **πρόσβαση** του εξωγενούς υποστρώματος στο κέντρο δέσμευσης (αυτό το αρχικό άνοιγμα φαίνεται να είναι μια αργή, ρυθμοκαθοριστική διεργασία)*

Smirnova et al., 2006

Smirnova et al., 2011

«Ο διαμεμβρανικός μεταφορέας» που έχει μελετηθεί διεξοδικά με ένα σύνολο διαφορετικών μεθοδολογιών από πολλά πεδία

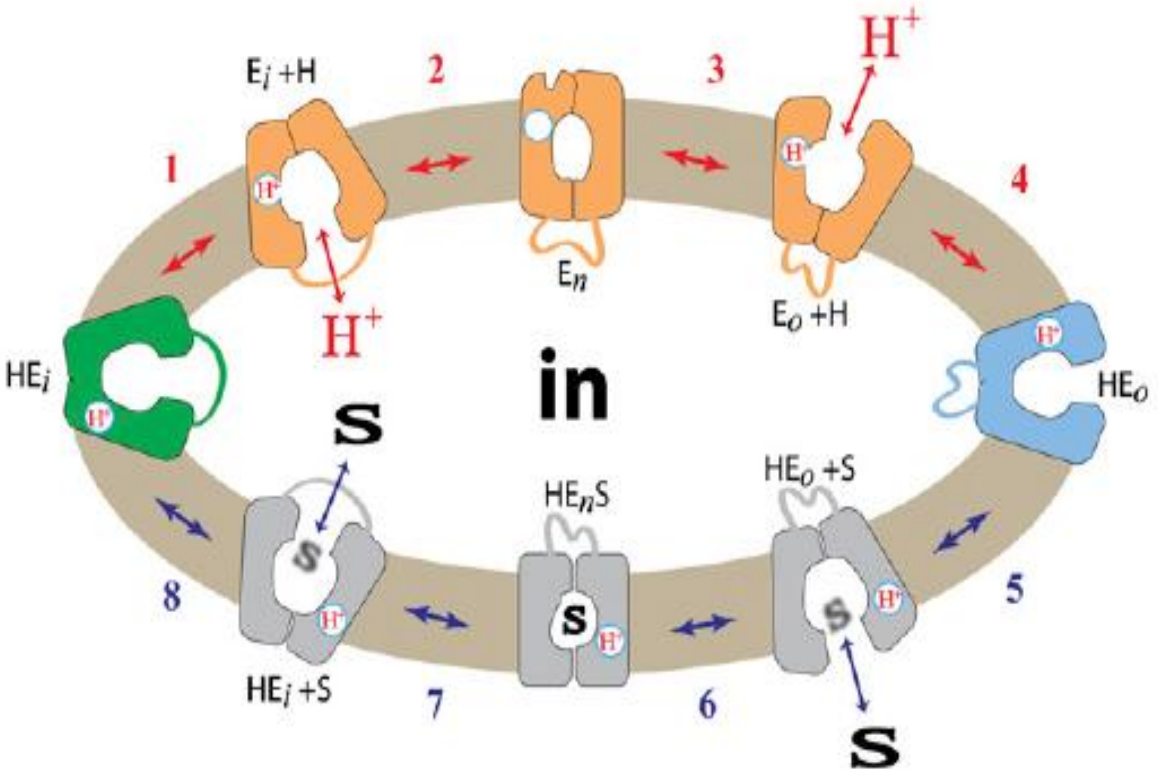

Madej et al., 2012

Smirnova et al., 2011

Binding site

The structure and mechanism of LacY

Abramson *et al.*, *Science* 301, 610 (2003)

Science. 2003 Aug 1;301(5633):610-5. Links
Comment in:
Science. 2003 Aug 1;301(5633):603-4.

Structure and mechanism of the lactose permease of Escherichia coli.

Abramson J, Smirnova I, Kasho V, Verner G, Kaback HR, Iwata S.
Department of Biological Sciences, Imperial College London, London SW7 2AZ, UK.

Membrane transport proteins that transduce free energy stored in electrochemical ion gradients into a concentration gradient are a major class of membrane proteins. We report the crystal structure at 3.5 angstroms of the Escherichia coli lactose permease, an intensively studied member of the major facilitator superfamily of transporters. The molecule is composed of N- and C-terminal domains, each with six transmembrane helices, symmetrically positioned within the permease. A large internal hydrophilic cavity open to the cytoplasmic side represents the inward-facing conformation of the transporter. The structure with a bound lactose homolog, beta-D-galactopyranosyl-1-thio-beta-D-galactopyranoside, reveals the sugar-binding site in the cavity, and residues that play major roles in substrate recognition and proton translocation are identified. We propose a possible mechanism for lactose/proton symport (co-transport) consistent with both the structure and a large body of experimental data.

PMID: 12893935 [PubMed - indexed for MEDLINE]

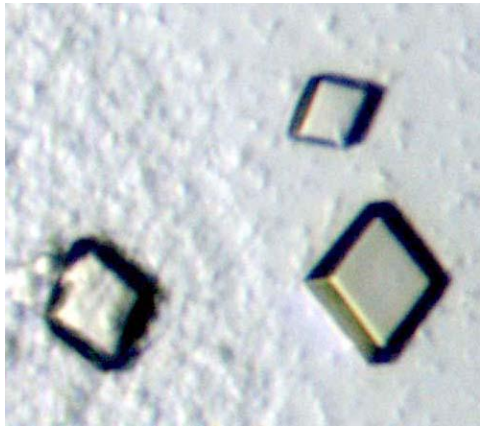

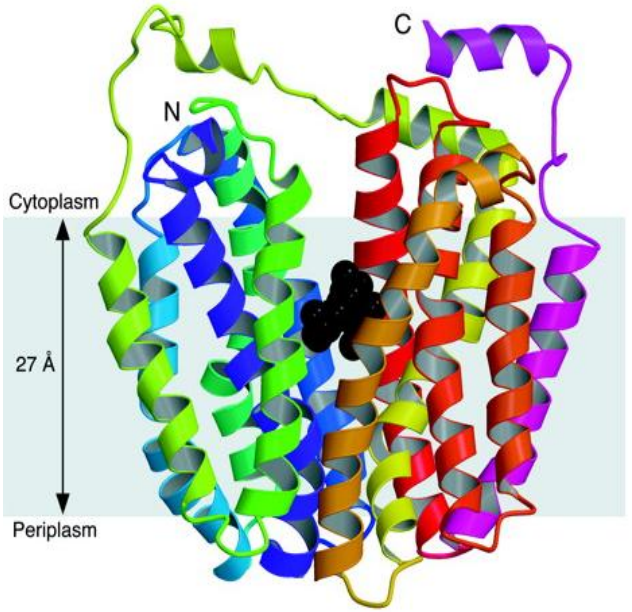

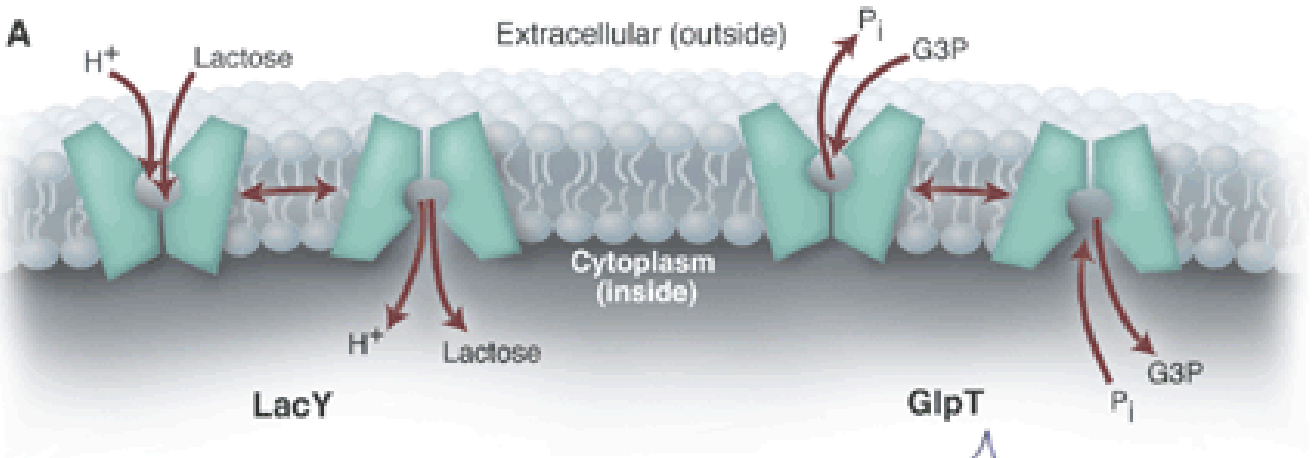

B

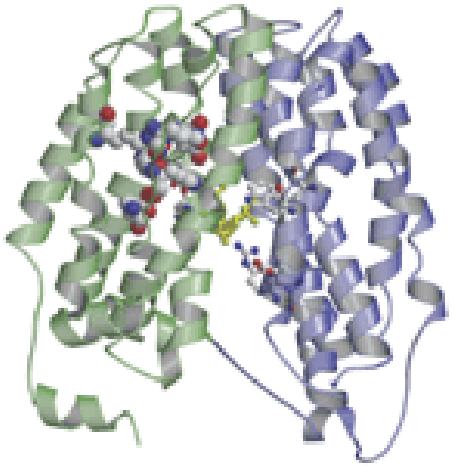

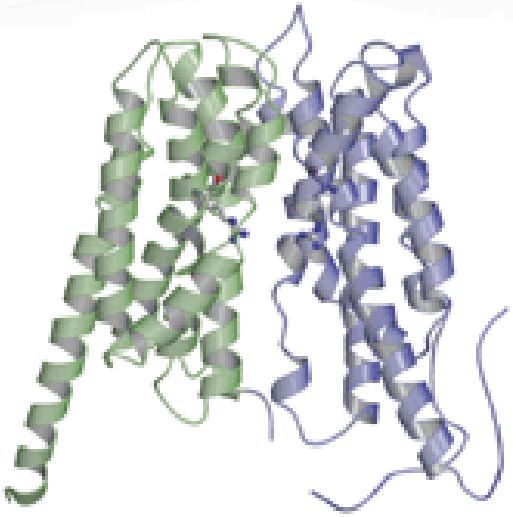

LacY

GlpT

3.5 Å

3.3 Å

«Ψευδοσυμμετρία» των δύο domains

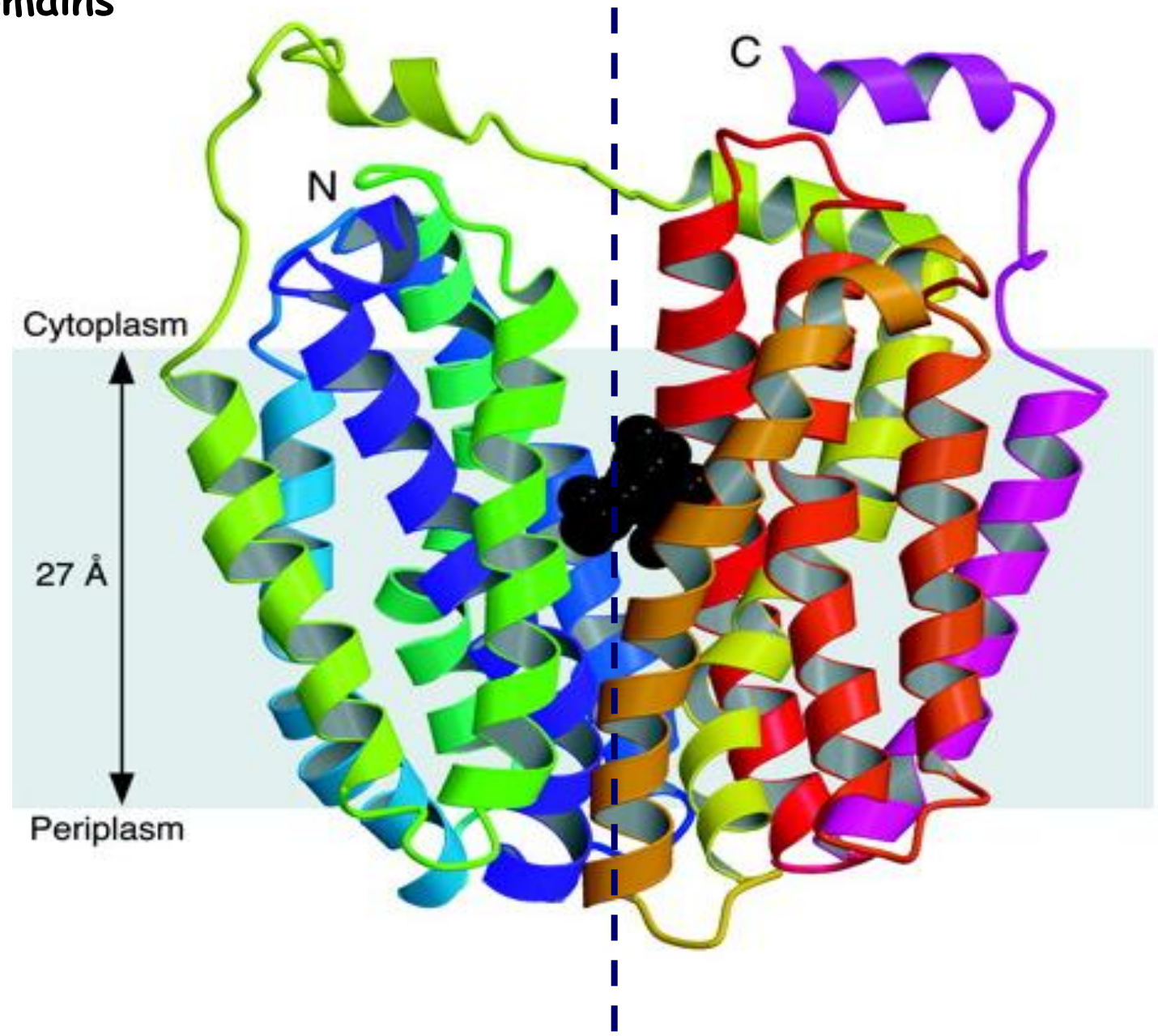

Το κέντρο δέσμευσης σχηματίζεται ανάμεσα στα δύο domains

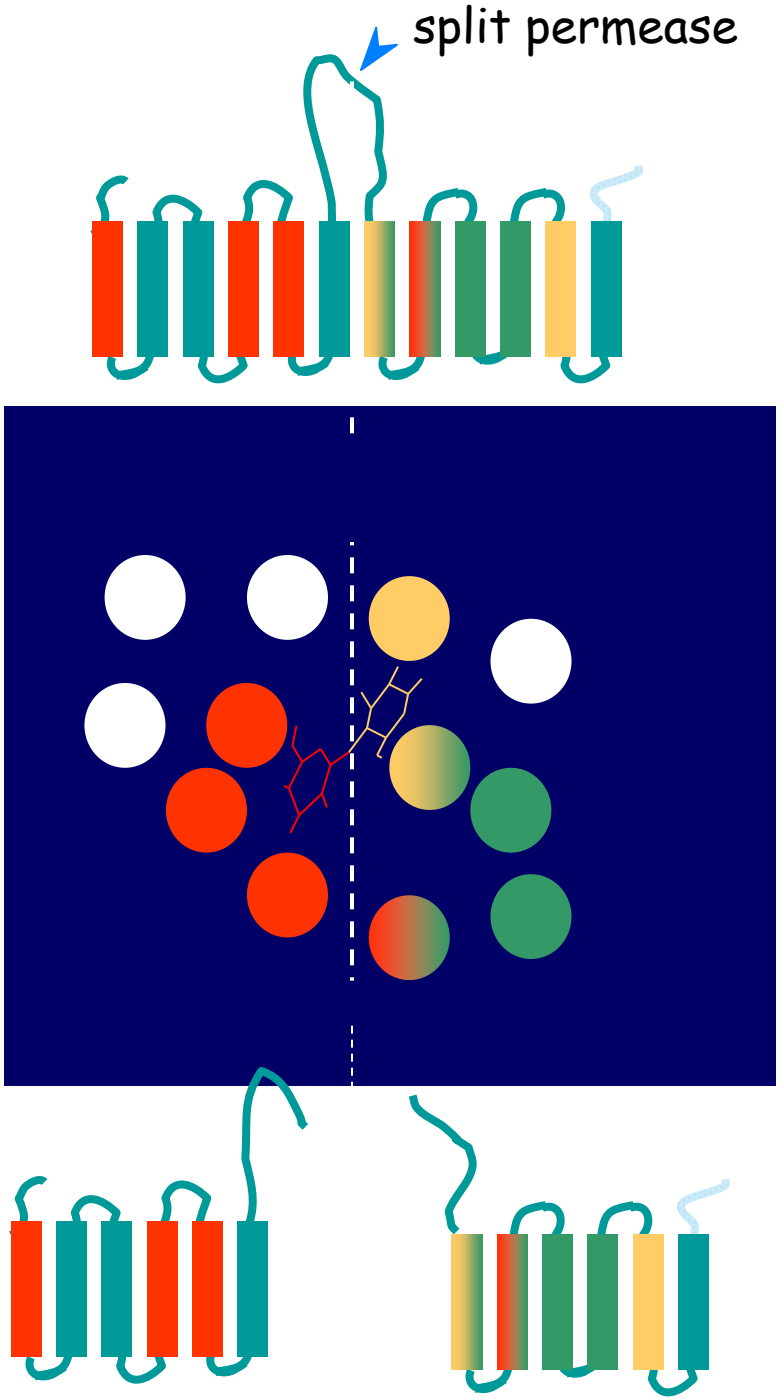

Το κέντρο δέσμευσης σχηματίζεται ανάμεσα στα δύο domains

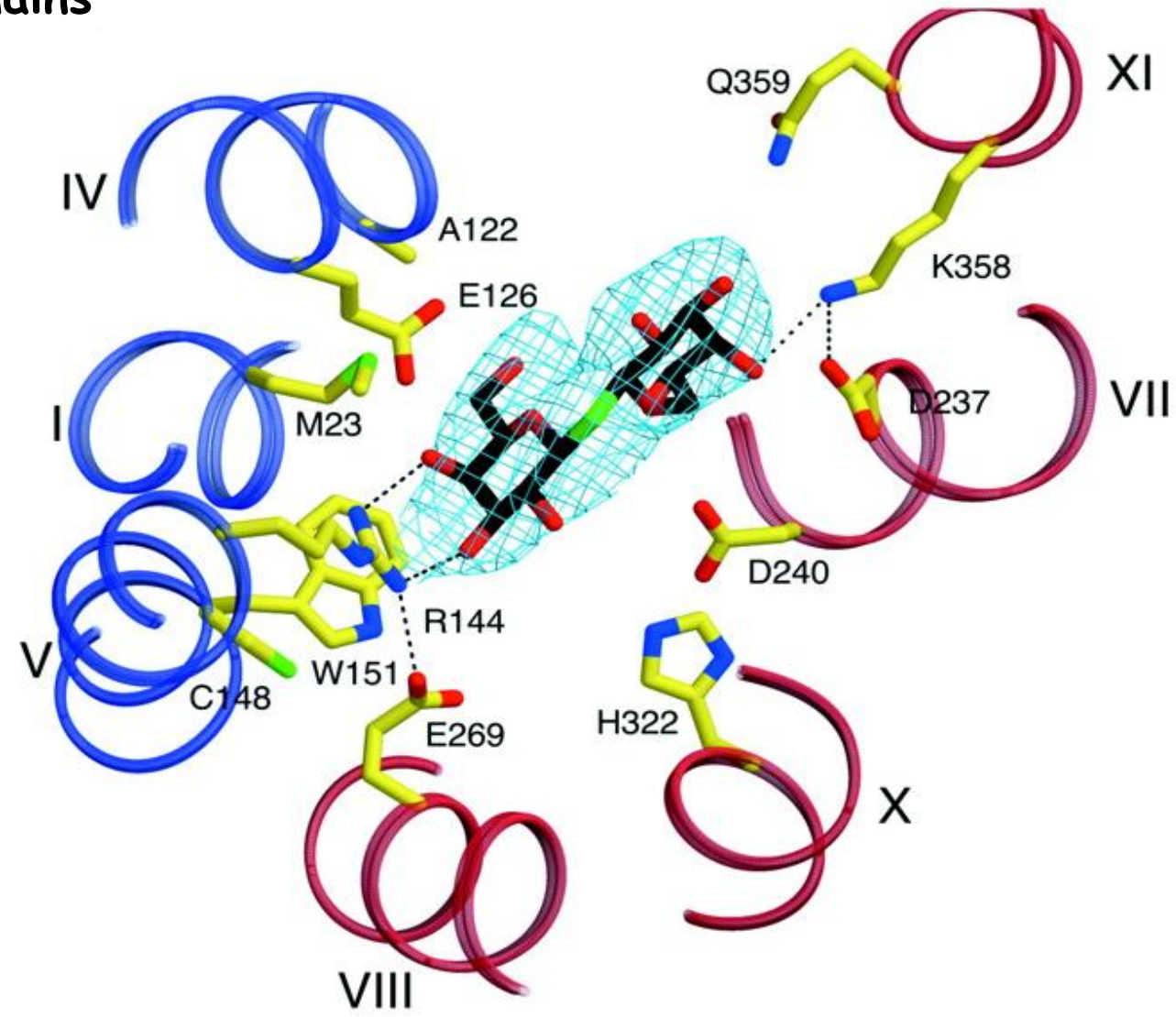

Το κέντρο δέσμευσης σχηματίζεται ανάμεσα στα δύο domains

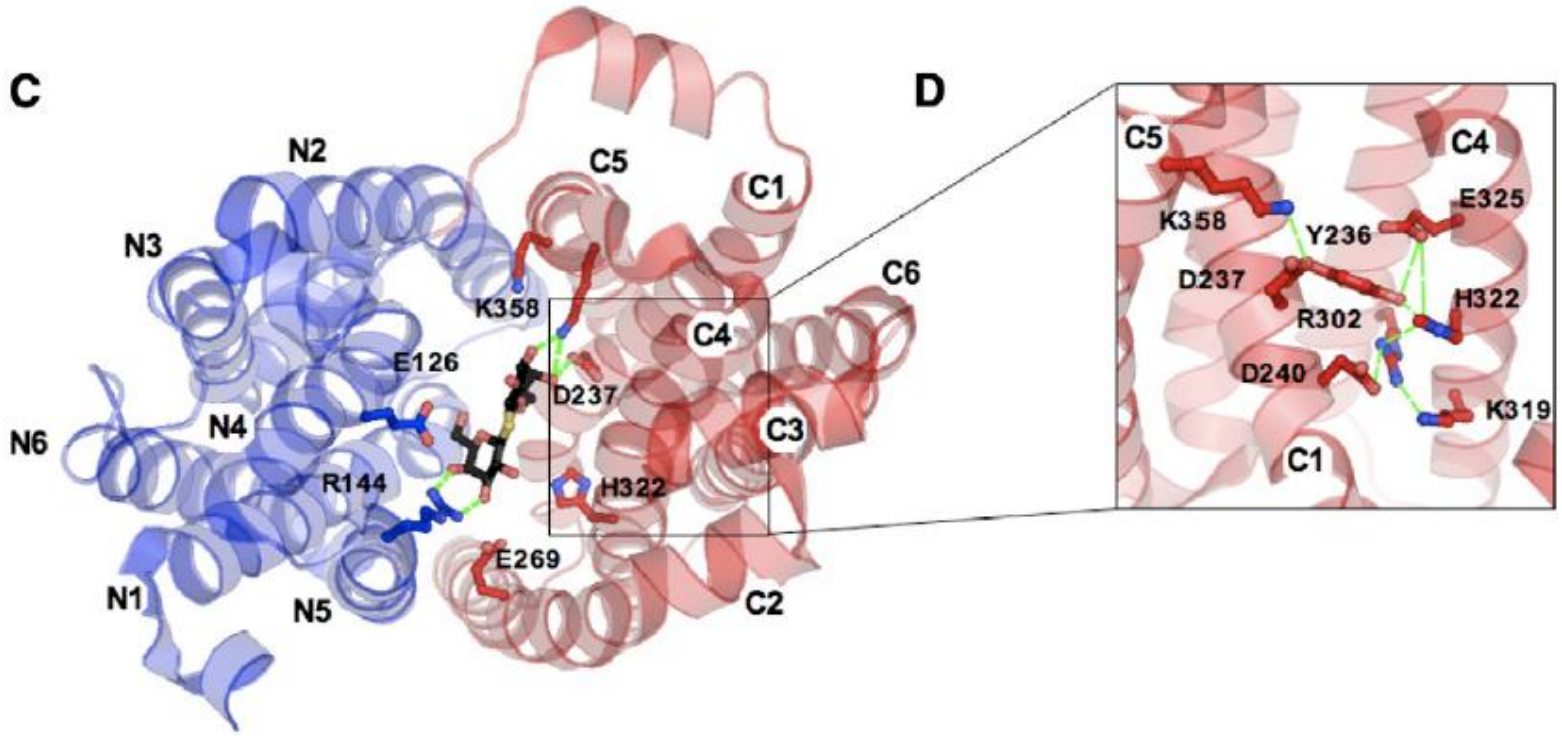

2003-2014: A compilation of MFS structures (περμεάση λακτόζης και ομόλογοι μεταφορείς)

x-ray crystallography (≥3.0 Å resolution)

Homology modeling/Molecular Dynamics

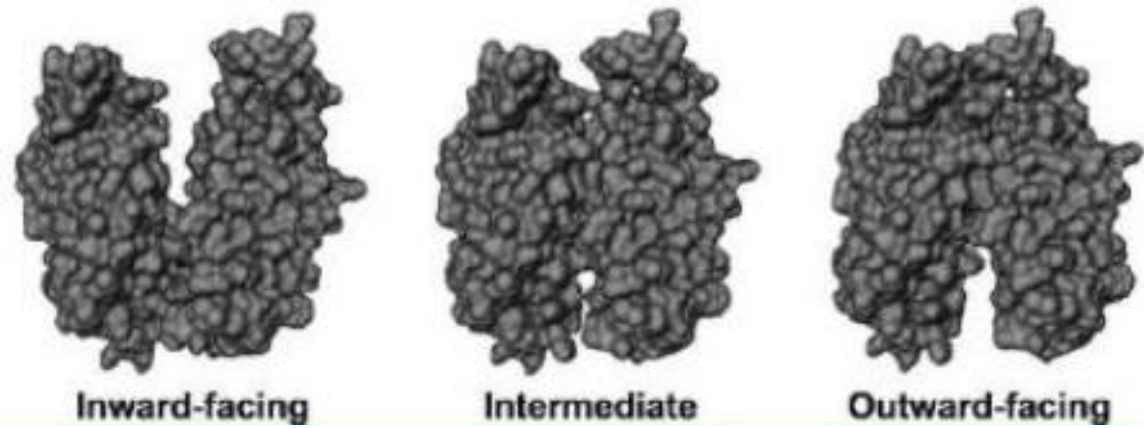

LacY (2003)
LacY (2006)
LacY (2006)
LacY (2007)
LacY (2011)
GlpT (2003)
GLUT1 (2014)

LacY (2014)
EmrD (2006)
PepT (2011)
NarK (2013)
NarU (2013)

FucP (2011)

Kumar et al., 2014

2003-2014: A compilation of MFS structures (περμεάση λακτόζης και ομόλογοι μεταφορείς)

x-ray crystallography (≥3.0 Å resolution)

Homology modeling/Molecular Dynamics

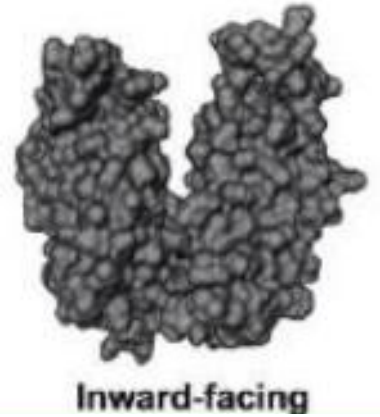

LacY (2003)	C154G	TDG	*Abramson et al., 2003*
LacY (2006)	C154G	_ (pH 6.5)	*Mirza et al., 2006*
LacY (2006)	C154G	_ (pH 5.6)	*Mirza et al., 2006*
LacY (2007)	wild-type	_	*Guan et al., 2007*
LacY (2011)	A122C	MTS-Gal	*Chaptal et al., 2011*

2003-2014: A compilation of MFS structures (περμεάση λακτόζης και ομόλογοι μεταφορείς)

x-ray crystallography (≥3.0 Å resolution)
Homology modeling/Molecular Dynamics

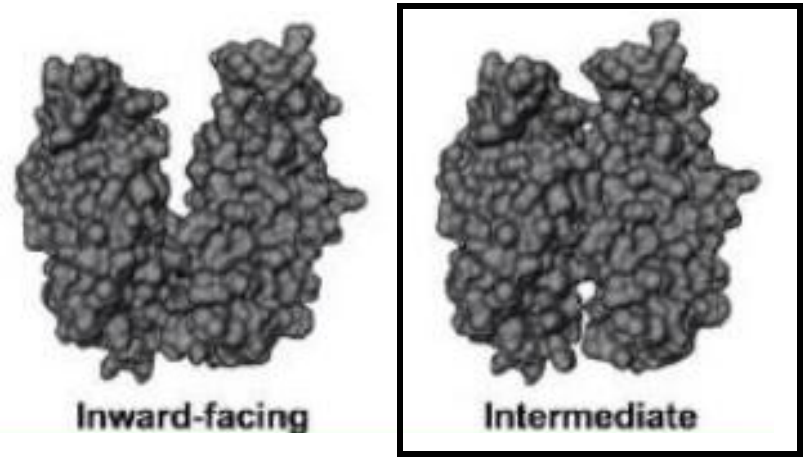

LacY (2003)	C154G	TDG	*Abramson et al., 2003*
LacY (2006)	C154G	_ (pH 6.5)	*Mirza et al., 2006*
LacY (2006)	C154G	_ (pH 5.6)	*Mirza et al., 2006*
LacY (2007)	wild-type	_	*Guan et al., 2007*
LacY (2011)	A122C	MTS-Gal	*Chaptal et al., 2011*
LacY (2014)	G46W/G262W	TDG	*Kumar et al., 2014; Smirnova et al., 2103*

2014: The first almost-occluded/outward-facing captured conformation in a LacY crystal structure

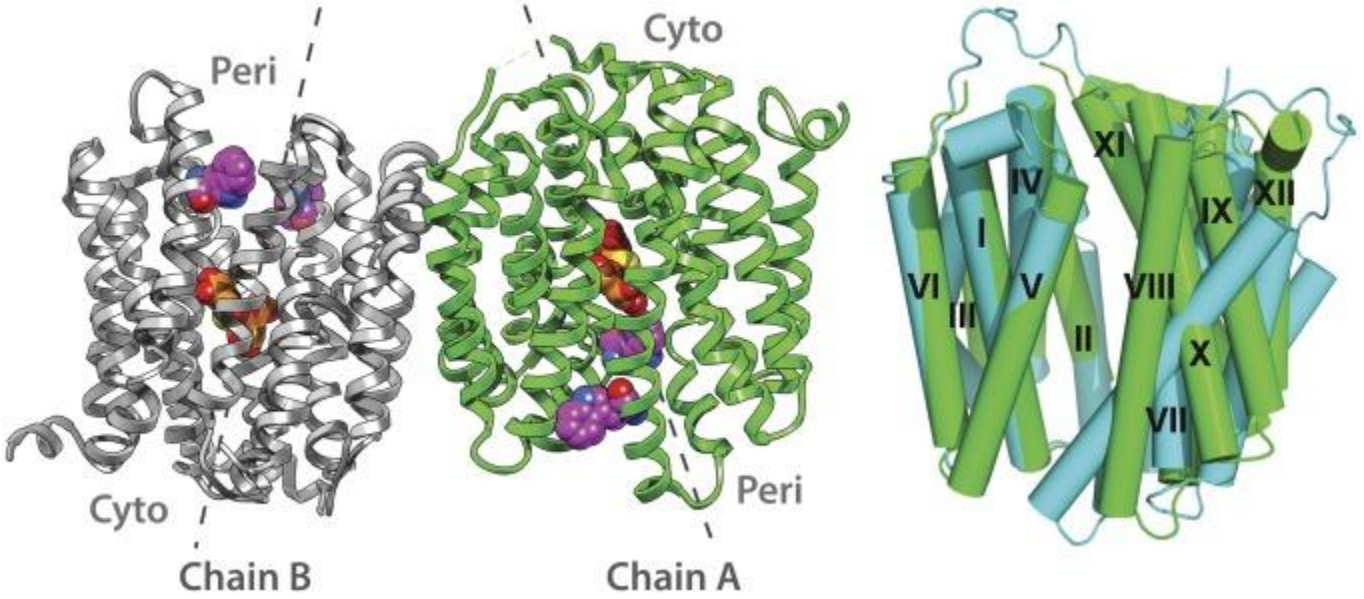

Kumar et al., 2014

Η δέσμευση υποστρώματος οδηγεί σε αναπροσαρμογή της διαμόρφωσης του ενεργού κέντρου (induced fit)

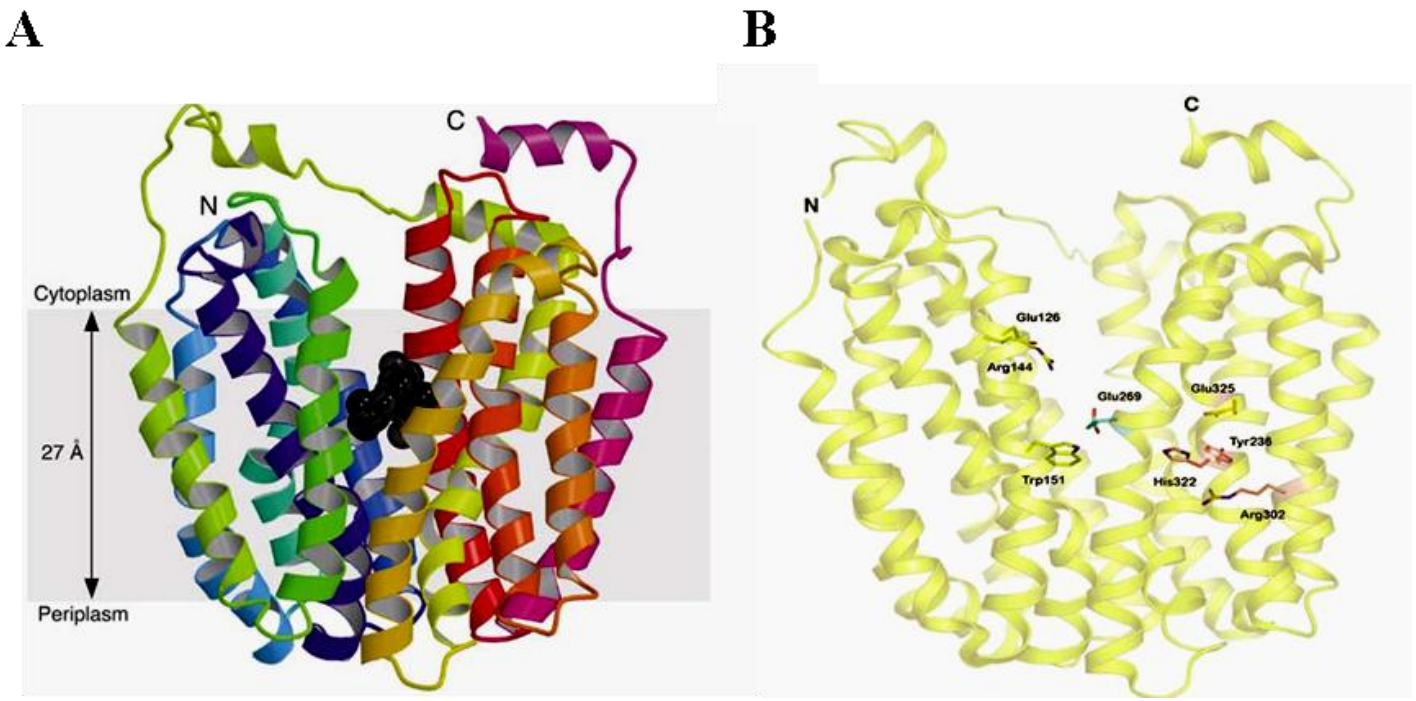

Abramson et al., 2003
with substrate (TDG)

Mirza et al., 2006
No substrate
pH 6.5, pH 5.6

Mirza et al., 2006

Η δέσμευση υποστρώματος οδηγεί σε αναπροσαρμογή της διαμόρφωσης του ενεργού κέντρου (induced fit)

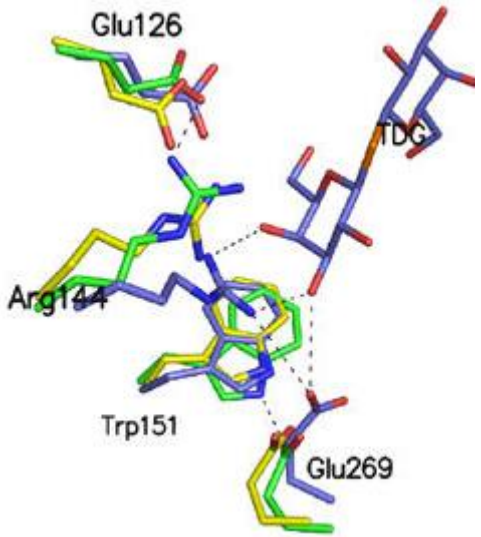

superimposition
of 3 structures

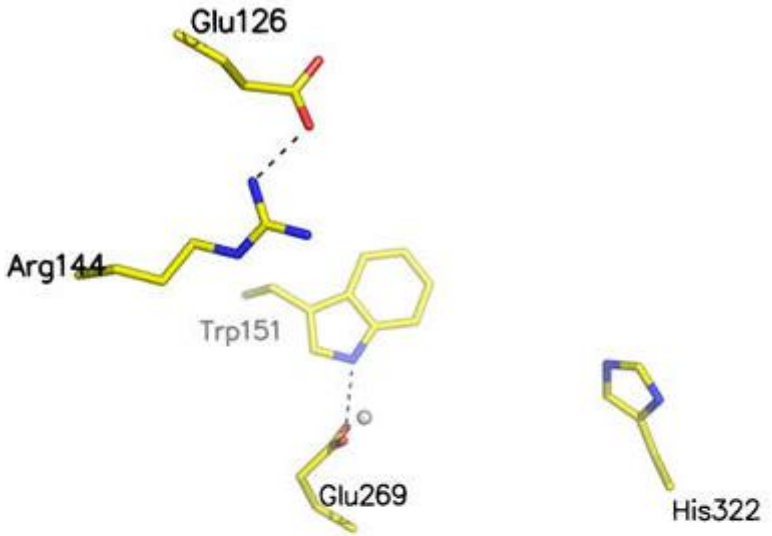

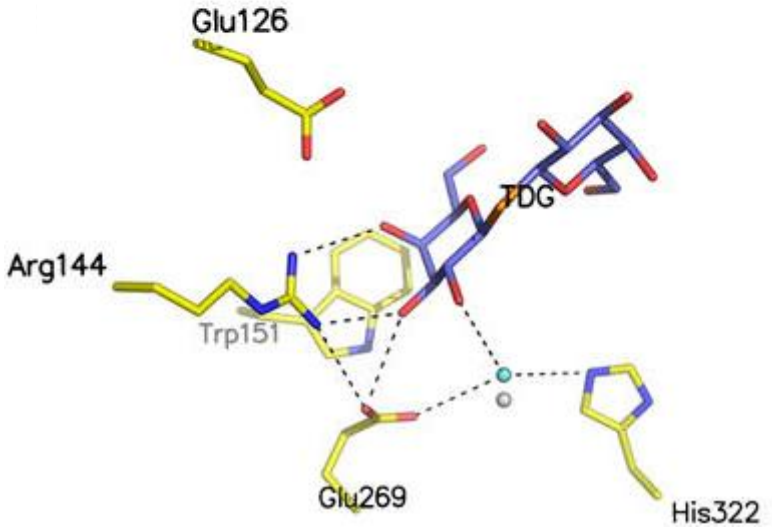

Mirza et al., 2006

Το ανενεργό μετάλλαγμα της LacY C154G εμφανίζει σφιχτή διαμόρφωση των TM1 και TM5 (Gly24-Gly154) η οποία δεν επιτρέπει την έναρξη των αλλαγών διαμόρφωσης που θα οδηγούσαν στην έξοδο του υποστρώματος από το ενεργό κέντρο (δεν γίνεται μεταφορά)

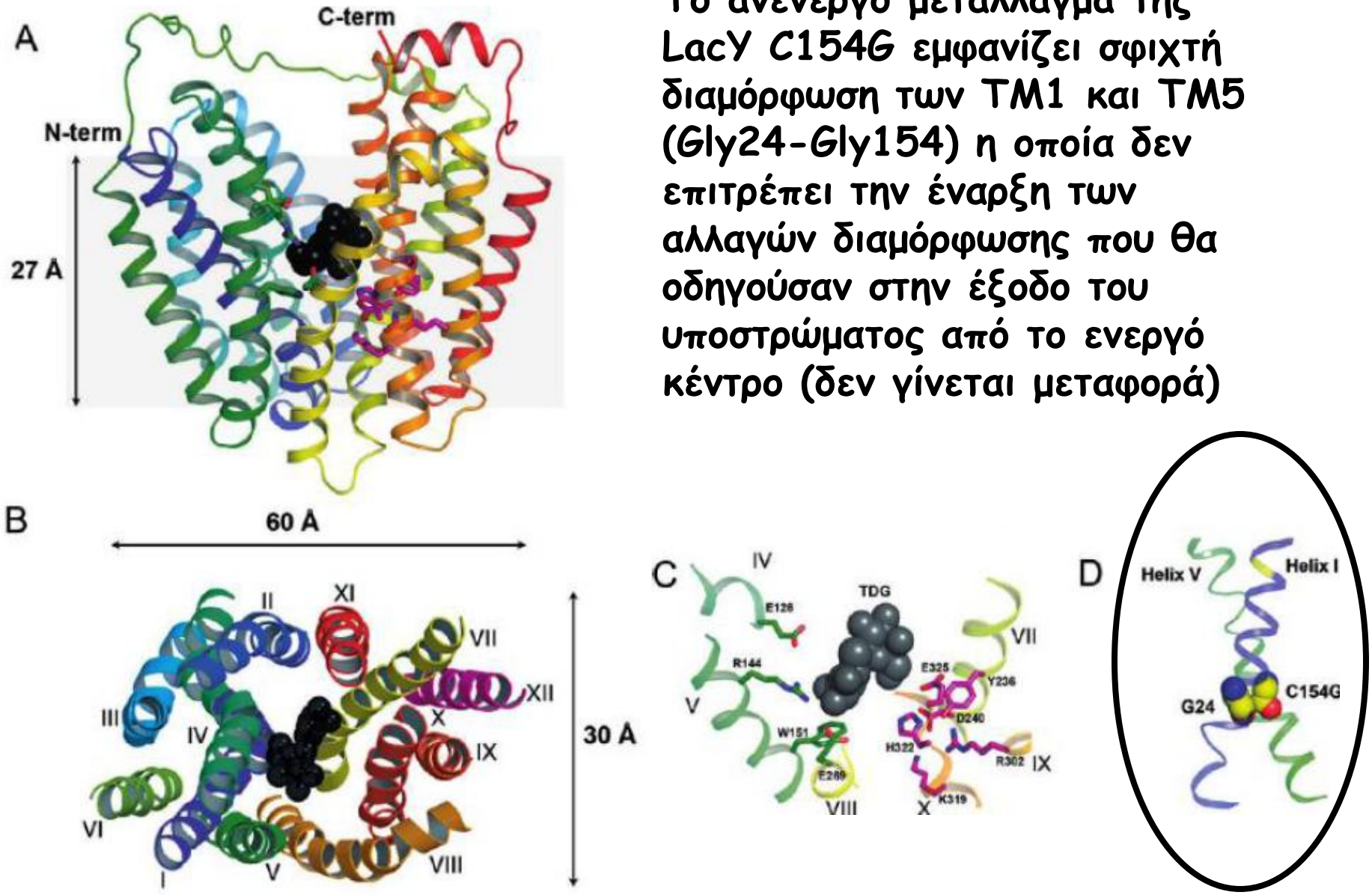

Guan et al., 2007

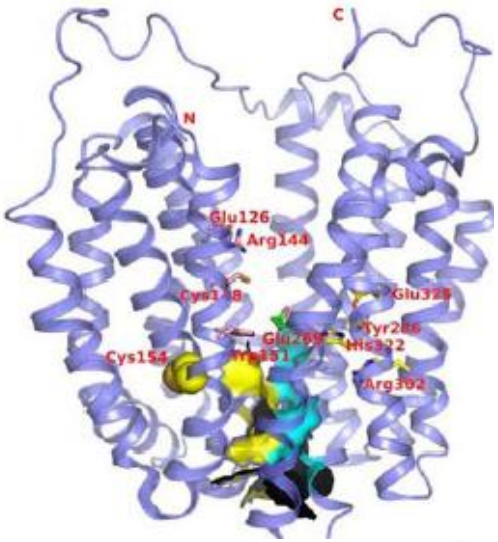

Αυτή είναι και η βασική διαφορά μεταξύ του ανενεργού μεταλλάγματος C154G και της LacY αγρίου τύπου (wild-type) [*κρυσταλλική δομή, 2007*]

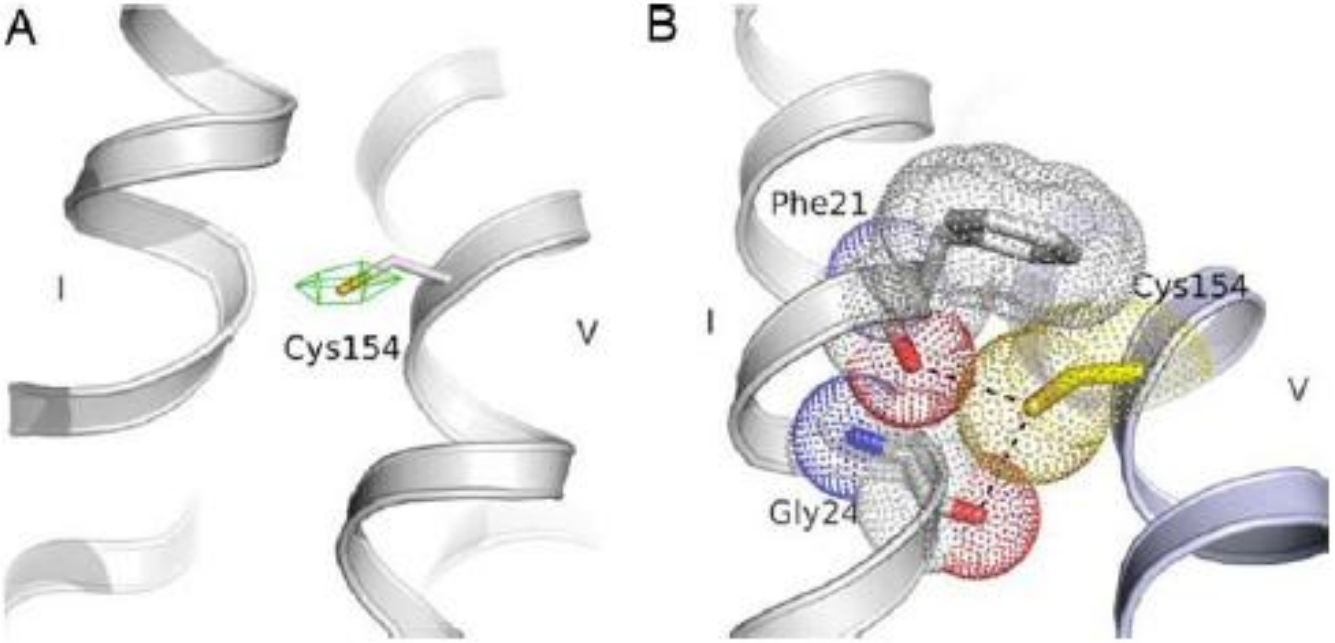

Guan et al., 2007

Ότι η αλλαγή διαμόρφωσης μεταξύ των TM1 και TM5 αποτελεί ένα αρχικό γεγονός απαραίτητο για την μεταφορά υποστρώματος έχει δειχθεί και με λειτουργικά πειράματα Cys-Cys cross-linking σε κυστίδια

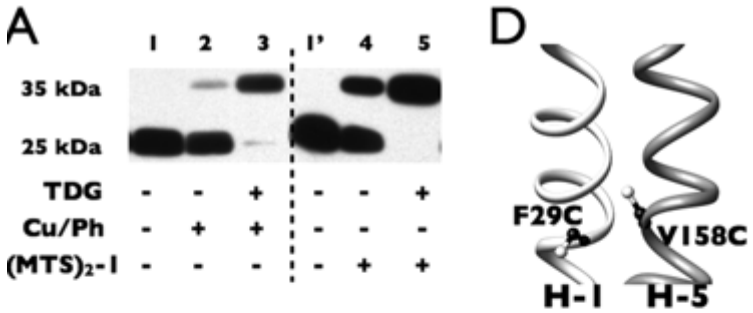

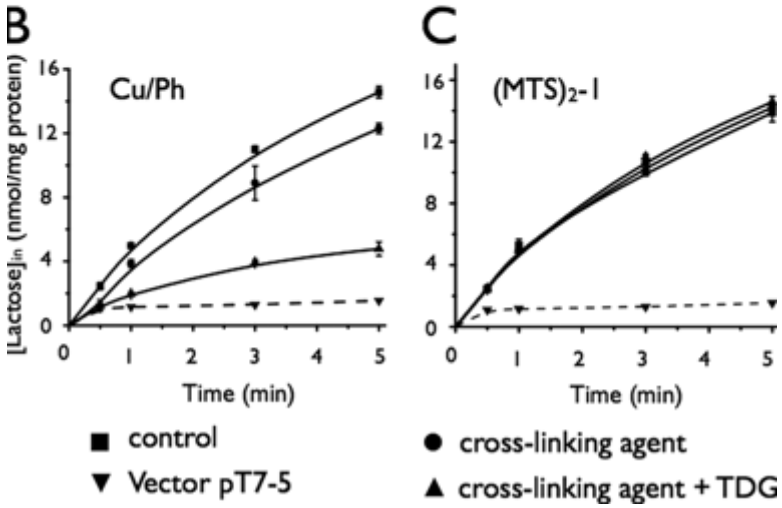

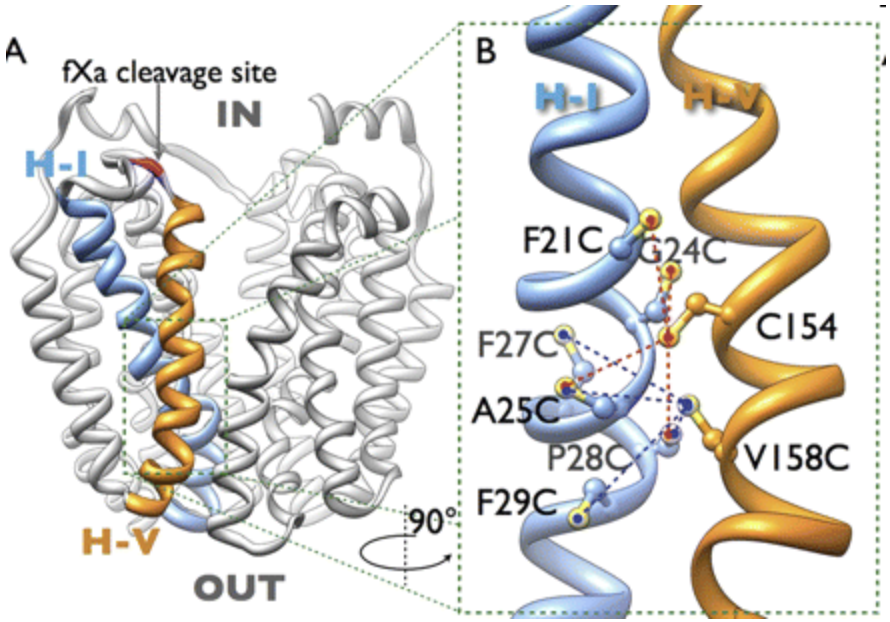

Zhou et al., 2011

Still-open questions

1. wild-type permease crystals (Guan et al., 2007); C154G mutant
2. more specified input from site-directed technology (Kaback, 2011)
3. Remaining conformations; link structure with function?
4. Resolution (3 Angstrom limit). Path of the proton?

Mechanism model

- **Recognition-part (substrate binding interactions)**
- **Conformation-part (protein turnover during the «catalytic» cycle)**
- **Energetics-part (proton-driven symport)**

Code: red, solved; purple, modeled; blue, unsolved

Binding site residues

Binding site residues

"before the structure"

Active site mapping (E269) - MS

Weinglass *et al.*, *EMBO J* 22, 1467 (2003)

The substrate-binding site (D126, R144)

Venkatesan & Kaback, *PNAS* 95, 9802 (1998)

C148 is a component of the binding site

Wu & Kaback, *Biochemistry* 33, 12166 (1994)

Η Cys-148 προστατεύεται πλήρως από αλκυλίωση με μια σειρά SH-αντιδραστηρίων παρουσία υποστρώματος (και από απενεργοποίηση)

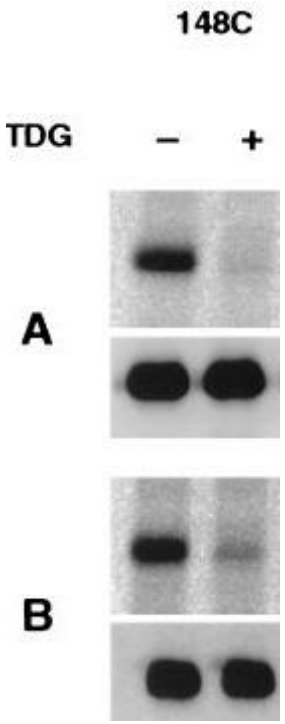

NEM

MTSES, MTSEA (solvent)

MIANS (fluorescent)

et al.

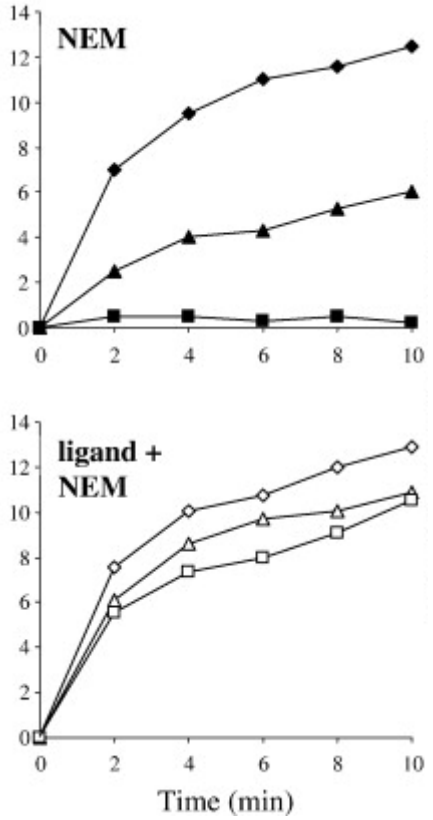

Frillingos & Kaback, 1996

Wu & Kaback, 1994

Ο συνδυασμός του Cys-148 με μεταλλαγές στις θέσεις Arg-144/Asp-126 οδηγεί σε <u>πλήρη</u> απώλεια της «αίσθησης» του υποστρώματος

Ι. Δεν δεσμεύεται (δεν προστατεύεται η Cys148)

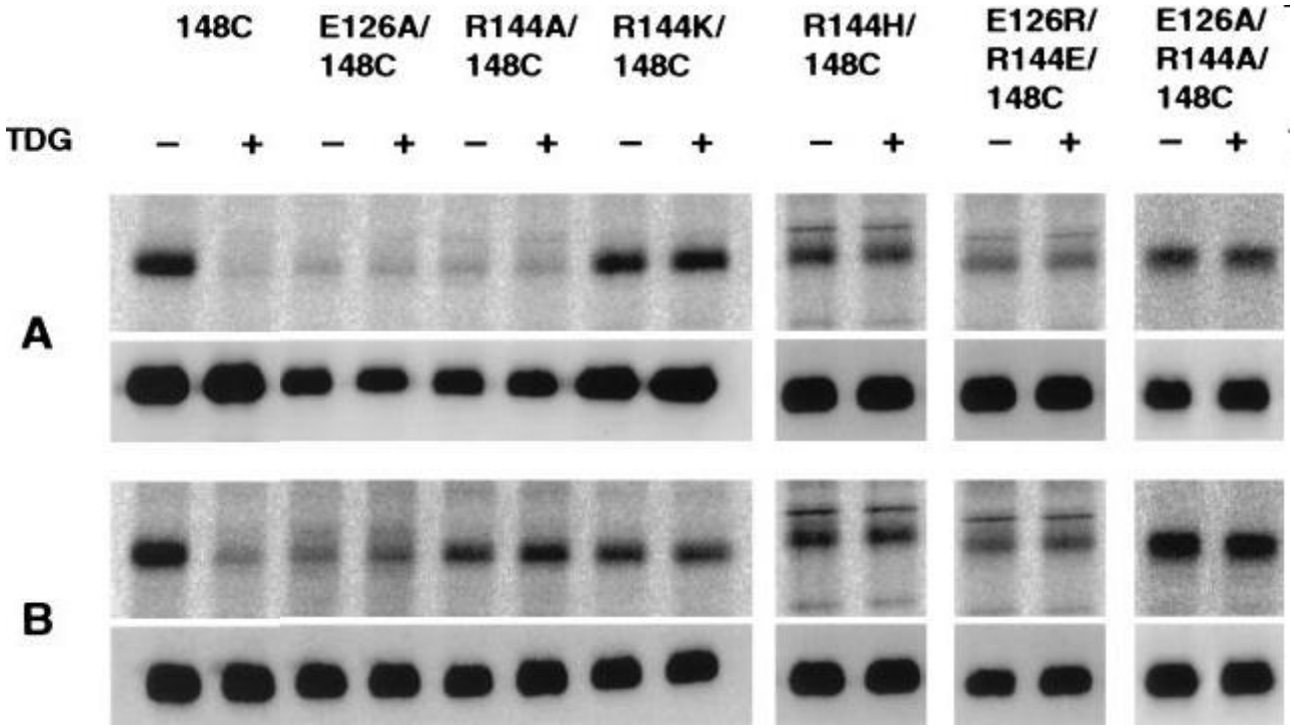

Venkatesan & Kaback, 1998

Ο συνδυασμός του Cys-148 με μεταλλαγές στις θέσεις Arg-144/Asp-126 οδηγεί σε <u>πλήρη</u> απώλεια της «αίσθησης» του υποστρώματος

ΙΙ. Δεν συμβαίνουν οι αναμενόμενες αλλαγές διαμόρφωσης

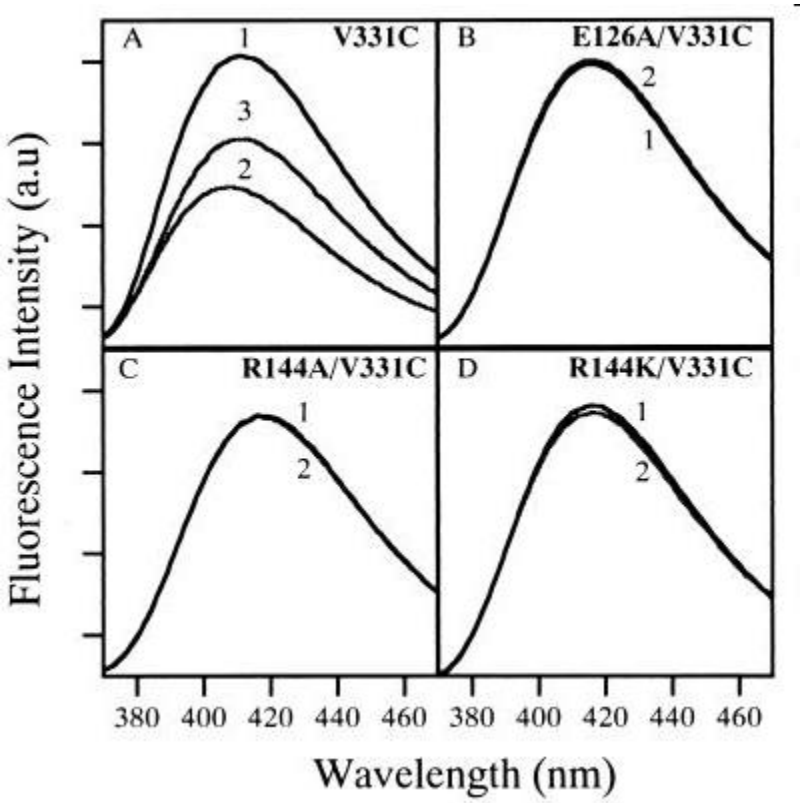

Venkatesan & Kaback, 1998

Lactose permease
Binding site

SITE-DIRECTED EVIDENCE

Arg144 (helix V)
Glu126 (helix IV)
Ala122 (helix IV)
Trp151 (helix V)

previous

CYS-SCANNING TECHNOLOGY

Native Cys residues

Cys148 (transmembrane α-helix V)

SH-modification reagents
(N-ethyl maleimide)

Effect of substrate / high-affinity ligand

current

ESI-MS, CARBODIIMIDES TECH

CNBr - peptides

Glu269 (transmembrane α-helix VIII)

Mass Spec

Effect of substrate / high-affinity ligand

EMBO J. 2003 Apr 1;22(7):1467-77. Links

Elucidation of substrate binding interactions in a membrane transport protein by mass spectrometry.

Weinglass AB, Whitelegge JP, Hu Y, Verner GE, Faull KF, Kaback HR.
Department of Physiology, Molecular Biology Institute, University of California Los Angeles, Los Angeles, CA 90095-1662, USA.

Integration of biochemical and biophysical data on the lactose permease of Escherichia coli has culminated in a molecular model that predicts substrate-protein proximities which include interaction of a hydroxyl group in the galactopyranosyl ring with Glu269. In order to test this hypothesis, we studied covalent modification of carboxyl groups with carbodiimides using electrospray ionization mass spectrometry (ESI-MS) and demonstrate that substrate protects the permease against carbodiimide reactivity. Further more, a significant proportion of the decrease in carbodiimide reactivity occurs specifically in a nanopeptide containing Glu269. In contrast, carbodiimide reactivity of mutant Glu269-->Asp that exhibits lower affinity is unaffected by substrate. By monitoring the ability of different substrate analogs to protect against carbodiimide modification of Glu269, it is suggested that the C-3 OH group of the galactopyranosyl ring may play an important role in specificity, possibly by H-bonding with Glu269. The approach demonstrates that mass spectrometry can provide a powerful means of analyzing ligand interactions with integral membrane proteins.

PMID: 12660154 [PubMed - indexed for MEDLINE]

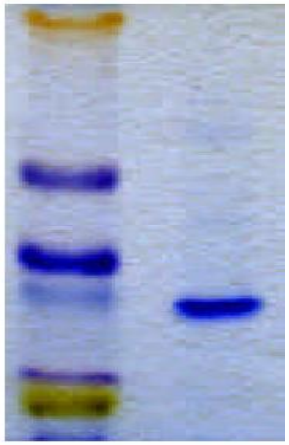

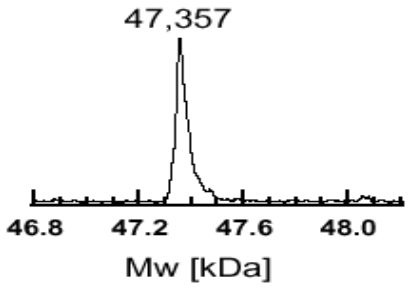

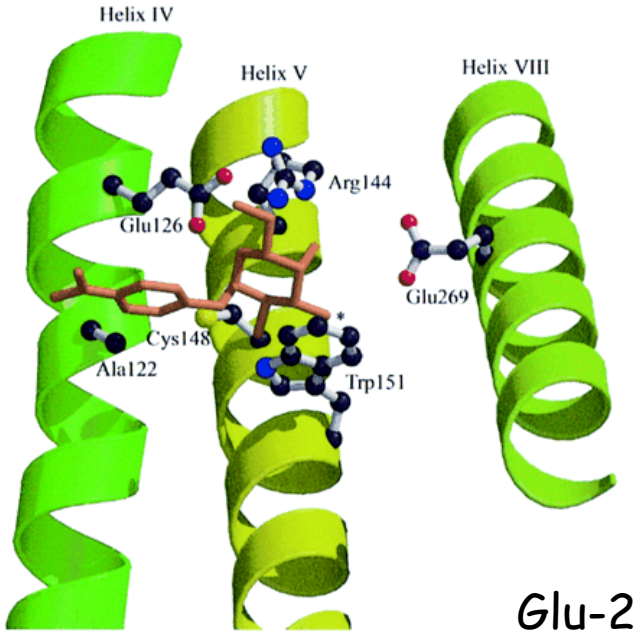

Glu-269 (TM8): Αναντικατάστατο!!

Πρωτεόλυση με βρωμιούχο κυάνιο (Met-): πεπτίδιο-9 που περιέχει το Glu-269

Φασματομετρία μαζών

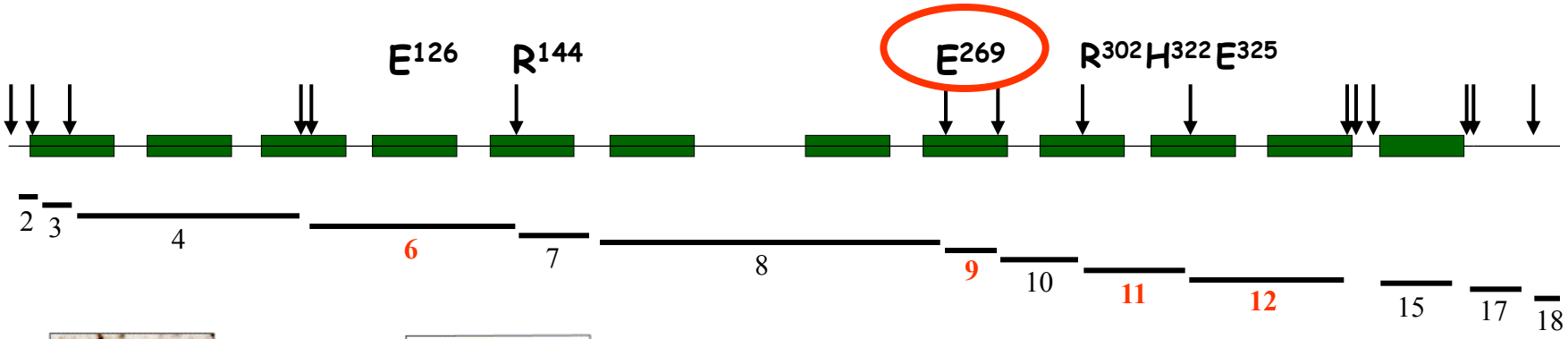

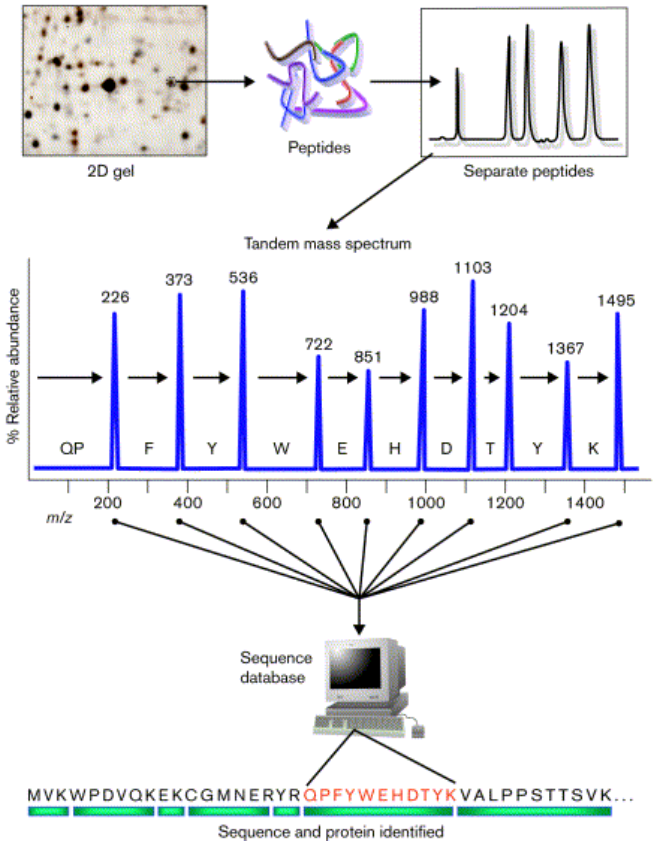

Peptide	M_{exp}	M_{obt}
1 (1)	102.1	N.D.
2 (2-13)	1331.5	1332.7
3 (12-23)	1577.9	1578.9
4 (24-83)	6810.1	6809
5 (84-86)	313.4	N.D.
6 (87-145)	**6503.6**	**6503**
7 (146-161)	1574.9	1573
8 (162-267)	11636.3	11666.3 (SE)
9 (268-276)	**899.4**	**899.7**
10 (277-299)	2395.9	2396
11(300-323)	**2525**	**2525.1**
12 (324-362)	**4541.3**	**4540**
13 (363-365)	361.4	N.D.
14 (366-372)	642.7	N.D.
15 (373-466)	9095.5	9097.3 (SE)
16 (467-468)	229.3	N.D.
17 (469-498)	2923.3	2922.4
18 (499-517)	2077.4	2079

Ομοιοπολική τροποποίηση του Glu-269 με καρβοδιϊμίδιο: πεπτίδιο-9 + 126 Da

Φασματομετρία μαζών

DiPC

COO⁻

LacY

Glu269

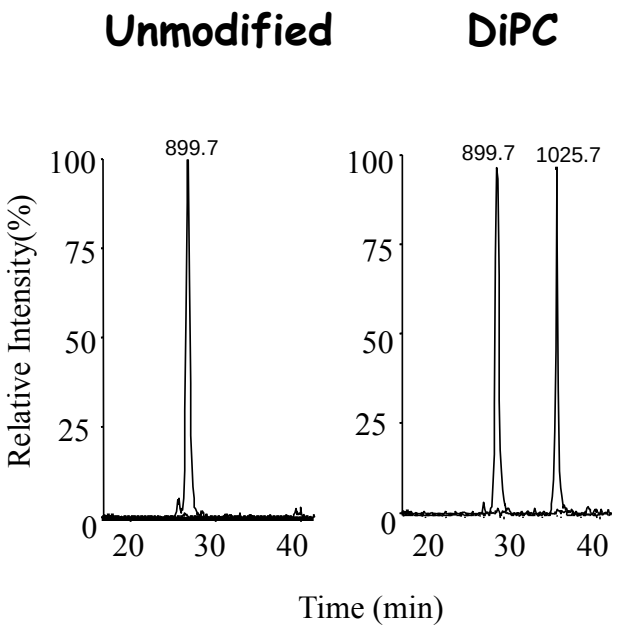

+126 Da

CO-urea

LacY

Glu269

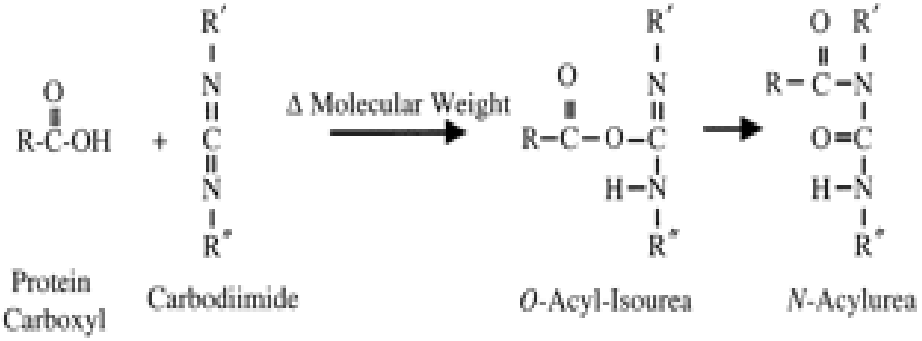

Ομοιοπολική τροποποίηση του Glu-269 με καρβοδιϊμίδιο παρουσία NPGal

Φασματομετρία μαζών

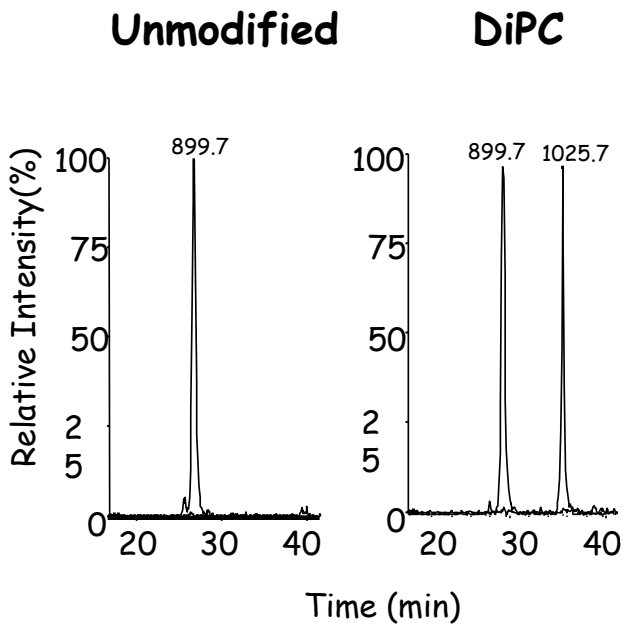

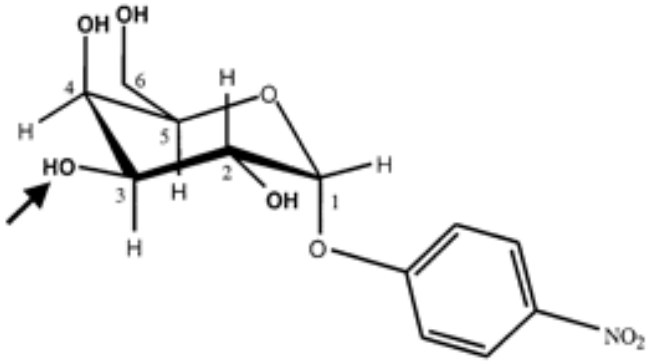

NPGal

Το Glu-269 προστατεύεται από τροποποίηση με καρβοδιϊμίδιο παρουσία NPGal

Φασματομετρία μαζών

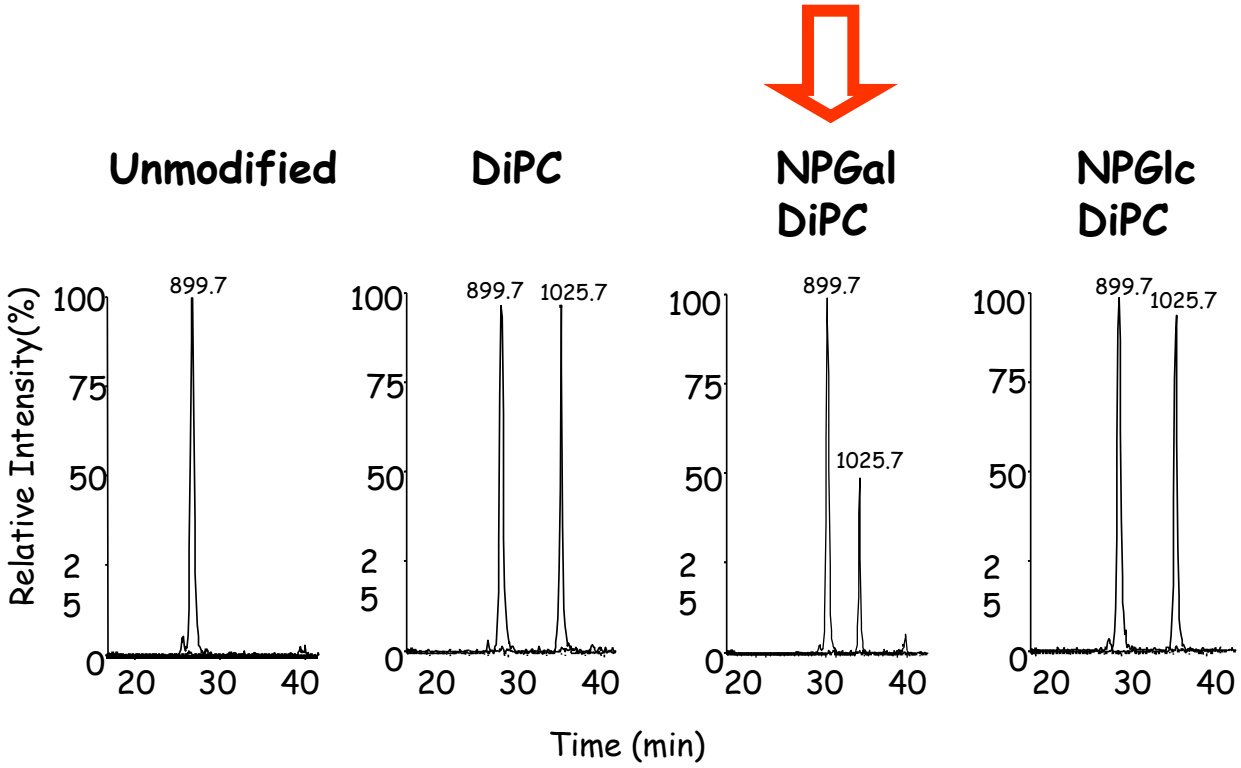

Binding site residues

"after the structure"

Active site mapping (W151) - FRET

Smirnova *et al.*, *Biochemistry* 45, 15279 (2006)

Structure with suicide substrate (A122) – MTS-Gal

Chaptal *et al.*, *PNAS* 108, 9361 (2011)

Αντίθετα με την Cys-148, η Ala-122Cys προστατεύεται από αλκυλίωση, αλλά όχι με όλα τα υποστρώματα (δεν προστατεύεται με γαλακτόζη)

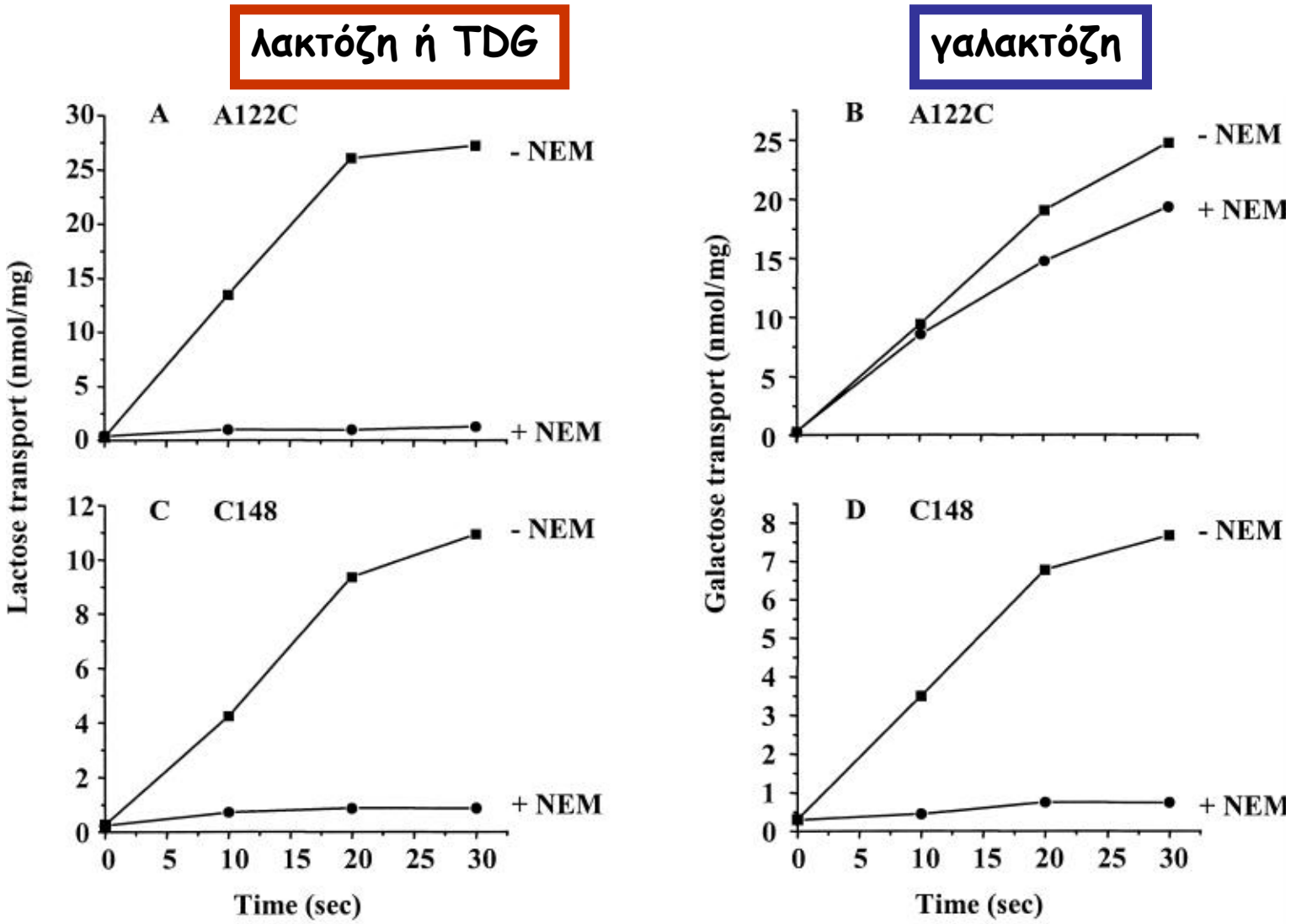

Guan et al., 2002

Αντικατάσταση της Ala-122 με μία ογκώδη πλευρική ομάδα (Phe,Tyr) «δημιουργεί» ένα μόριο LacY που δεν μεταφέρει λακτόζη, <u>αλλά μόνο γαλακτόζη</u>

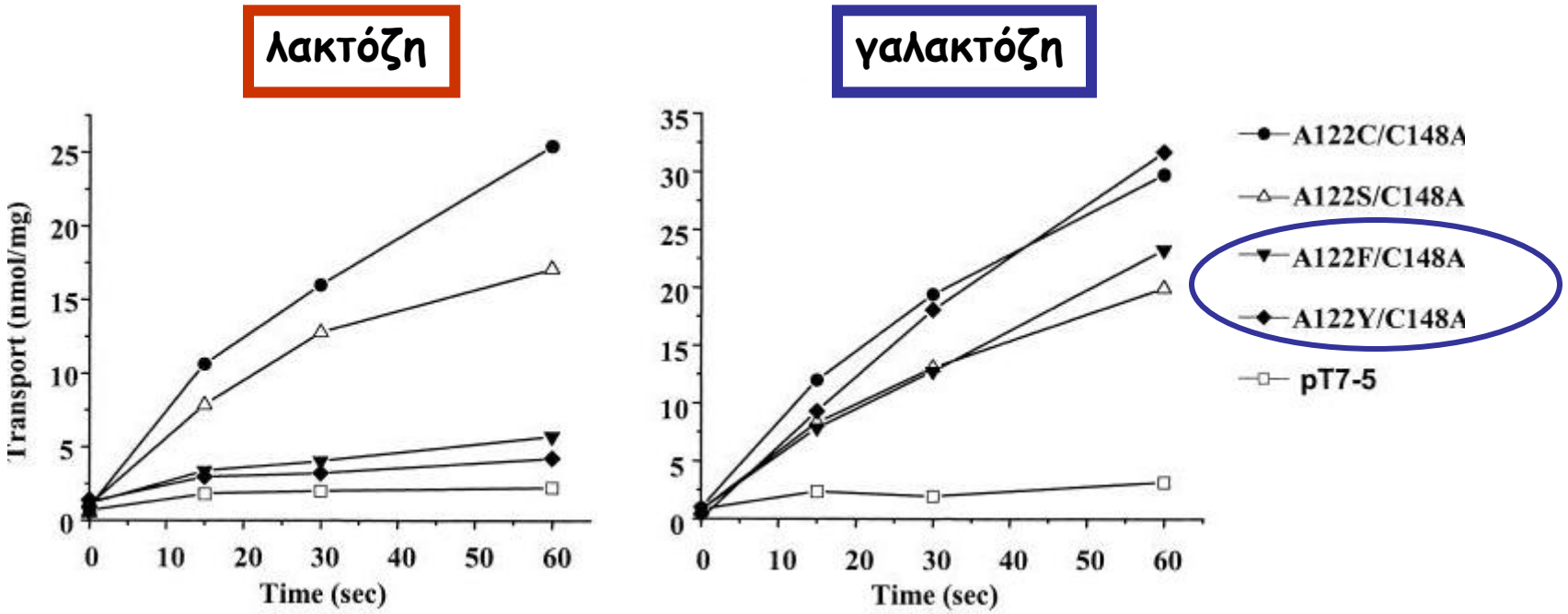

Guan et al., 2002

Απενεργοποίηση της LacY μέσω ενός υποστρώματος (MTS-Gal) που συνδέεται συγχρόνως ομοιοπολικά στην Ala-122 (affinity inactivator)

MTS-galactoside

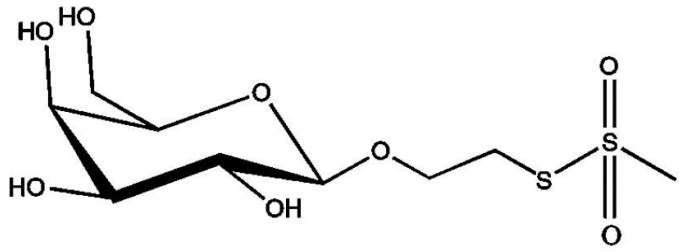

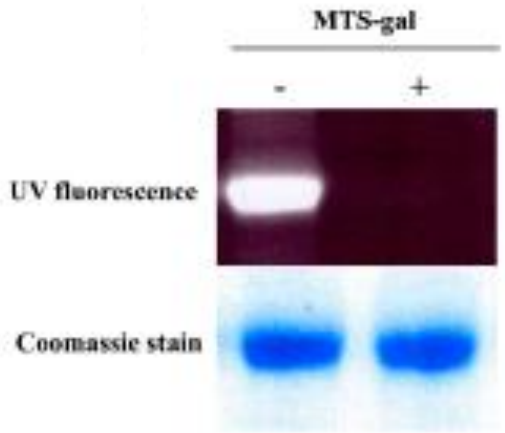

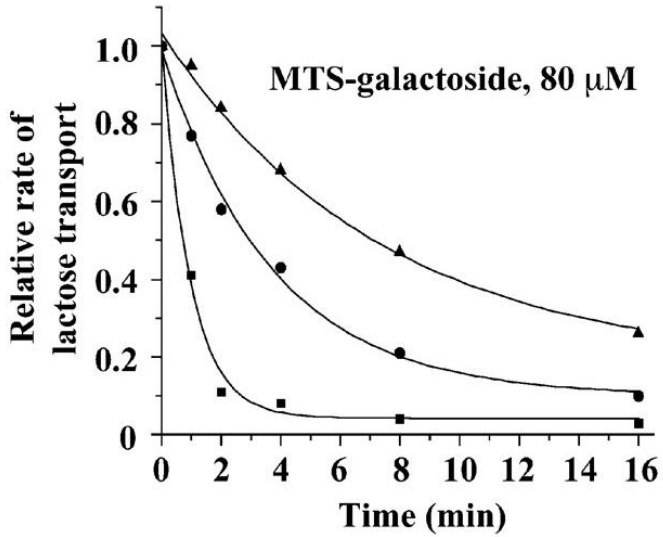

Guan et al., 2003

Συγκρυστάλλωση της LacY (Ala-122Cys) με το υπόστρωμα MTS-Gal

MTS-galactoside

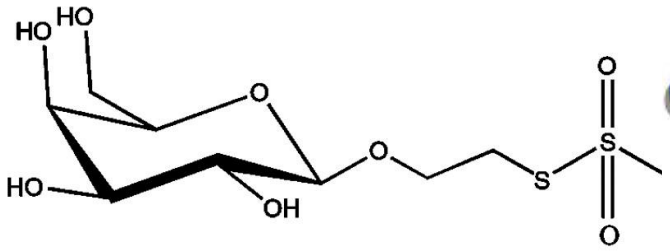

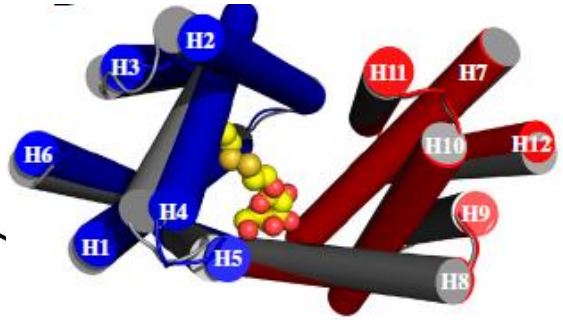

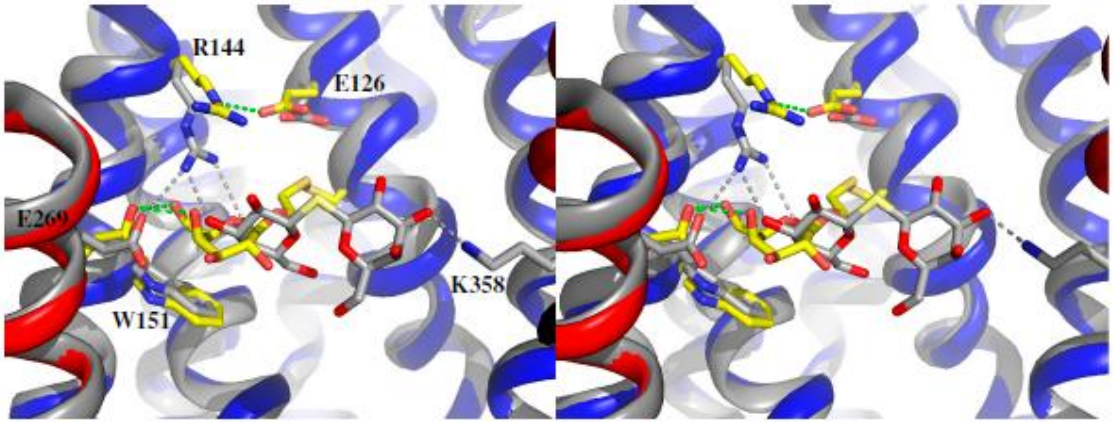

Chaptal et al., 2011

Biochemistry. 2006 Dec 26;45(51):15279-87. Epub 2006 Nov 29

Direct Sugar Binding to LacY Measured by Resonance Energy Transfer.

Smirnova IN, Kasho VN, Kaback HR.
Department of Physiology and Microbiology, Immunology & Molecular Genetics, Molecular Biology Institute, University of California Los Angeles, Los Angeles, California 90095-7327.

Trp151 in the lactose permease of Escherichia coli (LacY) is an important component of the sugar-binding site and the only Trp residue out of six that is in close proximity to the galactopyranoside in the structure (1PV7). The short distance between Trp151 and the sugar is favorable for Förster resonance energy transfer (FRET) to nitrophenyl or dansyl derivatives with the fluorophore at the anomeric position of galactose. Modeling of 4-nitrophenyl-alpha-d-galactopyranoside (alpha-NPG) in the binding-site of LacY places the nitrophenyl moiety about 12 A away from Trp151, a distance commensurate with the Förster distance for a Trp-nitrobenzoyl pair. We demonstrate here that alpha-NPG binding to LacY containing all six native Trp residues causes galactopyranoside-specific FRET from Trp151. Moreover, binding of alpha-NPG is sufficiently slow to resolve time-dependent fluorescence changes by stopped-flow. The rate of change in Trp --> alpha-NPG FRET is linearly dependent upon sugar concentration, which allows estimation of kinetic parameters for binding. Furthermore, 2-(4'-maleimidylanilino)naphthalene-6-sulfonic acid (MIANS) covalently attached to the cytoplasmic end of helix X is sensitive to sugar binding, reflecting a ligand-induced conformational change. Stopped-flow kinetics of Trp --> alpha-NPG FRET and sugar-induced changes in MIANS fluorescence in the same protein reveal a two-step process: a relatively rapid binding step detected by Trp151 --> alpha-NPG FRET followed by a slower conformational change detected by a change in MIANS fluorescence.
PMID: 17176050 [PubMed - in process]

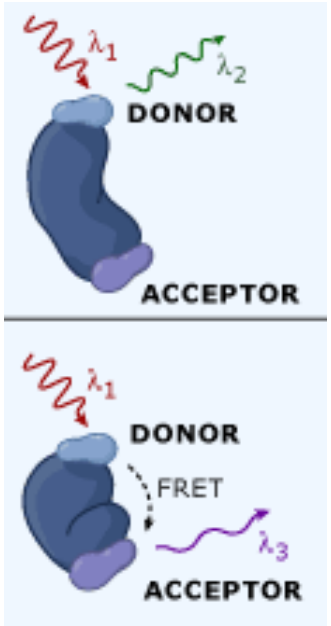

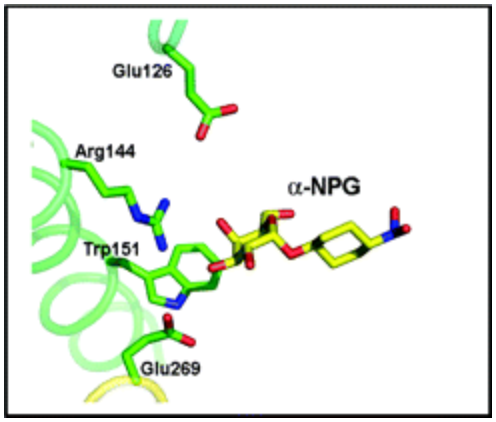

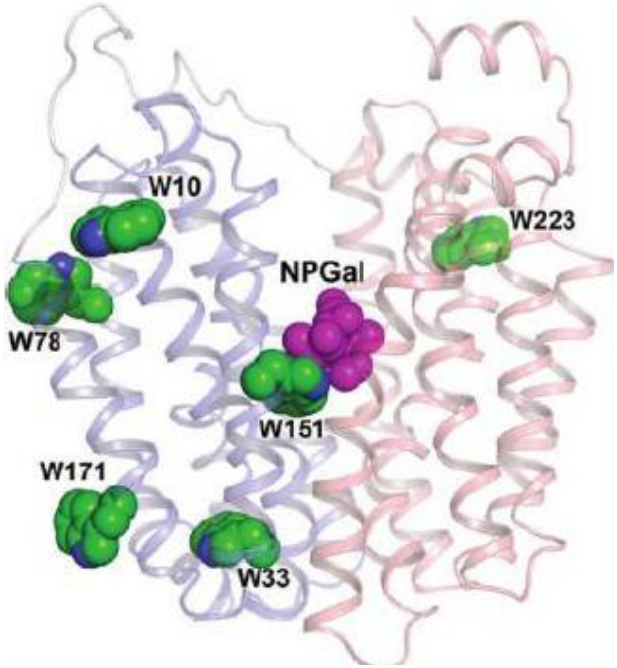

W151→α-NPG FRET evidence of substrate binding

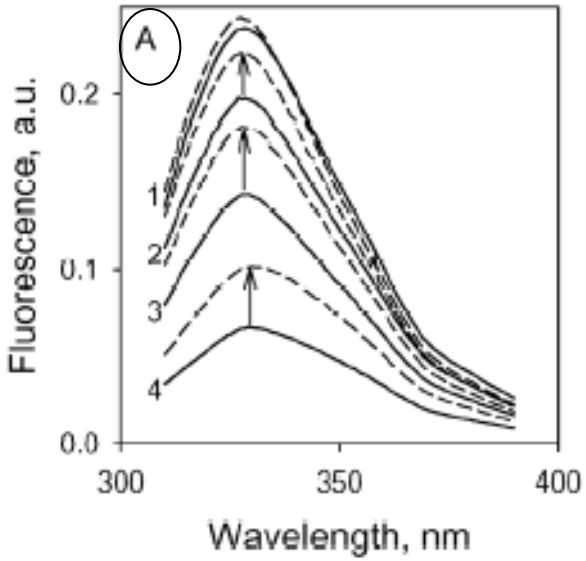

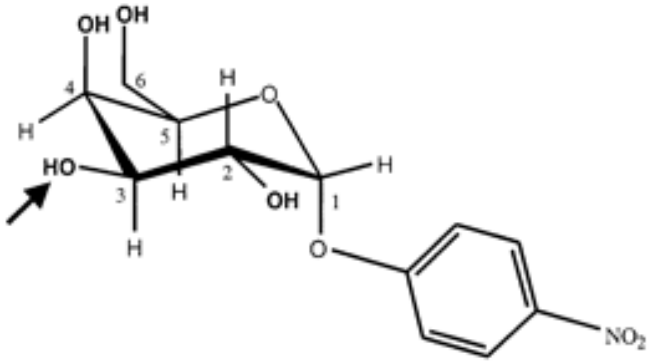

NPGal

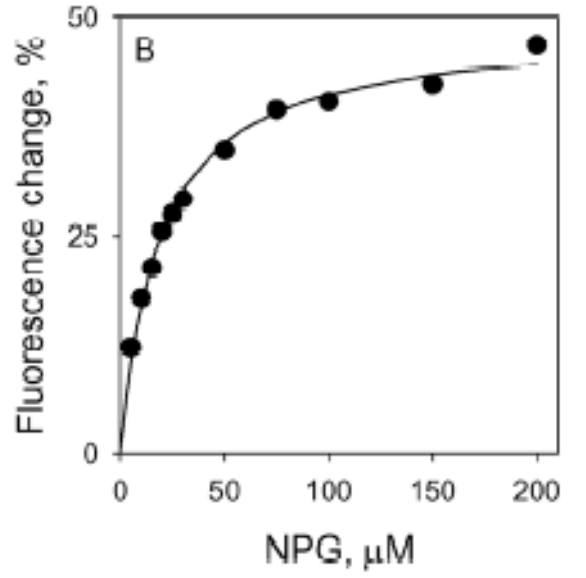

Solid lines: 5 – 50 μM α-NPG
Broken lines: displacement with TDG (10 mM) to distinguish FRET from inner-filter effect

Intrinsic Trp fluorescence (excitation 295 nm); absorption maximum of α-NPG at 306 nm

W151→α-NPG FRET data on binding specificity

Upper panel: different LacY variants

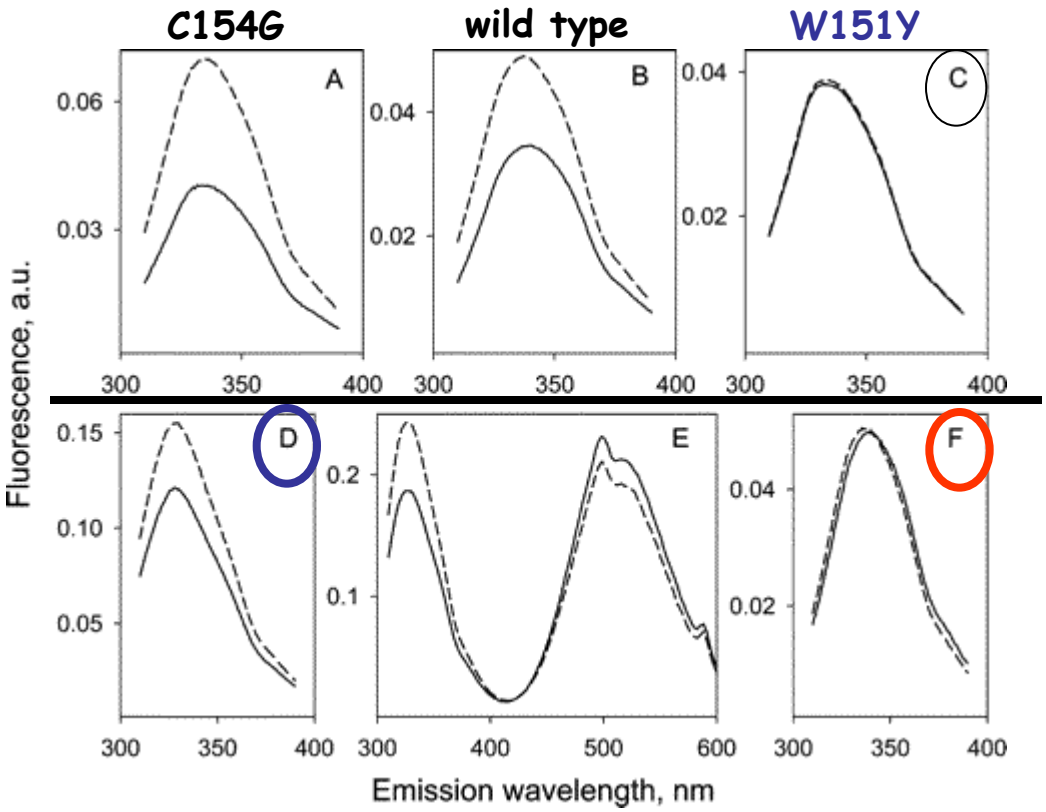

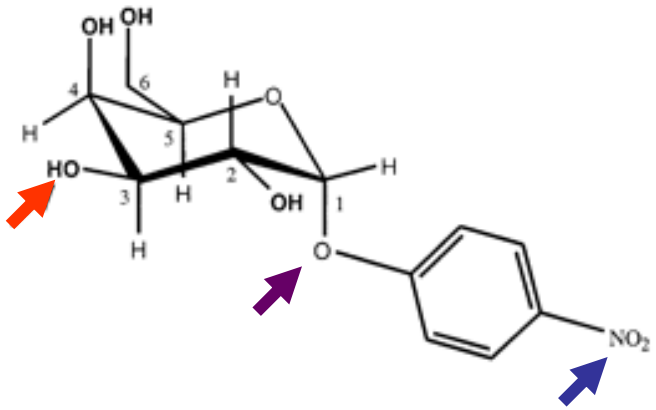

NPGal

A-C: (para) α-NPG
A: C154G ; B: wt ; C: W151Y/C154G

D: ortho α-NPG
E: FRET acceptor emission (Dns^{6}Gal)
F: α- or β-NPGlc, ortho or para β-NPG

Lower panel: different NPGal analogs

Six native Trp residues

W151→MIANS(Cys331) FRET evidence of conformation change

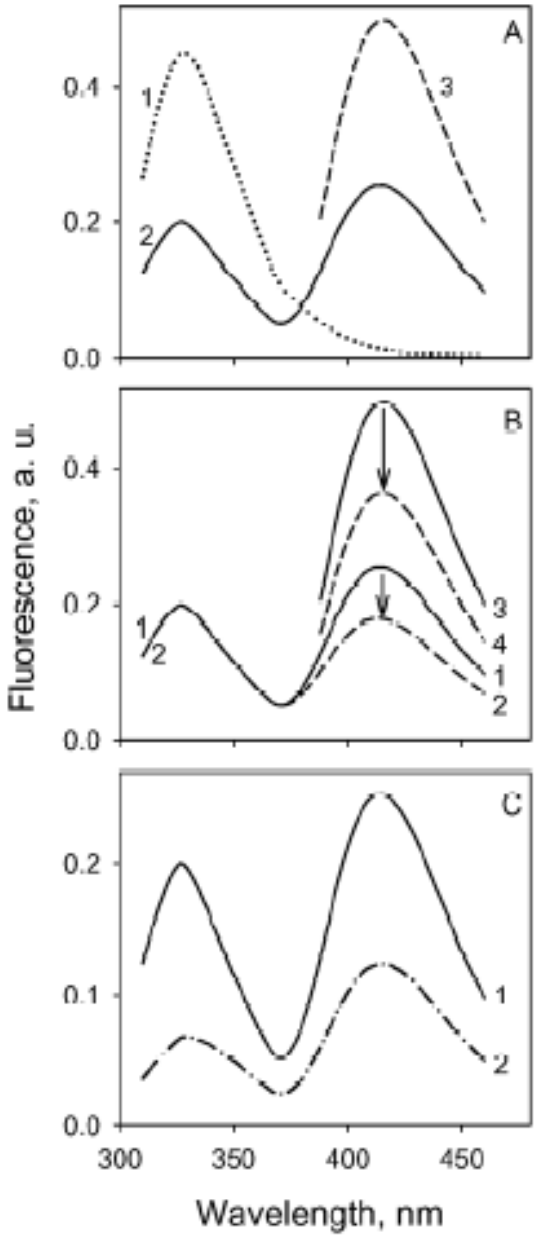

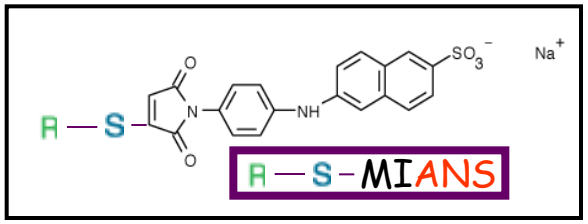

C154G/V331C LacY

A:
1: unlabeled, no substrate (exc. 295 nm)
2: MIANS-labeled, no substrate, exc. 295 nm
3: MIANS-labeled, no substrate, exc. 330 nm

B: MIANS-labeled
1: no substrate, exc. 295 nm
2: TDG, exc. 295 nm
3: no substrate, exc. 330 nm
4: TDG, exc. 330 nm

C: MIANS-labeled, exc. 295 nm
1: no α-NPG
2: with α-NPG

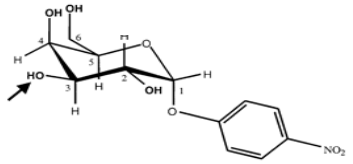

NPGal

CONCLUSIONS

LacY is a "prototype" for many transport proteins

…in structural features, mechanistic implications,

& research strategies

Many secondary active transporters can be threaded (modeled) to the known structure of LacY

…and allow meaningful interpretation of experimental data

Approaches used
in the research of LacY
are a guidance for

… developing strategies
to study other, unrelated or
distantly-related transporters

BIBLIOGRAPHY

Essential reading for the lesson

A chemiosmotic mechanism of symport

Kaback HR, *PNAS* 112, in press (2015)

http://www.ncbi.nlm.nih.gov/pubmed/25568085

Structure of Lactose Permease and a Chemiosmotic Mechanism of Symport

H. Ronald Kaback

Departments of Physiology and Microbiology, Immunology & Molecular Genetics, Molecular Biology Institute, University of California Los Angeles, Los Angeles, California 90095.

Lactose permease (LacY) catalyzes the coupled translocation of a galactoside and an H+ across the membrane of Escherichia coli (galactoside/H+ symport). Initial x-ray structures reveal N- and C-terminal domains, each with six largely irregular transmembrane helices surrounding an aqueous cavity open to the cytoplasm. Recently, a structure with a narrow periplasmic opening and an occluded, galactoside was obtained, which confirms many observations and indicates that sugar binding involves induced-fit. Residues involved in sugar and H+ transport become exposed reciprocally in the inward- or outward-open conformation allowing alternating access from either side of the membrane. The findings indicate: (i) The limiting step for lactose/H+ symport in the absence of the H+ electrochemical gradient (ΔμH+) is deprotonation, whereas in the presence of ΔμH+, the limiting step is probably opening of apo LacY on the other side of the membrane. (ii) LacY must be protonated to bind galactoside (pK for binding is ~10.5). (iii) Galactoside binding and dissociation--not ΔμH+--are the driving force for alternating access. (iv) Galactoside binding involves induced fit causing transition to an occluded intermediate that undergoes alternating access. (v) Galactoside dissociates, releasing the energy of binding. (vi) Arg302 comes into proximity with protonated Glu325 causing deprotonation. Accumulation of galactoside against a concentration gradient does not involve a change in KD on either side of the membrane, but the pKa (the affinity for H+) decreases markedly. Thus, transport is driven chemiosmotically, but contrary to expectation, ΔμH+ acts kinetically to control the rate of the process.

X-ray crystal structure | membrane proteins | transport | conformational change | MFS

The lactose permease of *Escherichia coli* (LacY), a paradigm for the Major Facilitator Superfamily (MFS), specifically binds and catalyzes symport of D-galactose and D-galactopyranosides with an H^+, but does not recognize the analogous glucopyranosides, which differ only in the orientation of the C4-OH of the pyranosyl ring (reviewed in 1, 2).

Typical of many MFS members, LacY couples the free energy released from downhill translocation of H^+ in response to an H^+ electrochemical gradient ($\Delta\tilde{\mu}_H+$) to drive accumulation of galactopyranosides against a concentration gradient. Since coupling between sugar and H^+ translocation is obligatory, in the absence of $\Delta\tilde{\mu}_H+$, LacY can also transduce the energy released from the downhill transport of sugar to drive uphill H^+ transport with the generation of $\Delta\tilde{\mu}_H+$, the polarity of which depends upon the direction of the sugar gradient. However, the mechanism by which this chemiosmotic process occurs remains obscure. This contribution aims at clarifying the specific steps underpinning the chemiosmotic mechanism of lactose/H^+ symport.

Structural evidence for an occluded intermediate. Initial x-ray structures of LacY were obtained with a conformationally restricted mutant C154G (3, 4) and WT LacY (5), and they are in an indistinguishable inward-facing conformation (**Fig. 1**). At the same time, a similar structure was determined for the glycerol-3-phosphate permease (GlpT) (6), which catalyzes phosphate/glycerol-3-phosphate exchange. The structures consist of two 6-helix bundles related by a quasi two-fold symmetry axis perpendicular to the membrane plane, linked by a long cytoplasmic loop between helices VI and VII. Furthermore, in each 6-helix bundle, there are two 3-helix bundles with inverted symmetry. The two 6-helix bundles surround a deep hydrophilic cavity tightly sealed on the periplasmic face and open to the cytoplasmic side only (an inward-open conformation). The initial structures led to the so-called "rocker-switch" model for transport in which the two 6-helix bundles rotate against each other around the middle of the protein, thereby exposing the substrate-binding site alternatively to either side of the membrane (*aka*, the alternating access model).

Although LacY contains 65-70% unequivocally hydrophobic side chains and crystal structures reflect only a single lowest energy conformation, the entire backbone appears to be accessible to water (7-9). In addition, an abundance of biochemical and spectroscopic data demonstrates that galactoside binding causes the molecule to open reciprocally on either side of the membrane, thereby providing almost unequivocal evidence for an alternating-access model {see below}. The first structure of LacY was obtained with a density at the apex of the central cavity, but because of limited resolution, the identity of the bound sugar and/or side-chain interactions were difficult to specify with certainty. However, biochemical and spectroscopic studies show that LacY contains a single galactoside-binding site and that the residues involved in sugar binding are located at or near the apex of the central, aqueous cavity in the approximate middle of the molecule.

Among the conserved residues in LacY and many other MFS members are two Gly-Gly pairs between the N- and C-terminal 6-helix bundles on the periplasmic side of LacY at the ends of helices II and XI (Gly46 and Gly370, respectively) and helices V and VIII (Gly159 and Gly262, respectively) (10). When Gly46 (helix II) and Gly262 (helix VIII) are replaced with bulky Trp residues (**Fig. 2**), transport activity is abrogated with little or no effect on galactoside affinity, but markedly increased accessibility of galactoside to the binding site is observed indicating that the G46W/G262W mutant is open on the periplasmic side (11). Moreover, site-directed alkylation and stopped-flow binding kinetics indicate that the G46W/G262W mutant is physically open on the periplasmic side (an outward-open conformation).

An x-ray structure of LacY mutant G46W/G262W co-crystallized in the presence of the relatively high-affinity, symmetrical lactose analogue β-D-galactopyranosyl-1-thio-β-D-galactopyranoside (TDG) was determined to 3.5-Å resolution, and importantly, crystals were not obtained in the absence of a galactoside (12). Two molecules in the asymmetric unit are adjacent to one another, but in opposite-facing orientations. Surprisingly, both molecules are in an almost occluded conformation with a narrow periplasmic opening and a single molecule of TDG in the central sugar-binding site. A space-filling view of the molecule from the periplasmic side (**Fig. 3**) reveals the bound TDG through

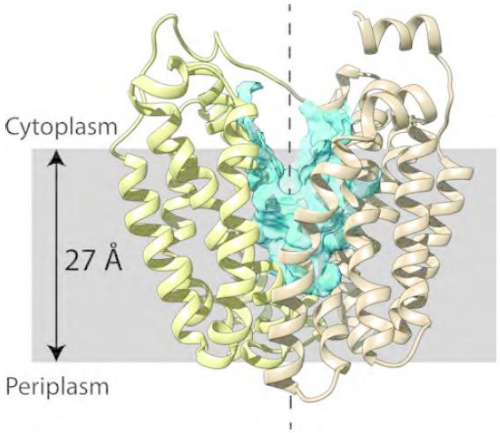

Fig. 1. LacY ribbon presentation in an inward-open conformation with a 2-fold axis of symmetry (broken line). Left, N-terminal helix bundle, light yellow; right, C-terminal helix bundle, tan. Cytoplasmic side at top. Blue region, hydrophilic cavity. Gray shaded area, membrane.

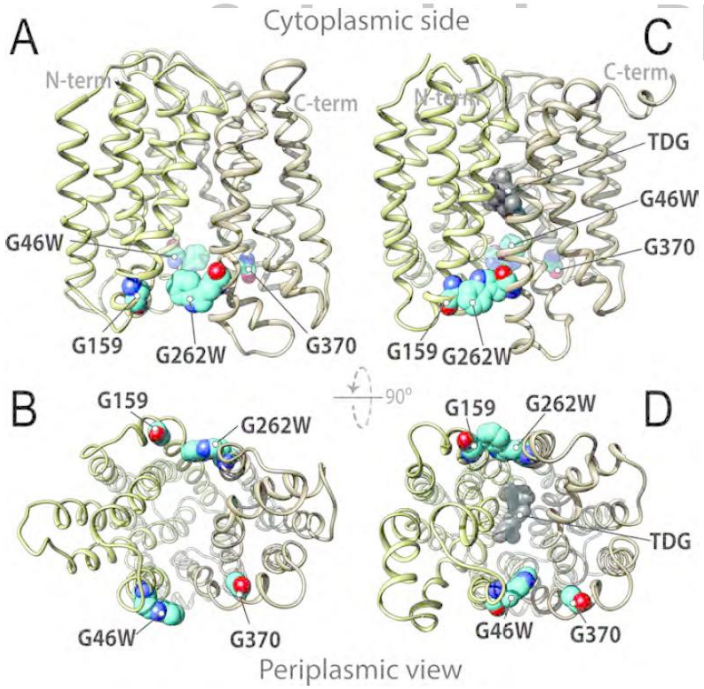

Fig. 2. Trp replacements in two pairs of Gly–Gly residues that connect the N- and C-terminal six-helix domains on the periplasmic side of LacY. The 12 transmembrane helices that make up LacY are light yellow (N-terminal bundle) and tan (C-terminal bundle). Gly residues 159 and 370 in helices V and XI, respectively, and Trp replacements G46W (helix II) and G262W (helix VIII) are indicated. The putative outward-open X-ray structure is viewed from the side (A) or from the periplasm (B). The crystal structure of the almost occluded, narrow outward-open conformer of LacY with Gly→Trp replacements at positions 46 and 262 and bound galactoside (dark gray) are viewed from the side (C) or the periplasm (D), respectively.

an opening that is too narrow to allow entrance or exit of the sugar (~3 Å at the narrowest point; Fig. 3B) (13). In contrast, the cytoplasmic side of the molecule is tightly sealed (Fig. 3C). The double-Trp mutant is sufficiently open to bind galactoside rapidly (11), but when binding occurs and the mutant attempts to transition into an occluded state, it cannot do so completely because the bulky Trp residues block complete closure. Thus, the mutant binds galactoside, which initiates transition into an intermediate occluded state, which it cannot complete, and this accounts for why the mutant is completely unable to catalyze transport of any type across the membrane. Therefore, it is apparent that the transport cycle includes an occluded intermediate conformer.

A TDG molecule is clearly defined in the almost occluded central cavity (**Fig. 4**) that allows assignment of likely H-bond interactions with the protein, although interatomic distances are only estimates at

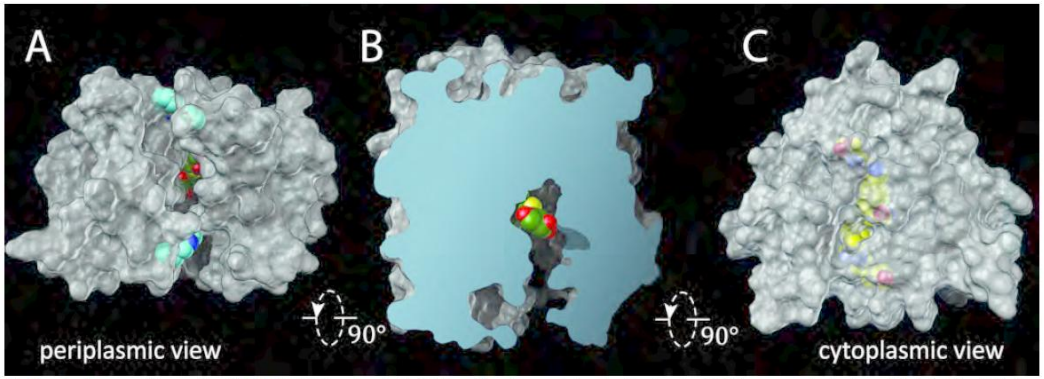

Fig. 3. : Surface renditions of LacY G46W/G262W molecule A. (A) View from the periplasmic side showing TDG (green and red spheres) just visible within the molecule; Trp residues shown in blue. (B) Slab view. (C) View from the cytoplasmic side with the residues that form a zipper-like motif to seal that side.

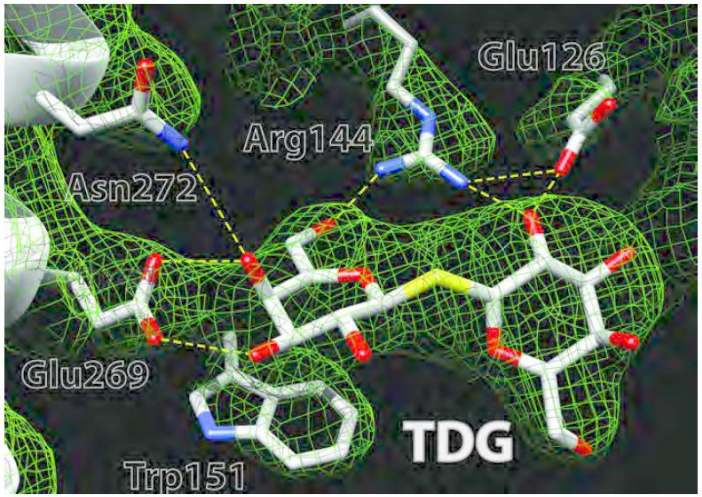

Fig. 4. : Electron density map contoured at 1σ (green mesh) of the sugar-binding site of LacY G46W/G262W. The density is superimposed on the structure, which is shown as sticks, with carbon atoms in gold, oxygen atoms in red, and nitrogen atoms in blue. Broken lines represent putative H bonds.

3.5-Å resolution. Specificity is directed towards the galactopyranoside ring, and α-galactosides bind with higher affinity than the β-anomers (14-18). One galactopyranosyl ring of TDG stacks hydrophobically with Trp151 (helix V), confirming biochemical (19) and spectroscopic (20) findings. Glu269 (helix VIII) is the acceptor of H bonds from the C4-OH and C3-OH groups of the galactopyranosyl ring, indicating that it is probably the primary determinant for specificity. Even conservative replacement with an Asp abolishes binding and inactivates lactose transport (21-23). The η1 NH_2 of Arg144 (helix V) donates an H bond to O5 in the ring and is also within H-bond distance of the C6-OH. The η2 NH_2 group of Arg144 donates H bonds to the C2'-OH of TDG and to Glu126 Oε2. Conservative replacement of Arg144 with Lys, as well as neutral replacements, virtually destroys binding and transport (23, 24). Glu126 (helix IV) acts as an H-bond acceptor from the C2'-OH of TDG and is an H-bond acceptor from theη2 NH_2 of Arg144. Replacement with Asp causes markedly diminished binding affinity and little or no transport activity; removal of the carboxyl group abolishes binding and transport (23, 25, 26).

Remarkably, His322 (helix X), long thought to be involved in H^+ transport by implication, likely acts as an H-bond donor/acceptor between the εNH of the imidazole ring and the C3-OH of TDG, and is stabilized by an H-bond donor/acceptor between the δNH of the imidazole and the OH of Tyr236, which was also thought to be involved in H^+ transport (**Fig. 5**). All replacements for His322 exhibit little or no binding and no transport activity (23, 25, 26). Finally, Asn272 (helix VIII) donates an H bond to the C4-OH of TDG; Gln is the only replacement tolerated by LacY with respect to binding and transport (27).

In addition to the residues involved in galactoside binding, Cys148 (helix V), well known with respect to substrate protection against alkylation (reviewed in 28), is close to bound TDG, but not sufficiently close to interact directly (**Fig. 5**). Similarly, replacement of Ala122 (helix IV) with bulky side chains, or alkylation of A122C with bulky thiol reagents causes LacY to become specific for the

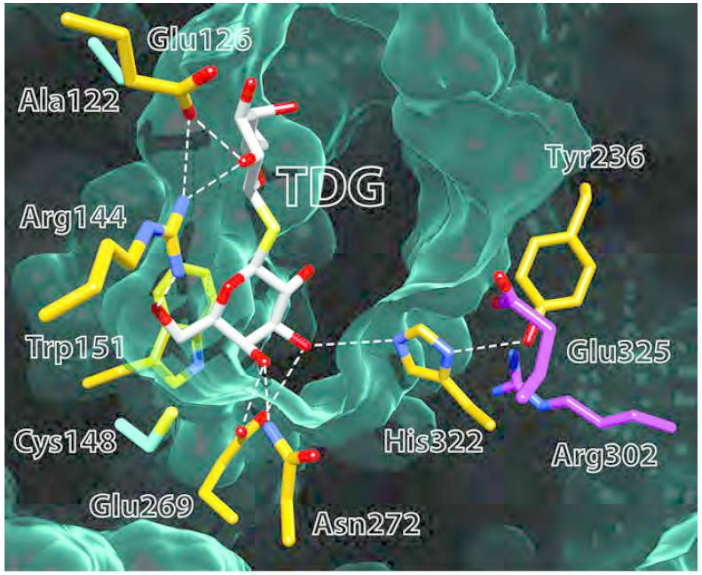

Fig. 5. . Cytoplasmic view of the active site in LacY. TDG is shown as green sticks, and side chains forming H bonds with TDG are in yellow. Broken lines represent likely H bonds. Ala122 and Cys148, which are close to TDG but do not make direct contact, are shown in cyan. Glu325 and Arg302 are purple. The green, felt-like area represents the Van der Waals lining of the cavity. Note the narrow opening on the periplasmic side.

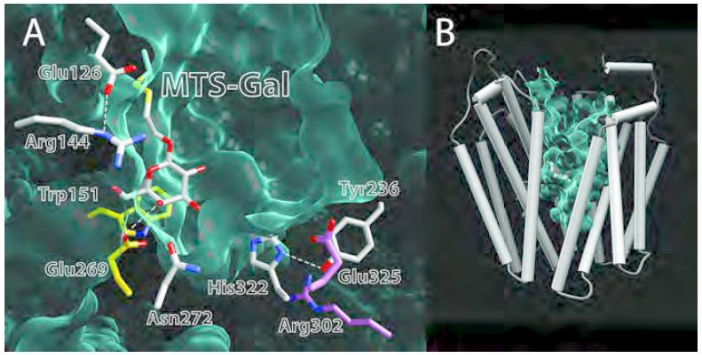

Fig. 6. Crystal structure of single-Cys122 LacY with covalently bound MTS-Gal. (A) Side chains are shown as sticks; those in yellow (Glu269 and Trp151) make direct contact with the galactopyranosyl ring of MTS-Gal covalently bound to a Cys at position 122. Side chains in gray are not sufficiently close to make contact with the galactopyranosyl ring. Glu325 and Arg302 (in purple) are involved in H^+ transport. The green, felt-like area represents the Van der Waals lining of the cavity. Note that the periplasmic side is closed. (B) Structure of single-Cys122 LacY with covalently bound MTS-Gal viewed from the side. Helices are depicted as rods, and MTS-Gal is shown as spheres colored by atom type with carbon in green. The aqueous central cavity open to the cytoplasmic side is colored light green.

monosaccharide galactose, and disaccharide binding and transport are blocked (29). However Ala122 does not make direct contact with TDG either. Asp240 (helix VII) and Lys 319 (helix X) interact relatively weakly (not shown), and mutants with double-neutral replacements (Cys or Ala) exhibit low but significant ability to catalyze lactose accumulation (30-32).

Although Glu325 (helix X) and Arg302 (helix IX) do not make direct contact with bound galactoside, both are critically involved in coupled H^+ translocation. Neutral replacement of either residue yields mutants that are defective in all transport reactions that involve net H^+ transport, but catalyze equilibrium exchange and/or counterflow as well or better than WT (1, 2).

Sugar binding involves induced fit. In the structure of single-Cys122 LacY with covalently bound MTS-Gal, a suicide inactivator for this mutant (33), the galactosyl moiety occupies the same position in the protein as in the double-Trp mutant (34). In addition, two important ligands—Trp151 and Glu269—interact with the galactopyranosyl ring (**Fig. 6A**). However, as opposed to the almost occluded, open-outward conformation of the double-Trp mutant, LacY with covalently bound MTS-Gal in the binding site exhibits an inward-open conformation (**Fig. 6B**), indicating that the galactoside must be fully liganded in order for LacY to transition into the occluded state. In view of this consideration and observations indicating that the alternating access mechanism of LacY is driven by galactoside binding and dissociation and not by $\Delta\tilde{\mu}_H+$ (1, 2, 35-37), it seems highly likely that sugar binding involves induced fit. By this means, the N- and C-terminal bundles converge as given side chains from both the N- and C-terminal helix bundles ligate the galactoside. The energetic cost of binding and the resultant conformational change is regained upon sugar

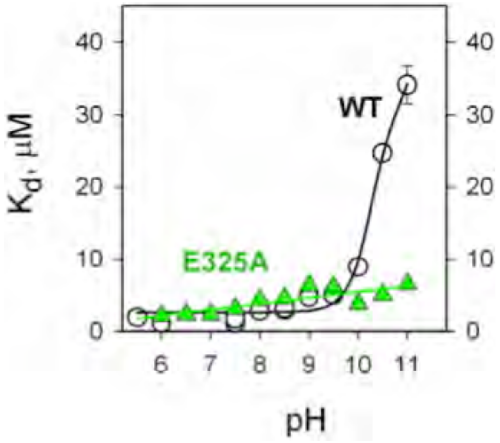

Fig. 7. : Effect of pH on the Kdapp for TDG binding to WT LacY (black) and the E325A mutant (green).

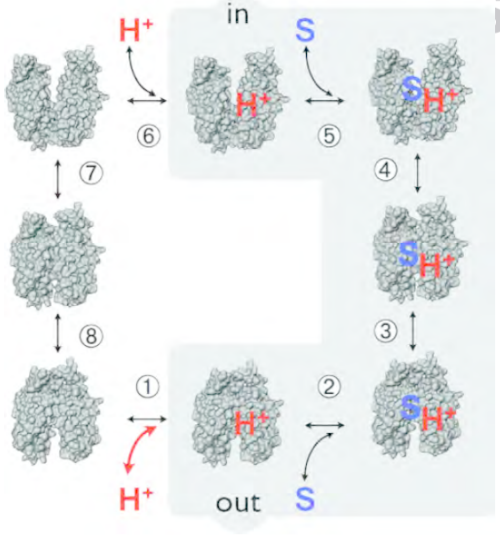

Fig. 8. Kinetic scheme for galactoside/H^+ symport, exchange and counterflow. Symport starts with protonation of LacY (step 1), which is required for high-affinity binding of lactose. Sugar binding to protonated LacY (step 2) causes a conformational change to an occluded state (step 3), which can relax to the inside where sugar dissociates first (step 5), followed by deprotonation (step 6) and return of unloaded LacY via an apo occluded intermediate (steps 7 and 8). Exchange or counterflow involves only steps 2-5 (gray shaded area).

dissociation and provides the energy for a further structural change that allows deprotonation. With respect to induced-fit, it is also notable that mutation of any single binding-site residue causes a marked decrease or complete loss of affinity (23). In brief, the mechanism of LacY resembles that of an enzyme, the difference being that the protein rather than the substrate forms the transition state.

Seven independent lines of support for the alternating access model. As postulated, alternating access involves reciprocal access of galactoside- and H^+-binding sites to either side of the membrane. Over the past few years, almost incontrovertible evidence for this structural mechanism has accrued with LacY (reviewed in 38, 39):

1. Since thiol crosslinking yields the closest distance between Cys residues, it was suggested that galactoside binding induces closure of the cytoplasmic cavity (3).

2. Site-directed alkylation of Cys replacements at every position in LacY shows that Cys replacements on the periplasmic side exhibit increased reactivity upon galactoside binding, while those on the cytoplasmic side show decreased reactivity (27, 40-44).

3. Single-molecule fluorescence energy transfer (smFRET) studies indicate that the periplasmic side opens and the cytoplasmic cavity closes upon sugar binding (45).

4. Double electron-electron resonance (DEER) reveals that LacY exists in at least 4 conformations even in the absence of galactoside and that galactoside binding induces a shift in the population

towards longer distances on the periplasmic side and shorter distances on the cytoplasmic side (46, 47).
5. Site-directed thiol cross-linking shows that the periplasmic cavity must open and close for transport to occur. Furthermore, the periplasmic side opens upon galactoside binding to approximately the same extent as observed with DEER (48).
6. Trp151→*p*-nitrophenyl-α-D-galactopyranoside (NPG) FRET exhibits practically identical kinetics of galactoside binding and displacement with LacY in inward- and outward-facing conformations (11, 49).
7. Utilization of Trp→bimane or His→Trp FRET to determine opening/closing of periplasmic or cytoplasmic cavities combined with Trp151→NPG FRET to measure galactoside binding, both in real time, shows that opening/closing are reciprocal and that opening of the periplasmic cavity controls closing of the cytoplasmic cavity (50-53).

Mechanism of lactose/H^+ symport. The affinity of WT LacY for galactosides (K_D) varies with pH to yield a pK of ~10.5 (23, 50, 54). In addition, sugar binding to purified LacY in detergent does not induce a change in ambient pH under conditions where binding or release of 1 H^+/LacY can be determined (54). Therefore, LacY is protonated over the physiological range of pH (**Fig. 7**). These observations and many others (see 1, 2) provide evidence for a symmetrical ordered kinetic mechanism in which protonation precedes galactoside binding on one side of the membrane, and follows sugar dissociation on the other side (**Fig. 8**). Recent observations (see 55) also suggest that a similar ordered mechanism may be common to other members of the MFS as well. Importantly, as mentioned above, mutants with neutral replacements for Glu325 catalyze equilibrium exchange and counterflow (the shaded reactions in **Fig. 8**), but do not catalyze any reaction involving net H^+ transport (56, 57). Dramatically, the titration observed in **Fig. 7** is abolished in mutant E325A and mutants with other neutral replacements for Glu325, which bind with high affinity up to pH 11 when LacY begins to denature. This behavior is highly unusual and suggests that Glu325 may be the sole residue directly involved in H^+ binding and transport [all 417 residues in LacY have been mutated and tested for transport activity (22)]. Thus, LacY cannot sustain a negative charge on Glu325 and bind galactoside simultaneously, and Glu325 must be protonated to bind sugar.

But deprotonation is also critical for turnover, but with an apparent pK of 10.5, how does deprotonation occur? One possibility is that the pK_a of Glu325, which is in a hydrophobic pocket, may decrease by becoming more accessible to water. However, evidence has been presented indicating that Arg302 is important in this capacity (58). Like neutral replacements for Glu325, mutants R302A and R302S are also specifically defective in translocation reactions that involve H^+ translocation--accumulation of lactose against a concentration gradient, as well as efflux—but they bind ligand and catalyze equilibrium exchange. Perhaps the positively charged guanidium group at position 302 facilitates deprotonation of Glu325. Although Tyr236 lies between Arg302 and Glu325 in the current structure (**Fig. 5**), double-mutant R302C/E325C exhibits excimer fluorescence when labeled with pyrene maleimide (59) and double-mutant R302H/E325H binds Mn(II) with μM affinity (60). Therefore, Arg302 and Glu325 may assume closer proximity in another conformation of LacY. Interestingly, a similar mechanism has been suggested for H^+ transport through the F_o portion of F_1/F_o-ATPase where an Arg residue in the *a* subunit is postulated to facilitate deprotonation of an Asp residue in the *c* subunit (reviewed in 61, 62).

Since equilibrium exchange and counterflow are unaffected by imposition of $\Delta\tilde{\mu}_H+$, it is apparent that the conformational change resulting in alternating accessibility of galactoside- and H^+-binding sites to either side of the membrane is the result of sugar binding and dissociation, and not $\Delta\tilde{\mu}_H+$ (reviewed in 1, 2). Moreover, lactose/H^+ symport from a high to a low lactose concentration in the absence of $\Delta\tilde{\mu}_H+$ exhibits a primary deuterium isotope effect that is not observed for $\Delta\tilde{\mu}_H+$-driven lactose/H^+ symport, equilibrium exchange or counterflow (63, 64). Thus, it is likely that the rate-limiting step for lactose/H^+ symport in the absence of $\Delta\tilde{\mu}_H+$ is deprotonation (also see 65, 66), while in the presence of $\Delta\tilde{\mu}_H+$, opening of apo LacY on the other side of the membrane and/or opening is probably rate limiting. In other words, by changing the rate-limiting step, $\Delta\tilde{\mu}_H+$ causes more rapid cycling.

A mechanism for chemiosmotic lactose/H^+ symport. Taken as a whole, the observations suggest the following considerations regarding the mechanism of chemiosmotic coupling in LacY: (i) Symport in the absence or presence of $\Delta\tilde{\mu}_H+$ is the same overall reaction. The limiting step for lactose/H^+ symport in the absence of $\Delta\tilde{\mu}_H+$ is deprotonation (a kinetic isotope effect is observed with D_2O). The limiting step in the presence of a $\Delta\tilde{\mu}_H+$ is probably the conformational change associated with opening of the cavity on the other side of the membrane. (ii) LacY must be protonated (possibly Glu325 specifically) to bind sugar (the pK for binding is ~10.5 and abolished in mutants with neutral replacements for Glu325). (iii) Sugar binding and dissociation--not $\Delta\tilde{\mu}_H+$--are the driving force for alternating access. (iv) Sugar binding involves induced fit causing transition to an occluded intermediate that undergoes alternating access. (v) Sugar dissociates, releasing the energy of binding. (vi) A conformational change allows Arg302 to approximate protonated Glu325, resulting in deprotonation. (vii) Apo LacY opens on the other side of the membrane, and the cycle is reinitiated.

Strikingly, accumulation of galactoside against a concentration gradient does not involve a change in K_D on either side of the membrane, but the pK (the affinity for H^+) decreases markedly. Moreover, it is apparent that $\Delta\tilde{\mu}_H+$ does not have a direct effect on the global structural change that corresponds to alternating access. Thus, transport is driven chemiosmotically, and $\Delta\tilde{\mu}_H+$ acts kinetically to control the rate of the process.

Acknowledgements.

I am deeply indebted to the members of my research group and my collaborators over the past 40 years who contributed their minds, hearts and hands to this work. At one time or another, the studies were supported financially by the National Heart (now Heart and Lung) Institute, the Roche Institute of Molecular Biology, the Howard Hughes Medical Institute, and National Institutes of Health Grants DK51131, DK069463, and GM073210, as well as National Science Foundation Grant MCB-1129551.

Reserved for Publication Footnotes

1. Guan L & Kaback HR (2006) Lessons from lactose permease. *Annu Rev Biophys Biomol Struct* 35:67-91.
2. Madej MG, Kaback, H. R. (2014) The Life and Times of Lac Permease: Crystals Ain't Enough, but They Certainly do Help. *Membrane transporter function: to structure and beyond*, eds Ziegler C & Kraemer R (Springer Series in Biophysics: Transporters), Vol 17, pp 121-158.
3. Abramson J, *et al.* (2003) Structure and mechanism of the lactose permease of Escherichia coli. *Science* 301(5633):610-615.
4. Mirza O, Guan L, Verner G, Iwata S, & Kaback HR (2006) Structural evidence for induced fit and a mechanism for sugar/H(+) symport in LacY. *Embo J* 25:1177-1183.

5. Guan L, Mirza O, Verner G, Iwata S, & Kaback HR (2007) Structural determination of wild-type lactose permease. *Proc Natl Acad Sci U S A* 104(39):15294-15298.
6. Huang Y, Lemieux MJ, Song J, Auer M, & Wang DN (2003) Structure and mechanism of the glycerol-3-phosphate transporter from Escherichia coli. *Science* 301(5633):616-620.
7. le Coutre J, Kaback HR, Patel CK, Heginbotham L, & Miller C (1998) Fourier transform infrared spectroscopy reveals a rigid alpha-helical assembly for the tetrameric Streptomyces lividans K+ channel. *Proc Natl Acad Sci U S A* 95(11):6114-6117.
8. Patzlaff JS, Moeller JA, Barry BA, & Brooker RJ (1998) Fourier transform infrared analysis of purified lactose permease: a monodisperse lactose permease preparation is stably folded, alpha-helical, and highly accessible to deuterium exchange. *Biochemistry* 37(44):15363-15375.
9. Sayeed WM & Baenziger JE (2009) Structural characterization of the osmosensor ProP. *Biochim Biophys Acta* 1788(5):1108-1115.
10. Kasho VN, Smirnova IN, & Kaback HR (2006) Sequence alignment and homology threading reveals prokaryotic and eukaryotic proteins similar to lactose permease. *J Mol Biol* 358(4):1060-1070.
11. Smirnova I, Kasho V, Sugihara J, & Kaback HR (2013) Trp replacements for tightly interacting Gly-Gly pairs in LacY stabilize an outward-facing conformation. *Proc Natl Acad Sci U S A* 110(22):8876-8881.
12. Kumar H, *et al.* (2014) Structure of sugar-bound LacY. *Proc Natl Acad Sci U S A* 111(5):1784-1788.
13. Pellegrini-Calace M, Maiwald T, & Thornton JM (2009) PoreWalker: a novel tool for the identification and characterization of channels in transmembrane proteins from their three-dimensional structure. *PLoS Comput Biol* 5(7):e1000440.
14. Sandermann H, Jr. (1977) b-D-Galactoside transport in *Escherichia coli*: substrate recognition. *Eur J Biochem* 80(2):507-515.
15. Sahin-Toth M, Lawrence MC, Nishio T, & Kaback HR (2001) The C-4 hydroxyl group of galactopyranosides is the major determinant for ligand recognition by the lactose permease of Escherichia coli. *Biochemistry* 40(43):13015-13019.
16. Sahin-Tóth M, Akhoon KM, Runner J, & Kaback HR (2000) Ligand recognition by the lactose permease of *Escherichia coli*: specificity and affinity are defined by distinct structural elements of galactopyranosides. *Biochemistry* 39:5097-5103.
17. Sahin-Tóth M, Lawrence MC, Nishio T, & Kaback HR (2001) The C-4 hydroxyl group of galactopyranosides is the major determinant for ligand recognition by the lactose permease of *Escherichia coli*. *Biochemistry* 43:13015-13019.
18. Sahin-Tóth M, Gunawan P, Lawrence MC, Toyokuni T, & Kaback HR (2002) Binding of hydrophobic D-galactopyranosides to the lactose permease of Escherichia coli. *Biochemistry* 41(43):13039-13045.
19. Guan L, Hu Y, & Kaback HR (2003) Aromatic stacking in the sugar binding site of the lactose permease. *Biochemistry* 42(6):1377-1382.
20. Vazquez-Ibar JL, Guan L, Svrakic M, & Kaback HR (2003) Exploiting luminescence spectroscopy to elucidate the interaction between sugar and a tryptophan residue in the lactose permease of *Escherichia coli*. *Proc Natl Acad Sci U S A* 100(22):12706-12711.
21. Ujwal R, *et al.* (2008) The crystal structure of mouse VDAC1 at 2.3 A resolution reveals mechanistic insights into metabolite gating. *Proc Natl Acad Sci U S A* 105(46):17742-17747.
22. Frillingos S, Sahin-Toth M, Wu J, & Kaback HR (1998) Cys-scanning mutagenesis: a novel approach to structure function relationships in polytopic membrane proteins. *Faseb J* 12(13):1281-1299.
23. Smirnova I, Kasho V, Sugihara J, Choe JY, & Kaback HR (2009) Residues in the H+ translocation site define the pKa for sugar binding to LacY. *Biochemistry* 48(37):8852-8860.
24. Frillingos S, Gonzalez A, & Kaback HR (1997) Cysteine-scanning mutagenesis of helix IV and the adjoining loops in the lactose permease of Escherichia coli: Glu126 and Arg144 are essential. *Biochemistry* 36(47):14284-14290.
25. Padan E, Sarkar HK, Viitanen PV, Poonian MS, & Kaback HR (1985) Site-specific mutagenesis of histidine residues in the *lac* permease of *Escherichia coli*. *Proc Natl Acad Sci USA* 82:6765-6768.
26. Puttner IB, Sarkar HK, Poonian MS, & Kaback HR (1986) lac permease of Escherichia coli: histidine-205 and histidine-322 play different roles in lactose/H+ symport. *Biochemistry* 25(16):4483-4485.
27. Jiang X, Driessen AJ, Feringa BL, & Kaback HR (2013) The Periplasmic Cavity of LacY Mutant Cys154-->Gly: How Open Is Open? *Biochemistry* 52(37):6568-6574.
28. Kaback HR, Sahin-Toth M, & Weinglass AB (2001) The kamikaze approach to membrane transport. *Nat Rev Mol Cell Biol* 2(8):610-620.
29. Guan L, Sahin-Toth M, & Kaback HR (2002) Changing the lactose permease of Escherichia coli into a galactose-specific symporter. *Proc Natl Acad Sci U S A* 99(10):6613-6618.
30. King SC, Hansen CL, & Wilson TH (1991) The interaction between aspartic acid 237 and lysine 358 in the lactose carrier of *Escherichia coli*. *Biochem Biophys Acta* 1062:177-186.
31. Sahin-Toth M, Dunten RL, Gonzalez A, & Kaback HR (1992) Functional interactions between putative intramembrane charged residues in the lactose permease of Escherichia coli. *Proc Natl Acad Sci U S A* 89(21):10547-10551.
32. Sahin-Toth M & Kaback HR (1993) Properties of interacting aspartic acid and lysine residues in the lactose permease of Escherichia coli. *Biochemistry* 32(38):10027-10035.
33. Guan L, Sahin-Toth M, Kalai T, Hideg K, & Kaback HR (2003) Probing the mechanism of a membrane transport protein with affinity inactivators. *J Biol Chem* 278(12):10641-10648.
34. Chaptal V, *et al.* (2011) Crystal structure of lactose permease in complex with an affinity inactivator yields unique insight into sugar recognition. *Proc Natl Acad Sci U S A* 108:9361-9366.
35. Kaczorowski GJ & Kaback HR (1979) Mechanism of lactose translocation in membrane vesicles from Escherichia coli. 1. Effect of pH on efflux, exchange, and counterflow. *Biochemistry* 18(17):3691-3697.
36. Kaczorowski GJ, Robertson DE, & Kaback HR (1979) Mechanism of lactose translocation in membrane vesicles from Escherichia coli. 2. Effect of imposed delata psi, delta pH, and Delta mu H+. *Biochemistry* 18(17):3697-3704.
37. Garcia ML, Viitanen P, Foster DL, & Kaback HR (1983) Mechanism of lactose translocation in proteoliposomes reconstituted with lac carrier protein purified from Escherichia coli. 1. Effect of pH and imposed membrane potential on efflux, exchange, and counterflow. *Biochemistry* 22(10):2524-2531.
38. Kaback HR, Smirnova I, Kasho V, Nie Y, & Zhou Y (2011) The alternating access transport mechanism in LacY. *J Membr Biol* 239(1-2):85-93.
39. Smirnova I, Kasho V, & Kaback HR (2011) Lactose permease and the alternating access mechanism. *Biochemistry* 50(45):9684-9693.
40. Kaback HR, *et al.* (2007) Site-directed alkylation and the alternating access model for LacY. *Proc Natl Acad Sci U S A* 104(2):491-494.
41. Jiang X, Nie Y, & Kaback HR (2011) Site-Directed Alkylation Studies with LacY Provide Evidence for the Alternating Access Model of Transport. *Biochemistry* 50(10):1634-1640.
42. Jiang X, *et al.* (2012) Evidence for an intermediate conformational state of LacY. *Proc Natl Acad Sci U S A* 109(12):E698-704.
43. Nie Y, Ermolova N, & Kaback HR (2007) Site-directed Alkylation of LacY: Effect of the Proton Electrochemical Gradient. *J Mol Biol* 374(2):356-364.
44. Nie Y & Kaback HR (2010) Sugar binding induces the same global conformational change in purified LacY as in the native bacterial membrane. *Proc Natl Acad Sci U S A* 107(21):9903-9908.
45. Majumdar DS, *et al.* (2007) Single-molecule FRET reveals sugar-induced conformational dynamics in LacY. *Proc Natl Acad Sci U S A* 104(31):12640-12645.
46. Smirnova I, *et al.* (2007) Sugar binding induces an outward facing conformation of LacY. *Proc Natl Acad Sci U S A* 104:16504-16509.
47. Madej MG, Soro SN, & Kaback HR (2012) Apo-intermediate in the transport cycle of lactose permease (LacY). *Proc Natl Acad Sci U S A* 109(44):E2970-2978.
48. Zhou Y, Guan L, Freites JA, & Kaback HR (2008) Opening and closing of the periplasmic gate in lactose permease. *Proc Natl Acad Sci U S A* 105(10):3774-3778.
49. Smirnova IN, Kasho VN, & Kaback HR (2006) Direct Sugar Binding to LacY Measured by Resonance Energy Transfer. *Biochemistry* 45(51):15279-15287.
50. Smirnova IN, Kasho V, & Kaback HR (2008) Protonation and sugar binding to LacY. *Proc Natl Acad Sci U S A* 105(26):8896-8901.
51. Smirnova I, Kasho V, Sugihara J, & Kaback HR (2009) Probing of the rates of alternating access in LacY with Trp fluorescence. *Proc Natl Acad Sci U S A* 106(51):21561-21566.
52. Smirnova I, Kasho V, Sugihara J, & Kaback HR (2011) Opening the periplasmic cavity in lactose permease is the limiting step for sugar binding. *Proc Natl Acad Sci U S A* 108(37):15147-15151.
53. Smirnova I, Kasho, V, Kaback, HR (2014) Real-time conformational changes in LacY". *Proc Natl Acad Sci U S A* in press.
54. Smirnova I, Kasho V, Sugihara J, Vazquez-Ibar JL, & Kaback HR (2012) Role of protons in sugar binding to LacY. *Proc Natl Acad Sci U S A* 109(42):16835-16840.
55. Madej MG & Kaback HR (2013) Evolutionary mix-and-match with MFS transporters II. *Proc Natl Acad Sci U S A*.
56. Carrasco N, Antes LM, Poonian MS, & Kaback HR (1986) *Lac* permease of *Escherichia coli*: histidine-322 and glutamic acid-325 may be components of a charge-relay system. *Biochemistry* 25(16):4486-4488.
57. Carrasco N, *et al.* (1989) Characterization of site-directed mutants in the lac permease of Escherichia coli. 2. Glutamate-325 replacements. *Biochemistry* 28(6):2533-2539.
58. Sahin-Tóth M & Kaback HR (2001) Arg-302 facilitates deprotonation of Glu-325 in the transport mechanism of the lactose permease from *Escherichia coli*. *Proc Natl Acad Sci U S A* 98(11):6068-6073.
59. Jung K, Jung H, Wu J, Privé GG, & Kaback HR (1993) Use of site-directed fluorescence labeling to study proximity relationships in the lactose permease of *Escherichia coli*. *Biochemistry* 32:12273-12278.
60. He MM, Voss J, Hubbell WL, & Kaback HR (1995) Use of designed metal-binding sites to study helix proximity in the lactose permease of Escherichia coli. 2. Proximity of helix IX (Arg302) with helix X (His322 and Glu325). *Biochemistry* 34(48):15667-15670.
61. Fillingame RH, Angevine CM, & Dmitriev OY (2002) Coupling proton movements to c-ring rotation in F(1)F(o) ATP synthase: aqueous access channels and helix rotations at the a-c interface. *Biochim Biophys Acta* 1555(1-3):29-36.
62. Fillingame RH & Steed PR (2014) Half channels mediating H(+) transport and the mechanism of gating in the Fo sector of Escherichia coli F1Fo ATP synthase. *Biochim Biophys Acta* 1837(7):1063-1068.
63. Viitanen P, Garcia ML, Foster DL, Kaczorowski GJ, & Kaback HR (1983) Mechanism of lactose translocation in proteoliposomes reconstituted with lac carrier protein purified from *Escherichia coli*. 2. Deuterium solvent isotope effects. *Biochemistry* 22(10):2531-2536.
64. Gaiko O, Bazzone A, Fendler K, & Kaback HR (2013) Electrophysiological Characterization of Uncoupled Mutants of LacY. *Biochemistry* 52(46):8261-8266.
65. Garcia-Celma JJ, Smirnova IN, Kaback HR, & Fendler K (2009) Electrophysiological characterization of LacY. *Proc Natl Acad Sci U S A* 106(18):7373-7378.
66. Garcia-Celma JJ, Ploch J, Smirnova I, Kaback HR, & Fendler K (2010) Delineating electrogenic reactions during lactose/H+ symport. *Biochemistry* 49(29):6115-6121.

Further reading / update

In search for outward-facing LacY conformers

Smirnova *et al.*, *PNAS* 111, 18548-53 (2014)

http://www.ncbi.nlm.nih.gov/pubmed/25512549

Outward-facing conformers of LacY stabilized by nanobodies

Irina Smirnova[a], Vladimir Kasho[a], Xiaoxu Jiang[a], Els Pardon[b,c], Jan Steyaert[b,c,1], and H. Ronald Kaback[a,d,e,1]

[a]Department of Physiology, [d]Department of Microbiology, Immunology, and Molecular Genetics, and [e]Molecular Biology Institute, University of California, Los Angeles, CA 90095-7327; [b]Structural Biology Research Center, VIB, Pleinlaan 2, 1050 Brussels, Belgium; and [c]Structural Biology Brussels, Vrije Universiteit Brussel, Pleinlaan 2, 1050 Brussel, Belgium

Contributed by H. Ronald Kaback, November 21, 2014 (sent for review October 31, 2014)

The lactose permease of *Escherichia coli* (LacY), a highly dynamic polytopic membrane protein, catalyzes stoichiometric galactoside/H^+ symport by an alternating access mechanism and exhibits multiple conformations, the distribution of which is altered by sugar binding. We have developed single-domain camelid nanobodies (Nbs) against a LacY mutant in an outward (periplasmic)-open conformation to stabilize this state of the WT protein. Twelve purified Nbs inhibit lactose transport in right-side–out membrane vesicles, indicating that the Nbs recognize epitopes on the periplasmic side of LacY. Stopped-flow kinetics of sugar binding by WT LacY in detergent micelles or reconstituted into proteoliposomes reveals dramatic increases in galactoside-binding rates induced by interaction with the Nbs. Thus, WT LacY in complex with the great majority of the Nbs exhibits varied increases in access of sugar to the binding site with an increase in association rate constants (k_{on}) of up to ~50-fold (reaching 10^7 $M^{-1}\cdot s^{-1}$). In contrast, with the double-Trp mutant, which is already open on the periplasmic side, the Nbs have little effect. The findings are clearly consistent with stabilization of WT conformers with an open periplasmic cavity. Remarkably, some Nbs drastically decrease the rate of dissociation of bound sugar leading to increased affinity (greater than 200-fold for lactose).

membrane transport proteins | fluorescence | major facilitator superfamily

Typical of many transport proteins, from organisms as widely separated evolutionarily as *Archaea* and *Homo sapiens*, the lactose permease of *Escherichia coli* (LacY), a paradigm for the Major Facilitator Superfamily (1), catalyzes the coupled, stoichiometric translocation of a galactopyranoside and an H^+ (galactoside/H^+ symport) across the cytoplasmic membrane (reviewed in refs. 2 and 3). Although it is now generally accepted that membrane transport proteins operate by an alternating access mechanism, this has been documented almost exclusively for LacY (reviewed in refs. 4 and 5). By this means, galactoside- and H^+-binding sites become alternatively accessible to either side of the membrane as the result of reciprocal opening/closing of cavities on the periplasmic and cytoplasmic sides of the molecule. LacY is highly dynamic, and alternates between different conformations (6, 7).

Until recently, six X-ray structures of LacY have exhibited the same inward-facing conformation with an aqueous cavity open to the cytoplasmic side, a tightly sealed periplasmic side, and sugar- and H^+-binding sites in the middle of the molecule (8–11). Numerous studies confirm that this conformation prevails in the absence of sugar (12–16). Recently, however, the X-ray structure of double-Trp mutant G46W/G262W with bound sugar reveals a conformation with a narrowly open periplasmic pathway and a tightly sealed cytoplasmic side (PDB ID code 4OAA) (17), thereby providing structural evidence that an intermediate occluded conformation occurs between the outward- and inward-facing conformations in the transport cycle.

Rates of opening/closing of periplasmic and cytoplasmic cavities have been determined in real time from changes in fluorescence of Trp or attached fluorophores with LacY either in detergent micelles or in reconstituted proteoliposomes (PLs) (15, 18, 19). Sugar-binding rates with WT LacY in PLs measured by Trp151→4-nitrophenyl-α-D-galactopyranoside (NPG) FRET are independent of sugar concentration, whereas the mutant with an open periplasmic cavity is characterized by a linear concentration dependence of sugar binding rates with k_{on} of ~10 $\mu M^{-1}\cdot s^{-1}$ (18, 20), which approximates diffusion controlled access to the binding site (21). Therefore, with WT LacY embedded in PLs, the periplasmic side is sealed, and substrate binding is limited by opening of the periplasmic cavity at a rate of 20–30 s^{-1} (19). This rate is very similar to the turnover number of WT LacY in right-side–out (RSO) membrane vesicles or reconstituted PLs (22) and is consistent with the notion that opening of the periplasmic cavity may be a limiting step in the overall transport mechanism.

To define and characterize partial reactions in the LacY transport cycle, stable conformers would be particularly useful. In this regard, remarkable progress has been made with G protein-coupled receptors through the use of camelid single-domain nanobodies (Nbs), which stabilize specific conformers (23–27). Advantages of Nbs include small size and a unique structure that allows flexible antigen-binding loops to insert into clefts and cavities. Here we report that Nbs prepared against the outward (periplasmic)-open LacY mutant G46W/G262W effectively bind to WT LacY and inactivate transport activity. However, the sugar-binding site becomes much more accessible to galactosides as a result of Nb binding, indicating stabilization of the open-outward conformations of LacY, and providing the means for detailed studies of galactoside binding to these conformers. Remarkably, several Nbs significantly increase affinity for galactosides by slowing the dissociation rate of the sugar while maintaining a high association rate. It is also apparent that the

Significance

LacY, a paradigm for the major facilitator superfamily (the largest family of transport proteins) catalyzes the coupled symport of a galactoside and an H^+. Although a detailed mechanism has been postulated, to test its veracity stable conformers of different intermediates would be particularly informative. Camelid single-domain nanobodies (Nbs), which can stabilize specific conformers, are ~15 kDa in size and have a unique structure that allows flexible antigen-binding loops to insert into clefts and cavities. Nbs prepared against an outward (periplasmic)-open LacY mutant are described herein. The Nbs bind effectively to WT LacY and inactivate transport by stabilizing the symporter in outward-open conformations with increased accessibility to the sugar-binding site. Moreover, several Nbs dramatically increase affinity for galactosides.

Author contributions: I.S., V.K., J.S., and H.R.K. designed research; I.S., V.K., X.J., E.P., and J.S. performed research; I.S., V.K., E.P., and J.S. contributed new reagents/analytic tools; I.S., V.K., X.J., E.P., and H.R.K. analyzed data; and I.S., V.K., E.P., J.S., and H.R.K. wrote the paper.

The authors declare no conflict of interest.

[1]To whom correspondence may be addressed. Email: jan.steyaert@vub.ac.be or rkaback@mednet.ucla.edu.

This article contains supporting information online at www.pnas.org/lookup/suppl/doi:10.1073/pnas.1422265112/-/DCSupplemental.

Nbs have the potential for crystallizing LacY trapped as otherwise unstable transient intermediates.

Results

Generation of Nbs. To generate Nbs that recognize and stabilize outward-open conformations of LacY, llamas were immunized (28) with LacY mutant G46W/G262W (20) reconstituted into PLs as the antigen. In this mutant, double-Trp replacements for Gly46 (helix II) and Gly262 (helix VIII) were introduced on the periplasmic side of LacY at positions where the two six-helix bundles come into close contact. Introduction of bulky Trp residues at these positions prevents closure of the periplasmic cavity and completely abrogates all transport activity. The double-Trp mutant reconstituted into PLs is oriented physiologically, with the periplasmic side facing the external medium (20), as demonstrated previously (18, 29). Thus, it is presumed that the llama's immune system is presented with an antigen that has an accessible periplasmic surface of LacY with an open cavity. Selections were performed on the LacY mutant to find those nanobodies that would specifically recognize the outward-open conformation, as well as on WT LacY. Procedures used for production, selection, cloning, and purification of Nbs are provided in *Methods*.

Lactose Transport. Lactose/H^+ symport catalyzed by WT LacY was measured in RSO membrane vesicles preincubated with each of 13 nanobodies, and the data are summarized in Table 1 and Fig. S1. Nb 9051 has no significant effect on the rate of lactose transport, but Nb 9042, Nb 9035, and Nb 9034 inhibit by 60%, 80%, and 90%, respectively, and other nine Nbs block lactose transport completely. Because it is well known that vesicles prepared by osmotic lysis of spheroplasts have the same orientation as the membrane in intact cells (for examples, see refs. 30 and 31–34), the results demonstrate that inhibition of transport by the Nbs is specifically a result of binding epitopes on the periplasmic side of WT LacY.

Sugar Binding to Nb/LacY Complexes. Sugar binding rates were measured by Trp151→NPG FRET with WT LacY or the double-Trp mutant solubilized in *n*-dodecyl-β-D-maltopyranoside (DDM) by using stopped-flow fluorimetry, which allows determination of association and dissociation rate constants (k_{on} and k_{off}) of sugar binding. WT LacY exhibits a k_{on} of 0.2 $\mu M^{-1}\cdot s^{-1}$, whereas k_{on} for the double-Trp mutant is 5.7 $\mu M^{-1}\cdot s^{-1}$ (compare open circles in Fig. 1*A* with open diamonds in Fig. 1*B*), indicating much higher accessibility of the sugar-binding site in mutant G46W/G262W with an open periplasmic cavity. None of Nbs tested abolish sugar binding to LacY (Table 1). Two Nbs (9051 and 9035) practically do not affect sugar binding (k_{on} and k_{off} values are similar to those measured for WT LacY without Nbs). Interaction of Nb 9042 and Nb 9034 with WT LacY results in sugar binding with rates independent of NPG concentration (k_{obs} = 30 and 15 s^{-1}, respectively), suggesting that these two nanobodies do not alter galactoside binding. Rather, they may decrease conformational flexibility of LacY in such a manner that sugar access to the binding site is limited by a slow conformational change or slow opening of the periplasmic cavity, which could explain partial inhibition of transport.

Nine Nb /WT LacY complexes that completely block transport, demonstrate a significant increase of NPG binding rates (k_{on} increases from 5- to 50-fold) (Fig. 1*A* and Table 1). Dramatic increases in NPG accessibility are observed for WT LacY complexed with Nbs 9039, 9048, 9047, 9033, and 9065 to an extent comparable to that of mutant G46W/G262W (Table 1) (k_{on} = 4.4, 6.8, 6.9, 7.5, and 9.3 $\mu M^{-1}\cdot s^{-1}$, respectively). Several Nbs exhibit a smaller effect on the rates of sugar binding by WT LacY, with k_{on} values of 1.0, 1.2, 3.5, and 3.5 $\mu M^{-1}\cdot s^{-1}$ for Nbs 9036, 9055, 9063, and 9043, respectively (Fig. 1*A* and Table 1). Notably, the double-Trp mutant in complex with Nbs 9036, 9063, and 9043 is characterized by lower k_{on} values than observed without Nbs, whereas all other Nbs have essentially no effect (Fig. 1*B* and Table 1). Kinetic parameters measured by displacement of bound NPG using a high concentration of β-D-galactopyranosyl-1-thio-β-D-galactopyranoside (TDG) show that the majority of the Nbs, which block transport, significantly increase the affinity of WT LacY for NPG (K_ds decrease up to 10 times), whereas K_ds are mostly unaltered with the double-Trp mutant (Table 1, shaded columns). Surprisingly, similar effects of Nb 9036 are observed with both WT LacY, and mutant G46W/

Table 1. Effect of Nbs on lactose transport and kinetics of sugar binding to LacY

	WT LacY				G46W/G262W LacY		
			Displacement			Displacement	
Nb	Lactose transport (%)	Binding k_{on} ($\mu M^{-1}\cdot s^{-1}$)	k_{off} (s^{-1})	K_d (μM)	Binding k_{on} ($\mu M^{-1}\cdot s^{-1}$)	k_{off} (s^{-1})	K_d (μM)
None	100	0.2	41	28	5.7	31	6.1
9051	100	0.2	48				
9042	40	ND*	41				
9035	20	0.3	24				
9034	10	ND*	38	60	8.6	34	5.7
9036	No	1.0	0.05	0.05†	0.3	0.02	0.07†
9055	No	1.2	52	35	4.1	63	18
9063	No	3.5	2.7	2.2	1.2	1.4	3.3
9043	No	3.0	8	4	2.2	4.8	3.2
9039	No	4.4	54	13	5.3	45	18
9048	No	6.8	13	2.8	4.4	11	4.2
9047	No	6.9	32	5.2	5.8	31	3.8
9033	No	7.5	31	3.8	5.3	29	5.2
9065	No	9.3	40	5.3	9.5	58	9.1

Rates of lactose transport were measured as described in *Methods* and Fig. S1. Rates of NPG binding were measured as Trp151→NPG FRET by stopped-flow fluorimetry (*Methods*). Association rate constants (k_{on}) were measured as described in Figs. 1 and 2. Dissociation rate constants (k_{off}) and K_d values were measured in displacement experiments (data in shaded columns), as shown in Fig. S2. Statistical SDs were within 10% for each presented data point. Color coding is the same as in Figs. 1 and 2. Only those Nbs that completely block transport in WT LacY were tested with the double-Trp mutant.

*Binding rates do not change with NPG concentration.

†K_d values for Nb9036/LacY complexes were calculated (k_{off}/k_{on}).

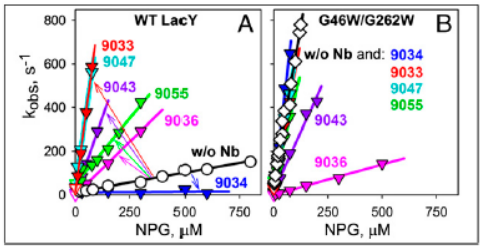

Fig. 1. Effect of six Nbs on kinetics of sugar binding by WT LacY (*A*) or mutant G46W/G262W (*B*) solubilized in DDM. Stopped-flow rates of NPG binding (k_{obs}) were measured by mixing LacY with NPG in the absence or presence of a given Nb. Stopped-flow traces of the decrease in Trp fluorescence were recorded and fitted with single-exponential equation for estimation of the sugar-binding rate (k_{obs}) at each NPG concentration. Concentration dependencies of k_{obs} for NPG binding to proteins without Nbs are shown in black (open circles, WT LacY; and open diamonds, double-Trp mutant). Data obtained with different Nbs are shown in the same colors as in Table 1. The slopes of the linear concentration dependencies of NPG binding rates ($k_{obs} = k_{off} + k_{on}$[NPG]) yielded the k_{on} values presented in Table 1 in the columns labeled "Binding." The arrows in *A* indicate the effect of each Nb on the accessibility of the sugar-binding site relative to WT LacY with no Nb.

G262W where NPG binding affinity is increased by orders of magnitude, which will be discussed in detail below.

Accessibility of the Sugar-Binding Site. Remarkable changes in sugar-binding rates are induced by interaction of Nb 9065 with WT LacY (Fig. 2*A* and Table 1). As estimated from the linear concentration dependence of binding rates, k_{on} increases from 0.2 to 9.3 $\mu M^{-1}\cdot s^{-1}$ (Fig. 2*B*), indicating free access to the sugar-binding site. Moreover, NPG binding rates are the same when the LacY/Nb 9065 complex is formed in the absence or presence of sugar (Fig. 2*B*, red triangles). WT LacY binding affinity for NPG is significantly increased by interaction with Nb 9065 (Table 1). The K_d value measured in displacement experiments decreases from 28 to 5.3 μM (Fig. S2 *A*, *C*, and *E*). Nb 9065 does not markedly alter NPG-binding kinetics with the G46W/G262W mutant (Fig. 2*B*, Table 1, and Fig. S2 *B*, *D*, and *F*).

Experiments with LacY solubilized in DDM do not specify whether Nb binding stabilizes conformers with an open periplasmic or cytoplasmic cavity. However, LacY reconstituted into PLs is oriented with the periplasmic side facing out, as in the native *E. coli* membrane (18, 20, 29). Therefore, a kinetic test was designed that allows discrimination between accessibility from the periplasmic or cytoplasmic sides of LacY by comparing sugar-binding rates with LacY solubilized in DDM versus reconstituted into PLs (Fig. S3). Mutants G46W/G262W or C154G with an open periplasmic or cytoplasmic cavity, respectively, are characterized by rapid sugar binding in DDM (Fig. S3 *A* and *D*) (k_{on} = 5 $\mu M^{-1}\cdot s^{-1}$). However, in PLs, sugar binding by mutant G46W/G262W is rapid and demonstrates a sharp concentration dependence of k_{obs} (with k_{on} = 14 $\mu M^{-1}\cdot s^{-1}$), whereas mutant C154G exhibits a relatively slow rate of sugar binding that is independent of galactoside concentration (k_{obs} = 50 s^{-1}) (Fig. S3 *B* and *E*). Thus, NPG has free access to the binding site from periplasmic side in the double-Trp mutant, but limited access in mutant C154G, where the rate of opening of the periplasmic cavity is limiting. However, k_{on} determined by displacement with reconstituted mutant C154G in PLs (Fig. S3*F*) (k_{on} = 14 $\mu M^{-1}\cdot s^{-1}$) is even higher than in DDM (k_{on} = 4.9 $\mu M^{-1}\cdot s^{-1}$). Thus, when the periplasmic cavity is open, the sugar binds with a diffusion-controlled rate.

Binding of NPG by WT LacY in DDM is characterized by k_{on} = 0.2 $\mu M^{-1}\cdot s^{-1}$ and consistent with reduced access to the sugar binding site (Fig. S3*G*). NPG binding by WT LacY reconstituted into PLs is slow (k_{obs} = 21 s^{-1}), and the rate is independent of sugar concentration, thereby indicating that binding is limited by opening of the periplasmic cavity (Fig. S3*H*). However, in displacement experiments with reconstituted WT LacY, opening of periplasmic cavity provides free access to binding site with a k_{on} of 10 $\mu M^{-1}\cdot s^{-1}$ (Fig. S3*I*), as shown for mutant C154G.

Binding of Nb 9065 to reconstituted WT LacY dramatically increases NPG binding rates, but no significant change is observed with the reconstituted double-Trp mutant (Fig. 2*C*). Linear fits of the data yield an estimated k_{on} of ~20 $\mu M^{-1}\cdot s^{-1}$ for both WT LacY and mutant G46W/G262W complexed with Nb 9065. Therefore, Nb 9065 binds to an epitope on reconstituted WT protein that is exposed to the external milieu, provides free access of NPG to the binding site, and blocks transport, thereby demonstrating clearly that Nb 9065 stabilizes an outward-facing conformer of WT LacY. Similar effects of Nb 9039 and 9047 on reconstituted WT LacY and of Nbs 9043, 9047 and 9065 on reconstituted mutant C154G are shown in Fig. S4.

Nb 9036 Induces High-Affinity Galactoside Binding. A striking effect of Nb 9036 on sugar binding is observed with both WT LacY and the double-Trp mutant. True k_{off} values for NPG determined in displacement experiments decrease in the presence of Nb 9036 by about three orders-of-magnitude from 41 to 0.05 s^{-1} and from 31 to 0.02 s^{-1} for the WT and mutant, respectively (Table 1). With the WT LacY/Nb 9036 complex, NPG binding rates increase (Fig. S5*A*), demonstrating greater accessibility of the sugar-binding site (k_{on} increases fivefold) (Fig. 1*A* and Table 1). Displacement rates are greatly decreased by Nb 9036 binding to WT LacY (Fig. S5*B*), resulting in a >500-fold increase in NPG affinity. A similar effect of Nb 9036 is observed with mutant G46W/G262W, although both k_{on} and k_{off} values are decreased (Table 1). Therefore, it appears that Nb 9036 binding stabilizes a specific outward-facing conformation of LacY in which the periplasmic cavity is partially open, but release of bound NPG is drastically hindered.

This effect of Nb 9036 allows characterization of the kinetic properties of lactose binding, the physiological substrate of LacY. The affinity of LacY for lactose in the absence of Nbs is extremely low with a K_d of ~10 mM (35, 36). The rate of lactose displacement was measured by Trp151→NPG FRET, where

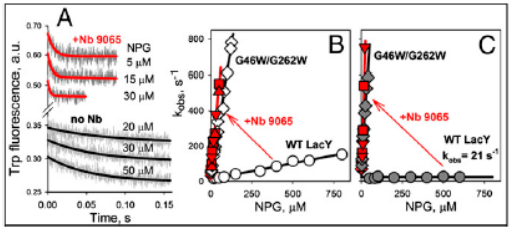

Fig. 2. Effect of Nb 9065 on accessibility of the sugar-binding site. NPG binding rates were measured directly by stopped-flow as Trp151→NPG FRET with WT LacY and G46W/G262W mutant in the absence of Nbs (black lines) or after preincubation with Nb 9065 (red lines). (*A*) Stopped-flow traces of Trp emission decreases were recorded with WT LacY in DDM after mixing with given concentrations of NPG. (*B*) Concentration dependencies of sugar binding rates measured in DDM with WT LacY (open circles and red triangles) or mutant (open diamonds and red squares). WT LacY preincubated with Nb 9065 in the absence or presence of sugar (red triangles pointed down or up, respectively) exhibits the same NPG binding rates. Estimated k_{on} values are presented in Table 1 in columns labeled "Binding." WT LacY/Nb 9065 complex in DDM solution exhibits ~50-fold increase in k_{on} (from 0.20 ± 0.01 to 9.3 ± 0.2 $\mu M^{-1}s^{-1}$). (*C*) Concentration dependencies of sugar binding rates measured with WT LacY (gray circles or red triangles) and mutant (gray diamonds and red squares) reconstituted into PLs. The red arrows indicate the change in concentration dependence of sugar binding rates after Nb 9065 binding to WT LacY.

a saturating concentration of NPG (0.2 mM) was mixed with WT LacY/Nb 9036 complex preincubated with given concentrations of lactose (Fig. 3*A*). The stopped-flow traces demonstrate that NPG binding occurs upon release of lactose at constant rate ($k_{off} = 1.8\ s^{-1}$). As estimated from the concentration dependence of the amplitudes of the fluorescence change (Fig. 3*B*), the K_d for lactose is 42 μM. The double-Trp mutant complexed with Nb 9036 yields a similar K_d of 49 μM (Fig. 3*B*), suggesting that Nb 9036 stabilizes similar conformers of both proteins.

Nbs Binding. Homology modeling of the 3D structures of each Nb described reveals Trp residues in the variable loops containing the complementarity determining regions (CDRs) that define the binding affinity of the Nbs (Fig. 4*A*). Therefore, interaction of the Nbs with LacY was studied by site-directed Trp-induced fluorescence quenching of bimane- or ATTO655-labeled LacY (19, 37, 38). WT LacY with a Cys replacement on the periplasmic side (I32C) labeled with bimane or ATTO655 exhibits a decrease in the fluorescence emission of either fluorophore upon addition of Nbs (Fig. S6). Time-courses of the fluorescence changes recorded with bimane-labeled (Fig. 4*B*) or ATTO655-labeled (Fig. 4*C*) mutant I32C LacY demonstrate various extents of fluorescence quenching after addition of Nbs 9036, 9055, and 9063, which likely reflect different distances between the Trp residues in the Nbs and the fluorophores in LacY when the Nb binds.

Stopped-flow mixing of various concentrations of Nb with 0.4 μM bimane-labeled LacY (Fig. S7) exhibits increased rates of binding with increasing Nb concentration. No change in the amplitude of the fluorescence decrease is observed even at lowest Nb concentrations (0.5–1 μM), which indicates that the affinity of Nbs for LacY is high with K_d values at least in the nanomolar range. Linear concentration dependencies of Nbs binding rates (Fig. 5) yield estimated k_{on} values that vary from 0.2 to 3.5 $\mu M^{-1}\cdot s^{-1}$, and extremely low k_{off} values for all five Nbs. In addition, the binding rates of Nb 9036 to bimane-labeled I32C LacY are identical in the absence or presence of 5 mM TDG ($k_{on} = 0.4\ \mu M^{-1}\cdot s^{-1}$), indicating that Nb recognizes the same LacY conformer with or without bound sugar.

When the Cys replacement is introduced on the cytoplasmic side of WT LacY (S401C), no significant Trp-induced fluorescence quenching is observed with bimane- or ATTO655-labeled LacY upon Nb binding (Fig. S8 *A–C*), although the effect of Nb 9036 on NPG binding kinetics for bimane-labeled S401C LacY is readily detected (Fig. S8*D*). In the bimane-labeled S401C LacY/Nb 9036 complex, both k_{on} and k_{off} values are altered to the same extent as observed with WT LacY/Nb 9036. Thus, the Nbs bind to the periplasmic side of LacY in DDM, and the method allows determination of Nb binding kinetics with LacY.

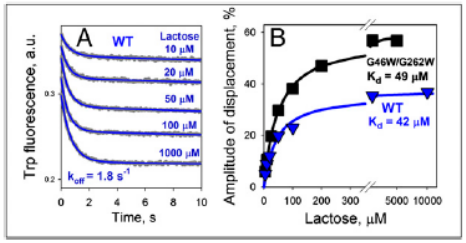

Fig. 3. Lactose binding affinity of WT LacY or mutant G46W/G262W complexed with Nb 9036. LacY/Nb complexes solubilized in DDM were preincubated with indicated concentrations of lactose and then mixed by stopped-flow with a saturating concentration of NPG (0.2 mM) that binds upon release of ligand and is an acceptor of FRET from Trp151. Binding of NPG to sugar-free protein is fast with observed rate estimated as ~200 s^{-1}. This rate is much faster than the lactose dissociation rate, and only the displacement rate for lactose (k_{off}) is measured. (*A*) Time traces of Trp fluorescence change were recorded with the WT LacY/Nb 9036 complex and fitted with a single-exponential equation (blue lines) that yield estimated rates of lactose dissociation ($k_{off} = 1.8 \pm 0.2\ s^{-1}$) by displacement with NPG. (*B*) Affinity of lactose binding was estimated from hyperbolic fits of the concentration dependence of the fluorescence changes at each lactose concentration in the stopped-flow traces for WT and mutant (triangles and squares, respectively). K_d values are 42 ± 5 and 49 ± 2 μM for the WT LacY and mutant complexes, respectively.

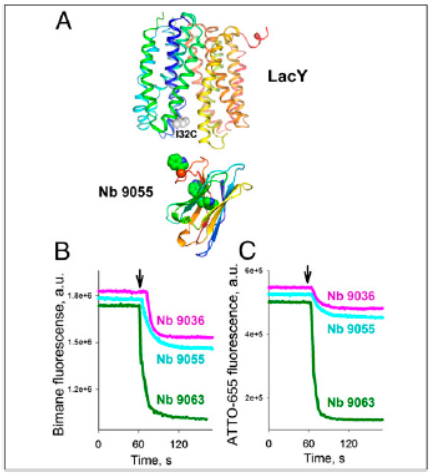

Fig. 4. Nb binding to periplasmic LacY I32C mutant labeled with fluorophores. Structural models of LacY and Nb 9055 (*A*) are shown as rainbow colored backbones (from blue to red) with highlighted Trp residues in the Nb (green spheres) and introduced Cys32 on periplasmic side of LacY (gray spheres) (PDB ID code 4OAA). Time courses of fluorescence quenching were recorded at excitation/emission wavelengths of 380/465 nm or 660/677 nm for bimane or ATTO655, respectively. Addition of 0.6 μM Nb 9036, Nb 9055, or Nb 9063 to 0.3 μM I32C LacY mutant labeled with bimane-maleimide (*B*) or ATTO655-maleimide (*C*) is indicated by black arrows. The effects of the Nbs on the emission spectra of fluorophore-labeled LacY are shown in Fig. S6.

Binding affinity of Nb 9036, Nb 9055, or Nb 9063 was measured by steady-state titration of bimane- or ATTO655-labeled I32C LacY at low protein concentration (20 nM). Estimated K_d values for all three Nbs are around 1 nM and do not depend on the structure of fluorophore attached to LacY (Fig. S9). The presence of sugar practically does not change Nbs binding affinity. Measured k_{on} (Fig. 5) and K_d values allow calculation of k_{off} as 1.2×10^{-3}, 0.4×10^{-3}, and $0.3 \times 10^{-3}\ s^{-1}$ for dissociation of Nbs 9063, 9055, and 9036, respectively.

Demonstration That Nb Binding Stabilizes a Conformer with an Open Periplasmic Cavity. Trp-induced bimane unquenching allows direct demonstration of opening of periplasmic cavity in LacY (19). Thus, bimane-labeled mutant F29W/G262C exhibits unquenching of bimane fluorescence after addition of sugar, indicating opening of the periplasmic cavity and even greater unquenching is observed after addition of Nb 9036 (Fig. 6*A*). The increased extent of bimane fluorescence unquenching caused by Nb binding compared with effect of TDG is most likely explained by stabilization of a specific outward-open conformation of LacY, whereas sugar binding results in dynamic equilibrium of several LacY conformers including those with an open periplasmic cavity (6). Furthermore, the rates of unquenching measured with bimane-labeled F29W/G262C at increasing concentrations of Nb 9036 exhibit a linear dependence with $k_{on} = 0.4\ \mu M^{-1}\cdot s^{-1}$ (Fig. 6*B*). This k_{on} value is identical to that measured by direct binding studies with Nb 9036 by using Trp-induced quenching of bimane-labeled I32C LacY (Fig. 5, pink circles), thereby demonstrating that binding of Nb 9036 stabilizes a conformer with an open periplasmic cavity.

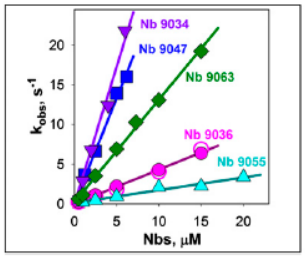

Fig. 5. Kinetics of Nbs binding to LacY. Rates of Nbs binding to bimane-labeled mutant I32C LacY were measured by stopped-flow as quenching of bimane fluorescence by Trp residues of the five Nbs indicated. Data were obtained with 0.4 μM LacY as described in Fig. S7. The linear dependencies of the observed rates on Nb concentrations yield estimated k_{on} values of 0.16 ± 0.01, 0.43 ± 0.01, 1.30 ± 0.02, 2.7 ± 0.1, and 3.5 ± 0.2 $\mu M^{-1}s^{-1}$ for Nbs 9055, 9036, 9063, 9047, and 9034, respectively. Nb 9036 binding rates were measured in the absence or presence of 5 mM TDG (open and closed pink circles, respectively).

Discussion

Nbs represent a unique type of single-domain antibodies with flexible antigen-binding loops containing CDR3, which is able to insert into clefts and cavities of membrane proteins and stabilize specific conformers (23–27). Therefore, Nbs were prepared against LacY mutant G46W/G262W, which is in an outward-open conformation, anticipating that such Nbs would interact with epitopes within the open periplasmic cavity to stabilize outward-facing conformers of WT LacY. As shown, 12 of the 13 Nbs characterized inhibit—and 9 totally block—lactose transport catalyzed by WT LacY in RSO membrane vesicles, indicating that they bind to periplasmic epitopes. However, sugar binding is not abolished. Rather, each of the nine Nbs significantly increases the rate of sugar binding with WT LacY solubilized in DDM, indicating that the sugar-binding site in the middle of the LacY molecule becomes much more accessible to the external medium in the presence of the Nbs. Even more impressive, WT LacY and C154G mutant reconstituted into PLs and then exposed to Nbs 9039, 9043, 9047, and 9065 exhibit virtually unrestricted sugar binding rates with high k_{on} values corresponding to stabilization of conformers with an open periplasmic cavity. It is also remarkable that with few exceptions (Nbs 9036, 9063, and 9043), the Nbs have little or no effect on sugar-binding rates with the double-Trp mutant presumably because the mutant is already open on the periplasmic side.

Although Nb binding to WT LacY generally increases accessibility of the binding site to NPG, the k_{on} values vary from 1 to 9 $\mu M^{-1}\cdot s^{-1}$ for different WT LacY/Nb complexes. Thus, the Nbs appear to recognize different epitopes and stabilize different outward-open conformers of LacY that may represent natural intermediates in the transport cycle.

Remarkably, three of the Nbs (9036, 9063, and 9043) significantly decrease k_{off} values measured for NPG with WT LacY/Nb complexes, and dissociation of sugar is slowed nearly 1,000-fold by Nb 9036 (Table 1), resulting in markedly increased affinity for galactosides. Thus, the K_d value of the Nb 9036/WT LacY complex for NPG decreases by >500-fold. This huge increase in affinity for galactoside allows determination of binding kinetics for lactose, the natural substrate of LacY where affinity increases >200-fold. Because Nb 9036 also decreases k_{off} and k_{on} values in complex with the double-Trp mutant to near those observed for WT LacY/Nb 9036 complex, it seems reasonable to suggest that this Nb stabilizes a conformer that approximates an occluded intermediate with fully liganded sugar.

A simple fluorescent method was developed for detection of Nb binding to LacY by using site-directed Trp-induced quenching of a fluorophore attached to the periplasmic side of LacY. Quenching of the fluorophore introduced on the periplasmic but not on cytoplasmic side of LacY also confirms that the Nbs bind to epitopes on the periplasmic side of LacY. Moreover, presteady-state kinetics of Nb binding to LacY were measured by stopped-flow. The linear concentration dependencies of binding rates reveal significant variations in k_{on} values for five tested Nbs (from 0.2 to 3.5 $\mu M^{-1}\cdot s^{-1}$) and exceedingly low k_{off} values. Multiple k_{on} values most likely correspond to interaction of the Nbs with different epitopes on periplasmic side of LacY that vary in complexity and structure. Binding affinities measured by steady-state titration are very high (K_d values are around 1 nM for Nbs 9036, 9055, and 9063), which explains extremely slow dissociation rates of the Nbs. Thus, calculated k_{off} values range from 0.3×10^{-3} to 1.2×10^{-3} s^{-1}, which are similar to published data for highly specific Nbs–antigen interactions (25).

Recognition of different epitopes in WT LacY by the Nbs results in stabilization of several conformational states of the symporter. These states may represent natural functional intermediates in overall transport cycle, as the Nbs do not interfere with sugar binding and therefore with protonation, because effective sugar binding requires the protonated form of LacY (39). Moreover, in vivo-matured Nbs do not apparently induce nonnative conformations of antigens (28). Thus, Nbs developed against the outward-open LacY mutant may be useful for crystallization of WT LacY in different conformations without the use of mutagenesis.

Methods

Construction of mutants, purification of LacY, reconstitution into PLs, and materials used in this study are described in *SI Methods*. All animal vaccination experiments were executed in strict accordance with good animal practices, following the EU animal welfare legislation and after approval of the local ethical committee (Ethical Committee for use of laboratory animals of the Vrije Universiteit Brussel, VUB project 13-601-1). Every effort was made to minimize suffering.

Generation of Nbs. Nbs were prepared against the G46W/G262W LacY mutant using a previously published protocol (28). In brief, one llama (*Lama glama*) received six weekly injections of 100 μg of purified G46W/G262W LacY reconstituted into PLs with lipid to protein ratio 5 (0.4 mg/mL LacY and 2 mg/mL

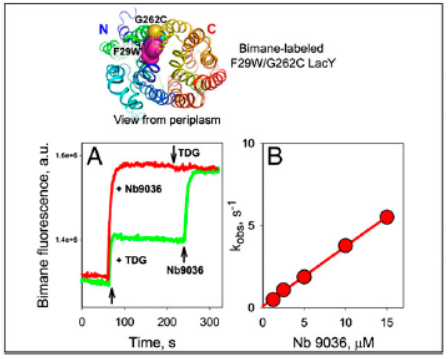

Fig. 6. Stabilizing the open periplasmic cavity by binding of Nb 9036. Structural model of mutant F29W/G262C in inward-facing conformation with a closed periplasmic cavity is shown on top with the backbone rainbow colored (from blue to red) and highlighted Trp- and Cys-replacements (magenta and yellow spheres, respectively) on the periplasmic side of the N- and C-terminal six-helix bundles of LacY. (*A*) Unquenching of fluorescence of bimane-labeled F29W/G262C LacY (0.3 μM) after addition of 5 mM TDG followed by 0.6 μM Nb 9036 (green line), or addition of 0.6 μM Nb 9036 followed by 5 mM TDG (red line). Time courses were recorded as described in Fig. 4*B*. (*B*) Rates of Nb 9036 binding were measured by stopped-flow as described in Fig. 5 by mixing indicated concentrations of Nb 9036 with bimane-labeled F29W/G262C LacY. Unquenching of bimane-labeled Cys262 in LacY results from separation of the fluorophore from Trp29 when the periplasmic cavity opens. Linear concentration dependence of the rates yields an estimated $k_{on} = 0.36 \pm 0.01$ $\mu M^{-1}s^{-1}$.

phospholipids). The Nb-encoding ORFs were amplified from total lymphocyte RNA and subcloned into the phage display/expression vector pMESy4. After one round of panning, clear enrichment was seen for the LacY double-Trp mutant. Ninety-two individual colonies were randomly picked, and the Nbs were produced as soluble His- and Capture Select C-tagged proteins (MW 12–15 kDa) in the periplasm of *E. coli*. Testing for specific binding to both the G46W/G262W mutant and WT LacY (with the fucose transporter as a negative control) resulted in 31 families with the highest signals with mutant G46W/G262W compared with WT LacY. All selections and screenings were done in the absence of sugar. Inducible periplasmic expression of Nbs in *E. coli* WK6 produces milligram quantities of >95% pure nanobody using immobilized metal ion affinity chromatography (Talon resin) from the periplasmic extract of a 1-L bacterial culture. Purified nanobodies (2–10 mg/mL) in 100 mM potassium phosphate (KP_i, pH 7.5) were frozen in liquid nitrogen and stored at −80 °C before use.

Transport Measurements. RSO vesides for transport assay were prepared from *E. coli* T184 harboring plasmid pT7-5 encoding WT LacY as described in *SI Methods*. The effect of the Nbs on lactose transport was measured after preincubation of vesicles (0.5 mg of total membrane protein) with 80 μg of each Nb (at ~5:1 molar ratio of Nb:LacY) in 100 mM KP_i/10 mM $MgSO_4$ (pH 7.2) for 20 min. Lactose transport was assayed with 0.4 mM [^{14}C]lactose (10 mCi/mmol) in the same buffer at room temperature (see *SI Methods* for details).

Fluorescence Measurements. Stopped-flow measurements were performed at 25 °C on a SFM-300 rapid kinetic system equipped with a TC-50/10 cuvette (dead-time 1.2 ms), and MOS-450 spectrofluorimeter (Bio-Logic). NPG binding was measured as Trp151→NPG FRET at excitation 295 nm with emission interference filters (Edmund Optics) at 340 nm. LacY/Nb complexes were formed by preincubation of purified LacY (20–30 μM) with 1.2 molar excess of each Nb in 50 mM NaP_i/0.02% DDM, pH 7.5 for 10 min at room temperature. Stopped-flow traces were recorded at final concentration 0.5–0.8 μM of LacY after mixing with NPG. In displacement experiments LacY/Nb complex was preincubated with NPG and then mixed with 15 mM TDG in stopped-flow. Measurements with purified protein in DDM were done in 50 mM NaP_i/0.02% DDM (pH 7.5). Experiments with PLs were carried out in 50 mM NaP_i (pH 7.5). To dissolve PLs, DDM was added to a final concentration of 0.3%, and after 10 min, the samples were used in stopped-flow experiments. Typically, 10–30 traces were recorded for each datapoint, averaged and fitted with an exponential equation using the built-in Bio-Kine32 software package or by using Sigmaplot 10 (Systat Software). Calculated SDs were within 10% for each presented datapoint. All given concentrations were final after mixing unless stated otherwise.

Rates of Nbs binding to LacY were measured as Trp-induced quenching of bimane-labeled LacY. Stopped-flow traces were recorded at an excitation wavelength of 380 nm with emission at 441–515 nm using cut-off filters (Edmund Optics).

Steady-state fluorescence emission spectra were measured at room temperature on a SPEX Fluorolog 3 spectrofluorometer (Edison) in 2.5 mL cuvette (1 × 1 cm) as previously described (15) with excitation at 380 nm (for bimane), and 650 nm (for ATTO655). Time courses were recorded at excitation/emission wavelengths 380/465 nm and 660/677 nm for bimane- and ATTO655-labeled protein, respectively.

Homology Modeling of Nb Structures. Modeling of the 3D structures of the Nbs was carried out on SWISS-Model web-based server (40, 41) using the X-ray structure of gelsolin nanobody (PDB ID code 2X1P) as a template, which has ~70% sequence identity with LacY-derived nanobodies.

ACKNOWLEDGMENTS. We thank Alison Lundqvist for the technical assistance in the preparation of the Nbs, and Balasubramanian Dhandayuthapani and Junichi Sugihara for their skillful technical assistance in purification of the nanobodies and preparation of mutants. This work was supported by NIH Grants DK51131, DK069463, and GM073210 (to H.R.K.).

1. Saier MH, Jr (2000) Families of transmembrane sugar transport proteins. *Mol Microbiol* 35(4):699–710.
2. Guan L, Kaback HR (2006) Lessons from lactose permease. *Annu Rev Biophys Biomol Struct* 35:67–91.
3. Madej MG, Kaback HR (2014) The life and times of Lac permease: Crystals ain't enough, but they certainly do help. *Membrane Transporter Function: To Structure and Beyond*, eds Ziegler C, Kraemer R, Springer Series in Biophysics: Transporters (Springer Heidelberg, Germany) Vol 17, pp 121–158.
4. Smirnova I, Kasho V, Kaback HR (2011) Lactose permease and the alternating access mechanism. *Biochemistry* 50(45):9684–9693.
5. Kaback HR, Smirnova I, Kasho V, Nie Y, Zhou Y (2011) The alternating access transport mechanism in LacY. *J Membr Biol* 239(1-2):85–93.
6. Smirnova I, et al. (2007) Sugar binding induces an outward facing conformation of LacY. *Proc Natl Acad Sci USA* 104(42):16504–16509.
7. Madej MG, Soro SN, Kaback HR (2012) Apo-intermediate in the transport cycle of lactose permease (LacY). *Proc Natl Acad Sci USA* 109(44):E2970–E2978.
8. Abramson J, et al. (2003) Structure and mechanism of the lactose permease of *Escherichia coli*. *Science* 301(5633):610–615.
9. Mirza O, Guan L, Verner G, Iwata S, Kaback HR (2006) Structural evidence for induced fit and a mechanism for sugar/H+ symport in LacY. *EMBO J* 25(6):1177–1183.
10. Guan L, Mirza O, Verner G, Iwata S, Kaback HR (2007) Structural determination of wild-type lactose permease. *Proc Natl Acad Sci USA* 104(39):15294–15298.
11. Chaptal V, et al. (2011) Crystal structure of lactose permease in complex with an affinity inactivator yields unique insight into sugar recognition. *Proc Natl Acad Sci USA* 108(23):9361–9366.
12. Majumdar DS, et al. (2007) Single-molecule FRET reveals sugar-induced conformational dynamics in LacY. *Proc Natl Acad Sci USA* 104(31):12640–12645.
13. Kaback HR, et al. (2007) Site-directed alkylation and the alternating access model for LacY. *Proc Natl Acad Sci USA* 104(2):491–494.
14. Zhou Y, Guan L, Freites JA, Kaback HR (2008) Opening and closing of the periplasmic gate in lactose permease. *Proc Natl Acad Sci USA* 105(10):3774–3778.
15. Smirnova I, Kasho V, Sugihara J, Kaback HR (2009) Probing of the rates of alternating access in LacY with Trp fluorescence. *Proc Natl Acad Sci USA* 106(51):21561–21566.
16. Nie Y, Kaback HR (2010) Sugar binding induces the same global conformational change in purified LacY as in the native bacterial membrane. *Proc Natl Acad Sci USA* 107(21):9903–9908.
17. Kumar H, et al. (2014) Structure of sugar-bound LacY. *Proc Natl Acad Sci USA* 111(5):1784–1788.
18. Smirnova I, Kasho V, Sugihara J, Kaback HR (2011) Opening the periplasmic cavity in lactose permease is the limiting step for sugar binding. *Proc Natl Acad Sci USA* 108(37):15147–15151.
19. Smirnova I, Kasho V, Kaback HR (2014) Real-time conformational changes in LacY. *Proc Natl Acad Sci USA* 111(23):8440–8445.
20. Smirnova I, Kasho V, Sugihara J, Kaback HR (2013) Trp replacements for tightly interacting Gly-Gly pairs in LacY stabilize an outward-facing conformation. *Proc Natl Acad Sci USA* 110(22):8876–8881.
21. Fersht A (1999) *Structure and Mechanism in Protein Science: A Guide to Enzyme Catalysis and Protein Folding* (W. H. Freeman, New York), pp xxi, 631 pp.
22. Viitanen P, Garcia ML, Kaback HR (1984) Purified reconstituted lac carrier protein from *Escherichia coli* is fully functional. *Proc Natl Acad Sci USA* 81(6):1629–1633.
23. Rasmussen SG, et al. (2011) Crystal structure of the β2 adrenergic receptor-Gs protein complex. *Nature* 477(7366):549–555.
24. Steyaert J, Kobilka BK (2011) Nanobody stabilization of G protein-coupled receptor conformational states. *Curr Opin Struct Biol* 21(4):567–572.
25. Muyldermans S (2013) Nanobodies: Natural single-domain antibodies. *Annu Rev Biochem* 82:775–797.
26. Ring AM, et al. (2013) Adrenaline-activated structure of β2-adrenoceptor stabilized by an engineered nanobody. *Nature* 502(7472):575–579.
27. Staus DP, et al. (2014) Regulation of β2-adrenergic receptor function by conformationally selective single-domain intrabodies. *Mol Pharmacol* 85(3):472–481.
28. Pardon E, et al. (2014) A general protocol for the generation of nanobodies for structural biology. *Nat Protoc* 9(3):674–693.
29. Herzlinger D, Viitanen P, Carrasco N, Kaback HR (1984) Monoclonal antibodies against the *lac* carrier protein from *Escherichia coli*. 2. Binding studies with membrane vesicles and proteoliposomes reconstituted with purified *lac* carrier protein. *Biochemistry* 23(16):3688–3693.
30. Kaback HR (1971) Bacterial membranes. *Methods in Enzymology*, eds Kaplan NP, Jakoby WB, Colowick NP (Elsevier, New York), Vol XXII, pp 99–120.
31. Short SA, et al. (1974) Determination of the absolute number of *Escherichia coli* membrane vesicles that catalyze active transport. *Proc Natl Acad Sci USA* 71(12):5032–5036.
32. Owen P, Kaback HR (1978) Molecular structure of membrane vesicles from *Escherichia coli*. *Proc Natl Acad Sci USA* 75(7):3148–3152.
33. Owen P, Kaback HR (1979) Antigenic architecture of membrane vesicles from *Escherichia coli*. *Biochemistry* 18(8):1422–1426.
34. Owen P, Kaback HR (1979) Immunochemical analysis of membrane vesicles from *Escherichia coli*. *Biochemistry* 18(8):1413–1422.
35. Wu J, Kaback HR (1994) Cysteine 148 in the lactose permease of *Escherichia coli* is a component of a substrate binding site. 2. Site-directed fluorescence studies. *Biochemistry* 33(40):12166–12171.
36. He MM, Kaback HR (1997) Interaction between residues Glu269 (helix VIII) and His322 (helix X) of the lactose permease of *Escherichia coli* is essential for substrate binding. *Biochemistry* 36(44):13688–13692.
37. Mansoor SE, Farrens DL (2004) High-throughput protein structural analysis using site-directed fluorescence labeling and the bimane derivative (2-pyridyl)dithiobimane. *Biochemistry* 43(29):9426–9438.
38. Mansoor SE, Dewitt MA, Farrens DL (2010) Distance mapping in proteins using fluorescence spectroscopy: The tryptophan-induced quenching (TrIQ) method. *Biochemistry* 49(45):9722–9731.
39. Smirnova IN, Kasho V, Kaback HR (2008) Protonation and sugar binding to LacY. *Proc Natl Acad Sci USA* 105(26):8896–8901.
40. Biasini M, et al. (2014) SWISS-MODEL: Modelling protein tertiary and quaternary structure using evolutionary information. *Nucleic Acids Res* 42(Web Server issue):W252–W258.
41. Guex N, Peitsch MC, Schwede T (2009) Automated comparative protein structure modeling with SWISS-MODEL and Swiss-PdbViewer: A historical perspective. *Electrophoresis* 30(Suppl 1):S162–S173.

Further reading / analysis

Alternating access transport in LacY

Kaback *et al.*, *J. Membr. Biol.* 239, 85-93 (2011)

http://www.ncbi.nlm.nih.gov/pubmed/2161516

The Alternating Access Transport Mechanism in LacY

H. Ronald Kaback · Irina Smirnova · Vladimir Kasho · Yiling Nie · Yonggang Zhou

Received: 23 September 2010 / Accepted: 5 November 2010

Abstract Lactose permease of *Escherichia coli* (LacY) is highly dynamic, and sugar binding causes closing of a large inward-facing cavity with opening of a wide outward-facing hydrophilic cavity. Therefore, lactose/H^+ symport via LacY very likely involves a global conformational change that allows alternating access of single sugar- and H^+-binding sites to either side of the membrane. Here, in honor of Stephan H. White's seventieth birthday, we review in camera the various biochemical/biophysical approaches that provide experimental evidence for the alternating access mechanism.

Keywords Lactose · Permease · Symport · Transport · Membrane · Membrane protein

H. R. Kaback · I. Smirnova · V. Kasho · Y. Nie · Y. Zhou
Department of Physiology and Department of Microbiology, University of California Los Angeles, Los Angeles, CA 90095, USA

H. R. Kaback
Immunology and Molecular Genetics, University of California Los Angeles, Los Angeles, CA 90095, USA

H. R. Kaback
Molecular Biology Institute, University of California Los Angeles, Los Angeles, CA 90095, USA

H. R. Kaback (✉)
MacDonald Research Laboratories (Rm 6720), UCLA, 675 Charles E. Young Drive South, Los Angeles, CA 90095-1662, USA
e-mail: rkaback@mednet.ucla.edu

Introduction

The lactose permease of *Escherichia coli* (LacY), which catalyzes the coupled symport of a galactopyranoside and an H^+, is a paradigm for the major facilitator superfamily (MFS) of membrane transport proteins. LacY has been solubilized, purified and reconstituted into proteoliposomes in a fully functional state (reviewed in Viitanen et al. 1986). Furthermore, X-ray crystal structures of the conformationally restricted mutant Cys154→Gly have been solved in an inward-facing conformation (Abramson et al. 2003; Mirza et al. 2006), and the crystal structure of wild-type LacY exhibits the same conformation (Guan and Kaback 2006; Guan et al. 2007). Both structures have 12 transmembrane α-helices, most of which are shaped irregularly, organized into two pseudosymmetrical six-helix bundles surrounding a large interior hydrophilic cavity open to the cytoplasm only (Fig. 1). The sugar-binding site and the residues involved in H^+ translocation are at the approximate middle of the molecule at the apex of the hydrophilic cavity and distributed so that the side chains important for sugar recognition are predominantly in the N-terminal helix bundle and the side chains that form an H^+-binding site are mainly in the C-terminal bundle (Smirnova et al. 2009b). The periplasmic side of LacY is tightly packed, and the sugar-binding site is inaccessible from that side of the molecule. A similar structure has been observed for the X-ray structure of GlpT, which has little or no sequence homology with LacY and catalyzes exchange of inorganic phosphate for glycerol-3-P across the membrane (Huang et al. 2003).

Wild-type LacY is highly dynamic. H/D exchange of backbone amide protons in wild-type LacY occurs at rapid rate (le Coutre et al. 1998; Patzlaff et al. 1998; Sayeed and Baenziger 2009), and sugar binding by wild-type LacY is

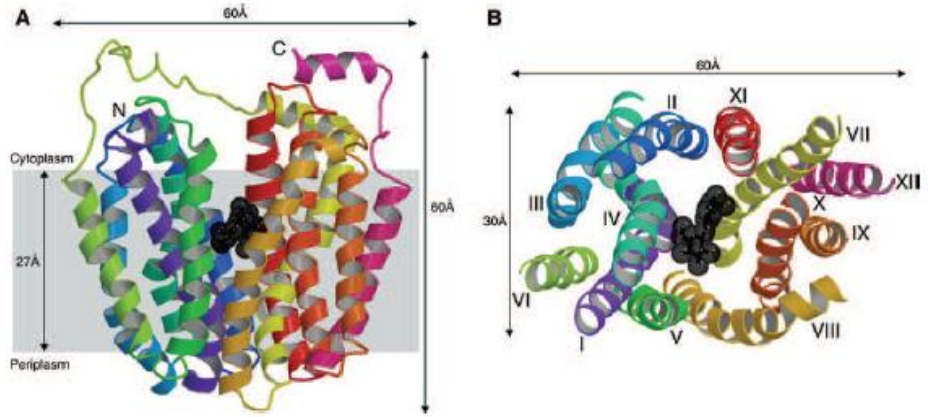

Fig. 1 Overall structure of LacY. **a** Ribbon representation of LacY viewed parallel to the membrane. **b** Ribbon representation of LacY viewed along the membrane normal from the cytoplasmic side. TDG is represented as *black spheres*

mostly entropic (Nie et al. 2006), inducing widespread conformational changes (reviewed in Guan and Kaback 2006; Kaback 2005; Kaback et al. 2001). More specifically, site-directed alkylation (reviewed in Kaback et al. 2007; Nie et al. 2007, 2008; Nie and Kaback 2010), single molecule fluorescence resonance energy transfer (Majumdar et al. 2007), double electron–electron resonance (Smirnova et al. 2007), site-directed cross-linking (Zhou et al. 2008) and Trp-quenching studies (Smirnova et al. 2009a) each provide independent evidence that sugar binding increases the open probability of a wide hydrophilic cleft on the periplasmic side of LacY with closing of the cytoplasmic cavity so that the sugar- and H^+-binding sites become alternatively accessible to either side of the membrane (the alternating access model). It has also been shown that the periplasmic cleft must close, as well as open, for translocation of sugar across the membrane to occur (Liu et al. 2010; Zhou et al. 2008, 2009).

Notably, in the conformationally restricted mutant C154G LacY, sugar binding is enthalpic and the periplasmic cleft is paralyzed in an open conformation (Majumdar et al. 2007; Nie et al. 2008; Smirnova et al. 2007). However, all X-ray structures of LacY (C154G as well as wild-type LacY) exhibit the same inward-facing conformation. Therefore, it is likely that the crystallization process selects a single conformer of LacY that is in the lowest free-energy state.

A functional LacY molecule devoid of its eight native Cys residues (C-less LacY) has been engineered by constructing a cassette *lacY* gene with unique restriction sites about every 100 bp (van Iwaarden et al. 1991). Utilizing this cassette *lacY* for Cys-scanning mutagenesis, a highly useful library of molecules with a single-Cys residue at virtually every position of LacY has been constructed (Frillingos and Kaback 1996). Cys is average in bulk, relatively hydrophobic and amenable to highly specific modification. Therefore, Cys-scanning mutagenesis has been used in combination with biochemical and biophysical techniques to reveal membrane topology, accessibility of intramembrane positions to the aqueous or lipid phase of the membrane and spatial proximity between transmembrane domains.

Here, the experimental approaches that provide a strong case for the alternating access model are reviewed cursorily.

Site-Directed Alkylation

Site-directed alkylation (SDA) of sylfhydryl thiols by radiolabeled *N*-ethylmaleimide (NEM) or fluorescent tetramethylrhodamine-5-maleimide (TMRM), which are membrane-permeant alkylating agents, has been used to study the reactivity of single-Cys LacY mutants in the C-less background in right-side-out (RSO) membrane vesicles. The approach provides important information about the structure, function and dynamics of LacY (reviewed in Guan and Kaback 2007). The reactivity/accessibility of Cys residues depend on the surrounding environment and are limited by close contacts between transmembrane helices and/or the low dielectric of the environment. Ligand binding increases NEM reactivity of single-Cys replacements located predominantly on the periplasmic side of LacY and decreases reactivity of those located predominantly on the cytoplasmic side (Guan and Kaback 2007). The pattern suggests that during sugar transport a periplasmic pathway opens with closing of the inward-facing cavity so that the

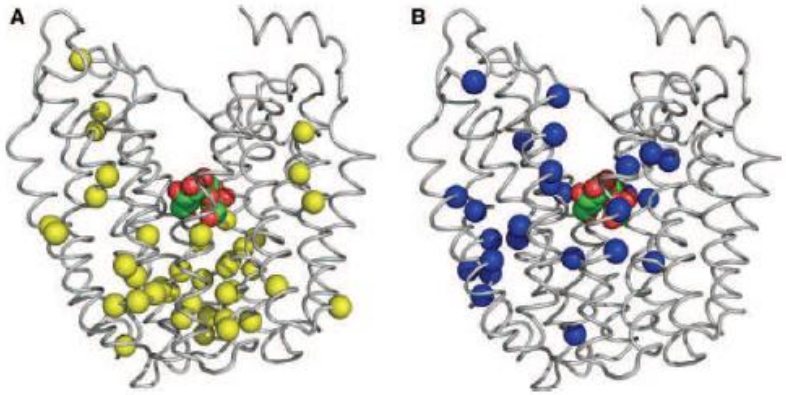

Fig. 2 Distribution of Cys replacements that exhibit changes in reactivity with NEM in the presence of TDG. **a** Positions of Cys replacements that exhibit a significant increase in reactivity with NEM (*gold spheres*) superimposed on the backbone of LacY viewed perpendicular to the plane of the membrane. TDG is shown as a CPK model at the apex of the inward-facing cavity. **b** Positions of Cys replacements that exhibit a significant decrease in reactivity with NEM (*blue spheres*) superimposed on the backbone of LacY viewed perpendicular to the plane of the membrane. The cytoplasmic surface is at the *top*, and TDG is shown as a CPK model at the apex of the inward-facing cavity (Color figure online)

sugar-binding site is alternatively accessible to either side of the membrane (Fig. 2).

Most recently, the simple, more facile alkylation method with TMRM (Nie et al. 2007, 2008, 2009) was utilized to examine the effect of sugar binding on alkylation of single-Cys LacY mutants either in RSO membrane vesicles or with purified proteins in dodecyl-β,D-maltopyranoside (DDM) micelles (Nie and Kaback 2010). Experiments were carried out at 0°C, where thermal motion is restricted (Venkatesan and Kaback 1998; Venkatesan et al. 2000a, 2000b), and linear rates of labeling were readily obtained (Fig. 3). TMRM labeling is almost negligible, with LacY containing each of five single-Cys residues at positions on the periplasmic side of the sugar-binding site in RSO membrane vesicles or with purified protein in DDM micelles. Therefore, each of these single-Cys replacements is unreactive and/or inaccessible to the alkylating agent. The observations are consistent with the interpretation that LacY in the native bacterial membrane is in a conformation similar to that of the X-ray crystal structures in the absence of ligand. The periplasmic side is tightly closed, and an open cavity is present facing the cytoplasm (the inward-facing conformation) (Abramson et al. 2003; Guan et al. 2007; Mirza et al. 2006).

As postulated by the alternating access model, on the cytoplasmic side of the sugar-binding site, each of five single-Cys replacement mutants labels at a rapid rate in the absence of sugar both in RSO membrane vesicles and with purified protein in DDM. Moreover, the tight-binding lactose homologue β-D-galactopyranosyl 1-thio-β,D-galactopyranoside (TDG) decreases the rate of TMRM labeling either in the membrane or with purified protein in DDM (Fig. 3; Table 1). The findings agree with a variety of other measurements (see below) showing that sugar binding induces closing of the cytoplasmic cavity and reduced reactivity/accessibility to alkylating agents.

The average increase in periplasmic TMRM labeling observed in the presence of TDG in RSO vesicles is ~10-fold, and the average cytoplasmic decrease in the presence of TDG is very similar (approximately ninefold) (Table 1). With purified single-Cys proteins in DDM, the comparable averages are approximately sixfold and approximately fivefold. Thus, the change in TMRM labeling induced by sugar on opposite faces of LacY appears to be about the same in RSO vesicles or with the purified single-Cys mutants in DDM. Therefore, the data provide further evidence not only that sugar binding markedly increases the open probability on the periplasmic side but that sugar binding also increases the probability of closing on the inside, the implication being that opening and closing may be reciprocal. However, reciprocity may not be obligatory as evidence has been presented showing that the periplasmic pathway is fixed in an open conformation in the C154G mutant, while the cytoplasmic cavity is able to close and open (Majumdar et al. 2007; Nie et al. 2008; Smirnova et al. 2007). It has also been demonstrated (Liu et al. 2010) that replacement of Asp68 with Glu at the cytoplasmic end of helix II blocks sugar-induced opening of the periplasmic cleft but has little or no effect on closing of the cytoplasmic cavity.

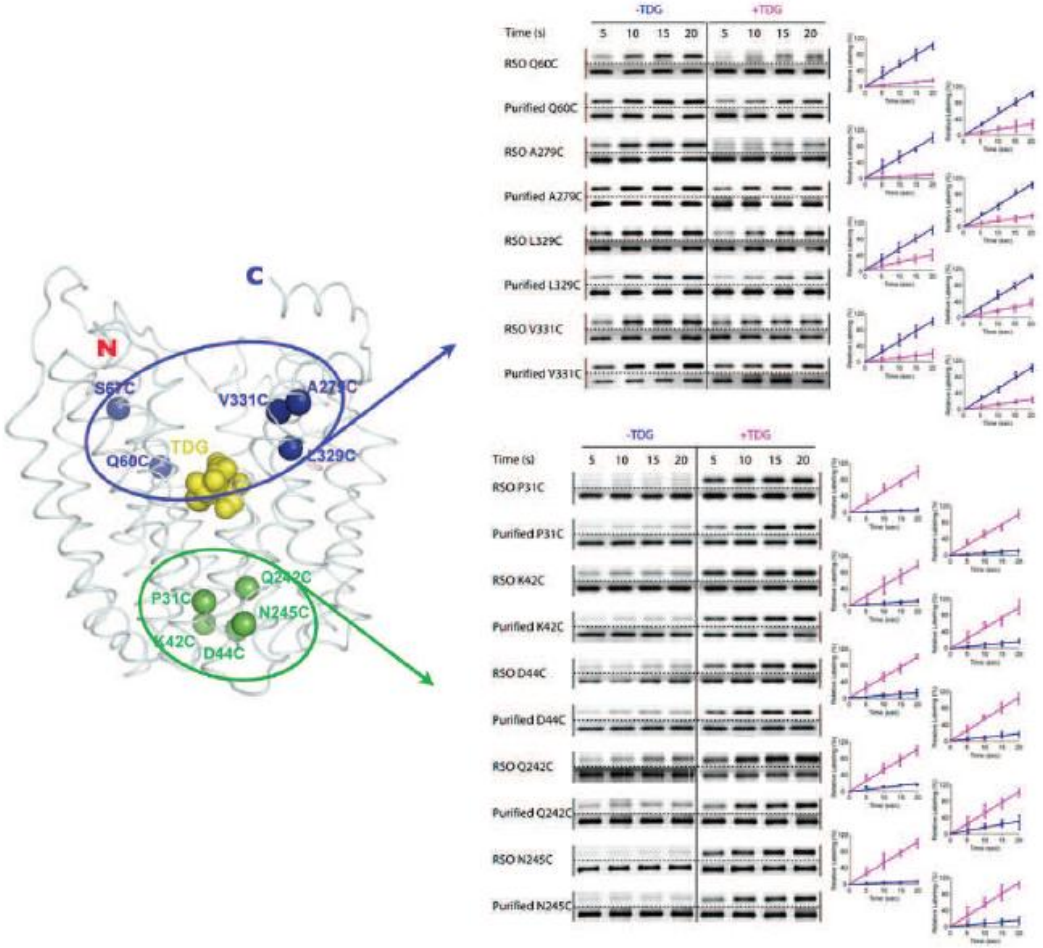

Fig. 3 TMRM labeling of cytoplasmic (*top*) or periplasmic (*bottom*) single-Cys mutants in RSO membrane vesicles or as purified proteins in DDM. Labeling of cytoplasmic single-Cys LacY mutants Q60C, S67C, A279C, L329C and V331C or periplasmic single-Cys LacY mutants Q31C, K42C, D44C, Q242C and N245C was performed with 40 μM TMRM (RSO membrane vesicles) or 4 μM TMRM (with purified proteins in DDM) for given times at 0°C in the absence of TDG (−TDG; *blue diamond*) or preincubated for 10 min with TDG prior to addition of TMRM (+TDG; *pink square*). Relative TMRM labeling rates were calculated as described (Nie and Kaback 2010); the data are plotted relative to the 20-s points in the absence (*top*) or presence (*bottom*) of TDG. For SDS/PAGE gels, *upper gel* displays the results of TMRM labeling and *bottom* is the silver-stained protein sample (Color figure online)

Although the sugar-induced changes in the global conformation of LacY are qualitatively similar in RSO membrane vesicles and with the purified mutants in DDM, it is notable that the magnitude of the effects is somewhat smaller with the purified mutant proteins (Table 1). Thus, the increases and decreases in TMRM labeling observed with the purified proteins upon addition of TDG are on average ~60% of those observed with RSO membrane vesicles. However, this is not surprising since it is known that a lipid bilayer (le Coutre et al. 1997) as well as its composition (Bogdanov et al. 2002) are important constraints on the structure of LacY.

Single-Molecule Fluorescence (Förster) Resonance Energy Transfer

Single-molecule fluorescence (Förster) resonance energy transfer (sm-FRET) has also been used to test the alternating access model with wild-type LacY and mutant

Table 1 TDG changes the rate of TMRM labeling of single-Cys mutants

LacY mutant	Helix	Fold change in TMRM labeling in RSO vesicles	Fold change in TMRM labeling in DDM
Periplasmic			
P31C	I	13.6	8.9
K42C	II	8.5	5.9
D44C	II	8.2	6.2
Q242C	II	5.2	3.2
N245C	VII	14.9	6.9
Cytoplasmic			
Q60C	II	−7.2	−3.8
S67C	II	−14.7	−8.3
A279C	IX	−13.1	−3.9
L329C	X	−2.6	−3.0
V331C	X	−5.1	−4.3

Rates of TMRM labeling were obtained from the time courses shown in Fig. 3 as described (Nie and Kaback 2010). For each mutant, the ratio of the estimated initial rate of TMRM labeling in the presence of TDG relative to that observed in the absence of TDG was calculated. Positive numbers indicate an increase in the relative labeling rate due to addition of TDG (periplasmic) and negative numbers indicate a decrease in the relative labeling rate due to addition of TDG (cytoplasmic)

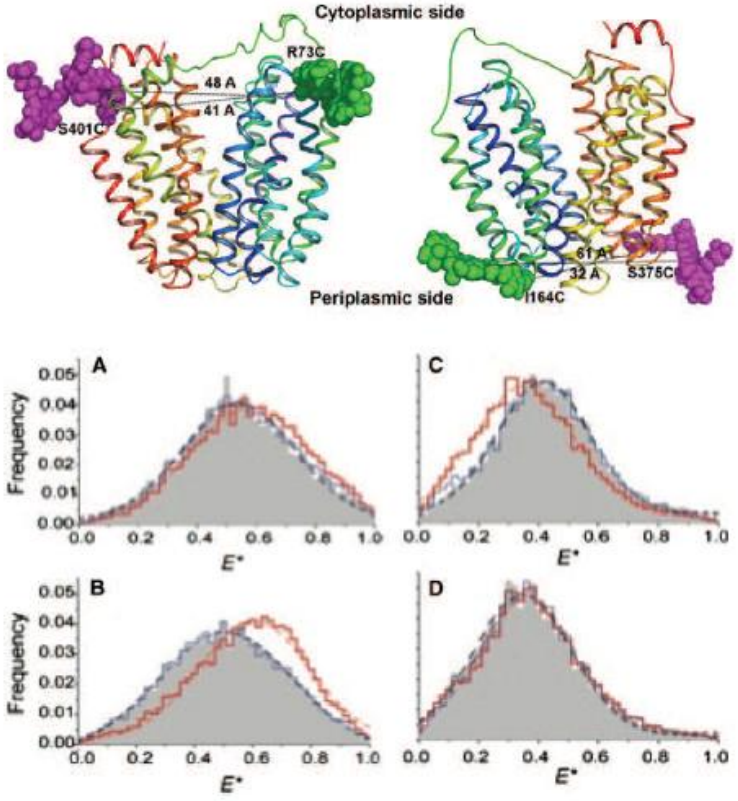

Fig. 4 Ligand-induced effects on the FRET distribution E^* at the cytoplasmic side of LacY (R73C/S401C, helices III and XII) or at the periplasmic side of LacY (I164C/S375C, helices V and XI). *Top* LacY backbone with donor (*magenta*) and acceptor fluorophores on the cytoplasmic or periplasmic side as indicated. *Bottom* **a** Frequency vs. E^* histograms corresponding to wild-type (**a**, **c**) and C154G mutant (**b**, **d**) LacY. Measurements for each construct were obtained in the absence of sugar (*gray*) and in the presence of 1 mM (saturating) galactosidic sugar concentration (*red*) or 1 mM glucosidic sugar (*blue*) (Nie et al. 2007). High E^* indicates high smFRET (i.e., closer distance between the fluorophores); low E^* indicates low smFRET (i.e., further distance) (Color figure online)

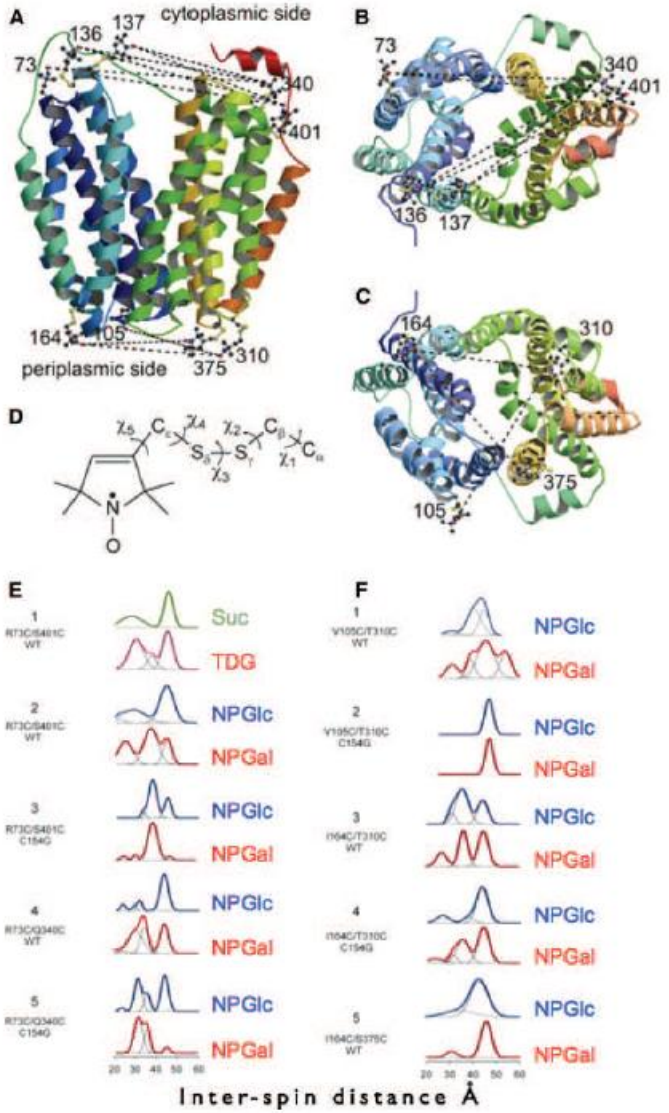

Fig. 5 *Top* Disulfide-linked nitroxide chains are modeled on the LacY X-ray structure (PDB ID 1PV6, rainbow-colored ribbons from *blue* [helix I] to *red* [helix XII]) with the cavity open to the cytoplasmic side. Nitroxides attached to the backbone of the protein are shown as *balls and sticks*. Interspin distances used for measurements are shown as *dashed lines*. Cytoplasmic pairs are viewed from the side (**a**) and from cytoplasm (**b**). Periplasmic pairs are viewed from the side (**a**) and from periplasm (**c**). Structure of the nitroxide side chain attached to the protein with indicated dihedral angles (**d**). *Bottom* DEER characterization of sugar-binding effects on interspin distances of nitroxide-labeled double-cysteine mutants located on the cytoplasmic (**e**) or the periplasmic (**f**) side of LacY. Distance distributions obtained by Tikhonov regularization are shown for protein with no sugar bound (glucosidic sugars sucrose or NP*Glc*—*green* or *blue*, respectively) and with bound sugar (galatosidic sugars TDG or NP*Gal*—*pink* or *red lines*, respectively), multi-gaussian fits (*black lines*) demonstrating relative distributions of conformational populations. See Smirnova et al. (2007) for details (Color figure online)

C154G in collaboration with Devdoot Majumdar and Shimon Weiss (Majumdar et al. 2007). Pairs of Cys residues at the ends of two helices on the cytoplasmic or periplasmic side of wild-type LacY and the mutant were labeled with appropriate donor and acceptor fluorophores, sm-FRET was determined in the absence and presence of sugar and distance changes were calculated. With wild-type LacY, binding of a galactopyranoside, but not a glucopyranoside, results in a decrease in distance on the cytoplasmic side and an increase in distance and in distance distribution on the periplasmic side (Fig. 4). In contrast, with the mutant, more pronounced decreases in distance and in distance distribution are observed on the cytoplasmic side but there is no change on the periplasmic side (Fig. 4). The results are consistent with the alternating access model and indicate that the translocation defect in the mutant is due to paralysis in the outward-facing conformation.

Double Electron–Electron Resonance

Double electron–electron resonance (DEER), a site-directed spin labeling technique, was applied to measure interhelical distance changes induced by sugar binding in collaboration with Christian Altenbach and Wayne Hubbell (Smirnova et al. 2007). Nitroxide-labeled paired-Cys replacements were constructed at the ends of transmembrane helices on the cytoplasmic or periplasmic side of LacY and in the conformationally restricted mutant C154G (Fig. 5a–d). Distances were then determined in the presence of galactosidic or nongalactosidic sugars (Fig. 5e, f). Strikingly, specific binding causes conformational rearrangements on both sides of the molecule. On the cytoplasmic side, each of six nitroxide-labeled pairs exhibits decreased interspin distances, ranging 4–21 Å. Conversely, on the periplasmic side, each of three spin-labeled pairs shows increased distances, ranging 4–14 Å. Thus, the inward-facing cytoplasmic cavity closes and a cavity opens on the tightly packed periplasmic side. In the C154G mutant, sugar-induced closing is observed on the cytoplasmic face but little or no change occurs on periplasmic side. DEER measurements in conjunction with molecular modeling based on the X-ray structure provide strong support for the alternative access model and suggest a structure for the outward-facing conformation of LacY.

Site-Directed Cross-Linking

As discussed, the residues essential for sugar recognition and H^+ translocation are located at the apex of the cavity and are inaccessible from the outside. On the periplasmic side, helices I/II and VII from the N and C six-helix bundles, respectively, participate in sealing the cavity from the outside. Three paired double-Cys mutants—Ile40 → Cys/Asn245 → Cys, Thr45 → Cys/Asn245 → Cys and Ile32 → Cys/Asn245 → Cys—located in the interface between helices I/II and VII on the periplasmic side of LacY were constructed with tandem factor Xa protease

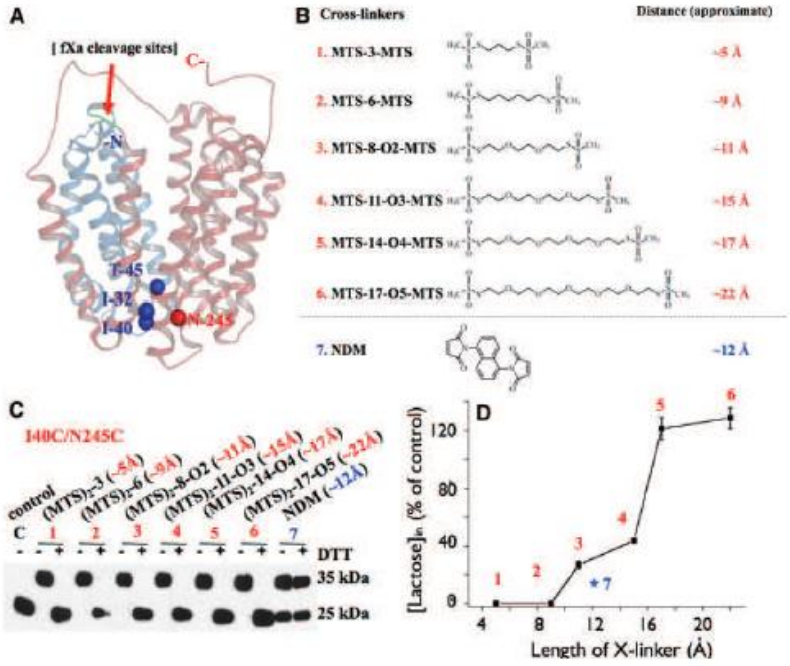

Fig. 6 **a** Structure model of LacY (PDB ID 2V8 N). Residues Ile32 (helix I), Ile40 (loop I/II) and Thr45 (helix II) are presented as *dark blue spheres*, and residue N245 (helix VII) is presented as a *red sphere*. The N-terminal four helices (N_4) and the C-terminal helices (C_8) are shown in *blue* and *red*, respectively, and separated by tandem factor Xa protease sites (*left side, green*), as indicated by the *red arrow*. **b** Homobifunctional cross-linking reagents. For MTS reagents, the approximate S–S distances between bridging sulfur atoms in the chains are as given by the manufacturer. The distance for NDM is from Green et al. (2001). Cross-linking (**c**) and lactose transport (**d**) with mutant I40C/N245C. All experiments were performed with RSO vesicles. *1*, MTS-3-MTS; *2*, MTS-6-MTS; *3*, MTS-8-O2-MTS; *4*, MTS-11-O3-MTS; *5*, MTS-14-O4-MTS; *6*, MTS-17-O5-MTS; *7*, NDM (Color figure online)

sites between the two Cys replacements (Fig. 6a) (Zhou et al. 2008). After quantitative cross-linking with flexible homo-bifunctional reagents less than about 15 Å in length, all three mutants lose the ability to catalyze lactose transport (Fig. 6b–d). Strikingly, however, full or partial activity is observed when cross-linking is mediated by flexible reagents greater than about 15 Å in length. Moreover, 17 Å is the minimum required for maximum activity, a distance very similar to that obtained from DEER (Smirnova et al. 2007). The results provide further support for the argument that transport via LacY involves opening and closing of a large periplasmic cavity.

Trp Quenching

Since Trp fluorescence is quenched by certain amino acyl side chains such as a protonated His or amino group, Trp residues were placed on either side of LacY where they are predicted to be in close proximity to the imidazole side chains of His in either the inward- or outward-facing conformation (Fig. 7, top) (Smirnova et al. 2009a). In the inward-facing conformation, LacY is tightly packed on the periplasmic side and Trp residues placed at position 245 (helix VII) or 378 (helix XII) are in close contact with His35 (helix I) or Lys42 (helix II), respectively. Sugar binding leads to *unquenching* of Trp fluorescence in both mutants, a finding clearly consistent with opening of the periplasmic cavity (Fig. 7a). The pH dependence of Trp245 unquenching exhibits a p*K*a of ~8, typical for a His side chain interacting with an aromatic group. On the cytoplasmic side, Phe140 (helix V) and Phe334 (helix X) are located on opposite sides of a wide open hydrophilic cavity. In precisely the opposite fashion from the periplasmic side, mutant Phe140 → Trp/Phe334 → His exhibits sugar-induced Trp *quenching* (Fig. 7b). Again,

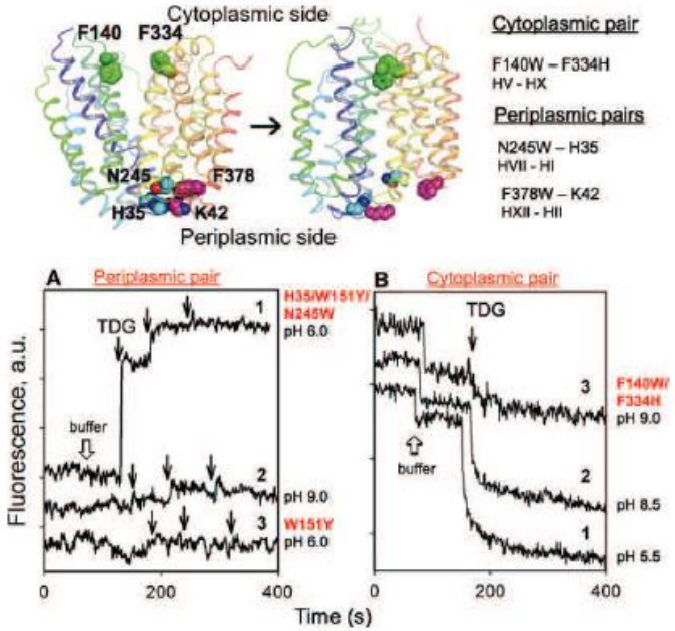

Fig. 7 *Top* Pairs of amino acid residues selected for Trp substitutions are shown on the backbone structure of LacY. The F140–F334 pair (helices V and X) on the cytoplasmic side is shown as *green spheres*. The H35–N245 (helices I and VII) and K42–F378 (helices II and XII) pairs on the periplasmic side are shown as *cyan* and *pink spheres*, respectively. A side view of the overall structure in the inward-facing conformation (PDB ID 2CFQ) is shown on the *left*, and the structure in the outward-facing conformation modeled (Smirnova et al. 2007) is shown on the *right*. Transmembrane helices are rainbow-colored from *blue* (helix I) to *red* (helix XII). *Arrow* indicates the conformational change resulting from sugar binding. The LacY structure is presented using Pymol0.97 (DeLano Scientific, San Carlos, CA). **a** TDG effect on fluorescence of Trp introduced on the periplasmic side. Sequential additions of 6 µl of buffer (*open arrow*) and 6-µl aliquots of 1.8 M TDG (*black arrows*) to the mutant W151Y/N245 W at pH 6.0 (*trace 1*) or at pH 9.0 (*trace 2*) and to the control mutant W151Y at pH 6.0 (*trace 3*). **b** TDG effect on Trp fluorescence of cytoplasmic pair F140 W–F334H at pH 5.5 (*trace 1*), pH 8.5 (*trace 2*) and pH 9.0 (*trace 3*). Additions of 20 µl of buffer (*open arrows*) or 20 µl of 1.5 M TDG (*black arrows*) were made into 2 ml of protein solutions (Color figure online)

quenching is pH-dependent with a p*K*a of ~8. The results provide yet another strong, independent line of evidence for the alternating access mechanism and demonstrate that the methodology described provides a sensitive probe to measure conformational changes in membrane transport proteins.

Acknowledgements The authors are indebted to M. Gregor Madej for embellishing the graphics and proofreading the manuscript. This work was supported by NIH grants DK051131, DK069463, GM073210 and GM074929 and NSF grant 0450970 (to H. R. K.).

References

Abramson J, Smirnova I, Kasho V, Verner G, Kaback HR, Iwata S (2003) Structure and mechanism of the lactose permease of *Escherichia coli*. Science 301:610–615

Bogdanov M, Heacock PN, Dowhan W (2002) A polytopic membrane protein displays a reversible topology dependent on membrane lipid composition. EMBO J 21:2107–2116

Frillingos S, Kaback HR (1996) Cysteine-scanning mutagenesis of helix VI and the flanking hydrophilic domains in the lactose permease of *Escherichia coli*. Biochemistry 35:5333–5338

Green NS, Reisler E, Houk KN (2001) Quantitative evaluation of the lengths of homobifunctional protein cross-linking reagents used as molecular rulers. Protein Sci 10:1293–1304

Guan L, Kaback HR (2006) Lessons from lactose permease. Annu Rev Biophys Biomol Struct 35:67–91

Guan L, Kaback HR (2007) Site-directed alkylation of cysteine to test solvent accessibility of membrane proteins. Nat Protoc 2:2012–2017

Guan L, Mirza O, Verner G, Iwata S, Kaback HR (2007) Structural determination of wild-type lactose permease. Proc Natl Acad Sci USA 104:15294–15298

Huang Y, Lemieux MJ, Song J, Auer M, Wang DN (2003) Structure and mechanism of the glycerol-3-phosphate transporter from *Escherichia coli*. Science 301:616–620

Kaback HR (2005) Structure and mechanism of the lactose permease. C R Biol 328:557–567

Kaback HR, Sahin-Toth M, Weinglass AB (2001) The kamikaze approach to membrane transport. Nat Rev Mol Cell Biol 2:610–620

Kaback HR, Dunten R, Frillingos S, Venkatesan P, Kwaw I, Zhang W, Ermolova N (2007) Site-directed alkylation and the alternating access model for LacY. Proc Natl Acad Sci USA 104:491–494

le Coutre J, Narasimhan LR, Patel CK, Kaback HR (1997) The lipid bilayer determines helical tilt angle and function in lactose permease of *Escherichia coli*. Proc Natl Acad Sci USA 94:10167–10171

le Coutre J, Kaback HR, Patel CK, Heginbotham L, Miller C (1998) Fourier transform infrared spectroscopy reveals a rigid alpha-helical assembly for the tetrameric *Streptomyces lividans* K^+ channel. Proc Natl Acad Sci USA 95:6114–6117

Liu Z, Madej MG, Kaback HR (2010) Helix dynamics in LacY: helices II and IV. J Mol Biol 396:617–626

Majumdar DS, Smirnova I, Kasho V, Nir E, Kong X, Weiss S, Kaback HR (2007) Single-molecule FRET reveals sugar-induced conformational dynamics in LacY. Proc Natl Acad Sci USA 104:12640–12645

Mirza O, Guan L, Verner G, Iwata S, Kaback HR (2006) Structural evidence for induced fit and a mechanism for sugar/H^+ symport in LacY. EMBO J 25:1177–1183

Nie Y, Kaback HR (2010) Sugar binding induces the same global conformational change in purified LacY as in the native bacterial membrane. Proc Natl Acad Sci USA 107:9903–9908

Nie Y, Smirnova I, Kasho V, Kaback HR (2006) Energetics of ligand-induced conformational flexibility in the lactose permease of *Escherichia coli*. J Biol Chem 281:35779–35784

Nie Y, Ermolova N, Kaback HR (2007) Site-directed alkylation of LacY: effect of the proton electrochemical gradient. J Mol Biol 374:356–364

Nie Y, Sabetfard FE, Kaback HR (2008) The Cys154 → Gly mutation in LacY causes constitutive opening of the hydrophilic periplasmic pathway. J Mol Biol 379:695–703

Nie Y, Zhou Y, Kaback HR (2009) Clogging the periplasmic pathway in LacY. Biochemistry 48:738–743

Patzlaff JS, Moeller JA, Barry BA, Brooker RJ (1998) Fourier transform infrared analysis of purified lactose permease: a monodisperse lactose permease preparation is stably folded, alpha-helical, and highly accessible to deuterium exchange. Biochemistry 37:15363–15375

Sayeed WM, Baenziger JE (2009) Structural characterization of the osmosensor ProP. Biochim Biophys Acta 1788:1108–1115

Smimova I, Kasho V, Choe JY, Altenbach C, Hubbell WL, Kaback HR (2007) Sugar binding induces an outward facing conformation of LacY. Proc Natl Acad Sci USA 104:16504–16509

Smimova I, Kasho V, Sugihara J, Kaback HR (2009a) Probing of the rates of alternating access in LacY with Trp fluorescence. Proc Natl Acad Sci USA 106:21561–21566

Smimova IN, Kasho VN, Sugihara J, Choe JY, Kaback HR (2009b) Residues in the H^+ translocation site define the pKa for sugar binding to LacY. Biochemistry 48:8852–8860

van Iwaarden PR, Driessen AJ, Menick DR, Kaback HR, Konings WN (1991) Characterization of purified, reconstituted site-directed cysteine mutants of the lactose permease of *Escherichia coli*. J Biol Chem 266:15688–15692

Venkatesan P, Kaback HR (1998) The substrate-binding site in the lactose permease of *Escherichia coli*. Proc Natl Acad Sci USA 95:9802–9807

Venkatesan P, Kwaw I, Hu Y, Kaback HR (2000a) Site-directed sulfhydryl labeling of the lactose permease of *Escherichia coli*: helix VII. Biochemistry 39:10641–10648

Venkatesan P, Liu Z, Hu Y, Kaback HR (2000b) Site-directed sulfhydryl labeling of the lactose permease of *Escherichia coli*: helix II. Biochemistry 39:10649–10655

Viitanen P, Newman MJ, Foster DL, Wilson TH, Kaback HR (1986) Purification, reconstitution, and characterization of the lac permease of *Escherichia coli*. Methods Enzymol 125:429–452

Zhou Y, Guan L, Freites JA, Kaback HR (2008) Opening and closing of the periplasmic gate in lactose permease. Proc Natl Acad Sci USA 105:3774–3778

Zhou Y, Nie Y, Kaback HR (2009) Residues gating the periplasmic pathway of LacY. J Mol Biol 394:219–225

Further reading / methods

Site-directed alkylation protocols

Gan & Kaback, *Nature Protocols* 2, 2012-2017 (2007)

http://www.ncbi.nlm.nih.gov/pubmed/17703213

Site-directed alkylation of cysteine to test solvent accessibility of membrane proteins

Lan Guan[1] & H Ronald Kaback[1–3]

[1]Department of Physiology, University of California Los Angeles, Los Angeles, California, USA. [2]Department of Microbiology, Immunology and Molecular Genetics, University of California Los Angeles, Los Angeles, California, USA. [3]Molecular Biology Institute, University of California Los Angeles, Los Angeles, California, USA. Correspondence should be addressed to H.R.K. (rkaback@mednet.ucla.edu).

Published online 16 August 2007; doi:10.1038/nprot.2007.275

This protocol describes a detailed method to study the static and dynamic features of membrane proteins, as well as solvent accessibility, by utilizing the lactose permease of *Escherichia coli* (LacY) as a model. The method relies on the use of functional single-Cys mutants, an affinity tag and a PhosphoImager. The membrane-permeant, radioactive thiol reagent *N*-[ethyl-1-^{14}C]ethylmaleimide ([^{14}C]NEM) is used to detect site-directed alkylation of engineered single-Cys mutants *in situ*. The solvent accessibility of the Cys residues is also determined by blockage of [^{14}C]NEM labeling with membrane-impermeant thiol reagents such as methanethiosulfonate ethylsulfonate (MTSES). The labeled proteins are purified by mini-scale affinity chromatography and analyzed by gel electrophoresis. Gels are dried and exposed to a PhosphoImager screen for 1–5 d, and incorporation of radioactivity is visualized. Initial results can be obtained in 24 h.

INTRODUCTION

Chemical modification is a simple, useful approach to study membrane protein structure and function. Among amino acids, Cys is average in steric bulk, relatively hydrophobic and amenable to highly specific modification. Cys-scanning mutagenesis takes advantage of these unique features of Cys combined with site-directed mutagenesis[1,2]. In order to optimize the approach, it may be necessary to construct a nonreactive or Cys-less mutant without inactivating the protein. On a functional Cys-less background, by systematically mutating each residue to Cys, a library of single Cys-mutant is generated, and the functional role of each position can be assessed by testing activity. A further advantage of the approach is that it enables studies of modification by Cys-specific reagents.

Site-directed sulfhydryl modification of single-Cys mutants *in situ* with radioactive *N*-ethylmaleimide (NEM) has been particularly useful for studying both static and dynamic features of the lactose permease of *Escherichia coli* (LacY)[3]. In this protocol, LacY is used as a prototype[4,5]. Alkylation with NEM is a measure of the reactivity and/or accessibility of a given Cys residue to this small, relatively hydrophobic, membrane-permeant thiol-specific reagent. Reactivity and/or accessibility are dependent primarily on the environment in the vicinity of a given Cys side chain and limited by close tertiary contacts between transmembrane helices and steric constraints of the lipid bilayer. Any change in reactivity of a Cys side chain upon substrate binding is indicative of an alteration in the local environment. Hence, determination of the reactivity of Cys replacement mutants with *N*-[ethyl-1-^{14}C]ethylmaleimide ([^{14}C]NEM) is a convenient way to assess the local environment of specific positions within the tertiary structure of the protein. Furthermore, *in situ* site-specific reaction with methanethiosulfonate ethylsulfonate (MTSES), a small hydrophilic, membrane-impermeant thiol reagent[6,7], can be utilized to study the accessibility of Cys residues to the aqueous milieu. Cys-scanning mutagenesis and site-directed sulfhydryl modification systematically applied to LacY has provided enormously valuable information with regard to structure, function and dynamics[2,3,5,8].

Here, we describe a simple, easy-to-handle protocol for measuring the reactivity of single-Cys mutants with various thiol reagents. Application allows (**Figs. 1** and **2**) (i) assessment of Cys reactivity with NEM under various conditions (e.g., absence or presence of ligand and/or an electrochemical proton gradient, temperature) (**Figs. 1a** and **2a**) and (ii) assessment of Cys reactivity with other nonradioactive thiol reagents by measuring blockade of radioactive NEM labeling (**Figs. 1b** and **2b**). Once Cys reacts with other thiol reagents, it cannot react with [^{14}C]NEM. One such application includes the use of impermeant MTSES[6,7,9] to study solvent accessibility; (iii) another application is estimation of apparent binding constants for a ligand by measuring ligand protection against alkylation with [^{14}C]NEM[10,11] (**Fig. 1c**), which will not be described here. In principle, NEM labeling and solvent accessibility approaches can be applied to identify residues buried in the core of a soluble protein by carrying out the analyses in the native or denatured condition. Furthermore, it is also useful for identifying positions located in the protein–protein interface of a protein

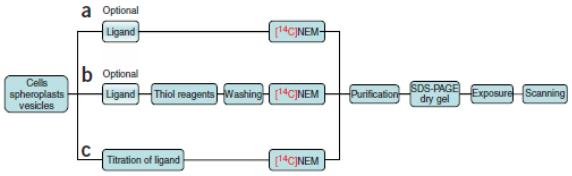

Figure 1 | Diagram for the application of *N*-ethylmaleimide (NEM) labeling. [^{14}C]NEM, *N*-[ethyl-1-14C]ethylmaleimide; SDS-PAGE, SDS–polyacrylamide gel electrophoresis.

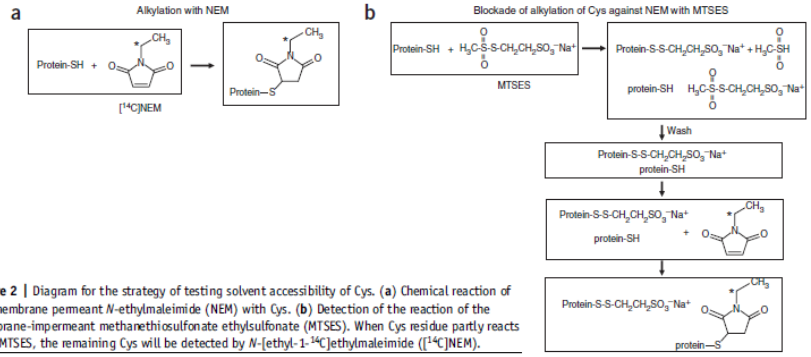

Figure 2 | Diagram for the strategy of testing solvent accessibility of Cys. (**a**) Chemical reaction of the membrane permeant *N*-ethylmaleimide (NEM) with Cys. (**b**) Detection of the reaction of the membrane-impermeant methanethiosulfonate ethylsulfonate (MTSES). When Cys residue partly reacts with MTSES, the remaining Cys will be detected by *N*-[ethyl-1-^{14}C]ethylmaleimide ([^{14}C]NEM).

complex by studying the effect of chemical modification on protein–protein interactions, solvent accessibility, as well as the protection against the alkylation of Cys residues.

Limitations of this particular protocol include requirement for radioactive NEM, use of an affinity tag fused to the target protein and a target protein containing only a single reactive Cys residue. Several affinity tags can be used to purify the target protein, examples being a His-tag on the target protein and metal affinity chromatography or other commercially available tags and protein purification kits. Here, we describe a protocol for purifying LacY containing a biotin acceptor domain at the C terminus by avidin chromatography[12,13].

It is important that the membrane permeability of the thiol reagent be tested in each system. In *E. coli*, NEM and MTSES are demonstrated to be permeant and impermeant, respectively, by analyzing labeling of cytoplasmic proteins[9]. It is also highly noteworthy that alternative methods with fluorescent thiol reactive reagents have been utilized[14–16].

MATERIALS

REAGENTS

- [^{14}C]NEM, 1.3 GBq mmol^{-1} (34.20 mCi mmol^{-1}) 0.5 ml Pentane (DuPont NEN, Boston, MA) ! CAUTION Pentane is volatile and irritant. It is harmful by inhalation, ingestion or skin absorption. ! CAUTION All experiments that involve the use of [^{14}C]NEM must be carried out following radiation safety guidelines.
- MTSES (Toronto Research Chemicals, Toronto, Ontario, Canada)
- Right-side out (RSO) membrane vesicles containing the target protein with an affinity tag can be prepared as described previously[17,18].
- 100 mM potassium phosphate (KP_i) or sodium phosphate (NaP_i), (pH 7.5)
- 100 mM KP_i (pH 7.5)/10 mM magnesium sulfate ($MgSO_4$)
- 10% Dodecyl-β-D-maltopyranoside (DDM; Anatrace, cat. no. D310A) ▲ CRITICAL Use NaP_i because KP_i will precipitate with SDS.
- 1 M DTT (Sigma-Aldrich, cat. no. D0632)
- Immobilized monomeric avidin gel (Pierce, cat. no. 20228) ▲ CRITICAL Further treatment with biotin is required, as described in the product information package from the supplier, Pierce.
- Column wash buffer (see REAGENT SETUP)
- Elution buffer (see REAGENT SETUP)
- Sample loading buffer [SDS–polyacrylamide gel electrophoresis (SDS-PAGE)]

EQUIPMENT

- 15-ml conical glass tube ! CAUTION Do not use plastic tubes with pentane, as this solvent may dissolve certain plastics.
- 1.5-ml conical screw cap tube with O-ring (VWR Scientific Products, cat. no. 20170-110)
- Argon gas
- Gel dryer (SpeedFel; Savant, cat. no. SG210D)
- Gel blot paper (Scheicher & Schuell, cat. no. BC 013)
- White light box
- Storage phosphor screen and exposure cassette (Molecular Dynamics)
- Kodak intensifying screen cleaner (Kodak, cat. no. 1064930)
- EL Mylar (Fralock, cat. no. F430052404, 0005 inch, 8 × 10)
- PhosphoImager
- –80 °C Freezer
- 3-ml Syringe barrels
- DNA miniprep column
- Vacuum manifold (Promega, cat. no. A7231) (**Fig. 3**)
- Microfuge
- Eppendorf tube
- Vertical electrophoresis apparatus

REAGENT SETUP

Column wash buffer 50 mM NaP_i (pH 7.4)/0.1 M NaCl/0.02 % DDM.
Elution buffer 5 mM Biotin in the column wash buffer given above; adjust to pH 7.5.

PROCEDURE

Preparation of [^{14}C]NEM solution ● TIMING 1–2 h

1| Add 0.5 ml H_20 to a 15-ml conical glass tube.

2| Tap the vial containing the [^{14}C]NEM solution on the bench top to force the reagent to the bottom of the vial.

3| Place vial containing [^{14}C]NEM on ice, in order to avoid pressure built-up, and file the top of the vial.

4| In a hood, break glass manually wearing gloves and using a kimwipe.

5| Immediately transfer the vial content to the 15-ml conical tube into the 0.5 ml H_2O (see Step 1) and mix on vortex immediately to avoid evaporation. Mark the interface of the two immiscible solvents.

6| Bubble the two-layer mixture gently with argon to evaporate the upper pentane layer (on completion, only one phase will be observed after mixing).

7| Aliquot the solution from Step 6 to a 1.5-ml conical screw cap tube with an O-ring screw top.
■ PAUSE POINT Store at −80°C until use. The NEM solution should be stable for at least a few months.

Figure 3 | Illustration of mini-scale purification using a vacuum manifold.

Preparation of membrane vesicle suspension ● TIMING 20 min

8| Place 50 µl of RSO membrane vesicles at a concentration of 20 mg protein ml^{-1} (approximately 0.1 mg of the target protein) in 100 mM KP_i (pH 7.5)/10 mM $MgSO_4$ in a 1.5-ml Eppendorf tube. The protein concentration can be estimated by the measurement at OD_{600}. To obtain an accurate measurement, vesicles must be diluted to a lower concentration (less than 1.0 at OD_{600}). An OD_{600} of 1 corresponds to approximately 1 mg protein ml^{-1}.

Blockade of [^{14}C]NEM labeling with MTSES ● TIMING 1–2 h (optional)

9| Add to the vesicle suspension MTSES to a final concentration of 0.2 mM, and incubate for 5 min in the absence or presence of ligand, (see **Figs. 1b** and **2b**). Stop reaction by dilution with 1.4 ml ice-cold 100 mM KP_i (pH 7.5)/10 mM $MgSO_4$ and centrifuge to remove excess reagents.

10| Wash another two times with 1.4 ml ice-cold 100 mM KP_i (pH 7.5)/10 mM $MgSO_4$ to remove the remaining MTSES (**Fig. 2b**).

11| Resuspend vesicles in 50 µl of 100 mM KP_i (pH 7.5)/10 mM $MgSO_4$.

12| For those samples to which a ligand had been added before the addition of MTSES (see Step 9), add the same concentration of ligand back to the samples.

[^{14}C]NEM labeling ● TIMING Approximately 30 min to 2h

13| To the Eppendorf tube, add 12 µl aqueous solution of [^{14}C]NEM from Step 7 to a final concentration of 0.5 mM, and start the timer.

14| At the appropriate time, add 1 µl of 1.0 M DTT to quench the reaction, mix on vortex and immediately place on ice. Time of labeling may vary with different membrane proteins or with different single-Cys mutants in the same protein. With LacY, labeling for 10 min may represent a rate of reaction for most positions[11,19]. When testing solvent accessibility (see Steps 9–12), the incubation time for [^{14}C]NEM labeling should be prolonged to 30–60 min.

Purification of biotinylated protein ● TIMING Approximately 30 min

15| Following reaction quenching with DTT, add 40 µl 100 mM KP_i or NaP_i (pH 7.5) to the suspension.

16| Add 25 µl 10% DDM to a final concentration of 2%.
▲ CRITICAL STEP Type of detergent and its concentration must be tested for each individual membrane protein. To obtain this information, a wide range of detergents must be screened in order to find those that solubilize the target membrane protein and maintain its stability in solution. This can be achieved by ultracentrifugation of the sample after addition of a given detergent and carrying out a western blot on the supernatant.

17| Mix by flicking the tube several times. The sample should clear immediately.

18| Add 40 µl immobilized monomeric avidin gel and mix by flicking the tube several times.

19| Incubate on a rotating platform at room temperature (~20 °C) for 5 min or at 4 °C for 30 min.

20| Place a Promega wizard column or any other DNA miniprep column on a vacuum manifold and prepare 3-ml syringe barrels (**Fig. 3**).

21| Spin down the sample, resuspend avidin gel with pipette tips and apply the sample to the column.

22| Turn on manifold just long enough to drain fluid.

23| Rinse sample tube with column wash buffer, apply to column and turn on the manifold briefly to drain the mixture.
▲ CRITICAL STEP Column wash buffer must have the detergent to avoid the aggregation of protein.

24| Attach syringe barrel to column.

25| Wash column with 6 ml column wash buffer.

26| Turn off manifold as soon as buffer is depleted.

27| Remove syringe barrel.

28| Place the column to a 1.5-ml Eppendorf tube.

29| Add 50 µl of 5 mM biotin in column wash buffer to top of column.

30| Wait for 2 min.

31| Spin at 12,000 r.p.m. for 20 s. Discard the columns in radioactive trash bin.

32| Purified protein samples in the Eppendorf tube are ready for analysis.

Separation and analysis of [^{14}C]NEM-modified LacY ● TIMING **3–4 h**

33| To the protein sample from Step 32 add 5 µl 10× SDS-PAGE sample loading buffer. Load two aliquots of 5 or 50 µl of the resulting solution onto two different 12% SDS-PAGE gels without heating the samples. Load protein markers to each gel.
▲ CRITICAL STEP Do not heat sample; heating causes aggregation of hydrophobic membrane proteins.

34| Run electrophoresis of the two gels at 20 mA and stop electrophoresis before the blue bands reach bottom (approximately 1–2 h).

35| Use one gel for western blot to detect the loaded protein. This works as an internal control.

36| Place the other gel onto gel blot paper, put onto Gel Dryer, covering gel with Saran wrap.

37| Dry gel at 80 °C for 1 h.

38| During this time, clean storage phosphor screen with Kodak intensifying screen cleaner and a soft cotton cloth. Erase the storage phosphor screen by placing facedown onto a light box until use (expose for approximately 1 h).
! CAUTION Carefully treat the storage phosphor screen as glass.

39| Trim the gel blot paper around the gel and tape the gel down to an exposure cassette.

40| Cover gel with a sheet of EL Mylar.

41| Expose by placing the blank storage phosphor screen directly onto the exposure cassette, lock the cassette and be sure that there is no exposure of the screen to light.

42| Label the exposure cassette with date, and store it flatly in a bench drawer at a room temperature.
■ PAUSE POINT Exposure usually takes 1–5 d.

Scan with PhosphoImager ● TIMING **1–5 d**

43| On the second day, scan the storage phosphor screen in PhosphoImager. Density of the band at the position corresponding to that of target protein represents [^{14}C]NEM-labeled protein. Save image as a 'tiff' file to be displayed through Adobe Photoshop software. This is the day-1 result, which should provide useful information to adjust the exposure time to obtain a high quality image. Intensity of the protein band is linear over a wide dynamic range. If the signal is weak, you need a longer exposure by simply erasing the image and exposing it again as described next.

44| Repeat Steps 38, 41 and 42. On the fifth day or the days after it, scan the storage phosphor screen in PhosphoImager to obtain a new image. If the image is still too weak, erase it and perform the exposure for a longer time.

45| When finished, discard gel in radioactive trash bin.

46| Clean the storage phosphor screen as described in Step 38 so that it is ready for further use, and return the screen to the exposure cassette.
? TROUBLESHOOTING

● **TIMING**
Cast SDS-PAGE: 2 h
Steps 1–7, preparation of [^{14}C]NEM solution: 1–2 h
Step 8, preparation of membrane vesicles suspension: 20 min
Steps 9–12, MTSES labeling: 1–2 h
Steps 13 and 14, [^{14}C]NEM labeling: approximately 30 min to 2h
Steps 15–32, purification of biotinylated protein: approximately 30 min
Steps 33–42, separation and analysis of [^{14}C]-NEM–modified LacY: 3–4 h
Steps 43–46, exposure: 1–5 d or longer

? TROUBLESHOOTING
Troubleshooting advice can be found in **Table 1**.

TABLE 1 | Troubleshooting table.

Problem	Possible reason	Solution
No protein band is present as probed with western blot and no radioactive band is visible	1. Immobilized monomeric avidin gel was not pretreated with biotin	1. Treat immobilized monomeric avidin gel with 3 mM biotin using a packed column; do not use the *batch method*
	2. Elution buffer did not contain biotin	2. Add biotin to elution buffer
	3. Elution buffer did not contain the proper concentration of detergent	3. Add detergent to elution buffer
	4. The sample was heated before SDS–polyacrylamide gel electrophoresis (SDS-PAGE)	4. Make sure not to heat the sample before running SDS-PAGE
A weak protein band detected using the PhosphoImager	Low level of expression	Increase level of membrane protein expression or expose the gel to the PhosphoImager for longer
Problematic extraction of *N*-[ethyl-1-^{14}C]ethylmaleimide from pentane	Pentane may react with certain plastic tubes	Use glass tubes
Partially exposed image of the labeled protein band	Cassette not closed completely (partly exposed to light)	Close the cassette tightly
Presence of superimposed images	Failure to erase storage phosphor screen	Clean well and expose the screen for longer time

ANTICIPATED RESULTS
The reactivity of Cys residues with NEM as well as the effect of ligand can be easily visualized by comparing the density of radioactive bands (**Fig. 4a**, upper panel). The total protein loaded, as visualized from western blot (**Fig. 4a**, lower panel) and data collected from a positive and a negative control for protein labeling are needed for a correct interpretation of the results. The following are examples for the interpretation of results as reported from studies on solvent accessibility of single-Cys residues determined by blockade of NEM labeling with MTSES following the protocol described above (**Fig. 4a**). The position studied is mapped in an x-ray crystal structure of LacY (**Fig. 4b**,**c**).

(1) *L329C LacY*^{20}. NEM labeling is nearly completely blocked by pretreatment with MTSES (compare lanes 1 and 3), showing that this Cys residue is highly accessible to solvent. The presence of the ligand β-D-galactopyranosyl 1-thio-β-D-galactopyranoside (TDG) at a saturating concentration does not alter accessibility (compare lanes 1 and 3 to lanes 2 and 4). Consistently, Leu^{329} (helix X) is exposed to the hydrophilic cavity of LacY (**Fig. 4b**,**c**).

(2) Q60C LacY^{21}. NEM labeling is blocked by MTSES (compare lane 5 to lane 7), showing that Cys at position 60 is highly accessible to solvent. In the presence of ligand, the side chain becomes less accessible to solvent, as shown by the decreased effectiveness of MTSES as a blocking agent (compare lanes 7 and 8). Gln^{60} (helix II) is fully exposed to the hydrophilic cavity (**Fig. 4b**,**c**).

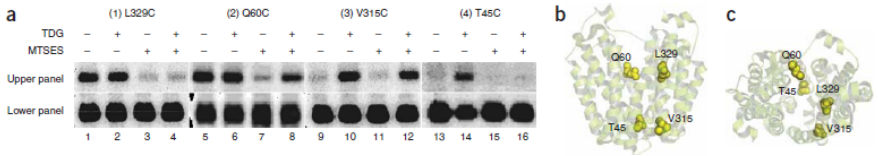

Figure 4 | Accessibility of single-Cys LacY mutants to methanethiosulfonate ethylsulfonate (MTSES) and effect of ligand. (**a**) Right-side out (RSO) membrane vesicles [approximately 1 mg protein in 50 µl 100 mM KP_i (pH 7.5)/10 mM $MgSO_4$] prepared from *Escherichia coli* T184 and transformed with plasmid encoding the indicated single-Cys LacY were incubated without or with MTSES (0.2 mM final concentration) for 5 min at 25 °C in the absence or presence of β-D-galactopyranosyl 1-thio-β-D-galactopyranoside (TDG), as indicated. Vesicles were washed two times with ice-cold buffer and resuspended in 50 µl of the same buffer and TDG (10 mM final concentration) was added back to the samples initially treated with TDG. Samples were then treated with *N*-[ethyl-1-^{14}C]ethylmaleimide ([^{14}C]NEM) (40 mCi mmol^{-1}; 0.5 mM final concentration) for 30 min at 25 °C. Reactions were quenched with DTT, and biotinylated LacY was solubilized and purified as described in the protocol. Aliquots containing approximately 5 µg protein were separated by SDS/12% polyacrylamide gel electrophoresis (PAGE). The gel was dried and exposed to a PhosphoImager screen for 5–8 d. Incorporation of [^{14}C]NEM (upper panel) was visualized and quantitated by a Storm 860 PhosphoImager (Molecular Dynamics). A fraction of the protein (0.5 µg) eluted from avidin gel was analyzed by western blotting with anti-C-terminal antibody (lower panel). (**b**) Mapping of the residues in the x-ray crystal structure of LacY (side view). (**c**) Cytoplasmic view.

Notably, Cys at positions 329 (native residue Leu) and 60 (native residue Gln) both are accessible to MTSES. Since these positions are located on the cytoplasmic side of transmembrane helices and MTSES is membrane impermeant, the reactivity observed may be due to conformational dynamics of LacY (i.e., exposure of positions lining the hydrophilic cavity).

(3) V315C LacY[20]. Although the presence of ligand markedly increases NEM labeling (compare lanes 9 and 10), a Cys side chain at position 315 is not accessible to MTSES (compare lanes 10 and 12), indicating lack of exposure to bulk solvent. Val[315] (helix X) is located between helical X and VII.

(4) T45C LacY[21]. In the presence of ligand, an increase in NEM labeling is observed (compare lanes 13 and 14), and the side chain is accessible to MTSES (compare lanes 14 and 16). Thr[45] (helix II) is located between helical II, I and VII.

ACKNOWLEDGMENTS The authors acknowledge support from National Institutes of Health (NIH) grants DK51131 and DK06946, GM074929 and National Science Foundation (NSF) grant 0450970 (to H.R.K.).

COMPETING INTERESTS STATEMENT The authors declare no competing financial interests.

Published online at http://www.natureprotocols.com
Reprints and permissions information is available online at http://npg.nature.com/reprintsandpermissions

1. Frillingos, S., Sahin-Tóth, M., Persson, B. & Kaback, H.R. Cysteine-scanning mutagenesis of putative helix VII in the lactose permease of *Escherichia coli*. *Biochemistry* **33**, 8074–8081 (1994).
2. Frillingos, S., Sahin-Toth, M., Wu, J. & Kaback, H.R. Cys-scanning mutagenesis: a novel approach to structure function relationships in polytopic membrane proteins. *FASEB J.* **12**, 1281–1299 (1998).
3. Kaback, H.R. *et al.* Site-directed alkylation and the alternating access model for LacY. *Proc. Natl. Acad. Sci. USA* **104**, 491–494 (2007).
4. Kaback, H.R., Sahin-Toth, M. & Weinglass, A.B. The kamikaze approach to membrane transport. *Nat. Rev. Mol. Cell Biol.* **2**, 610–620 (2001).
5. Guan, L. & Kaback, H.R. Lessons from lactose permease. *Annu. Rev. Biophys. Biomol. Struct.* **35**, 67–91 (2006).
6. Akabas, M.H., Stauffer, D.A., Xu, M. & Karlin, A. Acetylcholine receptor channel structure probed in cysteine-substitution mutants. *Science* **258**, 307–310 (1992).
7. Karlin, A. & Akabas, M.H. Substituted-cysteine accessibility method. *Methods Enzymol.* **293**, 123–145 (1998).
8. Guan, L., Sahin-Toth, M., Kalai, T., Hideg, K. & Kaback, H.R. Probing the mechanism of a membrane transport protein with affinity inactivators. *J. Biol. Chem.* **278**, 10641–10648 (2003).
9. Kwaw, I., Zen, K.C., Hu, Y. & Kaback, H.R. Site-directed sulfhydryl labeling of the lactose permease of *Escherichia coli*: helices IV and V that contain the major determinants for substrate binding. *Biochemistry* **40**, 10491–10499 (2001).
10. Frillingos, S. & Kaback, H.R. Probing the conformation of the lactose permease of *Escherichia coli* by *in situ* site-directed sulfhydryl modification. *Biochemistry* **35**, 3950–3956 (1996).
11. Sahin-Tóth, M., Akhoon, K.M., Runner, J. & Kaback, H.R. Ligand recognition by the lactose permease of *Escherichia coli*: specificity and affinity are defined by distinct structural elements of galactopyranosides. *Biochemistry* **39**, 5097–5103 (2000).
12. Consler, T.G. *et al.* Properties and purification of an active biotinylated lactose permease from *Escherichia coli*. *Proc. Natl. Acad. Sci. USA* **90**, 6934–6938 (1993).
13. Pouny, Y., Weitzman, C. & Kaback, H.R. *In vitro* biotinylation provides quantitative recovery of highly purified active lactose permease in a single step. *Biochemistry* **37**, 15713–15719 (1998).
14. Falke, J.J., Bass, R.B., Butler, S.L., Chervitz, S.A. & Danielson, M.A. The two-component signaling pathway of bacterial chemotaxis: a molecular view of signal transduction by receptors, kinases, and adaptation enzymes. *Annu. Rev. Cell Dev. Biol.* **13**, 457–512 (1997).
15. Yang, Q. *et al.* Experimental tests of a homology model for OxlT, the oxalate transporter of *Oxalobacter formigenes*. *Proc. Natl. Acad. Sci. USA* **102**, 8513–8518 (2005).
16. Koide, K., Maegawa, S., Ito, K. & Akiyama, Y. Environment of the active site region of RseP, an *Escherichia coli* regulated intramembrane proteolysis protease, assessed by site-directed cysteine alkylation. *J. Biol. Chem.* **282**, 4553–4560 (2007).
17. Kaback, H.R. Transport in isolated bacterial membrane vesicles. *Methods Enzymol.* **31**, 698–709 (1974).
18. Short, S.A., Kaback, H.R. & Kohn, L.D. Localization of d-lactate dehydrogenase in native and reconstituted *Escherichia coli* membrane vesicles. *J. Biol. Chem.* **250**, 4291–4296 (1975).
19. Guan, L. & Kaback, H.R. Binding affinity of lactose permease is not altered by the H^+ electrochemical gradient. *Proc. Natl. Acad. Sci. USA* **101**, 12148–12152 (2004).
20. Venkatesan, P., Hu, Y. & Kaback, H.R. Site-directed sulfhydryl labeling of the lactose permease of *Escherichia coli*: helix X. *Biochemistry* **39**, 10656–10661 (2000).
21. Venkatesan, P., Liu, Z., Hu, Y. & Kaback, H.R. Site-directed sulfhydryl labeling of the lactose permease of *Escherichia coli*: helix II. *Biochemistry* **39**, 10649–10655 (2000).